SH
11.A2
F53
Fish Mus

U.S. Department
of Commerce

Volume 107
Number 1
January 2009

Fishery Bulletin

SMITHSONIAN
MAR 09 2009
LIBRARIES

SHOUT
SHARE
IT

U.S. Department of Commerce
Carlos M. Gutierrez
Secretary

National Oceanic and Atmospheric Administration
William J. Brennan, Ph.D.
Acting Deputy Administrator of NOAA

National Marine Fisheries Service
James W. Balsiger, Ph.D.
Acting Assistant Administrator for Fisheries

Fishery Bulletin

Scientific Editor
Richard D. Brodeur, Ph.D.

Associate Editor
Julie Scheurer

National Marine Fisheries Service
Northwest Fisheries Science Center
2030 S. Marine Science Dr.
Newport, Oregon 97365-5296

Managing Editor
Sharyn Matriotti

National Marine Fisheries Service
Scientific Publications Office
7600 Sand Point Way NE
Seattle, Washington 98115-0070

Editorial Committee

John Carlson	National Marine Fisheries Service, Panama City, Florida
Kevin Craig	Florida State University, Tallahassee, Florida
Jeff Leis	Australia Museum, Sydney, New South Wales, Australia
Rich McBride	National Marine Fisheries Service, Woods Hole, Massachusetts
Rick Methot	National Marine Fisheries Service, Seattle, Washington
Adam Moles	National Marine Fisheries Service, Auke Bay, Alaska
Frank Parrish	National Marine Fisheries Service, Honolulu, Hawaii
Dave Somerton	National Marine Fisheries Service, Seattle, Washington
Ed Trippel	Department of Fisheries and Oceans, St. Andrews, New Brunswick, Canada
Mary Yoklavich	National Marine Fisheries Service, Santa Cruz, California

***Fishery Bulletin* web site: www.fishbull.noaa.gov**

The *Fishery Bulletin* (ISSN 0090-0656) is published quarterly by the Scientific Publications Office, National Marine Fisheries Service, NOAA, 7600 Sand Point Way NE, BIN C15700, Seattle, WA 98115-0070. Periodicals postage is paid at Seattle, WA. POSTMASTER: Send address changes for subscriptions to Fishery Bulletin, Superintendent of Documents, Attn.: Chief, Mail List Branch, Mail Stop SSOM, Washington, DC 20402-9373.

Although the contents of this publication have not been copyrighted and may be reprinted entirely, reference to source is appreciated.

The Secretary of Commerce has determined that the publication of this periodical is necessary according to law for the transaction of public business of this Department. Use of funds for printing of this periodical has been approved by the Director of the Office of Management and Budget.

For sale by the Superintendent of Documents, U.S. Government Printing Office, Washington, DC 20402. Subscription price per year: $36.00 domestic and $50.40 foreign. Cost per single issue: $21.00 domestic and $29.40 foreign. **See back for order form.**

The *Fishery Bulletin* carries original research reports and technical notes on investigations in fishery science, engineering, and economics. It began as the Bulletin of the United States Fish Commission in 1881; it became the Bulletin of the Bureau of Fisheries in 1904 and the *Fishery Bulletin* of the Fish and Wildlife Service in 1941. Separates were issued as documents through volume 46; the last document was No. 1103. Beginning with volume 47 in 1931 and continuing through volume 62 in 1963, each separate appeared as a numbered bulletin. A new system began in 1963 with volume 63 in which papers are bound together in a single issue of the bulletin. Beginning with volume 70, number 1, January 1972, the *Fishery Bulletin* became a periodical, issued quarterly. In this form, it is available by subscription from the Superintendent of Documents, U.S. Government Printing Office, Washington, DC 20402. It is also available free in limited numbers to libraries, research institutions, State and Federal agencies, and in exchange for other scientific publications.

U.S. Department of Commerce
Seattle, Washington

Volume 107
Number 1
January 2009

Fishery Bulletin

Contents

Articles

1–12 Stehlik, Linda L.
Effects of seasonal change on activity rhythms and swimming behavior of age-0 bluefish (*Pomotomus saltatrix*) and a description of gliding behavior

Companion papers

13–23 Anderson, Joel D., Dusty L. McDonald, Glen R. Sutton, and William J. Karel
Evolutionary associations between sand seatrout (*Cynoscion arenarius*) and silver seatrout (*C. nothus*) inferred from morphological characters, mitochondrial DNA, and microsatellite markers

24–35 McDonald, Dusty L., Joel D. Anderson, Britt W. Bumguardner, Fernando Martinez-Andrade, and Josh O. Harper
Spatial and seasonal abundance of sand seatrout (*Cynoscion arenarius*) and silver seatrout (*C. nothus*) off the coast of Texas, determined with twenty years of data (1987–2006)

36–44 Tolan, James M., and Mark Fisher
Biological response to changes in climate patterns: population increases of gray snapper (*Lutjanus griseus*) in Texas bays and estuaries

45–56 Candy, John R., R. Gregory Bonnell, Terry D. Beacham, Colin G. Wallace, and Ruth E. Withler
Dividing population genetic distance data with the software Partitioning Optimization with Restricted Growth Strings (PORGS): an application for Chinook salmon (*Oncorhynchus tshawytscha*), Vancouver Island, British Columbia

The National Marine Fisheries Service (NMFS) does not approve, recommend, or endorse any proprietary product or proprietary material mentioned in this publication. No reference shall be made to NMFS, or to this publication furnished by NMFS, in any advertising or sales promotion which would indicate or imply that NMFS approves, recommends, or endorses any proprietary product or proprietary material mentioned herein, or which has as its purpose an intent to cause directly or indirectly the advertised product to be used or purchased because of this NMFS publication.

The NMFS Scientific Publications Office is not responsible for the contents of the articles or for the standard of English used in them.

57–75 **Coulson, Peter G., S. Alex Hesp, Norman G. Hall, and Ian C. Potter**
The western blue groper (*Achoerodus gouldii*), a protogynous hermaphroditic labrid with exceptional longevity, late maturity, slow growth, and both late maturation and sex change

76–88 **Wood, Anthony D., Bradley M. Wetherbee, Francis Juanes, Nancy E. Kohler, and Cheryl Wilga**
Recalculated diet and daily ration of the shortfin mako (*Isurus oxyrinchus*), with a focus on quantifying predation on bluefish (*Pomatomus saltatrix*) in the northwest Atlantic Ocean

89–100 **Wood, Abby Jane M., Jeremy S. Collie, and Jonathan A. Hare**
A comparison between warm-water fish assemblages of Narragansett Bay and those of Long Island Sound waters

Note

101–105 **Staudinger, Michelle D., Francis Juanes, and Suzanne Carlson**
Reconstruction of original body size and estimation of allometric relationships for the longfin inshore squid (*Loligo pealeii*) and northern shortfin squid (*Illex illecebrosus*)

106 **Guidelines for authors**

108 **Subscription form**

Effects of seasonal change on activity rhythms and swimming behavior of age-0 bluefish (*Pomatomus saltatrix*) and a description of gliding behavior

Linda L. Stehlik

Email address: Linda.Stehlik@noaa.gov

National Marine Fisheries Service, NOAA
Northeast Fisheries Science Center
James J. Howard Marine Sciences Laboratory
74 Magruder Road
Highlands, New Jersey 07732

Abstract—Daily and seasonal activity rhythms, swimming speed, and modes of swimming were studied in a school of spring-spawned age-0 bluefish *(Pomatomus saltatrix)* for nine months in a 121-kL research aquarium. Temperature was lowered from 20° to 15°C, then returned to 20°C to match the seasonal cycle. The fish grew from a mean 198 mm to 320 mm (n=67). Bluefish swam faster and in a more organized school during day (overall mean 47 cm/s) than at night (31 cm/s). Swimming speed declined in fall as temperature declined and accelerated in spring in response to change in photoperiod.

Besides powered swimming, bluefish used a gliding-upswimming mode, which has not been previously described for this species. To glide, a bluefish rolled onto its side, ceased body and tail beating, and coasted diagonally downward. Bluefish glided in all months of the study, usually in the dark, and most intensely in winter. Energy savings while the fish is gliding and upswimming may be as much as 20% of the energy used in powered swimming. Additional savings accrue from increased lift due to the hydrofoil created by the horizontal body orientation and slightly concave shape. Energy-saving swimming would be advantageous during migration and overwintering.

Manuscript submitted 27 February 2008.
Manuscript accepted 1 August 2008.
Fish. Bull. 107(1):1–12 (2009).

The views and opinions expressed or implied in this article are those of the author and do not necessarily reflect the position of the National Marine Fisheries Service, NOAA.

Bluefish (*Pomatomus saltatrix*) are temperate-zone fish with seasonal cycles of activity that revolve around lengthy coastal migrations. Age-1 and older bluefish migrate northward from April through July along the continental shelf of the United States from Florida to as far north as Maine. They spawn in southern and middle-Atlantic waters. These bluefish are collected on the shelf in spring at a temperature range of 8–23°C, mainly 10–19°C (Shepherd and Packer, 2006). Spring- and summer-spawned cohorts of age-0 bluefish arrive in coastal waters and estuaries beginning in June and remain there throughout summer at temperatures of 14–25°C (Nyman and Conover, 1988; Able et al., 2003). Age-0 fish reside in estuaries and coastal waters until late October, whereas older age classes remain until late November (Scharf et al., 2004; Shepherd and Packer, 2006). Bluefish migrate southward along the Atlantic continental shelf from along the beaches to well offshore. Temperatures on the shelf where they are captured in fall are 10–27°C, mainly 17–25°C (Shepherd and Packer, 2006). Adults and the age-0 spring-spawned cohort spend winter on the outer continental shelf and slope from Virginia south to Florida (Shepherd and Packer, 2006; Shepherd et al., 2006). These lengthy migrations involve risks and are energetically costly.

With increasing temperature, the rates of metabolic processes of ectotherms increase (the bioenergetic response) (Fry, 1971; Brown et al., 2004). Within the thermal tolerance ranges of most fishes, as temperature increases, activity, food consumption, and growth increase (Beamish, 1978). Bluefish have a higher rate of increase in metabolism with temperature than their main competitors in the temperate zone, weakfish *(Cynoscion regalis)* and striped bass *(Morone saxatilis)* (Hartman and Brandt, 1995). The bioenergetic response in bluefish was observed experimentally in a school of 550–650 mm adults held in a 121-kL research aquarium under a summer photoperiod (Olla and Studholme, 1971). At 19.5°C, they swam at 40–60 cm/s. As the temperature increased to 30°C over a month, their swimming speed increased to 80–100 cm/s. The high food consumption rates of bluefish rival those of tropical species (Juanes and Conover, 1994; Buckel et al., 1995). Increased food consumption at higher temperatures is accompanied by increased growth rates in bluefish (Buckel et al., 1995; Hartman and Brant, 1995).

Diel activity cycles or rhythms in bluefish are known. Olla and Studholme (1972) examined effects of photoperiod upon the activity of six age-1+ bluefish in the aforementioned 121-kL aquarium. The mean swimming speed of the school increased after transition to daylight, peaked at midday, and slowed in afternoon. In darkness, the school was more dispersed, interfish distance increased, and speeds were more variable (Olla and Studholme, 1971, 1972). Less is known about seasonal rhythms in

bluefish. Under a winter photoperiod, as water temperature decreased, swimming speed correspondingly decreased (Olla and Studholme, 1971), but a longer study of behavior over a seasonal cycle has not been undertaken.

Bluefish use sustained or powered swimming for daily activity and long distance travel. They propel themselves by flexing the rear part of the body and tail and use their other fins mainly for stability and maneuvering. Powered swimming can be used for long periods without fatigue, although it has energetic costs (Beamish, 1978). For prey capture, bluefish use burst swimming at speeds recorded at up to 800–1000 cm/s (Olla et al., 1970). A novel and unexpected locomotory behavior was witnessed by Studholme and others during an unpublished study of a school of juvenile bluefish in the 12- kL research aquarium in 1984–85. At night, individual fish rolled onto their sides and, with their bodies and fins held still and slightly curved, glided downward diagonally, and then ascended. This behavior is remarkable in teleost fishes with laterally compressed bodies, because these fish are assumed to swim in a vertically oriented manner.

In 1995, a study was designed to expand upon previous bluefish research (Olla and Studholme, 1971, 1972; Olla et al., 1985) to examine in detail the seasonal cycle of activity in bluefish from fall through winter and spring. Unfortunately, the documentation of the cycle of behavior and gliding in age-0 bluefish from the 1984–85 study was lost in a fire. Therefore, a school of age-0 bluefish was brought to an aquarium of similar dimensions to that used earlier. Food consumption, swimming speed (as a measure of activity), and mode of swimming were recorded to determine their relationship to changing temperature and photoperiod. It was hoped that the previously observed but undescribed gliding behavior would recur. Particular attention was paid to changes in behavior that could be related to migration, overwintering, and the bioenergetic response.

Materials and methods

Source of fish and laboratory conditions

Spring-spawned age-0 bluefish were captured by hook and line from Sandy Hook Bay, NJ, over the period of a week. One hundred and five fish were placed in the research aquarium on 3 August 1995. The research aquarium, located at the National Oceanic and Atmospheric Administration James J. Howard Marine Sciences Laboratory, Sandy Hook, Highlands, NJ, held 121 kL (32,000 gallons), was 10.6 m by 4.5 m, and had a water depth of 2 m (Olla et al., 1967). Water originated from Sandy Hook Bay and salinity in the aquarium varied with ambient conditions (19 to 23 psu). The aquarium had a flow rate of 400 L /min and 10% of the water was replaced each week. Heaters and chillers were used to maintain the desired temperature (±0.5°C). Photoperiod matched that at the latitude of North Carolina (35°N) with a minimum of 9.3 hr of light at winter solstice. Light intensity at the bottom was 206 lux (0.0027 mEinsteins PAR) at midday and 0.17 lux at night, which allowed for video recording.

Water temperature was controlled to approximate that in migration and at summering and wintering areas, as determined from historical data from the NOAA National Data Buoy Center. The temperature was set at 20°C from the start of the experiment through 9 October. Then it was decreased incrementally over 8 wk (0.105°C/d) until it reached 15°C, the average minimum temperature off North Carolina south of Cape Hatteras. The temperature in the aquarium was raised from 15 to 20°C (0.194°C/d) over the period from 24 May to 23 June, simulating temperature increases in New Jersey coastal waters.

Feeding and growth

Bluefish were usually fed each afternoon, 5 d/wk. Live mummichogs *(Fundulus heteroclitus)* were weighed and tossed into the middle of the aquarium until the bluefish had fed to satiation. In winter, the bluefish did not feed as readily and therefore were left undisturbed to feed for an hour. Then the uneaten mummichogs were removed. A subset of fish was seined from the aquarium, anaesthetized, measured by total length (TL, to ~1 mm), and weighed (to ~1 g) every two months. The total weight of food consumed each week was divided by the calculated weight of all fish in the aquarium that week, and then divided by seven, to obtain the consumption rate in g food per g body weight per day (BW/d).

Daily and seasonal rhythms

Activity was measured by swimming speed. For each observation, an actively swimming bluefish was timed while it crossed a measured portion of the far wall of the aquarium. Only fish close to the wall were timed. During the first 5 minutes of each hour of the day, five randomly selected fish were timed and their speeds were averaged. When live observations could not be made, data were taken from videotapes made with a time-lapse video recorder and camera placed at a window opposite the far wall of the aquarium and set to record for five minutes at the start of each hour. Live observations were also made for longer periods during day and night. Every three or four weeks, or more often, a complete set of swimming speeds was recorded, in which 24 five-minute segments were observed on each of seven days, for a total of seventeen weeks. Speeds were expressed in cm/s and body lengths per second (BLl/s). For comparisons of day and night activity, a subset of the swimming speed observations were used, from 0900 through 1500 and 2100 through 0300.

Modes of swimming

The general behavior of the school, depth of swimming, and modes of swimming were noted in the first 5 min-

Table 1

Number of bluefish (*Pomatomus saltatrix*) measured, average total lengths (TL, mm), and weights (g), with ranges, at intervals during the activity rhythm experiment, 1995–96.

Date	Number of fish measured	Average total length (TL, mm)[1]	Length range (mm)	Average weight (g)	Weight range (g)
10 August 10 1995	110	161.5	125–192	34.8	16.6–60.5
12 October 1995	24	229.4	185–261	139.5	68.1–205.3
15 November 1995	26	251.8	210–278	196.7	100.7–259.5
17 January 1996	25	265.7	223–290	219.9	126.0–283.9
22 May 1996	27	302.6	268–334	285.2	186.7–389.7
28 June 1996	64	325.2	250–357	369.0	243.7–470.5

[1] Fork length = 0.8647 (TL) + 7.0656 for TL range 125 to 388 mm.

utes of each hour. During two weeks in January, counts were made to determine the proportion of fish that were gliding. All fish that passed in each 5-min observation period were counted, usually 300–600 observations. Then the videos were replayed and only the gliding fish were counted. Ascending fish were difficult to see and could not be counted.

Glide angles ($\acute{\alpha}$), upswimming (returning to initial depth) angles (β), and glide and upswim distances (a_1, a_2) (Weihs, 1973; Magnuson, 1978) were determined for individual fish from videotapes from the first week of January 1996. Angles were determined from successive still images and reported as the angle deviating from a horizontal path. Speeds of individuals over ground were also obtained from successive images.

An additional study was conducted from November 2006 through May 2007, under the same experimental conditions, to focus on details of gliding behavior. Age-0 summer-spawned bluefish (n=71, length range 135–216 mm TL) were used. Glide angles were measured as before, and body roll angles were measured from images of these fish gliding straight toward a video camera.

Results

Feeding and growth

At the start of the experiment, the mean length of the bluefish was 162 mm total length (TL) (147 mm fork length) and the mean weight was 35 g (Table 1). Their condition factor (Fulton's K) averaged 1.08. The day after placement into the aquarium the fish fed readily. In early September, at 20°C, they consumed 13% body weight/d (BW/d) (Table 2). Consumption rates decreased thereafter, falling to 2.0–3.8% BW/d while the water temperature was 15°C. After the temperature was raised once again to 20°C, food consumption rose to 5.9% BW/d. Fish grew throughout the experiment, but the rate of increase in length and weight slowed as fish size increased. At the end of the experiment on 28 June 1996, the mean length of the bluefish was 325 mm TL and the mean weight was 369 g (Table 2). At that time 67 bluefish survived in excellent health and their condition factor averaged 1.55. Growth rate over the entire experiment was 0.96 g/d.

From about 8 April to 4 May 1996, the fish were infested with the parasitic protozoa *Brooklynella hastili*. Swimming speed decreased, pale patches appeared on the skin, some scales were lost, and food consumption was unusually low (0.9% BW/d on week of 28 April to 4 May). Two fish died. The parasites were killed by lowering the salinity to 13 psu and then raising it to ambient psu from 1 May through 4 May. The following week the appetites and swimming speeds of the fish returned to levels similar to those before the infestation.

Daily and seasonal rhythms

After one week the bluefish settled into a pattern of swimming in a counterclockwise circle and individuals were spaced evenly around the aquarium perimeter. They occupied all depths of the aquarium. Individuals occasionally shot ahead or out of the circular path, but usually the fish remained apace with one another. In all months the bluefish swam faster during daylight than at night, accelerated each morning after light increased and usually attained maximum speed around noon. A representative diel rhythm during fall is shown for the week beginning 29 October 1995 (Fig. 1A). During the week of 31 December (Fig. 1B), the peaks of activity near noon were brief. Speeds in cm/s were highest when the fish had grown, as shown on the week of 26 May 1996 (Fig. 1C).

Activity varied seasonally in relation to water temperature and light in the aquarium. From early October through early December, mean swimming speeds decreased gradually from 38.3 to 31.2 cm/s (Fig. 2, Table 2). Mean speeds were irregular in winter, and at a minimum in early March (Fig. 2). Speeds increased

Table 2

Light, temperature, and biological measurements of bluefish (*Pomatomus saltatrix*), 1995–96. Seventeen weeks are presented in which observations of swimming were made at each hour of the day and averaged for the week. Total lengths and weights were calculated from subsamples measured on the dates in Table 1. All other quantities, hours of light per day, water temperature (°C), food consumption in percent body weight per day (% BW/d), and swimming speeds in cm/s and body lengths per second (BL/s), were averaged for the week.

Week	First day of week	Number of fish	Light (hr/d)	Mean temperature (°C)	Bluefish total length (mm)	Bluefish weight (g)	Food consumption (% BW/d)	Swimming speed (cm/s)	Swimming speed (BL/s)
7	10 Sep	89	12.6	20.7	198.3	78.8	13.0	35.8	1.81
11	8 Oct	72	11.4	19.2	228.2	137.3	8.8	38.3	1.68
14	29 Oct	72	10.5	17.9	242.0	170.0	9.3	40.0	1.65
18	26 Nov	71	9.6	15.3	254.7	201.3	4.1	33.6	1.32
20	10 Dec	71	9.4	15.1	257.7	206.3	3.8	31.2	1.21
23	31 Dec	71	9.4	15.0	262.3	214.1	2.5	35.0	1.33
27	28 Jan	71	10.1	15.0	269.3	225.9	3.1	38.5	1.43
31	25 Feb	71	11.2	15.0	277.2	239.3	3.1	34.8	1.25
32	3 Mar	71	11.6	15.0	279.2	242.8	2.0	34.3	1.23
33	10 Mar	71	11.9	15.0	281.2	246.3	2.2	31.1	1.11
34	17 Mar	71	12.2	15.0	283.3	249.9	3.6	37.0	1.31
35	24 Mar	70	12.5	15.0	285.3	253.6	2.1	46.0	1.61
36	31 Mar	69	12.8	15.0	287.4	257.2	3.2	45.0	1.56
40	28 Apr	67	13.9	15.5	295.8	272.5	0.9	38.2	1.29
44	26 May	67	14.8	17.2	306.3	298.1	4.7	44.2	1.44
46	9 Jun	67	15.0	19.2	315.3	330.4	4.5	51.2	1.62
47	16 Jun	67	15.0	20.4	319.9	347.9	5.9	53.3	1.67

in late March with increase in day length, although temperature was unchanged. When bluefish measured about 285 mm in late March, their mean speeds rose above 40 cm/s and they became capable of much higher maximum speeds. In June 1996, swimming speeds in cm/s were significantly greater than those in September 1995 (t-test, $P<0.01$, both at 20°C). Speeds in body lengths/s, however, showed no trend during the experiment (Table 2), because larger fish can swim faster.

When twilight speeds were removed from the dataset, there was no overlap in day and night speeds (cm/s) or their standard deviations (Fig. 3). In fall, the mean speed during daylight was >52 cm/s, and the mean night speed was between 28 and 38 cm/s. The decrease in mean speed in winter (Fig. 2), particularly in January, was due only to decreased day speed and briefer periods of peak activity (Fig. 1B). Night speeds were similar all year, except for certain periods of extremely slow swimming in spring, as described below. By mid-June, at the end of the study, the difference between day and night activity was greater because the mean daylight speed increased to 68.6 cm/s.

Modes of swimming

Bluefish used various modes of swimming in the research aquarium (Table 3). The most prevalent mode was powered swimming, which they performed by propelling themselves by beats or contractions of the muscles of the rear of the body and caudal peduncle. During powered swimming, the body orientation was vertical, while the pectoral and pelvic fins were folded except to make adjustments in direction. Fish in the aquarium used this mode primarily while circling in a level horizontal ring. At other times, powered swimming in a vertically undulating or sine-wave-like pattern was observed at all depths of the aquarium. The entire school participated in this behavior, often for hours.

During periods of undulatory swimming, some fish glided on their sides. To glide, a bluefish rolled onto its side, ceased body and tail movement, and its momentum carried it gradually downward (Figs. 4 and 5). The body was held flat or in a slightly convex shape. The dorsal, anal, and pelvic fins were stretched out and curved up or down slightly in response to water flow or for changing direction. The pectoral fins were pointed outward and sometimes sculled or steered, the tail was still, and the tail fin lobes were curved up or down slightly. The body rolled by less than 90° (i.e., not parallel to the bottom). Either side might be oriented downward and a fish sometimes switched sides in mid-glide. A fish encountering a side of the aquarium sometimes turned and continued to glide downward. Only a few members of the school glided at one time, and they accompanied

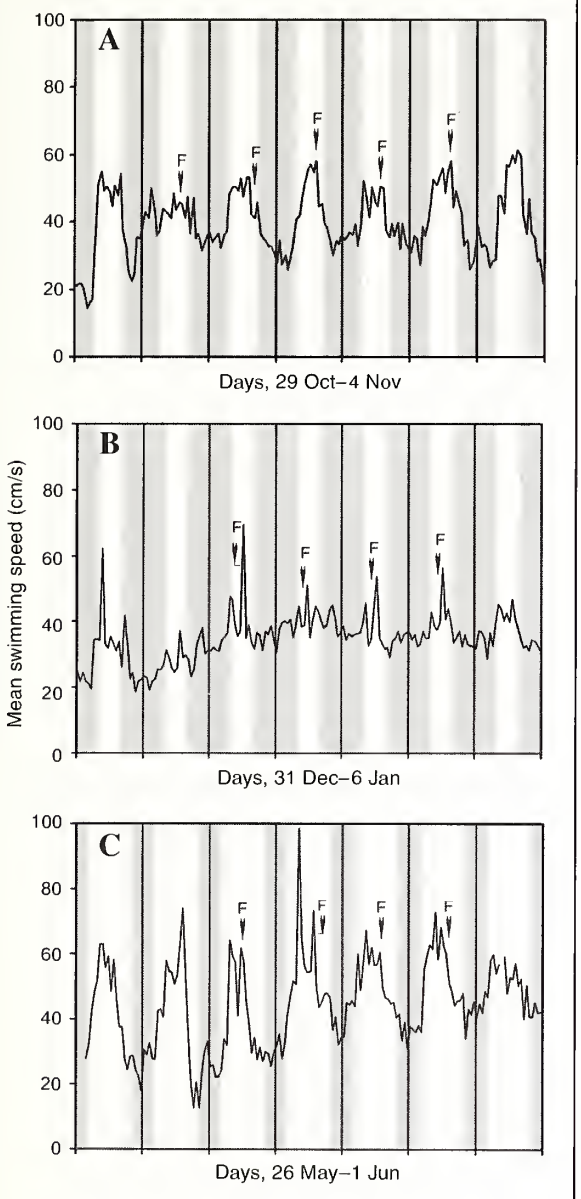

Figure 1

Diel patterns of swimming speed (cm/s) of bluefish (*Pomatomus saltatrix*) during representative weeks of fall (**A**), winter (**B**), and summer (**C**). Vertical gridlines mark midnight of each day, gray areas represent hours of darkness, and arrows with the letter "F" mark feeding times.

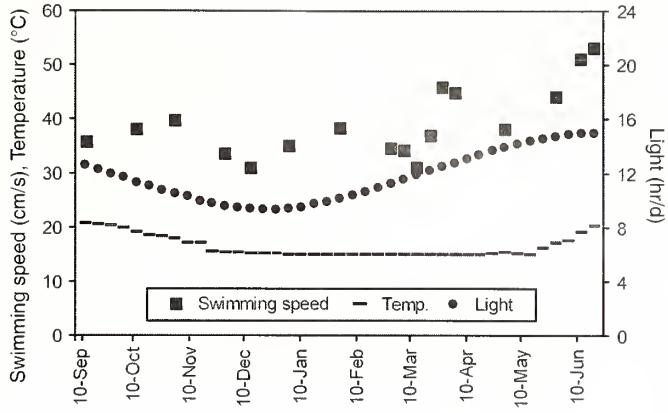

Figure 2

Mean swimming speeds (cm/s), water temperature (°C), and hours of light (hr/d) for bluefish (*Pomatomus saltatrix*), 10 Sept 1995–28 June 1996.

Table 3

Modes of swimming behavior seen in bluefish (*Pomatomus saltatrix*) in a laboratory aquarium over an annual cycle.

Mode of swimming	Description
Powered	Horizontal swimming in upright orientation, propelled by body and tail
Undulating	Powered swimming while fish continually changed depth
Burst	Brief, high-speed swimming
Gliding	No propulsion, oriented on side, descending or sinking diagonally
Upswimming	Powered swimming to ascend from a glide to the initial level
Milling	Upright orientation, swimming very slowly or almost motionless
Side-swimming	Powered swimming, oriented on side

nongliding fish at approximately the same speed and along the same path. A fish righted itself by rolling smoothly or by flexing the body and turning abruptly. After righting itself, a fish returned to its initial level or briefly swam horizontally. Gliding occurred only when the school was swimming briskly and in an undulating path. Gliding nearly always occurred at night in this study. In the dark, fish gliding with their bellies facing the camera could be seen by the reflection of light off their sides, but fish with their backs to the camera were difficult to detect.

Gliding was sometimes part of a sequence of side-oriented swimming behaviors. Side-swimming (Table 3) occurred during undulatory swimming, while a fish was descending, ascending, or moving horizontally, and often before or after a glide. Fish ascending from a glide sometimes side-swam up all or part of the distance. They usually returned smoothly along the undulating path of the rest of the school, but at times they ascended very steeply and swam against the direction of the school.

Gliding was prevalent throughout the study and occurred most frequently in fall and winter (Fig. 6). In

Table 4

Angles of gliding and upswimming, distances (cm), and horizontal speeds over ground (cm/s) of individual bluefish (*Pomatomus saltatrix*), January 1996, during the activity study. Angles of glides are in degrees below horizontal; angles of upswimming are in degrees above horizontal. Dashes indicate that no observations were available.

Angle of glide	Distance of glide (cm)	Horizontal speed (cm/s)	Angle of upswimming	Distance of upswimming (cm)	Horizontal speed (cm/s)
6.3	45	22.1	12.4	125	30.5
7.1	94	32.2	2.2	93	31.8
10.7	228	20.6	7.9	44	18.0
11.5	43	21.8	7.3	60	20.3
13.2	103	34.7	6.3	103	25.7
15.3	50	24.6	29.4	172	28.7
15.3	25	26.0	22.6	94	27.9
17.5	126	19.7	6.8	58	21.0
18.2	78	25.3	26.7	194	23.8
18.2	—	—	5.5	125	20.5
18.3	91	22.8	18.6	89	20.6
18.5	141	27.2	7.5	50	24.6
18.9	87	29.0	13.0	66	20.0
19.5	93	30.4	15.3	85	39.3
19.8	131	21.1	10.5	119	28.4
19.9	80	—	3.7	162	—
20.0	64	20.7	2.8	97	31.7
20.4	94	—	1.6	210	—
20.8	155	21.7	13.9	43	21.8
21.3	172	23.7	10.8	90	17.0
21.9	82	19.9	24.4	107	47.3
23.6	130	24.9	4.4	98	24.1

December and January, glides occurred during as many as 14 hr/d, even during daylight. During the greatest frequency of occurrence of the behavior in January, the proportion of fish gliding was also greatest, up to 14%.

Angles of descent during gliding ranged from 13–26° from the horizontal, and angles of ascent ranged from 2–29° (Table 4). The average angle of descent for all fish was 17.9° and for ascent by those that followed the undulating path of the school was 12.2°. The average speed of descent was 24.9 cm/s and of ascent was 26.3 cm/s. Using the gliding model of Weihs (1973), we diagrammed the path of a bluefish selected from Table 4. It glided at angle $\acute{\alpha}$=19.8° for a distance a_1=131 cm and ascended at angle β=10.5° for a distance a_2=119 cm, a total distance of 250 cm. If it had actively swum, the horizontal distance would have been 240 cm.

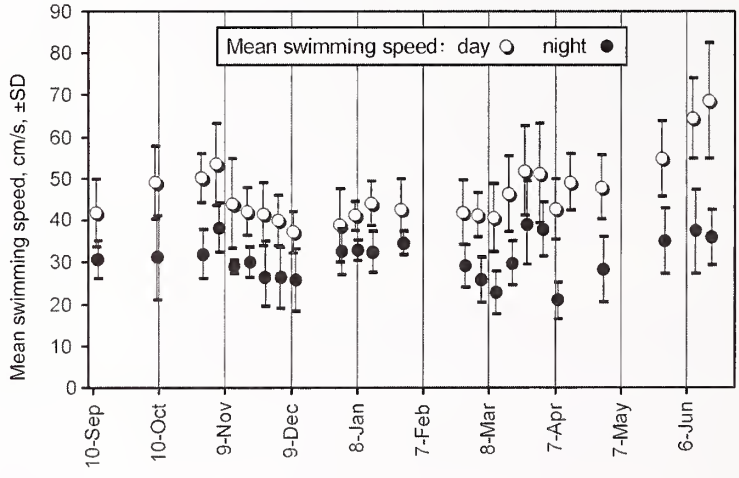

Figure 3

Swimming speeds (cm/s), with standard deviations (SD), from the 7 hours before and after midday and 7 hr before and after midnight for bluefish (*Pomatomus saltatrix*), 10 Sept. 1995–28 June 1996 (n=25 weeks).

Body roll angles were not measured in 1995–96, but in 2007 bluefish averaged 47° from vertical while gliding (n=33, maximum 65°). The glide angle $\acute{\alpha}$ averaged 19.7° (n=23) in 2007.

During periods when gliding was rare, bluefish sometimes moved very slowly at night in a swimming mode that can be called "milling." The orderly spac-

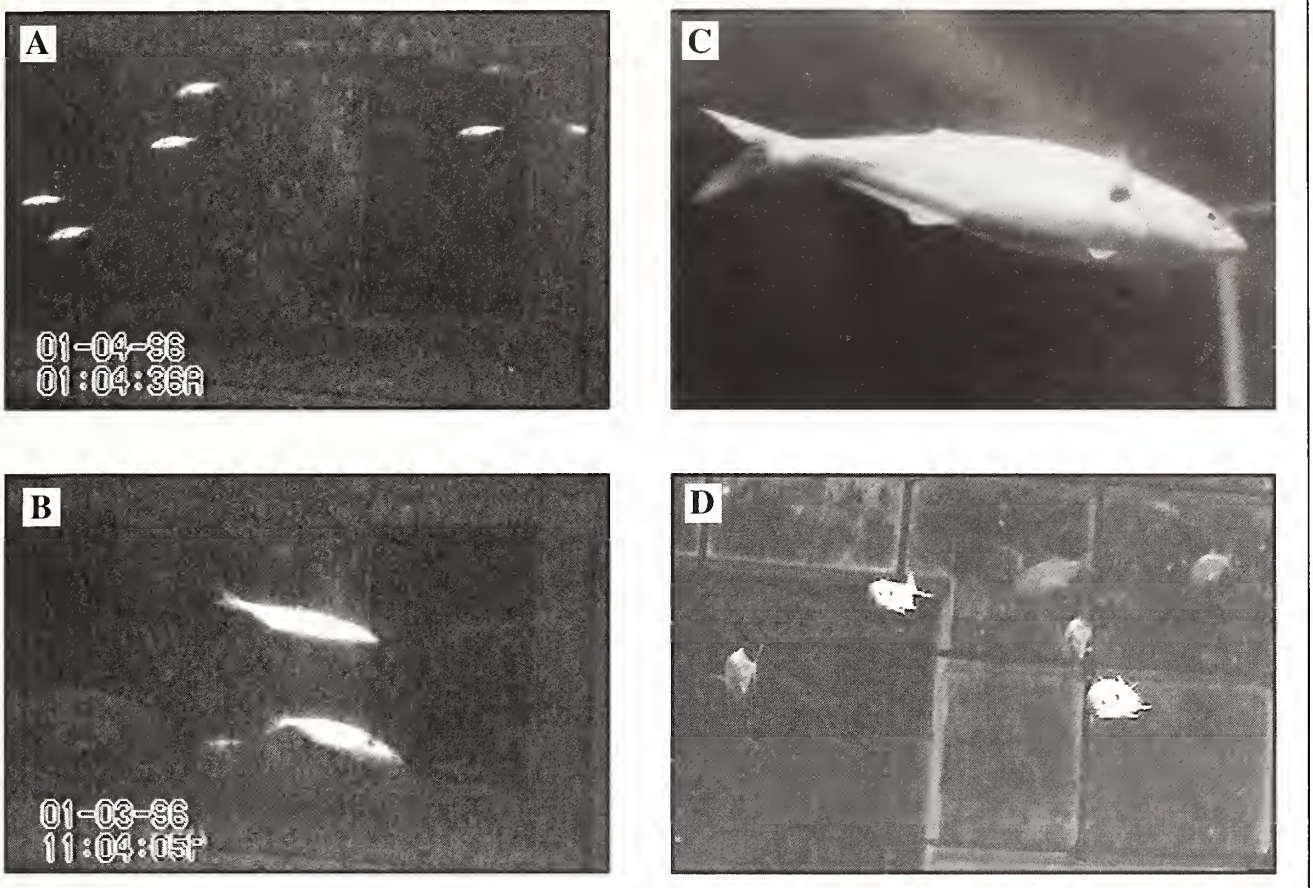

Figure 4

Still images of gliding bluefish (*Pomatomus saltatrix*) during the activity study. (**A**) Numerous gliding fish near the far side of the aquarium at night, recorded with a video camera, winter 1996, (**B**) one gliding (top fish) and one side-swimming fish (lower fish) close to the window near the video camera, winter 1996, (**C**) photograph from below a gliding fish, spring 1995, (**D**) gliding fish (lighter fish) are keeping pace with vertically oriented fish (gray-toned individuals) in the school, recorded with a video camera, spring 2007.

ing of the school was disrupted and fish dispersed with no common direction. Milling fish stayed near the water surface, apparently neutrally buoyant, and moved extremely slowly, propelled by occasional gentle flexes of the pectoral fins and tail. Milling was noticed beginning 6 February and was common through mid-March. Another period of milling occurred in the last week of April and the beginning of May during the parasite infestation.

Discussion

Feeding and growth

The period of extremely high food consumption and growth per body weight does not last very long in young bluefish. In this experiment, food consumption was greatest when the fish were smallest, as was anticipated from the literature. From 16% body weight per day (BW/d) in 35-g fish, food consumption rate decreased to 1–5% BW/d in 369-g fish the following spring. Similarly, in laboratory mesocosms at 21°C, growth rates of the smallest, (mean 2.6 g), age-0 fish were as high as 9.2% BW/d, but those of larger (mean 10.2-g) fish were 2.7% BW/d (Buckel et al., 1995). In small age-0 field-caught bluefish, food consumption rates were >30% BW/d (Juanes and Conover, 1994; Buckel et al., 1995). Rapid food intake permits rapid growth to a size where fish are less vulnerable to predators.

Growth in the research aquarium was continuous, and the increase in length was comparable to that of wild bluefish in the middle-Atlantic states. The fish in the aquarium grew to a mean total length of 300 mm (265 mm FL) by 22 May, whereas wild age-1 fish originating from a spring-spawned cohort are about 250 mm FL when they are caught in spring (Shepherd and Packer, 2006).

Daily and seasonal rhythms

In this and earlier studies (Olla and Studholme, 1972), bluefish in the laboratory were active during the day and schooled more cohesively during day than at night. Gliding and milling occurred at night. This timing of passive behaviors may alternate with active behaviors such as feeding during the day. Field studies corroborate these laboratory-observed rhythms. Stomach fullness in bluefish was greatest in the afternoon (Marks and Conover, 1993; Juanes and Conover, 1994). Bluefish were more vulnerable to otter trawls during daylight hours than at night (Munch, 1977; Wiedenmann and Essington, 2006). The latter authors hypothesized that bluefish descend to near-bottom during the day to feed upon schools of anchovies, *Anchoa* spp., and then ascend at night to where they are less accessible to otter trawls.

The present study is the first ever published on the behavior of bluefish over a yearly cycle in real time in a research aquarium. Bluefish changed activity patterns by season, as exemplified in the fall, when their swimming speeds and the day-night differences in speeds gradually decreased as temperature decreased. No period of restlessness or accelerated swimming was seen during the fall, as had been seen in an earlier study (Olla and Studholme, 1971). In that study, a school of adult bluefish was acclimated to 19.5°C, under a winter photoperiod, and were swimming at a mean speed of 20–30 cm/s. When the water was chilled to 11.5°C over 29 days (0.25°C/d), the fish, instead of swimming more slowly as predicted by the bioenergetic response, swam dramatically faster at 60–100 cm/s. Increased activity in reaction to chilling was also seen in tautog (*Tautoga onitis*) and sablefish (*Anoplopoma fimbria*) (Olla et al., 1980; Sogard and Olla, 1998). The fish in these latter studies may have been undergoing short-term stress responses associated with the urge to migrate or escape. In the present study, temperature was lowered half as fast (0.105°C/d in 57 days) as in the earlier study (Olla and Studholme, 1971), and the fish could adjust to the temperature change without a stress response.

In spring, the bluefish in the present study accelerated their swimming speed in response to the cue of increased daylength, without any cue of increased temperature. Similarly, bluefish on their wintering grounds respond to changes in day length and begin migration in time to arrive at their summer grounds when tolerable temperatures are available.

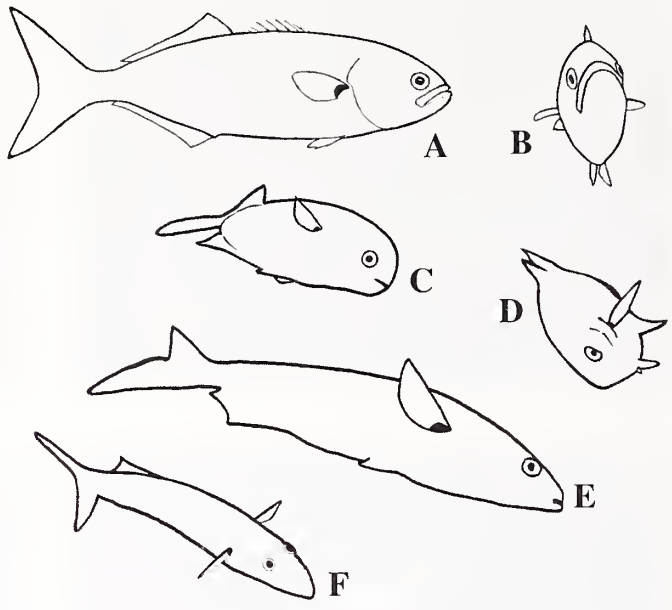

Figure 5

Line drawings from video images of bluefish (*Pomatomus saltatrix*). (**A**) Vertically-oriented 250-mm bluefish, all fins extended, (**B**) vertically oriented fish swimming toward the observer, pectoral and pelvic fins extended, (**C**) fish gliding toward the observer, rolled onto its left side, body curved downward and tail fin lobes curved up, (**D**) fish gliding toward the observer on its right side, dorsal, anal, and pelvic fins curved up, (**E**) side view of fish gliding with belly toward the observer, sculling with pectorals, tail fin lobes curved up, and (**F**) fish gliding with back toward the observer.

Modes of swimming

Bluefish exhibit speed and swimming endurance although they do not have the body and caudal-fin shapes optimally adapted for sustained swimming performance, as are found in pelagic taxa such as scombrids (Webb, 1978). The bodies of scombrids are cylindrical, elliptical in cross-section, and highly streamlined to minimize frictional drag. The optimal caudal fin for sustained swimming is stiff, has a high aspect ratio, and a lunate shape that reduces drag produced by the wake of the fish (Nursall, 1958; Webb, 1978). In the scombriform mode of propulsion, thrust is generated by the caudal peduncle and tail only (Blake, 2002). In contrast, bluefish use the anguilliform swimming mode, in which thrust is generated by muscular contractions along the body and tail (Webb, 1978). The tail of a bluefish produces 65% of the total thrust (Ogilvy and DuBois, 1982). Like scombrids, bluefish are streamlined and have elliptical body cross sections, but their tails are flexible and semilunate, suited for burst swimming as well.

To glide, an aquatic animal must be negatively buoyant, have sufficient forward momentum, and possess a foil shape that produces lift to counteract sinking. A foil has a downward-facing arch and an asymmetrical camber ratio that produces less pressure below it than above it. At sufficient speed, the horizontal body plan

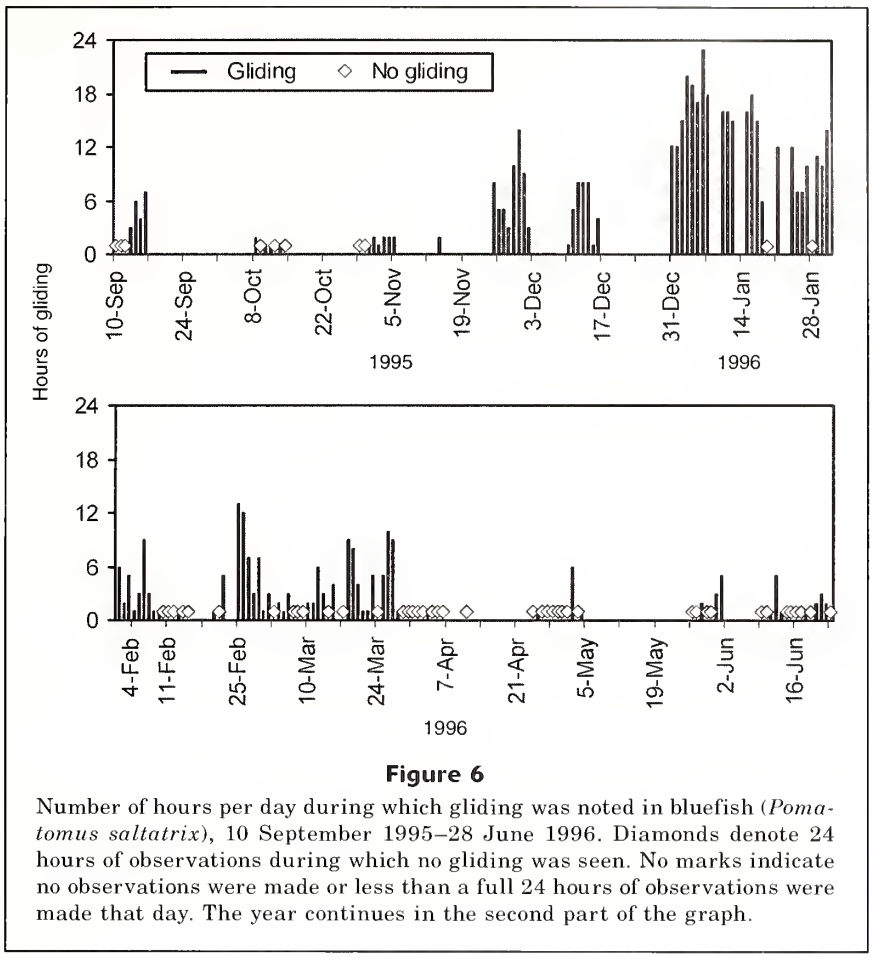

Figure 6

Number of hours per day during which gliding was noted in bluefish (*Pomatomus saltatrix*), 10 September 1995–28 June 1996. Diamonds denote 24 hours of observations during which no gliding was seen. No marks indicate no observations were made or less than a full 24 hours of observations were made that day. The year continues in the second part of the graph.

of flatfishes and the large area of the pectoral fins of certain sharks generate enough lift to permit gliding without stalling (Weihs, 1973). Sharks and flatfishes, which have no swim bladders, are always negatively buoyant. The shortfin mako (*Isurus oxyrinchus*), great white shark (*Carcharodon carcharias*), and blue shark (*Prionace glauca*) use bouts of gliding and upswimming in undulatory patterns over tens of meters (Klimley et al., 2002). Tuna (*Thunnus* spp.), billfish (Istiophoridae), and marine mammals glide while performing diving oscillations (Weihs, 1973; Klimley et al., 2002).

Reports of gliding in teleosts are scarce, and such reports have mostly been based on observations of flatfishes. American plaice (*Hippoglossoides platessoides*) used a glide-and-settle mode of swimming, gliding over 50 m while avoiding simulated trawl gear (Winger et al., 2004). Japanese flounder (*Paralichthys olivaceus*) used bouts of gliding and powered ascent in the field and in the laboratory (Kawabe et al., 2003, 2004). Ogilvy and DuBois (1982) stated that bluefish cannot glide, because the surface area of their pectoral fins is not enough to produce much lift, and if they stopped propelling themselves, they would stall. However, bluefish do not stall because they turn onto their sides and increase their horizontal surface area.

Energetics

Force required by a fish to swim forward must overcome pressure drag in front of the fish, frictional drag from distortion of water flow over the body, and turbulence from the swimming movements themselves. The drag in powered swimming is related to the drag created by gliding by a ratio, k: (Weihs, 1973; Magnuson, 1978),

$$k = Fs/Fg,$$

where Fs = the drag force of swimming; and
Fg = the drag force of gliding.

The ratio, k, varies between 1 and 4 (Weihs, 1973). In a scombriform lunate-tailed tuna, the kawakawa (*Euthynnus affinis*), k has been estimated at 1.2 (Magnuson, 1978). The streamlined body of the kawakawa generates relatively little drag during swimming; therefore gliding does not save it much energy. In contrast, a fish that uses anguilliform propulsion, such as a trout, dace, flatfish, or bluefish, may have a k of 3 to 4 (Weihs, 1973). A fish uses less energy or thrust during a cycle of gliding and upswimming than during horizontal powered swim-

ming over the same distance (Weihs, 1973; Webb, 1978). The smallest possible glide angle produces the greatest energy benefits. A fish having k=3, that achieves a glide angle $\acute{\alpha}$ of 11°, and uses the most advantageous upswim angle β of 37° saves 49% of the energy needed for a straight swim over the same distance, although it covers the distance in 12% more time (Weihs, 1973).

If k=3 for a bluefish and the glide and ascent angles are those measured in this study, namely, $\acute{\alpha}$ = 18° and β = 12°, a bluefish would save 20% of the energy it would use to actively swim the same horizontal distance. In January 1996, 14% of the bluefish in the aquarium were gliding at once, and if one multiplies by two to include the ascending fish that were unseen, more than one-quarter of the school was using this energy-saving mode at one time.

The function of gliding in migration has been studied outside the phylum of fishes. Some birds, particularly raptors, minimize the use of powered flight in migration by soaring upward on a rising heated air current and then gliding as far as possible to the next thermal current (Kerlinger, 1989). While soaring, birds flatten and extend their wings to increase their surface area. While gliding, they partially fold their wings to adjust their wing area and foil shape, to control the angle and speed of descent. Energy used in the soar and glide mode of flight for a hypothetical raptor, depending on its weight and wing area, is 10–40% of the energy used in powered flight. A broad-winged hawk (*Buteo platypterus*) in migration, given atmospheric conditions that produce consistent thermal currents, can fly 8 hr/d and travel 320 km/d with only occasional wing flapping (Kerlinger, 1989).

If a bluefish is turned onto its side, its tail shape is similar to that of the most energy-efficient tail shape of birds that glide. The most efficient lift-to-drag ratio is produced with a forked tail, the outermost feathers of which are twice the length of the innermost, and by a 120° angle when the tail is spread (Thomas, 1997). In juvenile bluefish, the ratio of the lengths of the outer to inner caudal fin rays (measured from a straight line across the narrowest part of the caudal peduncle) is about 2:1. The angle of the fork, however, is 65–80°.

Migration capability and swimming speed

When one compares information from bluefish tagging data with information on swimming capability ascertained in the laboratory, one concludes that migration is not a continuous activity. Recently, bluefish migration data from years of tagging studies along the U.S. eastern coast were summarized, and recoveries were grouped by season and distance (Shepherd et al., 2006). Among the southward-traveling bluefish, one group had a relatively short migratory path (about 600 km), having been tagged in the middle-Atlantic region and recaptured off North Carolina. Longer movements (up to 2000 km) were made by another group of fish tagged in the northern region (New England through New York Bight) and recaptured from the Carolinas south to Florida. The speeds calculated from the tag recoveries from fish at large for 2–3 mo, averaged 5.9 km/d (Shepherd et al., 2006), which are much less than speeds observed in laboratory studies. In the research aquarium, spring-spawned age-0 fish, in the late fall, including all hours of day and night and periods of gliding, averaged 33.6 cm/s (29 km/d). They would be able to travel the 600 km from the New York Bight to just south of Cape Hatteras, where age-0 fish overwinter, in 22 d. Older fish (500–550 mm) swim at sustained speeds up to 60 cm/s (52 km/d) (Olla et al., 1970) and could travel 2000 km in a minimum of 31 days. Age-2+ bluefish are the only fish captured regularly on Georges Bank and northward, and therefore would travel the farthest (Shepherd and Packer, 2006). Although a few tagged bluefish have attained speeds >20 km/d and one has attained >48 km/d (Shepherd et al., 2006), they are in the minority. Bluefish may not migrate directly, but intermittently. Their paths include detours, feeding stops, and searches for tolerable water conditions.

Little has been published on northward migration routes of bluefish. The timing of these migrations can be inferred from ichthyoplankton collections. From these, it is known that bluefish spawn in southeast U.S. continental shelf waters from March through May and continue to spawn in northeast U.S. continental shelf waters through August (Hare and Cowen, 1996; Berrien and Sibunka, 1999). Eggs from the spring spawning are entrained in currents off the southeast U.S. outer continental shelf waters and in the Gulf Stream (Kendall and Walford, 1979; Hare and Cowen, 1996). These currents travel northward at 50–100 cm/s (Hare and Cowen, 1996; Hare et al., 2002), and perhaps the bluefish themselves use them to migrate. Energy-conserving behavior would be extremely valuable to bluefish when they must migrate and produce eggs and sperm at the same time.

Overwintering

Bluefish are intolerant of cold, as is evident from their distribution range and from laboratory studies. A bluefish transferred from water 19.5°C to 10°C loses equilibrium and motor control, sinks, and soon dies (Olla et al., 1985). Gradual acclimation however allows them to endure longer. In North Carolina, age-0 bluefish survived for weeks in outdoor enclosures as temperatures declined gradually to 10°C, but a rapid temperature decline to 6°C killed many (Slater et al., 2007). The majority of bluefish, from age-0 spring-spawned to adults <45 cm, winter from south of Cape Hatteras, NC, to Florida (Shepherd et al., 2006; Morley et al., 2007), where surface waters do not decline below 15°C. Large adults, particularly >45 cm, also winter on the outer continental shelf and slope off Virginia and North Carolina (Shepherd et al., 2006). On the shelf-slope edge in that area, winter bottom temperatures vary among years from 10°C to >12°C (Bigelow, 1933). Age-0 bluefish can

endure more cold than adults and may not winter as far south as other age classes (Slater et al., 2007).

When fish cannot escape unfavorable temperatures, they resort to behavioral thermoregulation (Olla et al., 1985; Sogard and Olla, 1998). Starved walleye pollock (*Theragra chalcogramma*) reduce swimming speed and spend most of their time in colder waters below a thermocline, thus decreasing their metabolic cost (Sogard and Olla, 1996). Summer-spawned age-0 bluefish may use the same strategy to suppress metabolic rates by wintering in colder waters off North Carolina just south of Cape Hatteras instead of farther south (Morley et al., 2007; Slater et al., 2007). Milling is certainly another way in which bluefish reduce their activity in winter.

The 121-kL research aquarium is a large experimental space, but confinement may potentially alter fish behavior. Despite qualifications, the author believes gliding behavior in bluefish is authentic natural behavior. This behavior began in the first few weeks of captivity and persisted throughout the experiment. The researchers who initiated this line of investigation observed gliding in the aforementioned unpublished experiment in 1984–85, and the author witnessed it in a seven-month experiment in 2006–07. The behavior each time was composed of similar elements of body curvature, fin extension, glide distance, and glide angle. It is unknown, however, how far bluefish would glide given unlimited space.

Bluefish may be unique among laterally compressed teleosts in gliding on their sides, thus radically changing their hydrodynamic profiles. Although gliding has been witnessed in more than one group of age-0 bluefish in the laboratory, it has not been studied in very small age-0 fish or older age classes. Energy benefits may be different according to the age of a fish, because the bodies of adult bluefish are relatively more cylindrical and less flexible than age-0 fish, and perhaps cannot attain as efficient a foil shape.

Much remains to be discovered about daily behavior routines, migration routes, and overwintering in various cohorts and age classes of bluefish. Considerably less energy is spent during the glide and upswim mode, possibly comparable to energy savings by migrating raptors, and should be quantified or modeled. Internal archival tags that record depth would be valuable for field studies of gliding, in places where recovery is possible, such as a migration corridor. Bluefish with acoustic tags could be detected at strings of fixed or roving receivers at ocean observatories. Information from such tags may locate concentrations of milling bluefish in areas offshore that would be accessible to fishing. Daily vertical migrations of bluefish on the continental shelf should be investigated to determine their relation to feeding and long-distance travel. It was surprising that bluefish in the laboratory continued to glide briskly during midwinter when they would have reached wintering grounds in the wild. Perhaps the modes of swimming, speeds, and routes during migration and wintering in bluefish are more variable than we suspect.

Acknowledgments

This article is dedicated to A. Studholme and A. Bejda, who designed this experiment and ran a preliminary version of it in 1984. I acknowledge B. Olla, who established protocols and methods for studying behavior in fishes at the James J. Howard Marine Sciences Laboratory. D. Roe calculated energy savings for gliding bluefish. I acknowledge J. Buckel, B. Phelan, J. Rosendale, F. Scharf, and reviewers and editors for assistance.

Literature cited

Able, K. W., P. Rowe, M. Burlas, and D. Byrne.
2003. Use of ocean and estuarine habitats by young-of-year bluefish (*Pomatomus saltatrix*) in the New York Bight. Fish. Bull. 101:201–214.

Beamish, F. W. H.
1978. Swimming capacity. *In* Fish physiology, vol. 7 (W. S. Hoar, and D. J. Randall, eds.), p. 101–187. Academic Press, New York, NY.

Berrien, P., and J. Sibunka.
1999. Distribution patterns of fish eggs in the United States northeast continental shelf ecosystem, 1977–1987. NOAA Tech. Rep. NMFS 145, 301 p.

Bigelow, H. B.
1933. Studies of waters on the continental shelf, Cape Cod to Chesapeake Bay. I. The cycle of temperature. Papers Phys. Oceanogr. Meteorol. 2:1–135.

Blake, R. W.
2002. Fish functional design and swimming performance. J. Fish Biol. 65:1193–1222.

Brown, J. H., J. F. Gillooly, A. P. Allen, V. M. Savage, and G. B. West.
2004. Toward a metabolic theory of ecology. Ecology 85:1771–1785.

Buckel, J. A., N. D. Steinberg, and D. O. Conover.
1995. Effects of temperature, salinity, and fish size on growth and consumption of juvenile bluefish. J. Fish Biol. 47:696–706.

Fry, F. E. J.
1971. The effect of environmental factors on the physiology of fish. *In* Fish physiology, vol. 6 (W. S. Hoar, and D. J. Randall, eds.), p. 1–98. Academic Press, New York, NY.

Hare, J. A., and R. K. Cowen.
1996. Transport mechanisms of larval and pelagic juvenile bluefish (*Pomatomus saltatrix*) from South Atlantic Bight spawning grounds to Middle Atlantic Bight nursery habitats. Limnol. Oceanogr. 41:1264–1280.

Hare, J. A., J. H. Churchill, R. K. Cowen, T. J. Berger, P. C. Cornillon, P. Dragos, S. M. Glenn, J. J. Govoni, and T. N. Lee.
2002. Routes and rates of larval fish transport from the southeast to the northeast United States continental shelf. Limnol. Oceanogr. 47:1774–1789.

Hartman, K. J., and S. B. Brandt.
1995. Comparative energetics and the development of bioenergetics models for sympatric estuarine piscivores. Can. J. Fish. Aquat. Sci. 52:1647–1666.

Juanes, F., and D. O. Conover.
1994. Rapid growth, high feeding rates, and early piscivory in young-of-the-year bluefish (*Pomatomus saltatrix*). Can. J. Fish. Aquat. Sci. 51:1752–1761.

Kawabe, R., Y. Naito, K. Sato, K. Miyashita, and H. Yamashita.
2004. Direct measurement of the swimming speed, tail-beat, and body angle of Japanese flounder (*Paralichthys olivaceus*). ICES J. Mar. Sci. 61:1080–1087.

Kawabe, R., K. Nashimoto, T. Hiraishi, Y. Naito, and K. Sato.
2003. A new device for monitoring the activity of freely swimming flatfish, Japanese flounder (*Paralichthys olivaceus*). Fish. Sci. 69:3–10.

Kendall, A. W., Jr., and L. A. Walford.
1979. Sources and distribution of bluefish, *Pomatomus saltatrix*, larvae and juveniles off the east coast of the United States. Fish. Bull. 77:213–227.

Kerlinger, P.
1989. Flight strategies of migrating hawks, 375 p. Univ. Chicago Press, Chicago, IL.

Klimley, A. P., S. C. Beavers, T. H. Curtis, and S. J. Jorgensen.
2002. Movements and swimming behavior of three species of sharks in La Jolla Canyon, California. Environ. Biol. Fishes 63:117–135.

Magnuson, J. J.
1978. Locomotion by scombrid fishes: hydromechanics, morphology, and behavior. *In* Fish physiology, vol. 7 (W. S. Hoar, and D. J. Randall, eds.) p. 239–313. Academic Press, New York, NY.

Marks, R. E., and D. O. Conover.
1993. Ontogenetic shift in the diet of young-of-year bluefish *Pomatomus saltatrix* during the oceanic phase of the early life history. Fish. Bull. 91:97–106.

Morley, J. W., J. A. Buckel, and T. E. Langford.
2007. Winter energy dynamics and cohort structure of young-of-the-year bluefish (*Pomatomus saltatrix*) off North Carolina. Mar. Ecol. Prog. Ser. 334:273–286.

Munch, S. B.
1997. Recruitment dynamics of bluefish, *Pomatomus saltatrix*, from Cape Fear to Cape Cod, 1973–1995. M.S. thesis, 127 p. State Univ. New York, Stony Brook, NY.

Nursall, J. R.
1958. The caudal fin as a hydrofoil. Evolution 12:116–120.

Nyman, R. N., and D. O. Conover.
1988. The relation between spawning season and the recruitment of young-of-the-year bluefish, *Pomatomus saltatrix*, to New York. Fish. Bull. 86:237–250.

Ogilvy, C. S., and A. B. DuBois.
1982. Tail thrust of bluefish *Pomatomus saltatrix* at different buoyancies, speeds, and swimming angles. J. Exp. Biol. 98:105–117.

Olla, B. L., H. M. Katz, and A. L. Studholme.
1970. Prey capture and feeding motivation in the bluefish *Pomatomus saltatrix*. Copeia 1970:360–362.

Olla, B. L., W. W. Marchioni, and H. M. Katz.
1967. A large experimental aquarium system for marine pelagic fishes. Trans. Am. Fish. Soc. 96:143–150.

Olla, B. L., and A. L. Studholme.
1971. The effect of temperature on the activity of bluefish, *Pomatomus saltatrix* L. Biol. Bull. 141:337–349.
1972. Daily and seasonal rhythms of activity in the bluefish (*Pomatomus saltatrix*). *In* Behavior of marine animals, vol. 2: Vertebrates (H. E. Winn, and B. L. Olla, eds.), p. 303–326. Plenum Press, New York, NY.

Olla, B. L., A. L. Studholme, and A. J. Bejda.
1985. Behavior of juvenile bluefish *Pomatomus saltatrix* in vertical thermal gradients: influence of season, temperature acclimation and food. Mar. Ecol. Prog. Ser. 23:165–177.

Olla, B. L., A. L. Studholme, A. J. Bejda, and C. Samet.
1980. Role of temperature in triggering migratory behavior of the adult tautog *Tautoga onitis* under laboratory conditions. Mar. Biol. 59:23–30.

Scharf, F. S., J. P. Manderson, M. C. Fabrizio, J. P. Pessutti, J. E. Rosendale, R. J. Chant, and A. J. Bejda.
2004. Seasonal and interannual patterns of distribution and diet of bluefish within a middle Atlantic Bight estuary in relation to biotic and abiotic factors. Estuaries 27:426–436.

Shepherd, G. R., J. Moser, D. Deuel, and P. Carlsen.
2006. The migration patterns of bluefish (*Pomatomus saltatrix*) along the Atlantic coast determined from tag recoveries. Fish. Bull. 104:559–570.

Shepherd, G. R., and D. B. Packer.
2006. Essential fish habitat source document: Bluefish, *Pomatomus saltatrix*, life history and habitat characteristics. NOAA Tech. Memo. NMFS-NE-198, 89 p.

Slater, J. J., T. E. Lankford Jr., and J. A. Buckel.
2007. Overwintering ability of young-of-the-year bluefish *(Pomatomus saltatrix)*: effects of ration and cohort of origin on survival. Mar. Ecol. Prog. Ser. 339:259–269.

Sogard, S. M., and B. L. Olla.
1996. Food deprivation affects vertical distribution and activity on a marine fish in a thermal gradient: potential energy-conserving mechanisms. Mar. Ecol. Prog. Ser. 133:43–55.
1998. Contrasting behavioral responses to cold temperatures by two marine fish species during their pelagic juvenile interval. Environ. Biol. Fishes 53:405–412.

Thomas, A. L. R.
1997. On the tails of birds. BioScience 47:215–225.

Webb, P. W.
1978. Hydrodynamics: nonscombroid fish. *In* Fish physiology, vol. 7 (W. S. Hoar, and D. J. Randall, eds.), p. 189–237. Academic Press, New York, NY.

Weihs, D.
1973. Mechanically efficient swimming techniques for fish with negative buoyancy. J. Mar. Res. 31:194–209.

Wiedenmann, J., and T. E. Essington.
2006. Density-dependent overwinter survival in young-of-year bluefish (*Pomatomus saltatrix*)? A new approach for assessing stage-structured survival. Can. J. Fish. Aquat. Sci. 63:1934–1943.

Winger, P. D., S. J. Walsh, P. He, and J. A. Brown.
2004. Simulating trawl herding in flatfish: the role of fish length in behaviour and swimming characteristics. ICES J. Mar. Sci. 61:1179–1185.

Evolutionary associations between sand seatrout (*Cynoscion arenarius*) and silver seatrout (*C. nothus*) inferred from morphological characters, mitochondrial DNA, and microsatellite markers

Joel D. Anderson (contact author)[1]
Dusty L. McDonald[1]
Glen R. Sutton[2]
William J. Karel[1]

Email address for contact author: Joel.Anderson@tpwd.state.tx.us

[1] Perry R. Bass Marine Fisheries Research Station
Texas Parks and Wildlife Department
HC02 Box 385, Palacios, Texas 77465

[2] Galveston Bay Field Office
Texas Parks and Wildlife Department
1502 FM 517 East,
Dickinson, Texas 77539

Abstract—The evolutionary associations between closely related fish species, both contemporary and historical, are frequently assessed by using molecular markers, such as microsatellites. Here, the presence and variability of microsatellite loci in two closely related species of marine fishes, sand seatrout (*Cynoscion arenarius*) and silver seatrout (*C. nothus*), are explored by using heterologous primers from red drum (*Sciaenops ocellatus*). Data from these loci are used in conjunction with morphological characters and mitochondrial DNA haplotypes to explore the extent of genetic exchange between species offshore of Galveston Bay, TX. Despite seasonal overlap in distribution, low genetic divergence at microsatellite loci, and similar life history parameters of *C. arenarius* and *C. nothus*, all three data sets indicated that hybridization between these species does not occur or occurs only rarely and that historical admixture in Galveston Bay after divergence between these species was unlikely. These results shed light upon the evolutionary history of these fishes and highlight the genetic properties of each species that are influenced by their life history and ecology.

Manuscript submitted 24 April 2008.
Manuscript accepted 22 August 2008.
Fish. Bull. 107:13–23 (2009).

The views and opinions expressed or implied in this article are those of the author and do not necessarily reflect the position of the National Marine Fisheries Service, NOAA.

The molecular genetic associations between populations of sand seatrout (*Cynoscion arenarius*) and silver seatrout (*C. nothus*) have not been specifically examined on a large scale with DNA methods despite the close ties between the respective fisheries for the two species. In particular, the possibility of contemporary hybridization or historical admixture between these species remains to be explored by using a large panel of unlinked DNA markers. Sand and silver seatrout are so morphologically similar that they are collectively known as white trout by fishermen (Ginsburg, 1931). Both species are abundant throughout the Gulf of Mexico (hereafter, GOM); the distribution range for sand seatrout extends into the Atlantic Ocean, north to Georgia, and the distribution range for silver trout extends to Massachusetts (Hildebrand and Schroeder, 1928; Cordes and Graves, 2003). These seatrout make up a modest proportion of bycatch in shrimp and other commercial trawl operations (Warren, 1981), although commercial landings have decreased dramatically in the last 30 years (Fig. 1). Weinstein and Yerger (1976) completed perhaps the most comprehensive study of molecular evolution in the genus *Cynoscion*; they assessed protein electrophoresis variants in all four western North Atlantic species (*C. arenarius*, *C. nothus*, spotted seatrout [*C. nebulosus*], and gray weakfish [*C. regalis*]). Although these methods provided some insight into the evolutionary relationships among the species, the data of Weinstein and Yerger (1976) were insufficient to answer direct questions about rates of contemporary and recent historical gene flow within and among *Cynoscion* species. Enzyme electrophoresis has since been superceded by DNA-based methods on a broad scale. Microsatellite markers are likely more sensitive for studies involving high rates of gene flow and low levels of population identity (Wright and Bentzen, 1994). This is particularly true for marine fishes, whose populations are often characterized by enormous census sizes and higher rates of migration between subpopulations than freshwater and terrestrial organisms (DeWoody and Avise, 2000).

Previous morphological comparisons of sand and silver seatrout have resulted in a suite of distinct characteristics that vary between species in larval (Ditty, 1989) and adult stages (Ginsburg, 1929, 1931; Gunter, 1945; Moshin, 1973; Chao, 2002). However, both display a similar streamlined and fusiform body shape, and the ranges of numerous commonly used morphometric and meristic measures

overlap between the species. Additionally, hybridization, regional differentiation, or a combination of both, may often confound the trademark diagnostics used to distinguish between the two species. In any event, the superficial similarity of these species indicates that morphological divergence has been minimal and the concurrent bimodal timing of spawning indicates overlapping life history parameters (Sheridan et al., 1984). Distributional data seem to indicate that these species exhibit some habitat partitioning (primarily by water depth and distance from the shore) with the result that silver seatrout are found more frequently in deeper water farther from shore (Ginsburg, 1931; Byers, 1981).

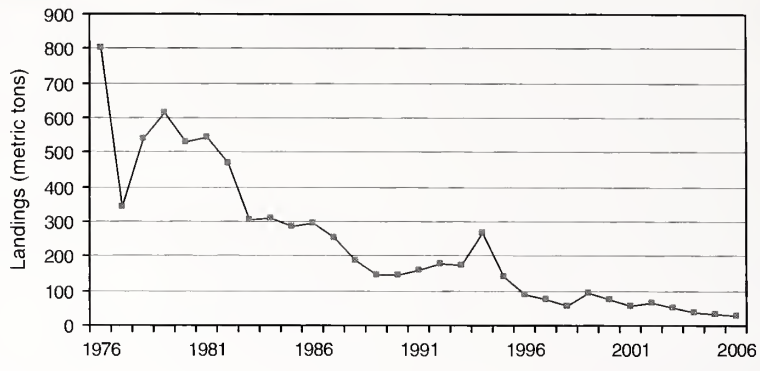

Figure 1

Commercial landings (in metric tons) of white trout (*Cynoscion nothus* and *C. arenarius* combined), from 1976 to 2006. Data provided by the Office of Science and Technology, National Marine Fisheries Service, Silver Spring, MD, 2007.

These life history and distributional data yield a framework for devising hypotheses to test the influence of niche overlap on historical associations between sand and silver seatrout populations. In particular, if hybridization between these species occurs, it is likely to occur in areas of contact such as nearshore marine waters used commonly by both species. Hybridization in the genus *Cynoscion* has been previously documented on the Atlantic coast of Florida (Cordes and Graves, 2003). In their initial examinations, Cordes and Graves (2003) characterized populations of gray weakfish using genetic techniques and in doing so also identified putative hybrids between gray weakfish and either sand or silver seatrout. This identification was accomplished by using four microsatellite markers and two nuclear intron gene regions (restriction fragment length polymorphisms, or RFLP's). Although these markers were appropriate for identification of hybrids with gray weakfish, they were ineffective for determining conclusively whether the second gametic contribution was made by sand or silver seatrout.

Here, both morphological and molecular (nuclear microsatellites and mitochondrial restriction fragments) data are used to characterize populations of sand and silver seatrout from the nearshore Gulf waters outside of Galveston Bay, Texas. Three competing hypotheses regarding genetic associations between these species are evaluated. First, in the case of contemporary hybridization, hybrids would appear as proportionate admixtures of both parental forms in microsatellite assignment tests. Moreover, the directionality of hybridization could be assessed with the use of mtDNA haplotypes (Wirtz, 1999), and hybrids would likely be found to be intermediate for diagnostic morphological characters (Hubbs, 1955; Campton, 1987). Second, in the case of historical association, such as lineage overlap during speciation or lineage admixture after speciation, mtDNA haplotypes might be shared between the species despite a mutually exclusive assignment of microsatellite genotypes (with the assumption of no contemporary hybridization). In such a case, assignment based on microsatellite genotypes should be more reliable than assignment by means of mtDNA haplotypes if mtDNA lineages have not been sorted categorically into contemporary populations (species). Third, in the case of no gene flow between the species, microsatellite assignment should be conclusive, mtDNA haplotypes should sort conclusively by species, and specimens should not reveal morphological intermediates for characters previously described as diagnostic among species. Each of these competing hypotheses was examined in light of evidence from the three data sets. The morphological and genetic similarities and differences between the species were examined as evidence for hybridization, and as an aid for future species identification. Finally, aspects of the ecology and life history of each species are invoked to explain the patterns of genetic variability within and between these congeneric species.

Materials and methods

Sample collection and laboratory methods

In July of 2007, whole fish were collected offshore of Galveston Bay, TX, during annual routine monitoring by the Texas Parks and Wildlife, Coastal Fisheries Division. White trout were collected with a 5.7-m otter trawl with 38-mm nylon multifilament mesh stretched throughout. Trawl tows (n=4) were conducted parallel to the fathom curve at a speed of three mph for ten minutes (Fig. 2). After collection, fish were frozen and transported to the Perry R. Bass Marine Fisheries Research Station in Palacios, Texas, for processing.

The sample consisted of 60 young adult sand seatrout and 60 young adult silver seatrout. A single researcher completed all morphological and meristic counts because considerable risk of extraneous variance has been demonstrated in data collected by mul-

tiple individuals (Palmeirim, 1998). Morphometric and meristic measurements were taken on the left side of each fish. In the event that fins or scales were damaged, the right side was used, and no measurements were taken if both sides were damaged. Body weight, standard length (SL), pectoral-fin length, pelvic-fin length, anal-fin base length, and eye diameter were measured in each specimen. Weight was taken in grams (g) and length measurements were taken in millimeters (mm). Unless otherwise indicated, statistical analyses were performed with SAS software (vers. 8.02, SAS Inst., Inc., Cary, NC). Differences in weight and length between the species were assessed with a Satterthwaite *t*-test for unequal variances (after failure of an equality-of-variance test). Length and weight were log-transformed to normalize extreme observations, and the interspecific difference between length-to-weight ratios was tested with a pooled *t*-test of transformed values. Meristic counts were made with a dissecting microscope and included anal-fin soft rays and lateral-line scale counts. For anal-fin soft-ray counts, the last branched soft ray was counted as one ray (McEachran and Fechhelm, 2005). Four commonly used diagnostics were evaluated for identification to species. The ratios of pectoral-fin length to pelvic-fin length (Chao, 2002) and also the ratio of anal-fin base-length to eye-diameter (DeVries and Chittenden, 1982) were calculated, and differences between species were assessed with a pooled *t*-test on untransformed data. Anal-fin soft rays (Ginsburg, 1929) and lateral-line scales (Hoese and Moore, 1998) were counted, and differences between these meristics were assessed with a chi-square test of homogeneity. Following morphological analyses, dorsal-fin soft tissue was excised from each specimen and placed in 70% denatured ethanol.

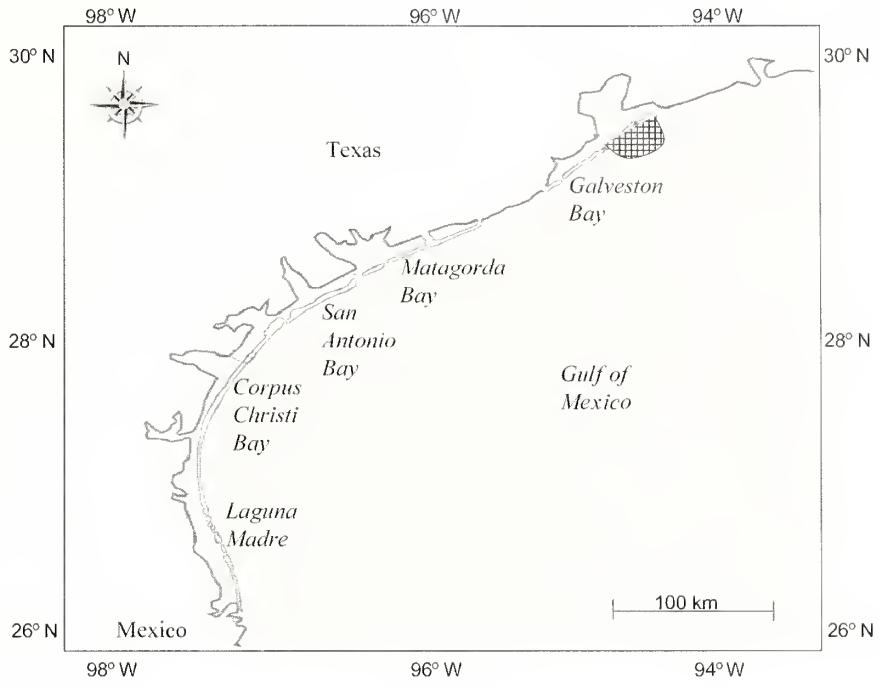

Figure 2

Map of the Texas gulf coast, showing the study area (hatched area), as well as major bays and inlets of Texas provided as points of reference. Trawls were collected in the offshore region of the gulf coast adjacent to Galveston Bay, TX, and sand seatrout (*C. arenarius*) and silver seatrout (*C. nothus*) were retained from each trawl.

Total genomic DNA was extracted from each fin-clip with a Puregene® miniprep kit (Gentra Systems, Minneapolis, MN) according to the manufacturer's instructions. The mtDNA methods used here were similar to those of Cordes et al. (2001) and Cordes and Graves (2003). A portion of the 12S/16S ribosomal gene locus of the mtDNA was amplified by polymerase chain reaction (PCR) with the primers 12SAL and 16SAH (Cordes et al., 2001). Amplification products were run through a 2% agarose gel next to a size standard spanning the ranges of 100–1500 base pairs (bp) to verify expected fragment length. Each amplicon was then digested with the restriction enzyme RsaI (New England Biolabs, Inc., Ipswich, MA) according to the standard protocol of the supplier, and restriction fragments were separated on a 2% agarose gel at 100 volts for 1 hour. A size standard was loaded onto each gel in order to approximate the size RFLPs. Gels were stained with ethidium bromide and RFLP bands were made visible (i.e., fluoresced) under an ultraviolet lamp.

Before initiation of this study, few microsatellite markers had been effectively characterized in the literature for sand or silver seatrout. However, a number of markers had been identified in a genomic library from the closely related sciaenid red drum (*Sciaenops ocellatus*) (Turner et al., 1998; Saillant et al., 2004), and some of these markers have subsequently been used successfully in members of the genus *Cynoscion* (Gold et al., 2003; Ward et al., 2007). Here, sixteen previously described microsatellite markers were chosen for examination: *SOC12*, *SOC50*, *SOC77*, *SOC85*, *SOC125*, and *SOC243* (Turner et al., 1998), *CNE133* (Gold et al., 2003), *SOC410*, *SOC412*, *SOC415*, *SOC416*, *SOC419*, *SOC423*, *SOC424*, *SOC428*, and *SOC432* (Saillant et al., 2004). Eight individuals of each species were genotyped with the suggested primers in each case. Each reverse oligonucleotide was previously labeled with a WellRED dye (Proligo USA LLC, Boulder, CO), and amplified products were produced at each locus by means of PCR. Products from individual reactions were diluted 1:20 with water and separated with a Beckman-Coulter CEQ™ 8000 automated capillary system (Beckman Coulter, Inc., Fullerton, CA), according

Table 1

Allele size ranges, in total DNA base pairs, for the microsatellite markers used to characterize populations of *Cynoscion arenarius* (sand seatrout) and *C. nothus* (silver seatrout) from offshore Galveston, TX, in July 2007. Each marker is listed by name as defined in the reference paper. The size range for *Sciaenops ocellatus* (red drum) was obtained from Saillant et al. (2004) and is included for reference.

Name	Allele range *C. arenarius*	Allele range *C. nothus*	Allele range *S. ocellatus*	Reference
SOC050	161–197	173–191	183–183	Turner et al., 1998
SOC243	100–112	106–127	94–106	Turner et al., 1998
SOC410	301–323	299–305	306–344	Saillant et al., 2004
SOC412	117–171	117–147	102–168	Saillant et al., 2004
SOC415	187–295	171–207	187–235	Saillant et al., 2004
SOC416	134–206	142–170	141–181	Saillant et al., 2004
SOC419	232–268	224–252	238–260	Saillant et al., 2004
SOC428	163–167	165–167	172–242	Saillant et al., 2004
SOC432	98–118	90–128	94–132	Saillant et al., 2004

to the manufacturer's protocol, and a 400-bp internal size standard (Beckman Coulter, Inc., Fullerton, CA) was included for fragment sizing. Each microsatellite locus was evaluated by a prioritized set of criteria: 1) amplification of the PCR product resulted in adequate signal intensity, 2) there were no excessive stepwise "stutter" bands preceding actual allele peaks, and 3) allelic polymorphism was present in both species. From the initial set of 16 loci, nine satisfied these criteria and consistently amplified a product (Table 1). Each experimental individual, for both species, was then genotyped at these nine loci.

Analysis of microsatellite data

The program FSTAT (Goudet, 1995) was used to calculate allele diversity (number of alleles per locus), gene diversity, and conformity with Hardy-Weinberg expectations at each locus within each population. The latter was approximated by testing the significance of the statistic F_{is} (Weir and Cockerham, 1984), which can be described as the within-population inbreeding coefficient. Significant departure of F_{is} from 0 represents significant deviation from Hardy-Weinberg expectations. FSTAT was used to detect the presence of linkage disequilibrium between loci within populations by using a nominal level of $\alpha = 0.05$ and Bonferroni adjustment for multiple tests. Finally, FSTAT was used to estimate genetic divergence between species as θ (Weir and Cockerham, 1984) at each locus and overall. The significance of θ was assessed by using the exact G-test of Goudet et al. (1996) with 1000 randomizations and an arbitrary $\alpha = 0.05$.

In order to determine which microsatellites were the most informative for species assignment, we used the critical population method of Banks et al. (2003) in assessing the discriminatory power of individual markers. The freeware program WHICHLOCI (Banks et al., 2003) was used to generate ten random sand seatrout populations (n=1000) based on empirical allele frequency data. These populations were used in simulated assignment procedures with constant assignment stringency (95% correct assignment of group members, 5% mis-assigned to critical population) and two conservative log odds ratio (LOD) assignment scores (LOD 2 and 3). The LOD assignment stringency is the log of the predetermined acceptable ratio of correctly assigned to incorrectly assigned individuals (thus LOD of 2=log10 of the ratio 100:1). The critical population (sand seatrout) used for simulations was also a conservative selection because it was chosen after observation of trial runs to discern which population routinely needed higher numbers of loci for correct assignment. The output from these simulations included a list of loci ranked by discriminatory power of assignment, the locus score based on both type-I and type-II errors, and the relative score of each locus weighted by the overall additive score of the entire microsatellite panel.

To identify hybrids resulting from crosses between these species, we used the Bayesian framework of Pritchard et al. (2000). The freeware program STRUCTURE (Pritchard et al., 2000) attempts to estimate the number of genetic clusters present while simultaneously assigning individuals to groups. This is done in part through progressive minimization of linkage disequilibrium and Hardy-Weinberg disequilibrium in iterative Markov chain Monte Carlo steps. Three sets of data were used in independent runs. In the initial run, we used data from the six highest-ranked microsatellite loci from WHICHLOCI analyses. A second run included data from all nine loci. Finally, a third run included the six highest-ranked loci, but mtDNA haplotype data were used to assign individuals *a priori* and microsatellite data were used to improve assignment. In each case, model parameters and run-times were specified as follows. The burn-in phase was set at 25,000 iterations and runs lasted 175,000 iterations under the admixture model. These values were chosen after inspection of model parameter normalization in preliminary runs. The Dirichlet parameter (α) was inferred from the data and was allowed to vary between populations. Allele

Table 2

Morphometric and meristic differences between two seatrout species, sand seatrout (*Cynoscion arenarius*) and silver seatrout (*C. nothus*), collected in trawls from Galveston Bay, TX, in July 2007. The range includes the overall range of data observations (*n*), followed by the mean and SE (standard error). The significance of each comparison was calculated by using either a standardized *t*-test (indictated as a lower-case a) or a chi-square test of homogeneity (indicated as a lower-case b).

	C. arenarius			*C. nothus*			
	n	Range	Mean ±SE	*n*	Range	Mean SE	*P*-value
Size measurements							
Standard length (mm)	60	83–175	107.9 ±8.3	60	100–163	119.5 ±4.7	<0.0001 [a]
Body weight (g)	60	10–95	26.4 ±7.3	60	20–75	33.4 ±4.1	0.0015 [a]
Ratios							
Pectoral fin/pelvic fin	60	0.9–1.2	1.10 ±0.04	48	0.9–1.3	1.09 ± 0.04	0.5978 [a]
Anal-fin base/eye diameter	60	1.2–2.4	1.59 ± 0.10	60	0.9–1.2	1.01 ± 0.03	<0.0001 [a]
Meristics							
Anal-fin soft rays	60	10–12	10.9 ± 0.2	60	8–9	8.8 ± 0.2	<0.0001 [b]
Lateral-line scales	57	57–61	59.3 ± 0.6	56	57–63	59.5 ± 0.8	0.9151 [b]

frequencies were assumed to be independent between populations. These model parameters were tested with a set $K = 2$, representing the two species as possible genetic contributors for each individual. The program was run under these model conditions for six trials to check for stability of resulting admixture coefficients (Q-values).

In order to evaluate the significance of individuals with extreme admixture coefficients values of Q, a set of simulated populations of 1000 individuals from each species was generated from allele-frequency data with WHICHLOCI. We analyzed these populations with STRUCTURE using identical model parameters to those in the experimental populations; the probability of obtaining a higher estimated level of admixture for any test individual was estimated as the frequency of higher admixture scores in the simulated population.

Results

Sample statistics and morphological characters

Samples of sand seatrout were collected from a combination of three grids, each of which was roughly one km from shore. The three grids were located at depths of three (one grid) and four (two grids) fathoms. For comparative purposes, trawl data for each species was combined and treated as a single random sample. All individual silver seatrout were collected from a single grid offshore from Galveston Bay. The grid was two km from land and had a depth of seven fathoms. The sand seatrout sample contained specimens that were significantly smaller than those obtained in the silver seatrout sample, in both mean standard length (t=–4.74, P<0.0001) and mean weight (t=–3.27, P=0.0015) (Table 2). The difference in mean size was not likely caused by gear selectivity because the size range of both species combined was from 83 to 175 mm, and larger fish are routinely caught in trawls. The mean ratio of weight to length was not significantly different between the species (t=0.07, P=0.800), indicating a similarity in growth trajectories between the species at the size examined, despite significant differences in overall size.

Two of four meristic measurements were useful in reliably sorting specimens to species. First, sand seatrout had overall larger anal-fin to eye-diameter ratios (t=21.32, P<0.0001); the sand seatrout ratio ranged from 1.23 to 2.44, whereas the range in silver seatrout was 0.85–1.19. Second, anal-fin soft rays were significantly different between species (χ^2=120, df=10, P<0.0001); sand seatrout possessed an average of 10.9, silver seatrout an average of 8.8 soft rays. In contrast, there was not a significant difference in pectoral-fin to pelvic-fin ratios between species (t=0.53, P=0.5978) (Fig. 3), nor was there a significant difference in the number of lateral line scales (χ^2=7.47, df=14, P=0.915). The anal-fin soft-ray meristic was the most practical morphological character for species discernment because the range of this character did not overlap between species in any specimen (range 10–12 for sand seatrout, 8–9 for silver seatrout), and this character was relatively easy to count.

Mitochondrial DNA

The fragments recovered from each mtDNA amplification were approximately 1500 bp, and this size did not vary between species. Two distinctive RFLP patterns were identified (Fig. 4). The first pattern contained four bands, at approximately 450, 290, 250, and 190 bp. This pattern was identified in each of the 60 sand seatrout assayed. The second pattern also contained four bands, at approximately 400, 290, 200, and 190 bp. This pattern was identified in each of the 60 silver seatrout assayed. Based upon the expected relative intensity of each band,

there was the likelihood that duplicate fragments were present in each haplotype at the 190 band. Additionally, multiple uncharacterized bands appeared that were <100 bp in length. These uncharacterized bands likely account for the remainder of digested DNA (~320 bp expected in *C. arenarius*, and ~420 bp expected in *C. nothus*) that was not accounted for by primary bands, although this assumption was not explicitly tested. Correct assignment of RFLP haplotypes to each species was confirmed by comparison with anal-fin ray counts and anal-fin to eye-diameter ratios.

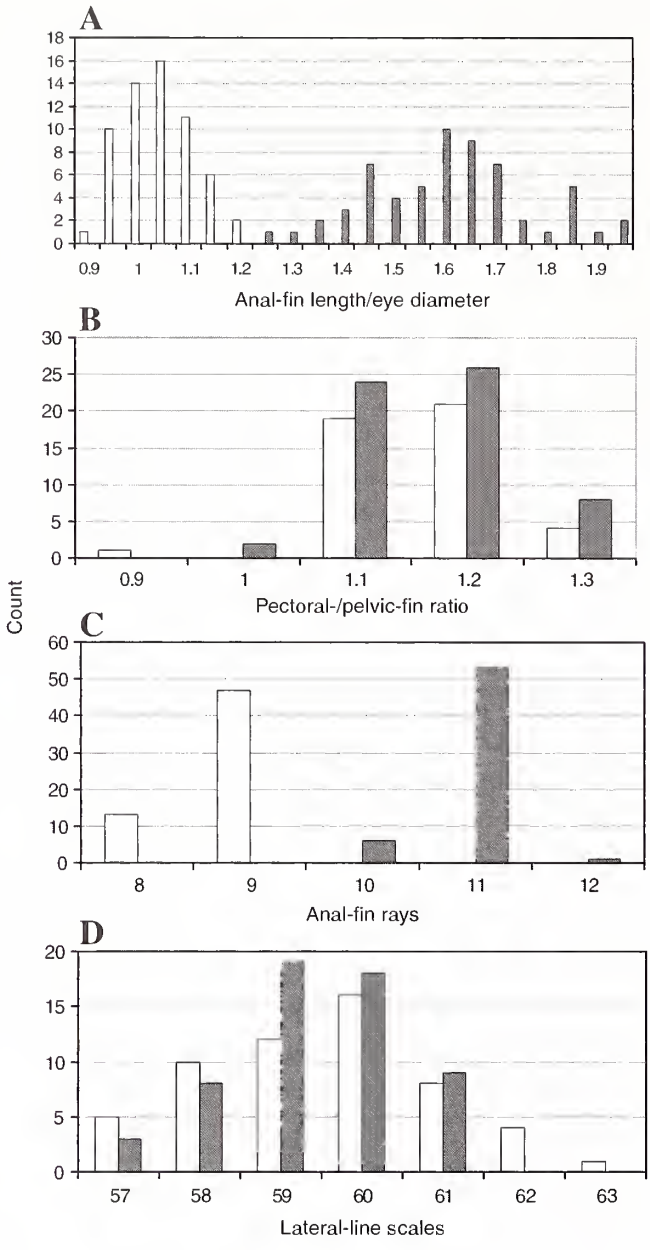

Figure 3

Histograms representing the distribution of meristic and morphometric characteristics of silver seatrout (*Cynoscion nothus*) (white bars) and sand seatrout (*C. arenarius*) (black bars) collected offshore from Galveston Bay, TX, in July 2007. The four main diagnostics examined included (**A**) anal-fin/eye- diameter ratio, (**B**) pectoral-fin/pelvic-fin ratio, (**C**) total anal-fin rays, and (**D**) total lateral-line scales. The abscissa represents each data class (ratio [A and B] or count [C and D] data), whereas the ordinate represents the total membership of each species sample in that class.

Microsatellite DNA

The nine microsatellites used for species comparisons had a range of three to 51 alleles overall. One locus (*SOC415*) had a dramatic allele range difference between the species (Table 1), which resulted in almost complete disjunction between allele distributions, possibly the result of a large insertion in sand seatrout, or deletion in silver seatrout. A deletion is most likely the reason because the allele range in sand seatrout is similar to that of the species in which the markers were initially cloned, *S. ocellatus*. Otherwise, the detected allele ranges of the remaining eight loci were similar between *Cynoscion* species and overlapped the range of *S. ocellatus*.

The average allele diversity was 16.44 alleles per locus in sand seatrout and 9.89 alleles per locus in silver seatrout, and diversity was (qualitatively) higher in sand seatrout at eight of nine loci (Table 3). Similarly, gene diversity was higher in sand seatrout at seven of nine loci and ranged from 0.11 to 0.97, compared to a range of 0.02 to 0.90 in silver seatrout. There was no indication of genotypic disequilibrium at any locus in any population because all *P*-values fell at or above the adjusted critical level of α = 0.0014. It should be noted, however, that a single combination of loci (*SOC243* and *SOC415*) did show evidence of significant linkage before adjustment for multiple tests ($P \approx 0.0014$). The inbreeding coefficient (F_{is}) was not significantly different from 0 at any locus in either population. As a result, all nine loci were included in downstream assignment assays.

Significant genetic divergence between the species was found at each of the nine loci, resulting in a range for θ of 0.025–0.464, with a mean value of θ=0.117 (Table 3). Six loci accounted for approximately 86% of the discriminatory power of the panel of microsatellites in Whichloci analyses (Table 4). Of these, only the four highest ranked loci were needed to correctly assign individuals to populations under an assignment stringency LOD-score of two. All six were needed when the assignment stringency was increased to a LOD-score of three. Unsuccessful assignment was due to stringency restrictions rather than to actual mis-assignment of individuals. In every case, all individuals were assigned correctly at a relaxed stringency.

Table 3

Genetic allele diversity, gene diversity, and the inbreeding coefficient (F_{is}) for nine microsatellite loci in sand seatrout (*Cynoscion arenarius*) and silver seatrout (*C. nothus*) collected from offshore Galveston Bay, Texas, in July 2007. No value of F_{is} was significantly different from 0. Genetic divergence between species (measured as θ) was significant at each locus. Summary statistics for overall variability are included on the bottom rows (mean above, SE below).

	C. arenarius			*C. nothus*			
Locus	Allele diversity	Gene diversity	F_{is}	Allele diversity	Gene diversity	F_{is}	θ
SOC050	11	0.77	−0.095	9	0.54	−0.045	0.059
SOC243	5	0.30	0.038	8	0.52	0.081	0.116
SOC415	40	0.97	0.021	15	0.90	0.107	0.066
SOC410	6	0.60	0.062	4	0.13	−0.048	0.464
SOC412	17	0.85	−0.056	11	0.80	−0.106	0.084
SOC416	30	0.94	0.045	15	0.89	−0.031	0.058
SOC419	16	0.77	0.050	13	0.86	−0.070	0.100
SOC428	3	0.11	−0.046	2	0.02	0.000	0.025
SOC432	20	0.91	−0.024	12	0.81	0.014	0.075
Overall	16.44	0.69	0.000	9.89	0.61	−0.010	0.117
(±SE)	(±8.01)	(±0.20)	(±0.037)	(±3.00)	(±0.22)	(±0.045)	(±0.087)

The performance of each of the three Bayesian assignment models was evaluated by examining the average membership proportion of each species in either of two genetic clusters after assignment. Under the assumption that the best assignment model should result in the highest proportion of membership (POM) of individuals to their correct species cluster (that is, assuming no admixture between the species), each model performed equally well for assignment of sand seatrout (POM=0.978), whereas the six-locus panel of markers (POM=0.989) performed better than the nine-locus panel (POM=0.985) for silver seatrout. The highest average POM of 0.994 and 0.996 for sand and silver seatrout, respectively, was attained by assigning group membership *a priori* based on mtDNA haplotype, and by refining group membership scores with the six highest-rated microsatellite loci. Using the six-locus model without mtDNA information, we found significant coancestry between the species for a single individual identified as belonging to the sand seatrout cluster, and an estimated proportion of silver seatrout ancestry of 0.303 (Table 5). In six successive iterations, the mean Q for this individual was 0.297 (range: 0.291–0.305). This value of Q was higher than any obtained in simulated populations ($P<0.05$). However, when mtDNA haplotype data were used to improve clustering, probability of admixture was not significant in this individual ($Q=0.119$). Furthermore, morphological evidence indicated no intermediacy at the diagnostic traits (anal-fin to eye-diameter ratio=1.8, anal-fin rays=12); both of these diagnostics indicated this individual was a sand seatrout.

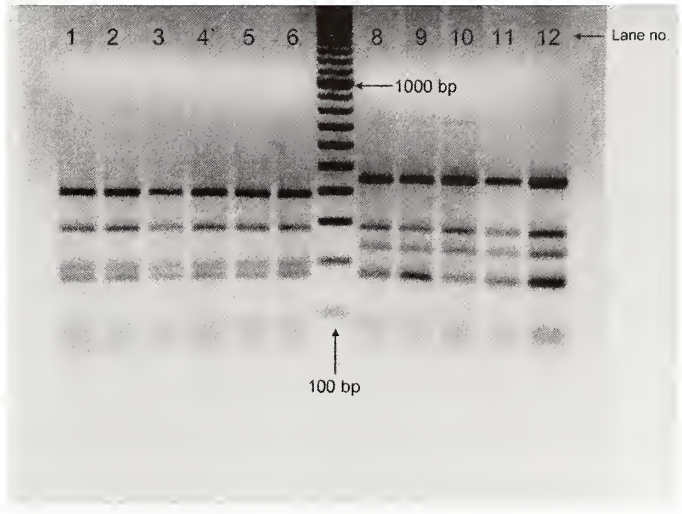

Figure 4

Sample gel image from mitochondrial DNA (mtDNA) restriction fragment length polymorphism (RFLP) analysis. Lanes 1–6 are restriction digests of silver seatrout (*Cynoscion nothus*) mtDNA with the enzyme RsaI, whereas lanes 8–12 are restriction digests of sand seatrout (*C. arenarius*) mt DNA. Lane 7 is a sizing ladder, where the 1000-base pair (bp) fragment is marked. The lightest ladder fragment is 100 bp.

Discussion

Morphological and genetic identification of white trout

Two of four commonly used morphological diagnostics are useful in distinguishing conclusively between sand

and silver seatrout. As previously described, the ratio of anal-fin base to eye diameter has a nonoverlapping distribution (DeVries and Chittenden, 1982), and this is due in part to a difference in eye size of each species, for which the mean diameter is lower in sand seatrout than in silver seatrout. Anal-fin soft-ray counts also are diagnostic in these samples, contrary to previous marine fish keys, which indicate overlap of these characters (Robins et al., 1986; Chao, 2002; McEachran and Fechhelm, 2005). The ineffectiveness of the remaining diagnostics (pectoral- to pelvic-fin length ratio, lateral-line scale counts) may be due to differences at various age classes; i.e., the previously described differences may be more apparent in older individuals. Also, it should be noted that several damaged pectoral fins (resulting in shorter fins) in the silver seatrout sample were encountered because of the nature of capturing fish with trawling nets. Therefore there was a smaller sample size for the pectoral- to pelvic-fin ratio measurement. Nevertheless, the morphological data in conjunction with completely diagnostic mtDNA haplotypes, should prove useful for future species identification issues between sand and silver seatrout.

Table 4

Locus scores and relative scores from WHICHLOCI analyses, ranked in order of population assignment power. The locus score is the power of each locus as a ratio of correctly assigned to incorrectly assigned individuals in data simulations. The relative score of each locus is obtained by summing all locus scores and then dividing an individual locus score into the total score.

Locus	Score	Relative score (%)
SOC415	0.97	20.8
SOC416	0.70	15.1
SOC419	0.63	13.4
SOC410	0.61	13.1
SOC432	0.58	12.5
SOC412	0.49	10.6
SOC50	0.32	6.8
SOC243	0.31	6.6
SOC428	0.05	1.1

In contrast to the diagnostic differences in morphological characters and in mtDNA haplotypes, no diagnostic microsatellite loci were identified in the present study. This is likely due to several factors. First, microsatellites have a more elevated rate of mutation than other loci (Ellegren, 2000) and tend to evolve in stepwise fashion (Ellegren, 2000; Xu et al., 2000), such that they may be subject to increased rates of homoplasy (Estoup et al., 2002). The result is that convergent electromorphs can obscure the actual rate of fixation for homologous microsatellite alleles. Second, the fixation of different alleles between the two species may be confounded by recombination, resulting in longer evolutionary timeframes for lineage assortment to occur than what would be expected for mtDNA, which is typically nonrecombinant and clonally inherited. Finally, the enormous population sizes characteristic of marine fish populations may partially mitigate the effects of genetic drift (Allendorf and Phelps, 1981), which is likely the main mechanism for divergence at neutral loci. Collectively these processes have resulted in similarity in allele ranges for all but a single microsatellite locus (*SOC415*), despite significant differences in θ at each individual locus. Thus although no single microsatellite is diagnostic, when used in concert they are adequate for reliable identification to species. Further, because of their high overall between-species divergence and within-species variability, these microsatellites are likely adequate for diagnosis of hybrids, in particular at the F_1 (first generation hybrid) level.

Genetic variability and divergence within and between species

Significant genetic divergence between these species (θ=0.117) is indicated by examination of microsatellite

Table 5

Admixture class (proportion of genetic contribution from the opposing species, in rows) membership in a randomized population sample (n=1000), compared to experimental populations (n=60) of silver seatrout (*Cynoscion nothus*) and sand seatrout (*C. arenarius*) collected from offshore Galveston Bay, TX, in July 2007. The admixture classes are defined arbitrarily by Q-score increments of 0.05. The value "P" represents the proportion of individuals in each population that fall into a particular admixture class (range of Q), and significance in experimental populations (indicated by a superscript "a") was assessed quantitatively by comparing membership in each class to expected values as assessed by examination of the randomized population.

Q-score	Randomized population	P	*C. nothus*	P	*C. arenarius*	P
0–0.050	980	0.98	59	0.98	56	0.93
0.060–0.100	13	0.01	0	0.00	2	0.03
0.011–0.150	5	0.01	1	0.02	1	0.02
0.016–0.200	1	0.00	0	0.00	0	0.00
0.210–0.250	1	0.00	0	0.00	0	0.00
>0.250	0	0.00	0	0.00	1^a	0.02

loci. This divergence is coupled with primarily nonsignificant estimates of admixture between species, although one individual did exhibit significant evidence of admixture ($Q>0$). Although it is plausible that this individual is an advanced backcross, this result more likely represents an outlier. Evidence for the outlier supposition includes the admixture model with mtDNA haplotypes used to improve clustering; in this scenario, the silver seatrout contribution for this individual is no longer significant. Additionally, no overlap occurred in the mtDNA haplotypes or in the two diagnostic morphological characters examined in this study. Thus, these data indicate that hybrid formation between sand and silver seatrout is either rare or nonexistent in the offshore Galveston Bay area, and enough generations have elapsed since divergence from an ancestral population that contemporary mtDNA haplotypes do not indicate either incomplete lineage sorting or admixture during the time of, or after, speciation. Altough the absence of hybridization seems to be the case in the Galveston Bay area, the present study was limited geographically, and the possibility of hybridization elsewhere within the overlapping ranges of these species must be further explored. Although narrow hybrid zones are rare in marine organisms (Palumbi, 1994), heterogeneity in the rate of hybridization has been demonstrated. For instance, the rate of hybridization in European shads (*Alosa* spp.) tends to be heterogeneous across the range of *A. alosa* and *A. fallax* (Alexandrino et al., 2006).

Estimates of genetic variability were systematically higher in sand seatrout than in silver seatrout, indicating possible demographic differences between populations of these species. For instance, both allelic richness and gene diversity are higher at almost every locus in sand seatrout. This observation is likely of biological significance, rather than a genetic ascertainment bias, because these markers were initially isolated from a species outside the genus *Cynoscion*. The direction of ascertainment bias would therefore be expected to vary from locus to locus, rather than to have comparable effects across a majority of loci. Demographic parameters such as population census size, rates of migration among neighboring populations, and variance in reproductive success can all affect effective population size (N_e), and heterogeneity in these parameters would result in different levels of measured genetic variability between the species. Thus the implication, based on systematically lower levels of genetic variability, is that silver seatrout have a lower N_e than sand seatrout.

The finding of higher genetic variability in sand seatrout is not likely the result of differences in migration rates because both species spawn primarily offshore in the GOM (Shlossman and Chittenden, 1981; DeVries and Chittenden, 1982); the pelagic nature of eggs and larvae in both species allow for long-distance dispersal and gene flow throughout the GOM. It is also unlikely that a difference in census sizes is the cause of elevated genetic variability in sand seatrout. The data of McDonald et al. (2009) indicates dramatically a higher abundance of *C. nothus* in the Galveston Bay offshore region, and the western GOM in general. The most likely explanation for the elevated genetic variability of sand seatrout is an overall higher level of individual reproductive success than that recorded for individuals in the silver seatrout population. Two key biological differences support this assertion. First, sand seatrout have an approximately 25% higher fecundity (mean 100,900 eggs per spawn than that of silver seatrout (mean 73,900 eggs per spawn) in the GOM (Sheridan et al., 1984). Second, individual sand seatrout are more likely to spawn on multiple occasions during their lifetime. Sand seatrout live longer (2–3 years, Shlossman and Chittenden, 1981) than silver seatrout (1–1.5 years, DeVries and Chittenden, 1982) and have two peak spawns per year in the western GOM, compared to a single relatively definitive peak in silver seatrout (McDonald et al., 2009). Both species mature before age one, and both species experience high mortality at early life stages. Hedgecock (1994) referred to the combination of high fecundity and high mortality at early life stages as a sweepstakes strategy, which is likely common in marine fishes. Such differences in fecundity and longevity between species likely result in a higher variance in reproductive success in silver seatrout, which concurrently results in lower effective population size and a decrease in genetic variability (Hedgecock, 1994; Hedrick, 2005). In any event, one caveat to this result is the fact that while the sand seatrout sample was collected during the course of three trawls, all silver seatrout specimens were collected from a single trawl. Thus sampling error or sample ascertainment bias cannot be ruled out completely as an explanation for differences in diversity estimates.

The morphological and ecological similarities among sand seatrout, silver seatrout, and gray weakfish have resulted in difficulty in distinguishing the taxonomic status of these species (Weinstein and Yerger, 1976). However, there is a fundamental difference between the distributions of the three species; whereas sand seatrout and gray weakfish are functionally parapatric in their distribution, inhabiting primarily the GOM and Atlantic Ocean, respectively, silver seatrout are found in relatively large populations in both areas. The shallow divergence previously reported between sand seatrout and gray weakfish (Weinstein and Yerger, 1976) was likely caused by highly stochastic sea level changes throughout the Pleistocene Epoch, resulting in regional differences between populations in the GOM and Atlantic Ocean. A similar pattern is typical among other marine, freshwater, and terrestrial vertebrates worldwide that diverged during this time period (Avise and Walker, 1998; Avise et al., 1998; Hewitt, 2000), and has been particularly well documented in peninsular Florida (Avise, 1992). However, these episodic sea level changes were likely not long enough for reproductive isolation between sand seatrout and gray weakfish to develop. Therefore, contemporary hybridization between these species is common on the Atlantic coast of Florida (Cordes and Graves, 2003); in contrast, no such patterns have been indicated between populations of sand

and silver seatrout, which have sympatric distributions in the GOM.

This finding supports the monophyly of an assemblage that includes sand seatrout and gray weakfish and may indicate that silver seatrout diverged from this group before the sea level changes of the last glacial maximum. The current data indicate complete divergence in two morphological characters and a single genetic (mtDNA) locus between sand and silver seatrout. In contrast, the morphological data of Aguirre and Shervette (2005) indicate a sister-species relationship between sand seatrout and weakfish. Interestingly, the silver seatrout is the only one of the three species that is not partially estuarine-dependent, indicating that estuarine independence may have evolved after the speciation process. Furthermore, because silver seatrout are not tied to shallow estuarine waters, they may have eluded the significant vicariance effects (that is, genetic divergence caused by the appearance of a transient or permanent boundary) caused by sea level shifts during periods of glacial advance. However, caution must be used in interpreting genetic data in light of contemporary distribution range because extant distributions are not necessarily good indicators of geographic ranges at the time of divergence (Losos and Glor, 2003). Whatever the case, trophic partitioning between the two species likely contributes to the heterogeneous offshore distribution of sand seatrout, in contrast to the relatively consistent offshore distribution of silver seatrout (Ginsberg, 1931; Byers, 1981; McDonald et al., 2009). These data indicate that partitioning may also play a role in the maintenance of reproductive barriers between species, resulting in distinctive genetic profiles, and little evidence of evolutionary association after speciation.

Acknowledgments

The fisheries monitoring staff at the Galveston Bay Field Office, Texas Parks and Wildlife (TPW), including ecosystem leaders R. Hensley and B. Balboa, were responsible for sample collection. Samples were collected during TPW routine monitoring, which is funded by Federal Aid in Sportfish Restoration Grant (FRM-34). Assistance during sample processing was provided by M. Jesberg, A. Mione, E. Young, and R. Vickers. Improvements to the first draft were provided by M. Fisher and B. Bumguardner (TPW), and three anonymous reviewers. This research project was funded in part by dedicated funds from a Federal Aid in Sportfish Restoration Grant (F-158-R).

Literature cited

Aguirre, W. E., and V. R. Shervette.
2005. Morphological diversity of the *Cynoscion* group (Perciformes: Sciaenidae) in the Gulf of Guayaquil region, Ecuador: a comparative approach. Environ. Biol. Fishes 73:403–413.

Alexandrino, P., R. Faria, D. Linhares, F. Castro, M. Le Corre, R. Sabaties, J. L. Beglinière, and S. Weiss.
2006. Interspecific differentiation and intraspecific substructure in two closely related clupeids with extensive hybridization, *Alosa alosa* and *Alosa fallax*. J. Fish Biol. 69(B):242–259.

Allendorf, F. W., and S. R. Phelps.
1981. Use of allelic frequencies to describe population structure. Can. J. Fish. Aquat. Sci. 38: 1507–1514.

Avise, J. C.
1992. Molecular population structure and the biogeographic history of a regional fauna: a case history with lessons for conservation biology. Oikos 63:62–76.

Avise, J. E., and D. Walker.
1998. Pleistocene phylogeographic effects on avian populations and the speciation process. Proc. R. Soc. Lond. B 265:457–463.

Avise, J. C., D. Walker, and G. C. Johns.
1998. Speciation durations and Pleistocene effects on vertebrate phylogeography. Proc. R. Soc. Lond. B 265:1707–1712.

Banks, M. A., W. Eichert, and J. B. Olsen.
2003. Which genetic loci have greater population assignment power? Bioinformatics 19:1436–1438.

Byers, S. M.
1981. Trophic relationships of two sympatric Sciaenid fishes, *Cynoscion arenarius* and *Cynoscion nothus*, in the north central Gulf of Mexico. M.S. thesis, 70 p. Univ. Southern Mississippi, Ocean Springs, MS.

Campton, D. E.
1987. Natural hybridization and introgression in fishes: methods of detection and genetic interpretations. *In* Population genetics and fishery management (N. Ryman, and F. Utter, eds.), p. 161–192. Univ. Washington Press, Seattle, WA.

Chao, N. L.
2002. Sciaenidae. *In* The living marine resources of the Western Central Atlantic, Vol. 3. Bony fishes, part 2 (K. E. Carpenter, ed.), p. 1583–1653. Special Publ. no. 5, American Society of Ichthyologists and Herpetologists. Food and Agriculture Organization, United Nations, Rome, Italy.

Cordes, J. F., S. L. Armknecht, E. A. Starkey, and J. E. Graves.
2001. Forensic identification of sixteen species of Chesapeake Bay sportfishes using mitochondrial DNA restriction fragment-length polymorphism (RFLP) analysis. Estuaries 24:49–58.

Cordes, J. F., and J. E. Graves.
2003. Investigation of congeneric hybridization in and stock structure of weakfish (*Cynoscion regalis*) inferred from analyses of nuclear and mitochondrial DNA loci. Fish. Bull. 101:443–450.

DeVries, D. A., and M. E. Chittenden.
1982. Spawning, age determination, longevity and mortality of the silver seatrout, *Cynoscion nothus*, in the Gulf of Mexico. Fish. Bull. 80(3):487–500.

DeWoody, J. A., and J. C. Avise.
2000. Microsatellite variation in marine, freshwater and anadromous fishes, compared with other animals. J. Fish Biol. 56: 461–473.

Ditty, J. G.
1989. Separating early larvae of sciaenids from the western North Atlantic: a review and comparison of larvae off Louisiana and Atlantic coast of the U.S. Bull. Mar. Sci. 44: 1083–1105.

Ellegren, H.
2000. Heterogeneous mutation processes in human microsatellite DNA sequences. Nat. Genet. 24:400–402.
Estoup, A., P. Jarne, and J-M Cornuet.
2002. Homoplasy and mutation model at microsatellite loci and their consequences for population genetics analysis. Mol. Ecol. 11:1591–1604.
Ginsburg, I.
1929. Review of the weakfishes (*Cynoscion*) of the Atlantic and gulf coasts of the United States, with a description of a new species. Fish. Bull. 45:71–85.
1931. On the difference in the habitat and the size of *Cynoscion arenarius* and *C. nothus*. Copeia 1931:144.
Gold, J. R., L. B. Stewart, and R. Ward.
2003. Population structure of the spotted seatrout (*Cynoscion nebulosus*) along the Texas Gulf coast, as revealed by genetic analysis. *In* Biology of the spotted seatrout (S. A. Bortone, ed.), p. 17–29. CRC Press, Boca Raton, FL.
Goudet, J.
1995. FSTAT (vers. 1.2): a computer program to calculate F-statistics. J. Hered. 86:485–486.
Goudet, J., M. Raymond, T. Demeeus, and F. Rousset,
1996. Testing differentiation in diploid populations. Genetics 144:1933–1940.
Gunter, G.
1945. Studies of marine fishes of Texas. Contrib. Mar. Sci. 1:1–190.
Hedgecock, D.
1994. Does variance in reproductive success limit effective population size in marine organisms? *In* Genetics and evolution of aquatic organisms (A. Beaumont, ed.), p. 122–134. Chapman and Hall, London, UK.
Hedrick, P.
2005. Large variance in reproductive success and the Ne/N ratio. Evolution 59:1596–1599.
Hewitt, G.
2000. The genetic legacy of the Quaternary ice ages. Nature 405:907–913.
Hildebrand, S. F., and W. S. Schroeder.
1928. Fishes of Chesapeake Bay. Fish. Bull. 43:1–336.
Hoese, H. D., and R. H. Moore.
1998. Fishes of the Gulf of Mexico, 2nd ed., 422 p. Texas A&M University Press, College Station, TX.
Hubbs, C. L.
1955. Hybridization between fish species in nature. Syst. Zool. 4:1–20.
Losos, J. B., and R. E. Glor.
2003. Phylogenetic comparative methods and the geography of speciation. Trends Ecol. Evol. 18:220–227.
McDonald, D. L., J. D. Anderson, B. L. Bumguardner, F. Marinez-Andrade, and J. Harper.
2009. Spatial and seasonal distribution of sand seatrout (*Cynoscion arenarius*) and silver seatrout (*C. nothus*) off the coast of Texas, determined with twenty years of data (1987–2006). Fish. Bull. 107:24–35.
McEachran, J. D., and J. D. Fechhelm.
2005. Fishes of the Gulf of Mexico, vol. 2: Scorpaeniformes to Tetraodontiformes, 1st ed., 1014 p. Univ. Texas Press, Austin, TX.
Moshin, A. K. M.
1973. Comparative osteology of weakfishes (*Cynoscion*) of the Atlantic and Gulf coasts of the United States. Ph.D. diss, 148 p. Texas A&M Univ., College Station, TX.
Palmeirim, J. M.
1998. Analysis of skull measurements and measurers: can we use data obtained by various observers? J. Mammal. 73:1021–1028.
Palumbi, S. R.
1994. Genetic divergence, reproductive isolation, and marine speciation. Annu. Rev. Ecol. Syst. 25:547–572.
Pritchard, J. K., M. Stephens, and P. Donnelly.
2000. Inference of population structure using multilocus genotype data. Genetics 55:945–959.
Robins C. R., G. C. Ray, and J. Douglass.
1986. A field guide to Atlantic coast fishes in North America. The Peterson field guide series (R. T. Peterson, ed.), 354 p. Houghton Mifflin Co., New York, NY.
Saillant, E., K. Cizdziel, K. G. O'Malley, T. F. Turner, C. L. Pruett, and J. R. Gold.
2004. Microsatellite markers for red drum, *Sciaenops ocellatus*. Gulf Mex. Sci. 22:101–107.
Sheridan, P. F., D. L. Trimm, and B. M. Baker.
1984. Reproduction and food habits of seven species of northern Gulf of Mexico fishes. Contrib. Mar. Sci. 27:175–204.
Shlossman, P. A., and M. E. Chittenden Jr.
1981. Reproduction, movements, and population dynamics of the sand seatrout, *Cynoscion arenarius*. Fish. Bull. 79: 649–669.
Turner, T. F., L. R. Richardson, and J. R. Gold.
1998. Polymorphic microsatellite DNA markers in red drum (*Sciaenops ocellatus*). Mol. Ecol. 7:1771–1773.
Ward, R., K. Bowers, R. Hensley, B. Mobley, and E. Belouski.
2007. Genetic variability in spotted seatrout (*Cynoscion nebulosus*), determined with microsatellite DNA markers. Fish. Bull. 105:197–206.
Warren, J. R.
1981. Population analyses of the juvenile groundfish on the traditional shrimping grounds in Mississippi Sound before and after the opening of the shrimp season. M.S. thesis, 93 p. Univ. Southern Mississippi, Ocean Springs, MS.
Weinstein, M. P., and R. W. Yerger.
1976. Protein taxonomy of the Gulf of Mexico and Atlantic Ocean seatrouts, genus *Cynoscion*. Fish. Bull. 74:599–607.
Weir, B. S., and C. C. Cockerham.
1984. Estimating F-Statistics for the analysis of population structure. Evolution 38:1358–1370.
Wirtz, P.
1999. Mother species-father species: unidirectional hybridization in animals with female choice. Anim. Behav. 58:1–12.
Wright, J. M., and P. Bentzen.
1994. Microsatellites: genetic markers for the future. Rev. Fish Biol. Fish. 4:384–388.
Xu, X., M. Peng, Z. Fang, and X. Xu.
2000. The direction of microsatellite mutations is dependent upon allele length. Nat. Genet. 24:396–399.

Spatial and seasonal abundance of sand seatrout (*Cynoscion arenarius*) and silver seatrout (*C. nothus*) off the coast of Texas, determined with twenty years of data (1987–2006)

Dusty L. McDonald (contact author)[1]
Joel D. Anderson[1]
Britt W. Bumguardner[1]
Fernando Martinez-Andrade[2]
Josh O. Harper[3]

Email address for contact author: Dusty.Mcdonald@tpwd.state.tx.us

[1] Perry R. Bass Marine Fisheries Research Station
Texas Parks and Wildlife Department
HC02 Box 385
Palacios, Texas 77465

[2] Corpus Christi Field Office
Texas Parks and Wildlife Department
5200 Ocean Dr.
Corpus Christi, Texas 78412

[3] Palacios Field Office
Texas Parks and Wildlife Department
2200 Harrison St.
Palacios, Texas 77465

Abstract—Sand seatrout (*Cynoscion arenarius*) and silver seatrout (*C. nothus*) are both found within the immediate offshore areas of the Gulf of Mexico, especially around Texas; however information is limited on how much distributional overlap really occurs between these species. In order to investigate spatial and seasonal differences between species, we analyzed twenty years of bay and offshore trawl data collected by biologists of the Coastal Fisheries Division, Texas Parks and Wildlife Department. Sand seatrout and silver seatrout were distributed differently among offshore sampling areas, and salinity and water depth appeared to correlate with their distribution. Additionally, within the northernmost sampling area of the gulf waters, water depth correlated significantly with the presence of silver seatrout, which were found at deeper depths than sand seatrout. There was also an overall significant decrease in silver seatrout abundance during the summer season, when temperatures were at their highest, and this decrease may have indicated a migration farther offshore. Sand seatrout abundance had an inverse relationship with salinity and water depth offshore. In addition, sand seatrout abundance was highest in bays with direct passes to the gulf and correlated with corresponding abundance in offshore areas. These data highlight the seasonal and spatial differences in abundance between sand and silver seatrout and relate these differences to the hydrological and geological features found along the Texas coastline.

Manuscript submitted 24 April 2008.
Manuscript accepted 22 August 2008.
Fish. Bull. 107:24–35 (2009).

The views and opinions expressed or implied in this article are those of the author and do not necessarily reflect the position of the National Marine Fisheries Service, NOAA.

The sand seatrout (*Cynoscion arenarius*) and the silver seatrout (*C. nothus*) from the family Sciaenidae are sympatric species that co-occur within the Gulf of Mexico (GOM). In the literature, the co-occurrence and distribution of these species has been noted, particularly in offshore areas where feeding grounds overlap (Miller, 1965; Chittenden and McEachran, 1976). These studies, in concert with previous life history data from Texas (Shlossman and Chittenden, 1981; DeVries and Chittenden, 1982) have provided some insight into when and why any distributional variation occurs in the western GOM. Nevertheless, most studies of the abundance of these species have been limited on a spatial and temporal scale. Additionally, the spatial and temporal abundance of these species in relation to hydrological characteristics such as water temperature, salinity, depth, and bay access to the gulf through a channel or pass has not been thoroughly investigated.

Sand seatrout use inshore waters extensively but also move offshore seasonally to evade the temperature extremes of the inshore bays and to spawn (Shlossman and Chittenden, 1981; Vetter, 1982). In contrast silver seatrout, although on occasion they can be collected inshore, live their entire lives offshore (Gunter, 1945; Miller, 1965). In addition to their distributional difference, differences exist in their hydrological preference, particularly in salinity and water depth, adding to the complexity of the distributional preferences of these two species (Chittenden and McEachran, 1976). However, a great deal of distributional overlap of these species occurs within the immediate offshore area, year-round (Gunter, 1938; Sheridan et al., 1984), although the spatial and temporal dynamics of this overlap are poorly understood.

Furthermore, information is limited on whether the distribution of sand seatrout offshore correlates with what is found inshore (bays) (Shlossman and Chittenden, 1981). Each of the bays along the Texas coastline is unique in their geological and hydrological characteristics, giving rise to differences in species assemblages between the bays (Blackburn, 2004).

Table 1

Sampling locations, location abbreviations, pass presence at locations (yes or no), and number of trawls (monthly and overall) conducted to sample sand seatrout (*Cynoscion arenarius*) and silver seatrout (*C. nothus*) in inshore and offshore waters off Texas. Geographic locations of the inshore and offshore trawling surveys are indicated in Figure 1. Offshore sampling sites (gulf stations) extended 16.7 km from the state boundary of Texas.

Location	Abbreviation for location	Pass presence	Sample size (no. of trawls /month)	Sample size (no. of trawls, overall)
Inshore sites				
Sabine Lake	SL	Yes	10	2760
Galveston Bay	GB	Yes	20	4800
East Matagorda Bay	EMB	No	10	2370
Matagorda Bay	MB	Yes	20	4800
San Antonio Bay	SAB	No	20	4800
Aransas Bay	AB	Yes	20	4800
Corpus Christi Bay	CCB	Yes	20	4800
Upper Laguna Madre	ULM	No	10	2400
Lower Laguna Madre	LLM	Yes	10	2400
Offshore sites				
Gulf station A	Gulf A	Yes	16	3840
Gulf station B	Gulf B	Yes	16	3814
Gulf station C	Gulf C	Yes	16	3822
Gulf station D	Gulf D	Yes	16	3792
Gulf station E	Gulf E	Yes	16	3829

Sand seatrout use functioning offshore passes to facilitate egg and larval transport from spawning areas (the immediate offshore) to nurseries (estuaries within bays) (Simmons and Hoese, 1959). However, the seasonal change in distribution of sand seatrout between these two locales has not been thoroughly examined. Furthermore, the differences in abundance of sand seatrout inhabiting bays with direct passes to the GOM and sand seatrout inhabiting bays with limited access to these passes have not been determined.

The purpose of this study was to expand current information regarding the distribution of sand and silver seatrout in the western GOM. To this end, two major objectives were identified 1) to compare the spatial and seasonal abundance of sand seatrout and silver seatrout within the immediate GOM, within the boundaries of Texas, and relate any distributional differences between the two species to specific hydrological variables (i.e., temperature, salinity, depth) and 2) to investigate the spatial and seasonal abundance of sand seatrout between the immediate offshore and the inshore areas (the bays) where there were direct passes to the gulf.

Materials and methods

Collections

We analyzed twenty years (1987–2006) of standardized offshore and inshore trawling data from Texas. The Coastal Fisheries Division of the Texas Parks and Wildlife Department (CF-TPWD) conducts annual monitoring of five gulf areas, as well as nine inshore bay systems (bays) within Texas waters (Table 1, Fig. 1). All of the major bay systems in Texas are protected from the GOM by geographical features such as islands or peninsulas. As such, bays were designated as all waters contained within the area between the Texas terrestrial shoreline and the associated barrier island or peninsula. Some of these bays have access to the GOM by means of a large navigable pass or cut directly through the geographical barrier, whereas other bays have limited access because of their distance from the gulf or to the navigational barrier presented by islands (Table 1). Gulf areas were those areas immediately offshore (outside the geographical barriers) and each was situated around major passes and extended 16.7 km from shore. Sampling by trawling was divided between the first half of the month (days 1–15) and the second half of the month (days 16- end of month) throughout all years. Sampling locations for gulf areas and bays were chosen randomly from a matrix of 1.85-km square grids. Grids were not sampled more than once a month. All samples were taken during daylight hours when both species are susceptible to trawling (Shlossman and Chittenden, 1981; DeVries and Chittenden, 1982).

Trawling was conducted with a 5.7-m otter trawl with 38-mm nylon multifilament mesh, for both locations (gulf areas and major bays). Trawls were towed at the bottom parallel to the fathom curve at a speed of 4.83 km/hr for ten minutes. Abundance was determined for all trawls as individuals collected per hour (ind.

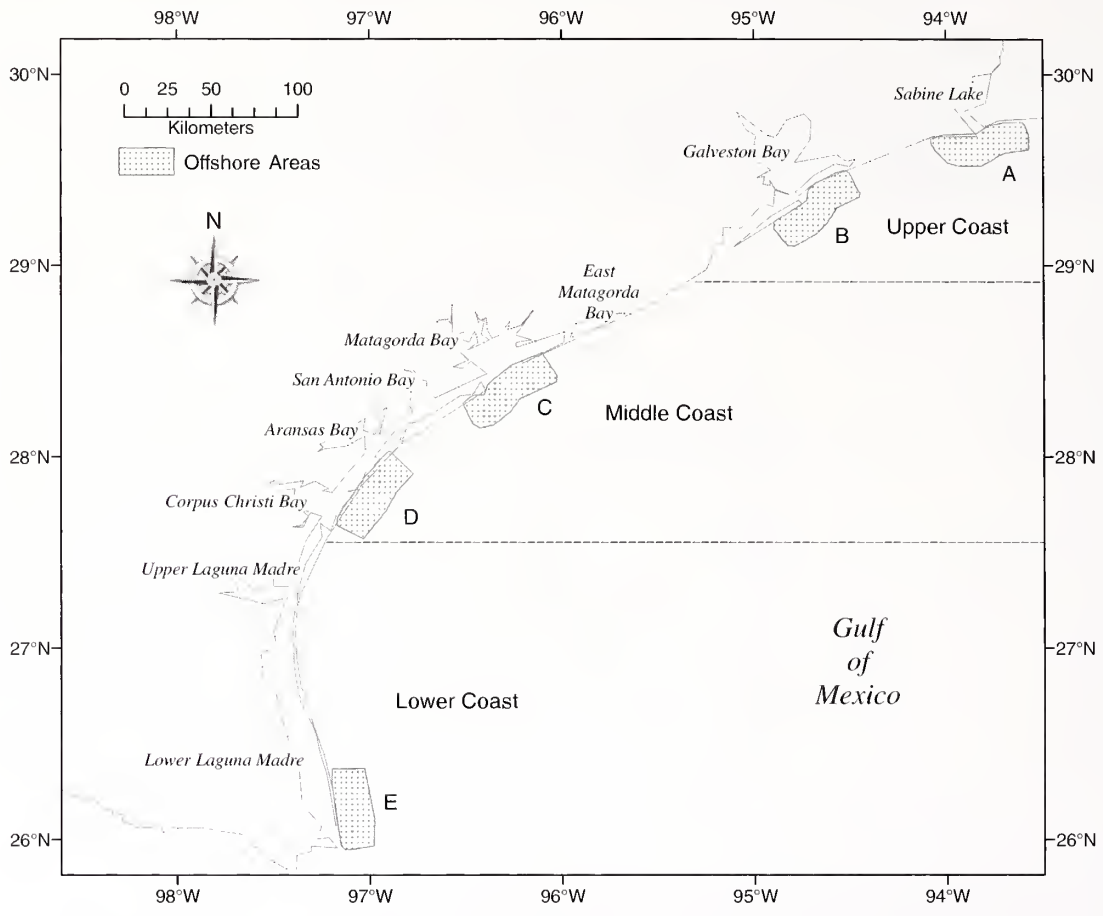

Figure 1

Map of the Texas coastline identifying major bay systems and offshore sampling areas routinely monitored by the Coastal Fisheries Division of the Texas Parks and Wildlife Department. Major bays are labeled by name, gulf areas discussed in the text are indicated by a shaded area and are labeled (A–E).

collected/hr) and served as a form of catch per unit of effort. Temporal variation in abundance was assessed from data by averaging the abundance of all trawls within a given season within a year and then averaging across all twenty years, and these results represented our temporal investigation. Seasons were designated as a three-month group: fall (October–December), winter (January–March), spring (April–June), and summer (July–September). In addition we recorded the mean total length (TL, mm) of each species and the following environmental variables: water temperature (°C) at depth of trawl (0.3 m off bottom); salinity (psu); and water depth (m) with each trawl.

Distribution of sand seatrout and silver seatrout

The abundance of sand seatrout and silver seatrout among offshore sampling areas was analyzed to determine 1) overall abundance of each species, within each gulf area, and 2) seasonal and species differentiation among gulf areas. First, overall differences in abundance between species were tested by using a t-test for species mean abundance (averaged over all years) at each gulf area. Then, a three-factor ANOVA was used, involving the following factors: gulf areas (n=5; all offshore sampling areas); seasons (n=4; all seasons); and species (n=2; both species) with all interactions. Species abundance was then correlated against each environmental variable by using Pearson correlation coefficients for each gulf area and season to determine the significance of the regressions.

Length-frequency histograms were created from the twenty-year data set by using catch-length data set, separated by month, and averaged over years for individual species collected across offshore areas. These histograms were created by partitioning individuals into 10-mm (TL) size classes and were used to describe cohort strength between species, by month.

Distribution of sand seatrout inshore

The abundance of sand seatrout at combined gulf areas (offshore) and at major bays (inshore) was analyzed to identify any spatial and temporal differentiation. To this end a two-factor ANOVA was employed involving the factors: location (n=2; combined gulf areas and combined

Table 2

Summary of ANOVA results of abundance data for sand seatrout (*Cynoscion arenarius*) and silver seatrout (*C. nothus*) from gulf areas (three-factor ANOVAs) and abundance of sand seatrout compared between locations, pass or no pass, and bays with pass presence (two-factor ANOVAs) averaged across twenty years (1987–2006) of trawl capture monitoring by Texas Parks and Wildlife. Log-transformed abundance data were the dependent variable in all analyses. Degrees of freedom (df), mean squares (MS), *F*-values (*F*), and *P*-values (*P*) reported. ns = $P>0.05$; * = $P<0.05$

Dependent variable	Factors	df	MS	*F*	*P*
Sand seatrout and silver seatrout (Log_{10} abundance)	Gulf areas	4	18.27	60.41*	<0.0001
	Season	3	4.15	13.73*	<0.0001
	Species	1	34.66	114.58*	<0.0001
	Gulf areas × season	12	1.79	5.93*	<0.0001
	Gulf areas × species	4	10.24	33.86*	<0.0001
	Season × species	3	5.48	18.12*	<0.0001
	Gulf areas × season × species	12	0.40	1.34 ns	0.1906
Sand seatrout (Log_{10} abundance)	Location	1	6.60	101.16*	<0.0001
	Season	2	0.35	5.31*	0.0062
	Location × season	2	0.14	2.17 ns	0.1192
Sand seatrout (Log_{10} abundance)	Pass	1	15.47	192.74*	<0.0001
	Season	2	0.70	8.70*	0.0003
	Pass × season	2	0.17	2.11 ns	0.1255
Sand seatrout (Log_{10} abundance)	Bays	5	3.68	22.72*	<0.0001
	Season	2	1.79	11.08*	<0.0001
	Bays × season	10	0.18	1.14 ns	0.3337

major bays) and seasons ($n=3$; fall, spring and summer), and interaction (the winter season was excluded from this analysis because of the invariably low counts of sand seatrout within both locations, across all years).

To determine whether abundance differed between bays with direct GOM passes and bays either without these passes or with limited offshore access, a two-factor ANOVA was used involving the following factors: pass presence ($n=2$; bays with a direct offshore pass and bays without a direct pass) and seasons ($n=3$), with interaction. Analyses were then focused on bays with direct passes in order to determine whether distribution differed among individual bays with passes, seasonally. This analysis employed a two-factor ANOVA, involving the following factors: bays ($n=6$; all major bays with passes) and seasons ($n=3$), with interaction. Length-frequency histograms of inshore sand seatrout were then created in a similar fashion to that used for the previously created offshore length-frequency histograms in order to qualitatively evaluate differences in monthly cohort size and size classes of sand seatrout between locations (i.e., offshore and inshore).

Statistical analyses

All data were first averaged across seasons for each year and then analyzed across years for all dependent variables in all parametric tests. All dependent variables in these analyses were first tested for normality by using a Shapiro-Wilk test; however, in the case of non-normality, data were log_{10}-transformed before analysis. All abundance data for ANOVAs involved all catch (zero catches included) so that catches were not overestimated. Statistical analyses and length-frequency histograms were carried out with SAS software (SAS vers. 8.02, SAS Inst., Inc., Cary, NC) and illustrated by using SigmaPlot (SigmaPlot vers. 10.0, Systat Software, Inc., Point Richmond, CA).

Results

Distribution of sand seatrout and silver seatrout

Sand seatrout abundance was significantly lower (13.2 ±6.7) than that of silver seatrout (37.2 ±17.7) ($t=-8.55$, $P<0.0001$). In addition, significant spatial and seasonal differences existed between sand and silver seatrout abundance, including significant interactive effects, and differences between species accounted for a majority of the variance in abundance in trawls in the 3-factor model (Table 2). The first interaction, season×species, revealed a lower abundance of silver seatrout throughout the summer season (Fig. 2A). Sand seatrout abundance was high during July and decreased by August, whereas silver seatrout abundance peaked in April, declined in June, and was minimal by July (Fig. 3). The second interaction, gulf area × species, revealed a high abundance of sand seatrout and low abundance of silver seatrout in the gulf area A (Fig. 4). The gulf area × season interaction although significant, explained only a minimal amount of variance in abundance and

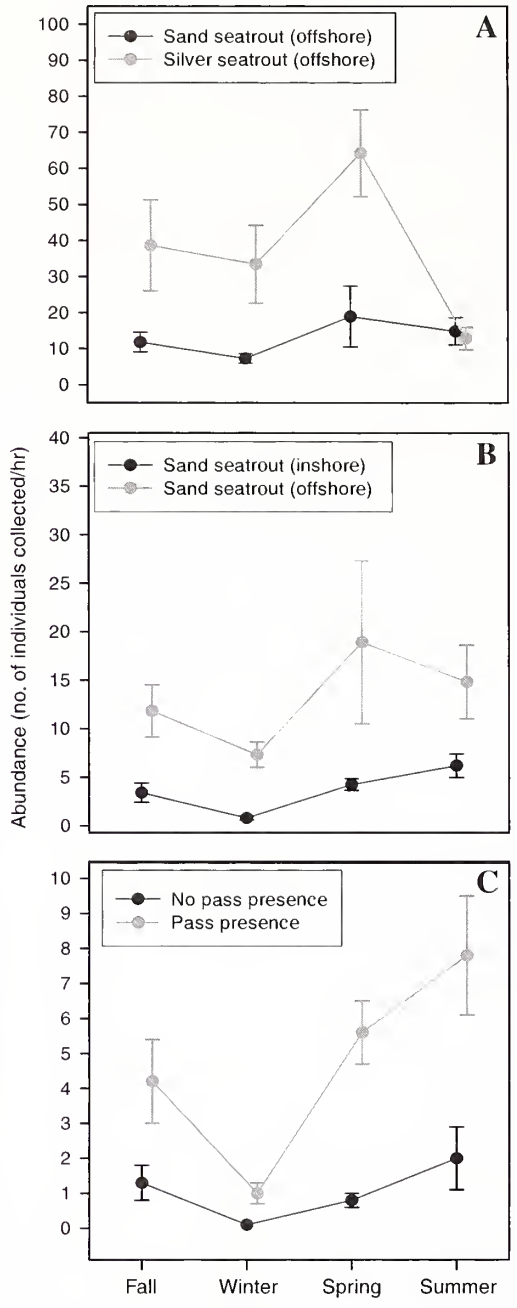

Figure 2

Differences in seasonal mean abundances (individuals collected/hr, mean ±standard error), averaged over twenty years of trawl data (1987–2006), for (A) a comparison of sand seatrout (*Cynoscion arenarius*) collected off the coast of Texas (offshore) and silver seatrout (*C. nothus*) collected offshore, and (B) a comparison of sand seatrout collected inshore (combined major bays) and offshore (combined Gulf of Mexico sampling areas), and (C) a comparison of sand seatrout collected inshore between bays with direct passes to the gulf and sand seatrout collected in bays without direct access to the gulf.

did not warrant further investigation for the primary objectives of this study. When comparing species across gulf areas, we found significant differences in species abundance across seasons. Sand seatrout appear to be in their highest abundance along the upper coast, whereas silver seatrout are found primarily in the middle coast, especially in gulf areas C and D (Figs. 1 and 5).

Water depths between our offshore sampling areas increased from north to south. Water depths (range, mean depth ±standard deviation [SD]) among gulf areas were as follows: gulf area A (1.2–12.8, 7.6 ±2.8), gulf area B (0.9–18.0, 10.5 ±3.4), gulf area C (1.2–26.5, 14.9 ±4.8), gulf area D (0.4–23.8, 15.2 ±4.7), and gulf area E (2.4–30.0, 18.6 ±5.2). Within gulf areas, silver seatrout were more abundant at deeper water depths, and this trend was particularly strong during the fall season in gulf areas A, C, and D ($P<0.05$) and during the winter season in gulf areas of A–D ($P<0.01$). In contrast, sand seatrout abundance was inversely related to water depth within these gulf areas (Fig. 6). However, sand seatrout abundance was inversely related to water depth among gulf areas ($r=-0.61$, $P<0.0001$) (Fig. 7), whereas silver seatrout abundance was not significantly correlated with depth among offshore areas ($r=0.06$, $P=0.49$). Water temperature correlation coefficients exhibited no correlation with the presence of sand seatrout, whereas the presence of silver seatrout appear to have a strong positive relationship with water temperature specifically for the winter season in gulf areas (A–D) ($P<0.01$) (Fig. 8C).

Salinity between our offshore sampling areas increased from north to south. Salinity among gulf areas were (range, mean salinity ±SD); gulf area A (3.2–40.0, 26.4 ±4.8), gulf area B (9.0–42.0, 29.1 ±4.6), gulf area C (2.4–43.0, 31.4 ±3.5), gulf area D (2.4–44.0, 32.4 ±3.4), and gulf area E (23.0–42.6, 33.6 ±2.6). Although there were no significant differences in abundance between these species at different salinities locally (Fig. 8B), salinity did appear to play a role in the broad-scale geographic distribution of the two species, particularly that of sand seatrout. Sand seatrout displayed a strong inverse relationship with salinity among gulf areas, across years ($r=-0.56$, $P<0.0001$) (Fig. 9), whereas silver seatrout displayed no relationship with salinity among gulf areas, across years ($r=-0.02$, $P=0.8003$).

Distribution of sand seatrout inshore

Sand seatrout were much less common inshore than in offshore catches. Sand seatrout abundance inshore (mean ±standard error of ind. collected/hr) (4.6 ±0.6) was significantly lower ($P<0.0001$) than abundance offshore (15.2 ±3.3). There was also a significantly higher abundance ($P=0.0062$) of sand seatrout collected in both summer (10.5 ±2.4) and spring (11.6 ±4.7) seasons than during the fall season (7.6 ±1.9). The interactive effects of location and season did not reveal a significant effect on sand seatrout abundance ($P=0.1192$); this result was due to trends in inshore abundance among seasons being generally predictive of trends in offshore

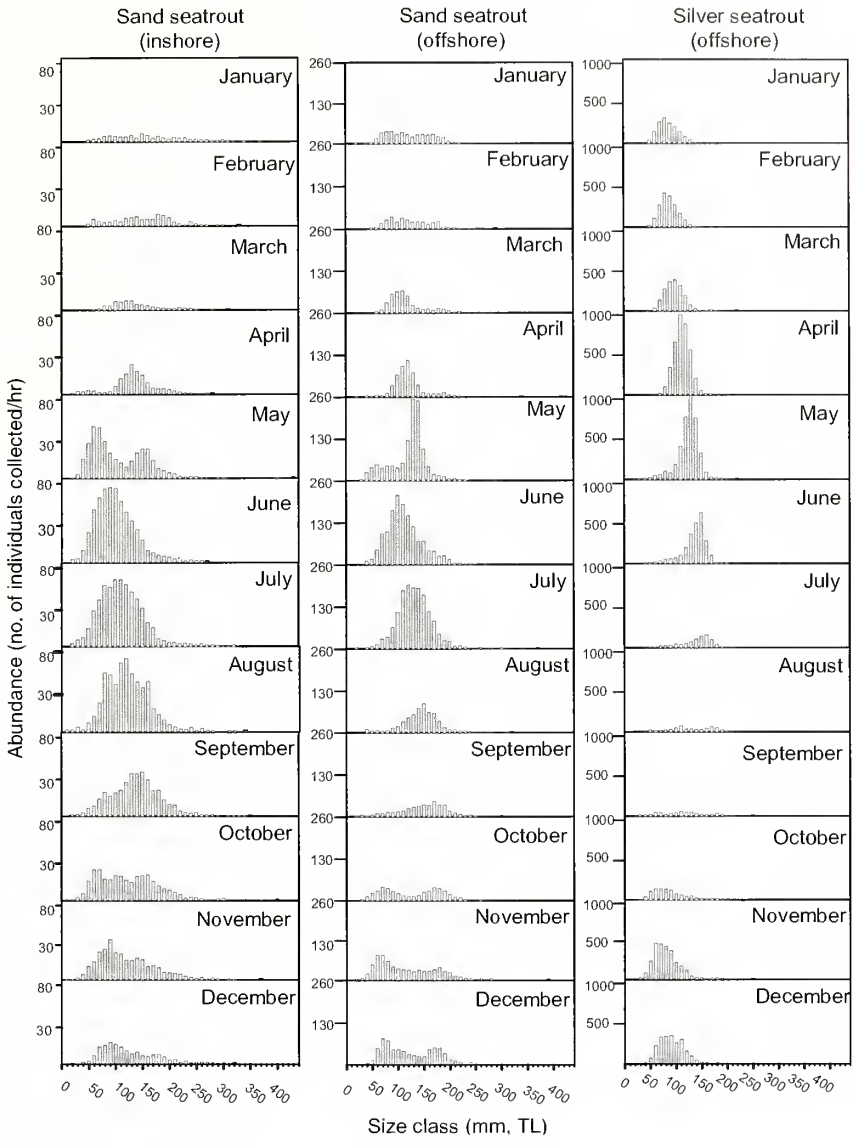

Figure 3

Monthly length-frequency histograms (averaged over twenty years of trawl data (1987–2006)) for combined major bays (inshore) in the Gulf of Mexico for sand seatrout (*Cynoscion arenarius*), combined gulf sampling areas (offshore) for sand seatrout, and for combined offshore sampling areas for silver seatrout (*C. nothus*), by 10-mm total length (TL) size classes.

abundance, although overall abundance remained higher offshore (Fig. 2A). The length-frequency histograms further illustrated differences in abundance among locations (Fig. 3). Sand seatrout collected inshore appeared to decrease in abundance after August, whereas offshore sand seatrout began to decrease in abundance after spring, specifically after July. Additionally, clear bimodal peaks in abundance were evident for May in both inshore and offshore areas, reflecting the bimodal spring and late-summer+fall spawning times of sand seatrout (Shlossman and Chittenden, 1981).

Sand seatrout were significantly higher ($P<0.0001$) in abundance in major bays with passes (mean ±SE) (5.9 ±0.8) than in bays without direct passes (1.4 ±0.4) (Table 2). There was also significant seasonal difference ($P=0.0003$) inshore; abundance was higher in the summer (4.9 ±1.3) than in spring (3.2 ±0.9) and fall (2.8 ±0.8). The interactive effects of pass presence and season were not significant ($P=0.1255$) (Fig. 2B). However, sand seatrout differed significantly in abundance among bays with passes ($P<0.0001$) (Table 2), and all bays were significantly greater in abundance than the

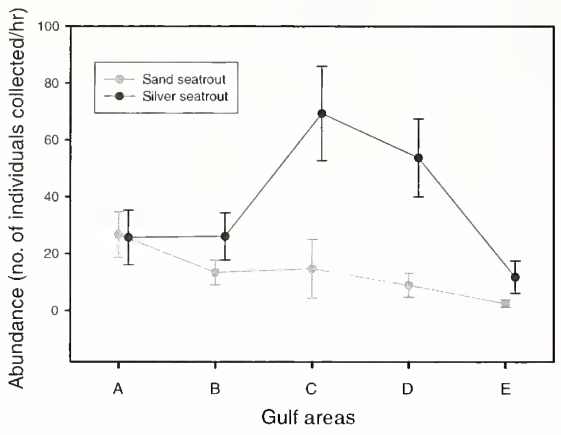

Figure 4

Differences in annual mean abundance (individuals collected/hr, mean ±standard error), averaged over twenty years of trawl data (1987–2006), of sand seatrout (*Cynoscion arenarius*) and silver seatrout (*C. nothus*) collected offshore within sampling areas of the Gulf of Mexico (A–E).

Lower Laguna Madre (Fig. 10). There was a significant seasonal difference ($P<0.0001$) among bays with passes; abundance was greater in summer (7.6 ±1.5) than in spring (5.3 ±1.0) and fall (4.1 ±0.8). No significant interactive effects were reported for bays with direct passes and seasons ($P=0.3337$), and this result was due to parallel seasonal patterns among the bays. Abundance of sand seatrout was highest for inshore areas from Corpus Christi Bay north, for all seasons (Fig. 11).

Discussion

Distribution between species offshore

Evidence from this study established a significantly lower concentration of sand seatrout than that of silver seatrout within 16.7 km of the immediate GOM, within the boundaries of Texas. Miller (1965) and Chittenden and McEachran (1976) also recorded a lower abundance of sand seatrout than silver seatrout, but they did not investigate the cause. The lower abundance of sand seatrout than silver seatrout is most likely due to differences in their life histories and environmental preferences. Sand seatrout use both the offshore and inshore bays in contrast to silver seatrout which use the offshore throughout their lives (Shlossman and Chittenden, 1981; DeVries and Chittenden, 1982). Sand seatrout primarily use these estuaries during early life stages, most probably because of the relatively sensitive tolerances of juveniles to salinity. In contrast, silver seatrout have a much higher salinity tolerance and are more likely to be abundant off the coast of Texas where salinities are higher than off the coasts of Louisiana or Mississippi, where salinities are reduced by the productive Mississippi and Atchafalaya rivers (Dinnel and Wiseman, 1986).

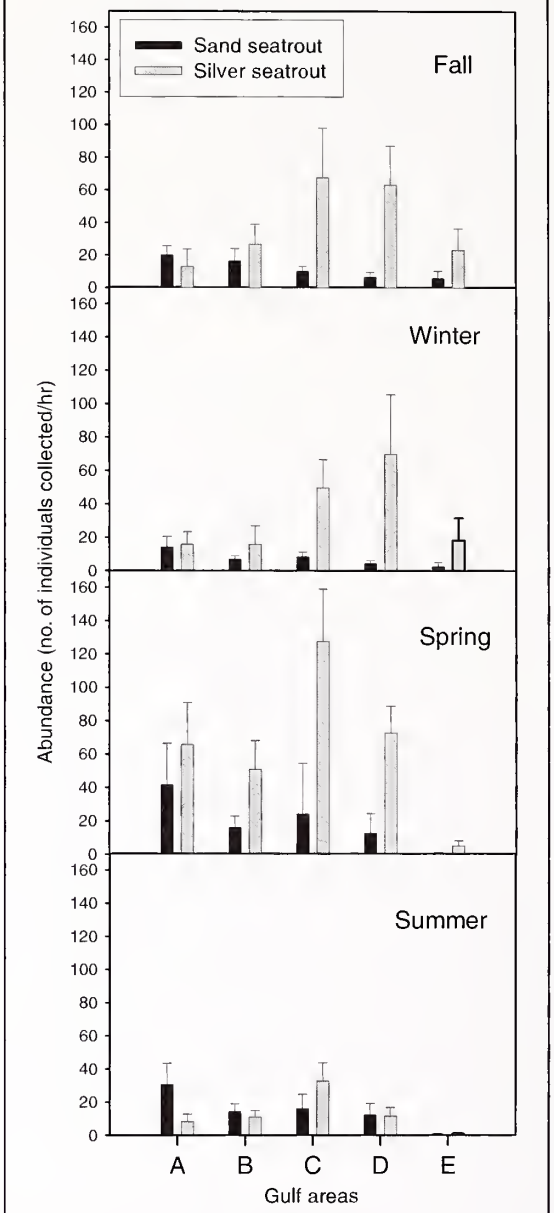

Figure 5

Differences in seasonal mean abundance (individuals collected/hr, mean ±standard error), averaged over twenty years of trawl data (1987–2006), for sand seatrout (*Cynoscion arenarius*) (black bars) and silver seatrout (*C. nothus*) (gray bars) in sampling areas of the Gulf of Mexico (A–E).

The offshore abundance of sand seatrout was lower than that of silver seatrout for every season other than summer. In the summer season, offshore silver seatrout

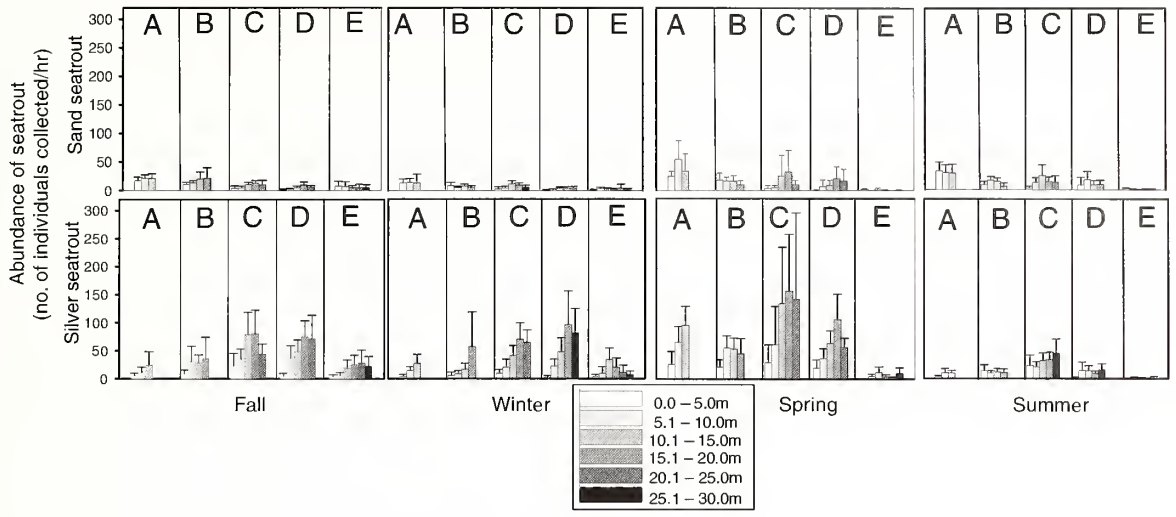

Figure 6

Average seasonal abundance (individuals collected/hr, mean ±standard error), averaged over twenty years of trawl data (1987–2006), for sand seatrout (*Cynoscion arenarius*) (top) and silver seatrout (*C. nothus*) (bottom) averaged by different water depths collected in sampling areas of the Gulf of Mexico (A–E). Depths are represented by shades.

abundance tended to drop dramatically. This finding is similar to the results of DeVries and Chittenden (1982) who also described a reduction in silver seatrout abundance offshore in summer and may also be due to offshore migrations, die offs, or sampling errors.

Low silver seatrout abundance during the summer season may be due to their migrations farther offshore. Although summer migration outside of CF-TPWD sampling areas (>16.7 km from shoreline) has not been reported for silver seatrout, they do migrate during winter (DeVries and Chittenden, 1982) and summer migrations occur in similar species (Vetter, 1982). A spatial analysis of offshore sampling areas indicated that samples of both species were commonly collected in the outermost (most offshore) grids sampled (data not shown). Thus, it is possible that the true center of distribution of silver seatrout was not sampled in our study and that offshore migration during summer months is reflective of seasonal movements into deeper water.

Low silver seatrout abundance during the summer season may also be due to adult die offs of a species with a short life span. DeVries and Chittenden (1982) estimated a maximum life span for silver seatrout of one to one-and-a-half years of age. Not only are they short-lived, but they are also summer spawners. Thus, the reduction in abundance in summer may reflect cyclic spawning, followed by the die-off of spawners.

Finally, low silver seatrout abundance during the summer season may be due to sampling bias in that the capture of the larger-size silver seatrout may have been limited. Sheridan et al. (1984) captured numerous silver seatrout >200 mm TL; our samples were rarely >200 mm TL. However, Sheridan et al. (1984) did not describe their trawl methods, specifically their

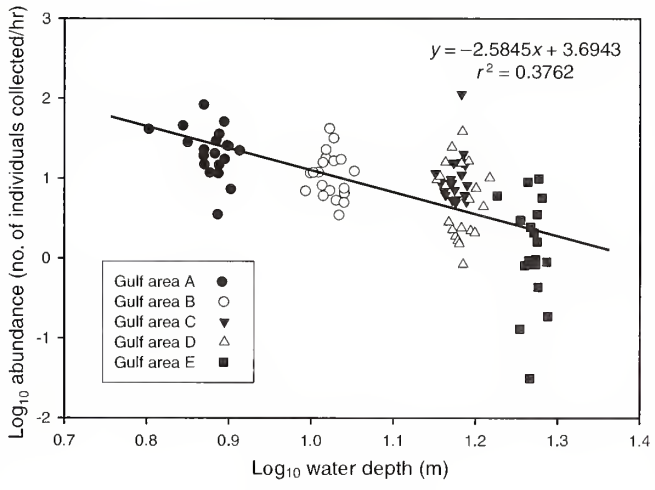

Figure 7

Least-square regression for annual mean water depth (m) and annual mean abundance (individuals collected/hr), averaged over twenty years of trawl data (1987–2006) for sand seatrout (*Cynoscion arenarius*) collected across sampling areas in the Gulf of Mexico. Each gulf area (A–E) is represented by a different symbol.

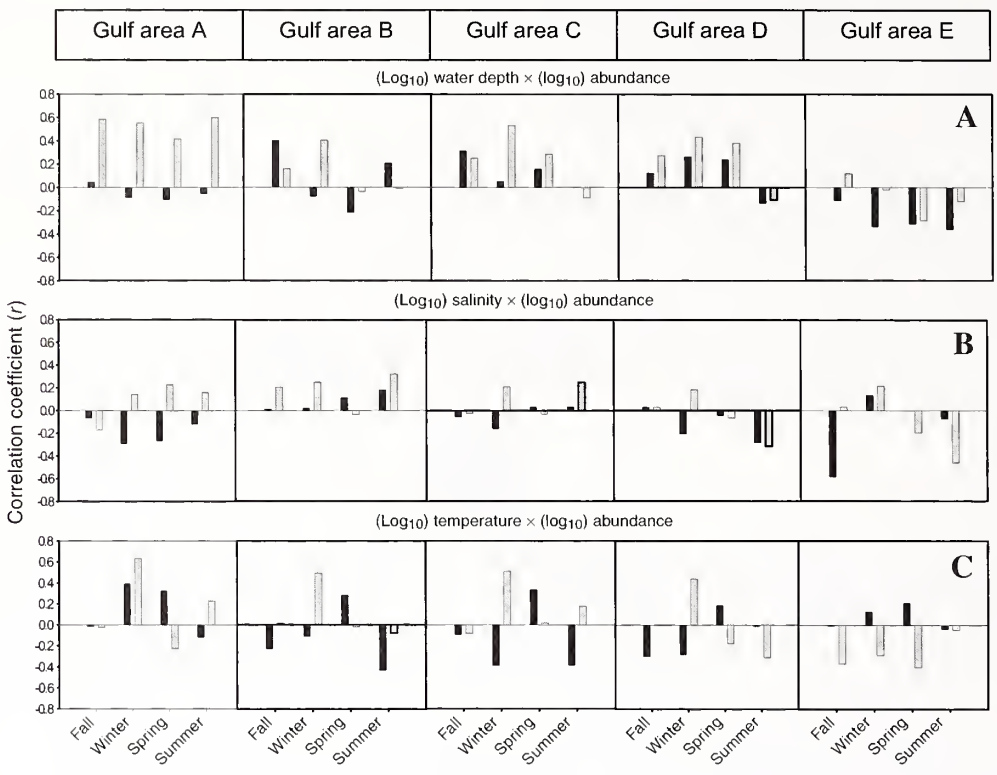

Figure 8

Correlation coefficients (r) describing the relation between annual mean abundance (individuals collected/hr), averaged over twenty years of trawl data (1987–2006) for sand seatrout (*Cynoscion arenarius*) and silver seatrout (*C. nothus*) collected across all sampling areas in the Gulf of Mexico (A–E) (black bars=sand seatrout, gray bars=silver seatrout) and (**A**) water depth (m), (**B**) water salinity (psu), and (**C**) water temperature (°C).

mesh sizes, and therefore a direct comparison of data cannot be made. Depending on their ability and size, fishes attempt to avoid contact with trawl gear by either maintaining position at the net opening (Wardle, 1983) or by falling back along the taper of the body panel of the trawl net towards the codend opening (Wardle, 1983), as discussed by Broadhurst et al. (2000). Thus trawl configuration can play a role in limiting the size and condition of fishes that are captured. In contrast to silver seatrout, sand seatrout are found offshore within gulf areas in highest abundance during the spring and summer seasons. Increased spring abundance may be due to both the mature-size individuals emigrating from bays to the offshore in order to spawn as well as to the presence of recently spawned young of the year during May–July (Fig. 3). In any case, the relative abundance of sand seatrout off the coast of Texas is dramatically lower than that of silver seatrout, in all seasons other than summer.

There is a difference in the distribution of both sand and silver seatrout in offshore gulf areas. Whereas silver seatrout are found predominately along the middle coast, sand seatrout, although lower in overall abundance, appear to decrease in abundance from north to south. Moore et al. (1970) described somewhat similar results, namely a higher abundance of sand seatrout within Louisiana waters and more silver seatrout in Texas waters. The distributional distinctions between species in our study correlated well with both salinity and water depth. Sand seatrout were shown to have a preference for lower salinities, whereas silver seatrout prefer higher salinities (ranging from 7.5 to 38.6 psu) (Swingle, 1971). In addition, Ginsburg (1931) and Miller (1965) have reported the water depth preferences for sand seatrout (shallower depths) and silver seatrout (deeper depths). Gulf area A, because it is shallower and less saline than the other gulf areas, appears to be ideal habitat for sand seatrout, whereas silver seatrout prefer the deeper and more saline gulf areas C and D. Correlation between depth and abundance also occurred locally, within selected sampling areas. For instance, within gulf area A, silver seatrout were found specifically within the deepest grids, for all seasons. Also, silver seatrout were found in deeper waters during fall and winter, across most sampling areas, indicating the occurrence of an offshore winter migration during

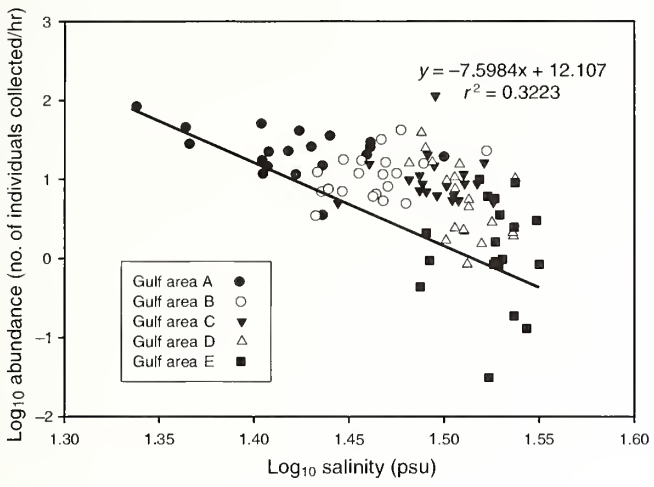

Figure 9

Least-square regression for annual mean salinity (psu) and annual mean abundance of sand seatrout (*Cynoscion arenarius*, individuals collected/hr) in Gulf of Mexico areas, averaged over twenty years of trawl data (1987–2006). Each gulf sampling area (A–E) is represented by a different symbol.

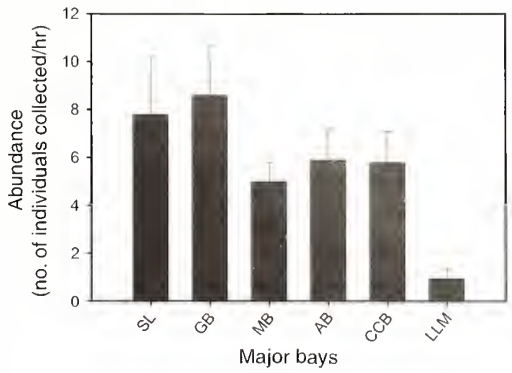

Figure 10

Differences in annual mean abundance (individuals collected/hr, mean ±standard error), averaged over twenty years of trawl data (1987–2006) for sand seatrout (*Cynoscion arenarius*) collected in bays with direct access to the Gulf of Mexico. (SL=Sabine Lake, GB=Galveston Bay, MB=Matagorda Bay, AB=Aransas Bay, CCB=Corpus Christi Bay, and LLM=Lower Laguna Madre).

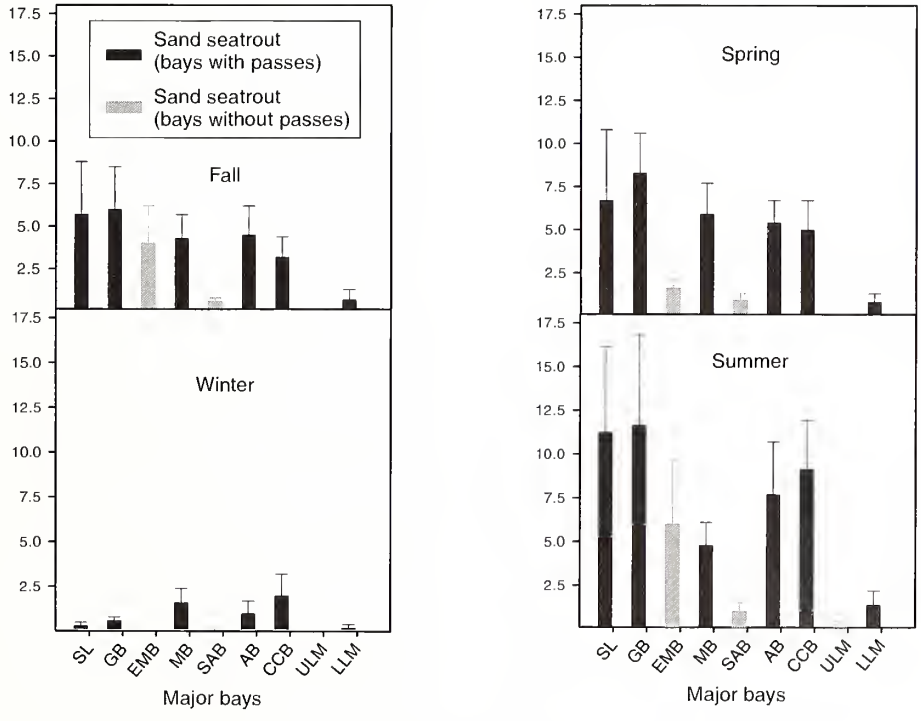

Figure 11

Differences in seasonal mean abundance (individuals collected/hr, mean ±standard error), averaged over twenty years of trawl data (1987–2006) for sand seatrout (*Cynoscion arenarius*) collected within bays with passes (black bars) and without direct passes to the Gulf of Mexico (gray bars) (SL=Sabine Lake, GB=Galveston Bay, EMB=East Matagorda Bay, MB=Matagorda Bay, SAB=San Antonio Bay, AB=Aransas Bay, CCB=Corpus Christi Bay ULM=Upper Laguna Madre, and LLM=Lower Laguna Madre).

cooler months, as reported by DeVries and Chittenden (1982). Sand seatrout also may migrate to the deeper waters of the GOM in response to either photoperiod or temperature extremes of winter and summer (Vetter, 1982), although they tend to be found at shallower depths than those occupied by silver seatrout in the gulf areas. The environmental variables for Gulf area E formed an exception in our data; there were no correlations found with the presence of either species. This result may have been caused by environmental factors that were outside the optimum for both species, which resulted in neither species being found in high abundance in this area.

Water temperature displayed some correlation with the preference of silver seatrout for warmer waters, during the winter season across relevant gulf areas (A–D). This correlation, in conjunction with the propensity of silver seatrout to be found deep in the water column, may indicate that they have less temperature tolerance than sand seatrout.

Distribution of sand seatrout inshore

Sand seatrout are unique among their GOM congenerics in their extensive use of both inshore and offshore areas, compared to spotted seatrout (a primarily inshore species) and silver seatrout (a primarily offshore species). Therefore the intent of the second objective of our study was to relate the abundance of sand seatrout between these two locations and further to characterize factors that correlated with their inshore distribution. To this end, the overall abundance at the offshore and inshore locations was compared. Second, the effectiveness of direct passes between the inshore and offshore areas in predicting sand seatrout abundance was examined. Finally, the correlation between abundance inshore and offshore was examined in order to demonstrate whether increased inshore abundance was predictive of increased offshore abundance in the same area.

Despite using both offshore and inshore areas, sand seatrout were significantly less abundant inshore than offshore, in all seasons. Additionally, trends in inshore abundance appeared to mirror trends in offshore abundance, with abundance increasing in spring and summer and decreasing in fall and winter. These trends correspond with spawning cycles followed by spawning inactivity, and are comparable to trends suggested by Shlossman and Chittenden (1981). For instance, sand seatrout migrate offshore from inshore areas during temperature extremes (Vetter, 1982) and for spawning (Gunter, 1945). Additionally, older fish may become more tolerant of higher salinity levels with age, in general resulting in older fish using offshore areas more frequently. The offshore abundance of sand seatrout may also result from nutritional preferences of mature fish. Sand seatrout found offshore are generalists, preying on both fish and crustaceans that are found at offshore depths of 3.5–22 m (known white shrimp grounds) during June–September and that are most common in the depths of 22–91 m (known brown shrimp grounds) during January–March (Chittenden and McEachran, 1976; Byers, 1981). Finally, sand seatrout are found in highest abundance inshore during the summer, a finding that is similar to what has been indicated by Byers (1981). Shlossman and Chittenden (1981) suggested that this abundance is due to the introduction of the recently spring-spawned offspring to the inshore population (Shlossman and Chittenden, 1981), which thus consists primarily of age-1 individuals that have not yet moved offshore.

Inshore sand seatrout abundance was different among locations, and correlated closely with the presence or absence of direct access to GOM spawning grounds. It has previously been noted that sand seatrout have a higher affinity for bays with direct passes to the offshore than to bays with no direct passes. For instance, Simmons and Hoese (1959) suggested that pass presence is imperative for seasonal sand seatrout migration, although they did not directly quantify the effect of pass presence on abundance. The data in the present study demonstrated a disparity in abundance between bays with direct access to offshore water and bays with some limitations to offshore water, whether it is distance or a barrier by islands. In fact, pass presence is the most influential global factor in affecting abundance among the various inshore bays. Pass presence clearly affects movements of fishes offshore and inshore; therefore, for a migratory species that moves between the two areas annually, pass presence is critical to inshore abundance. Shlossman and Chittenden (1981) suggested that although sand seatrout nurseries may be found both in estuarine and offshore habitats, estuarine areas may be the most important habitat for late summer age-1 fish. Finally, Shlossman and Chittenden (1981) noted that the spawning of sand seatrout coincides with onshore winds and surface currents that facilitate passive transport of eggs and larvae to inshore nurseries; thus pass presence would have a significant effect on abundance within bays, particularly during early life stages.

A second factor that significantly indicated inshore abundance of sand seatrout was abundance in the contiguous offshore area. Sand seatrout abundance within bays with direct passes is significantly higher in bays from Corpus Christi Bay, north, and this high abundance correlates with the overall abundance of sand seatrout offshore, year round. For major bays with low sand seatrout abundance, such as the Lower Laguna Madre, there is a corresponding lower overall abundance offshore (i.e., in gulf area E). One exception to this finding is the unique assemblage of species found in the hypersaline Lower Laguna Madre—species that are not seen elsewhere along the Texas coast. In this instance, it is likely that both hypersaline conditions and low offshore abundance have limited the abundance of sand seatrout inshore of Lower Laguna Madre.

Sand seatrout inshore abundance is thus related to a host of different factors. Access to offshore waters is the most significant factor, but it is important to note that inshore transport of eggs and larvae and offshore mi-

gration of adults are limited by pass size, configuration, and distance. However, there are also global factors such as the population abundance within offshore areas that affect inshore abundance, which decreases from north to south along the Texas coast. In turn, offshore abundance is likely related to hydrological factors such as depth and salinity, such that inshore populations of sand seatrout are not independent of offshore abiotic conditions. However, offshore abundance may be equally affected by the presence and availability of estuarine nursery areas, because estuaries are highly productive and offer an alternative location for the growth of age-1 individuals. This supposition was not explicitly tested in our study because all offshore gulf areas in this study were located near estuarine passes. However, it is clear that offshore and inshore abundance are closely linked, and the presence of a pass between the two likely affects abundance of local populations as a whole.

Acknowledgments

We thank biologists of the Texas Parks and Wildlife Department-Coastal Fisheries Division (TPWD-CF), specifically the countless dedicated technicians and biologists who collected the data as part of their routine monitoring activities that are funded in part by Federal Aid in Sportfish Restoration Grant (FRM-34). We thank B. Balboa for his expertise and time. Improvements to the first draft were provided by M. Fisher (TPWD), B. Karel (TPWD), C. Williams (TSU), and wife Christa (of Dusty McDonald), and three anonymous reviewers. This research project was funded in part by dedicated funds from a Federal Aid in Sportfish Restoration Grant (F-158-R).

Literature cited

Blackburn, J.
2004. The book of Texas bays (Gulf coast studies), 1st ed., 290 p. Texas A&M Univ. Press, College Station, TX.

Broadhurst, M. K., P. E. McShane, and R. B. Larsen.
2000. Effects of twine diameter and mesh size in the body of prawn trawls on bycatch in Gulf St. Vincent, Australia. Fish. Bull. 98:463–473.

Byers, S. M.
1981. Trophic relationships of two sympatric sciaenid fishes, *Cynoscion arenarius* and *Cynoscion nothus*, in the north central Gulf of Mexico. M.S. thesis, 70 p. Univ. Southern Mississippi, Hattiesburg, MS.

Chittenden, M. E., and J. D. McEachran.
1976. Composition, ecology, and dynamics of demersal fish communities on the northwestern Gulf of Mexico continental shelf, with a similar synopsis for the entire Gulf, 104 p. Sea Grant Publication TAMU-SG-76-208, Texas A&M Univ., College Station, TX.

DeVries, D. A., and M. E. Chittenden.
1982. Spawning, age determination, longevity and mortality of the silver seatrout, *Cynoscion nothus*, in the Gulf of Mexico. Fish. Bull. 80(3):487–500.

Dinnel, S. P., and W. J. Wiseman.
1986. Freshwater on the Louisiana and Texas shelf. Cont. Shelf Res. 6:765–784.

Ginsburg, I.
1931. On the difference in the habitat and the size of *Cynoscion arenarius* and *C. nothus*. Copeia 1931:1–144.

Gunter, G.
1938. Notes on invasion of fresh water by fishes of the Gulf of Mexico, with special reference to the Mississippi-Atchafalaya River system. Copeia 1938:69–72.
1945. Studies of marine fishes of Texas. Contrib. Mar. Sci. 1:1–190.

Miller, J. M.
1965. A trawl survey of the shallow Gulf fishes near Port Aransas, Texas. Contrib. Mar. Sci. 10:80–107.

Moore, D., H. A. Brusher, and L. Trent.
1970. Relative abundance, seasonal distribution, and species composition of demersal fishes off Louisiana and Texas, 1962–1964. Contrib. Mar. Sci. 15:45–70.

Sheridan, P. F., D. L. Trimm, and B. M. Baker.
1984. Reproduction and food habits of seven species of northern Gulf of Mexico fishes. Contrib. Mar. Sci. 27:175–204.

Shlossman, P. A., and M. E. Chittenden Jr.
1981. Reproduction, movements, and population dynamics of the sand seatrout, *Cynoscion arenarius*. Fish. Bull. 79:649–669.

Simmons, E. G., and H. D. Hoese.
1959. Studies on the hydrography and fish migrations of Cedar Bayou, a natural tidal inlet on the central Texas coast. Contrib. Mar. Sci. 7:56–80.

Swingle, H. A.
1971. Biology of Alabama estuarine areas-cooperative Gulf of Mexico estuarine inventory. Ala. Mar. Resour. Bull. 5:1–123.

Vetter, R. D.
1982. Seasonal metabolic compensation in sympatric seatrout: adaptation to the estuary. Trans. Am. Fish. Soc. 111:193–198.

Wardle, C. S.
1983. Fish reactions to towed fishing gears. *In* Experimental biology at sea (A. MacDonald, and I. G. Priede, eds.), p.167–195. Academic Press, New York, NY.

Biological response to changes in climate patterns: population increases of gray snapper (*Lutjanus griseus*) in Texas bays and estuaries

James M. Tolan (contact author)[1]

Mark Fisher[2]

Email address for contact author: james.tolan@tpwd.state.tx.us

[1] Texas Parks and Wildlife Department, Coastal Fisheries Division
6300 Ocean Dr., Natural Resources Center, Suite 2501, Unit 5846
Corpus Christi, Texas 78412

[2] Texas Parks and Wildlife Department, Coastal Fisheries Division
Rockport Marine Science Laboratory
Rockport, Texas 78382

Abstract—The increase in the abundance of gray snapper (*Lutjanus griseus*) in Texas bays and estuaries over the past 30 years is correlated to increased wintertime surface water temperatures. Trends in the relative abundance of gray snapper are evaluated by using monthly fishery-independent monitoring data from each of the seven major estuaries along the Texas coast from 1978 through 2006. Environmental conditions during this period demonstrated increasing annual sea surface temperatures, although this increase was not seasonally uniform. The largest proportion of temperature increases was attributed to higher winter temperature minimums since 1993. Positive phases of the North Atlantic Oscillation, resulting in wetter, warmer winters in the eastern United States have occurred nearly uninterrupted since the late 1970s, and unprecedented positive index values occurred between 1989 and 1995. Increases in water temperature in Texas estuaries, beginning in the early 1990s, are postulated to provide both favorable over-wintering conditions for the newly settled juveniles and increased recruitment success. In the absence of cold winters, this species has established semipermanent estuarine populations across the entire Texas coast. A shift to negative phases of the North Atlantic Oscillation will likely result in returns to colder winter temperature minimums that could reverse any recent population gains.

Manuscript submitted 21 March 2008.
Manuscript accepted 5 September 2008.
Fish. Bull. 107:36–44 (2009).

The views and opinions expressed or implied in this article are those of the author and do not necessarily reflect the position of the National Marine Fisheries Service, NOAA.

Decadal and multidecadal climate variability in the eastern United States and North Atlantic Ocean are sensitive to natural climate variability associated with the North Atlantic Oscillation-Arctic Oscillation (NAO-AO; Okumura et al., 2001). Ocean-atmosphere interactions between sea-level atmospheric pressure and sea surface temperature have resulted in periods of intensified climate variability at 50–80 year cycles (Enfield et al., 2001; Cronin et al., 2003). Interannual fluctuations in fishery catches that are linked to climate variability occur in many marine systems; the best examples are found in the North Pacific Ocean and Bering Sea (reviewed in Roessig et al., 2004, but also see Perry et al., 2005; Zeeburg et al., 2008). Huge increases in fish populations in the North Atlantic Ocean ("fish outbursts" in Hare and Able [2007]) have been linked to decadal-scale fluctuations in both atmospheric pressure gradients and water temperatures. Examples include dramatic fluctuations in gadoids (Sirabella et al., 2001), sciaenids (Hare and Able, 2007), pleuronectids (Sullivan et al., 2005), and in the size of fish assemblages—the latter caused by changes to the estuarine ecosystem (Attrill and Power, 2002). Changes in fish populations along the west coast of the Americas have also been related to shorter time-scale climate variation associated with El Niño patterns (Arcos et al., 2001; Smith and Moser, 2003). Few studies have examined the link between ecosystem structure, fisheries production, and climatic forcing along the southeastern coasts of the United States (including "the Gulf" of Mexico, hereafter referred to as "the gulf"), but those that have (Parker and Dixon, 1998; Sullivan et al., 2005) generally identify warmer winter temperatures as the cause of distributional changes in fish populations (Oviatt, 2004; Preston, 2004).

The gray snapper (*Lutjanus griseus*) is a temperate and tropical reef fish, commonly found in marine and estuarine waters in the western Atlantic Ocean from Florida through Brazil, including Bermuda, the Caribbean, and the northern Gulf (Randall, 1968; Rutherford et al., 1989a). Although the young of this species have been collected as far north as Cape Cod, Massachusetts (Denit and Sponaugle, 2004), they are most prevalent in continental and island shelf waters in the vicinity of south Florida, Cuba, and Venezuela (Allman and Grimes, 2002). Larvae and juvenile fish are common inshore in seagrass and mangrove nursery areas and have been even found in freshwater estuaries. Adults are usually associated with complex structures (such as rocky areas, coral reefs, pilings, and docks) and mangrove sloughs (gaining them the often-used local name

of mangrove snapper). Because of their affinity for hard bottom substrates, gray snapper are especially common on the numerous artificial reefs, such as oil and gas platforms, and on other man-made structures located on the northern gulf continental shelf from Alabama to Texas (Fischer et al., 2005).

Studies of the life history characteristics of gray snapper (Rutherford et al., 1989b; Burton, 2001) have revealed this species to be both euryhaline (they have been observed in salinities ranging from 0 to 67) and thermally tolerant (in temperatures ranging from 12.8° to 31.7°C). The lower lethal temperature limit is reported to be 11–14°C (Starck and Schroeder, 1971) and increased mortalities accompany sudden temperature drops. Cold kills of gray snapper (along with other estuarine and coastal fishes) have been reported at numerous times along the Texas Gulf coast (Gunter, 1941, 1951; McEachron et al., 1994). These cold kills of tropical species in Texas waters have previously been associated with warmer than usual summer and fall temperatures that stimulate tropical species either to move inshore or to remain inshore much later into the winter than would otherwise occur, thereby leaving them more vulnerable to sudden cold spells (Moore, 1976, Holt and Holt, 1983).

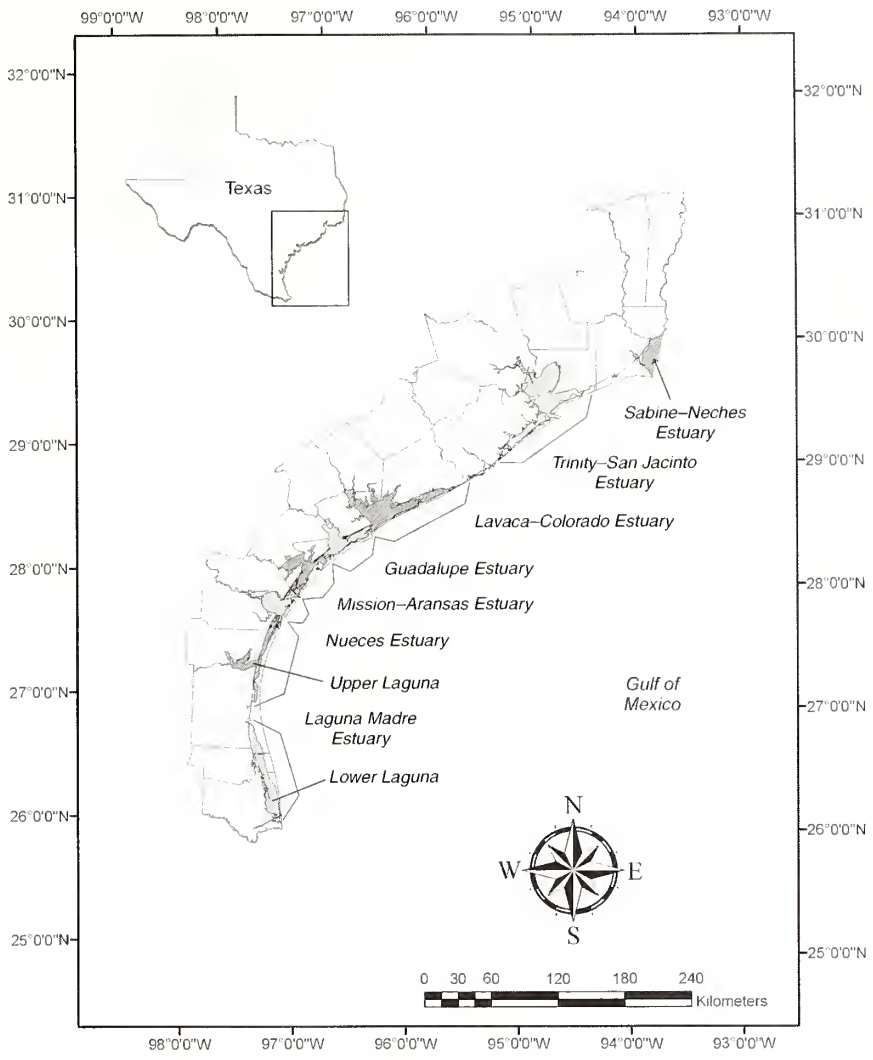

Figure 1

Map of the Texas coastline showing the location along the coast of each of the major estuarine systems sampled as part of the Resource Monitoring Program conducted by the Texas Parks and Wildlife Department from 1978 through December 2006. The fine line trailing the coastline represents the outline of the barrier island that runs from the pass at Sabine to Brazos-Santiago Pass, just north of Rio Grande.

Texas Parks and Wildlife Department (TPWD) has used various gears systematically in Texas estuaries since 1975 to assess changes in the abundance and size of organisms, their spatial and temporal distributions, species compositions of the community, and selected environmental parameters known to influence their distribution and abundance. The purpose of this study was to examine the relationship between water temperature and population trends in juvenile and adult gray snapper within the seven major estuaries along the Texas gulf coast.

Methods and materials

Gray snappers were collected from November 1978 through December 2006 with bag seines, otter trawls, and gill nets as part of a survey conducted by the Resource Monitoring Program of the Texas Parks and Wildlife Department within each of the seven major estuaries on the Texas Gulf coast: Sabine-Neches, Trinity-San Jacinto, Lavaca-Colorado, Guadalupe, Mission-Aransas, Nueces, and Laguna Madre (further subdivided into an Upper and Lower section, see Fig. 1). Bag seines (18.3 m wide, 1.8 m deep, and equipped with 1.3-cm stretched nylon multifilament mesh in the 1.8-m wide central bag and with 1.9-cm stretched mesh in the remaining webbing) were pulled parallel to the shoreline for 15.2 m for a total area swept of 0.03 ha. Sampling frequencies of the bag seines have not been uniform since the inception of the Routine Monitoring Program. Before 1981, only six bag seine samples were collected in each month in each bay (except for June 1978 when none was collected). From January 1982 through August 1984, 10 samples were

Table 1

Numbers of gray snapper (Lutjanus griseus) collected by each of the fishery-independent gears used in the eight major estuaries along the Texas coast. The increase in numbers of gray snapper from before to after the 1993 time period is presented as an ×-fold increase.

	Bag seine			Otter trawl			Gill net		
Estuary	Before 1993	After 1993	×-fold increase	Before 1993	After 1993	×-fold increase	Before 1993	After 1993	×-fold increase
Sabine-Neches	0	6	—	0	8	—	0	4	—
Trinity-San Jacinto	4	20	5.0	0	5	—	3	52	7.3
Lavaca-Colorado	17	72	4.2	1	6	6.0	14	232	16.6
Guadalupe	26	71	2.7	1	10	10.0	8	163	20.4
Mission-Aransas	7	73	10.4	3	22	7.3	8	103	12.9
Nueces	13	35	2.7	0	1	—	233	926	3.9
Upper Laguna Madre	2	6	3.0	0	2	—	6	46	7.7
Lower Laguna Madre	4	34	8.5	22	159	7.2	64	461	7.2
Total	73	317	4.3	27	213	7.9	336	1987	5.9

collected each month in each bay, except Sabine Lake (Sabine Lake sampling began in 1986). From August 1984 through January 1992, sampling frequency within each estuary increased to 12 samples per month, then to 16 per month, and finally to 20 samples each month. Since 1992, a total of 20 bag-seine samples have been collected from randomly selected locations within each bay in each month, resulting in 1920 samples per year. Otter trawls (6.1 m wide and with 3.8-cm stretched nylon multifilament mesh) were pulled for 10 minutes in water ≥1.0 m depth. Twenty trawl samples were taken from randomly selected sites in each bay each month (except for 10 per month in Nueces and the upper Laguna Madre). A total of 1920 trawl samples were collected each year. Gill nets (monofilament, 183 m long, 1.2 m deep, and equipped with separate 45.7-m sections of 7.6-, 10.2-, 12.7-, and 15.2-cm stretched mesh tied together in a sequence of ascending mesh size) were set overnight during each spring and fall season. The spring season begins with the second full week in April and extends for 10 weeks; the fall season begins with the second full week in September and also extends for 10 weeks. Gill nets were set perpendicular to the shore with the smallest mesh facing shoreward. Nets were set within 1 hour before sunset and retrieved within 4 hours after the following sunrise. In each bay, a total of 90 gill nets were set at randomly selected sites (720 samples per year).

Total lengths (TL) of gray snapper were measured for each gear type. Catch rates (relative abundance expressed as catch per unit of effort) from each gear were calculated for each bay, month, season, or year. Environmental measurements of surface salinity, water temperature (°C), and dissolved oxygen (mg/L and percent saturation) were measured both before the set and retrieval of gear for each gillnet collection and before each bag-seine collection. Bottom salinity, water temperature, and dissolved oxygen were measured before each trawl sample.

Analytical techniques

In order to directly compare the time series of abundance patterns of gray snapper across the disparate gears, relative abundance estimates for each gear were first Z-transformed (Snedecor and Cochran, 1980). The temperature records from each estuary were aggregated by month and year and expressed as monthly arithmetic averages to produce a time series compatible with the monthly abundance series. The temperature records were then analyzed with an empirical orthogonal function (EOF), a statistical tool used to decompose a spatially multivariate data set into its principal components. With this tool, the bulk of the variance can be described by a few orthogonal modes, so that the major properties of the data set can be more easily understood (Keiner and Yan, 1997). Principal modes of the spatial EOFs were seasonally detrended (multiplicative seasonal adjustment; SYSTAT, vers. 12, SYSTAT Software Inc., San Jose, CA) to reveal either periodicity or trends in the data. Detrended EOF slopes were assessed with linear regressions to test any departure from zero.

Results

From 1978 through 2006, a total of 2953 gray snappers were sampled from Texas bays and estuaries. The seasonal patterns revealed with the fishery-independent gears agreed well with published reports of spawning and movement patterns. Most juvenile and subadults taken in the bag seines and otter trawls were collected in the late summer to early fall, from August to October. Adult gray snapper were collected with gill nets in every month when this gear was deployed and were most prevalent during the fall from September to November. The vast majority of individuals were collected with gill nets from the middle Texas coast (from Lavaca-Colorado Estuary

Table 2

Percent and cumulative percent of the total variation explained by the eight empirical orthogonal function (EOF) modes. The eight modes correspond to the eight major Texas estuaries, spatially interpolated by means of an objective analysis scheme by means of a series consisting of 288 monthly averaged mean salinity readings collected from the Resource Monitoring Program of the Texas Parks and Wildlife Department.

	EOF							
	1	2	3	4	5	6	7	8
Percent	96.40	0.81	0.65	0.55	0.47	0.41	0.39	0.33
Cumulative percent	96.40	97.21	97.86	98.26	98.73	99.14	99.53	100

to the Nueces Estuary; see Table 1). Given the affinity of this species for structured habitats, it is no surprise that the otter trawl was the least effective gear for capturing this species.

Environmental data during this same period demonstrated increasing annual water temperatures, although these increases were not seasonally uniform. Summer maximum water temperatures remained relatively stable, whereas winter minimums increased through time. The largest proportion of temperature increases were attributed to higher winter temperature minimums since 1993 (Fig. 2). Before 1993, winter minimum temperatures routinely fell below the lower lethal limit for gray snapper, and these events were especially common in the upper coast estuaries of Sabine-Neches, Trinity-San Jacinto, and Lavaca-Colorado. Since 1993, winter temperatures along the coast of Texas have generally been mild, although particularly powerful polar fronts caused dramatic declines in surface water temperatures in both 1997 and 2001.

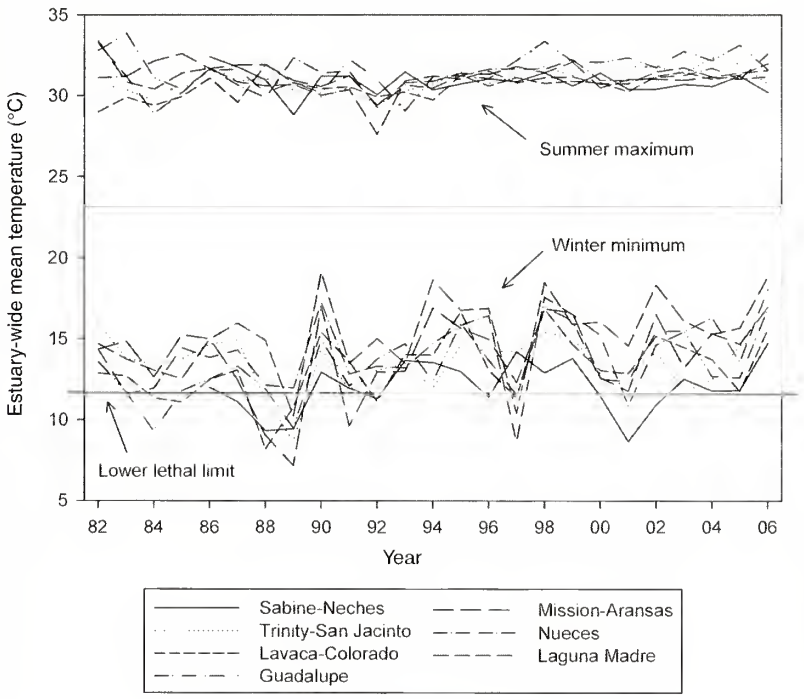

Figure 2

Time series of mean yearly temperatures (summer maximum and winter minimums, in °C) of Texas coastal estuaries. The solid horizontal line identifies the lower lethal limit (12°C) for gray snapper (Lutjanus griseus).

The 288 months of average surface temperatures from the seven major estuaries along the Texas coast were combined into a data matrix and interpreted with a spatial EOF. The variance pattern for the principal EOF mode is shown in Figure 3. The fundamental periodicity within the first mode (capturing 96% of the total variability, Table 2) represents the yearly signal inherent in the series (0.083 cycles per month, or 1 cycle per year). Temperature structure in each estuary was effectively described by the first mode of the EOF, and positive component loadings ranged from 0.976 to 0.985 for each estuary. Seasonally detrended EOF mode 1 revealed that increases in winter minimum temperatures, especially after 1993, corresponded to the largest positive amplitude values seen in the series. Before 1993, the slope of the detrended temperature record was not significantly different from zero ($F_{1,\ 143}$=1.194; P=0.276), whereas after 1993, the trend in water temperature was significantly upward and warmer ($F_{1,\ 153}$=5.055; P=0.026).

Before 1993, gray snapper were generally uncommon in all estuaries on the Texas gulf coast, but since then, increases in abundances have ranged from near 3- to over 20-fold (see Table 1). The temporal pattern of increasing abundances, especially within the mid-coast estuaries where gray snapper are most prevalent, is shown in Figure 4. A winter temperature minimum near or below the lower lethal limit appears to inhibit

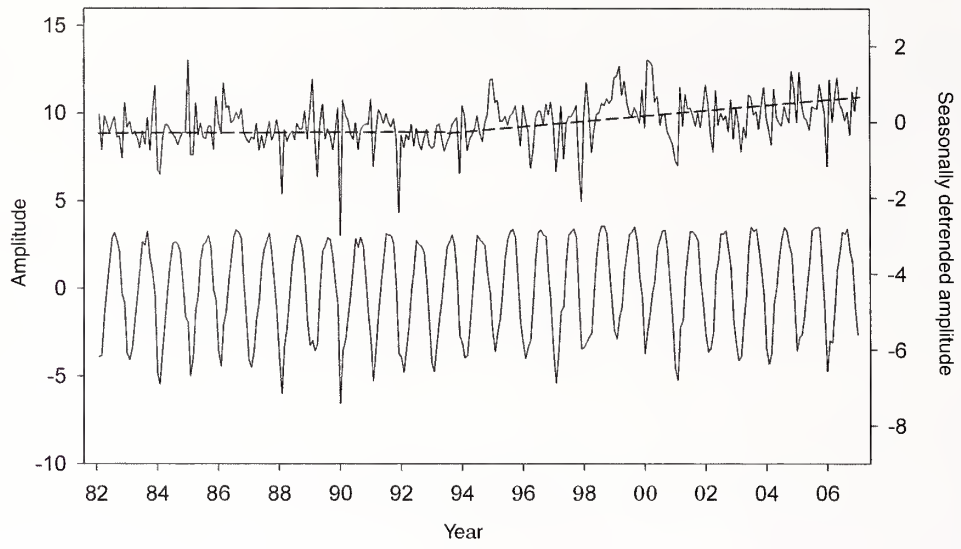

Figure 3

Amplitudes of the spatial empirical orthogonal function, mode 1. Lower panel is the seasonal signal, upper panel is the seasonally detrended signal. Dashed line within the upper panel is the slope derived independently for the period before 1993 and after 1993. Amplitudes are nondimensional.

Table 3

Separate variance t-test results from a comparison of the mean size and standard deviation (SD) of gray snapper (Lutjanus griseus) collected with bag seines, otter trawls, and gill nets (before and after 1993) from Texas estuaries, pooled by sampling gear and time period. Effective degrees of freedom (df) for each test were approximated with the Welch-Satterthwaite equation; therefore degrees of freedom (df) are not reported as whole numbers.

	Bag seine		Otter trawl		Gill net	
	Before	After	Before	After	Before	After
Mean size (mm)	50.1	61.4	110.7	138.9	268.8	308.0
SD	19.2	22.8	44.3	49.1	59.0	36.3
t-test value		2.77		2.24		9.62
df		38.5		16.7		230.6
P value		0.008		0.039		<0.001

recruitment (as evidenced by the young-of-the-year abundance estimates determined from the bag-seine collections), as well as limit the survival of over-wintering juveniles. An absence of cold winters has allowed for dramatic increases in the abundance of gray snapper in nearly every estuary along Texas gulf coast. Accompanying these increases there has been a concomitant increase in the mean size of gray snapper collected with all gear types. Separate variance *t*-tests revealed that coast-wide post-1993 collections of gray snapper were significantly greater in numbers (for all gear types) than the pre-1993 collections (Table 3).

The exponential increase in estuarine abundance of gray snapper in Texas, as recorded with the fisheries-independent gill nets, has been confirmed with fishery-dependent data of population trends from nearby locations. A time series of state-wide recreational landings from both Texas (primarily bay and estuary landings) and Louisiana (primarily nearshore continental shelf landings) virtually mirrors the exponential increase in abundance recorded with the gill nets (Fig. 5).

Discussion

Time series have become increasingly important in the studies of climate influences on biological patterns (Reid et al., 2001; Edwards et al., 2002), especially

during recent years when unusual climate trends have been reported and major events have affected living resources and fisheries management (Rebstock, 2003; Woehrling et al., 2005). The uninterrupted, 30+ year record of systematic monitoring within every estuary on the Texas Gulf coast is almost unprecedented in terms of both spatial and temporal coverage. These collections encompass a scale sufficient to document ecosystem-level responses to climate variation and may provide insight into any biological responses that are revealed. Analyses of proxy-based reconstructions of temperatures, with particular emphasis on the Atlantic Coast region during the past millennium, have shown patterns of multidecadal variation in sea surface temperature with a distinct oscillatory mode of variation at an approximate time scale of 70 years (Delworth and Mann, 2000; Cronin et al., 2003). Embedded within this climate signal is an overall warming trend on the order of 0.16°C to 0.21°C per decade (Preston, 2004). Some researchers have reported that this warming trend accelerated during the latter half of the 20th century (Hoerling et al., 2004; Zeeburg et al., 2008). A general trend of increasing water temperature was also found along the Texas coast, but this increase was not seasonally consistent. Maximum water temperatures during summer months were relatively stable over the study period, whereas increases in winter minimum temperatures were seen to drive this mean increase. Seasonally nonlinear temperature patterns have also been reported in other estuarine systems (Nixon et al., 2004; Hare and Able, 2007), along with the common feature of warming winter surface waters.

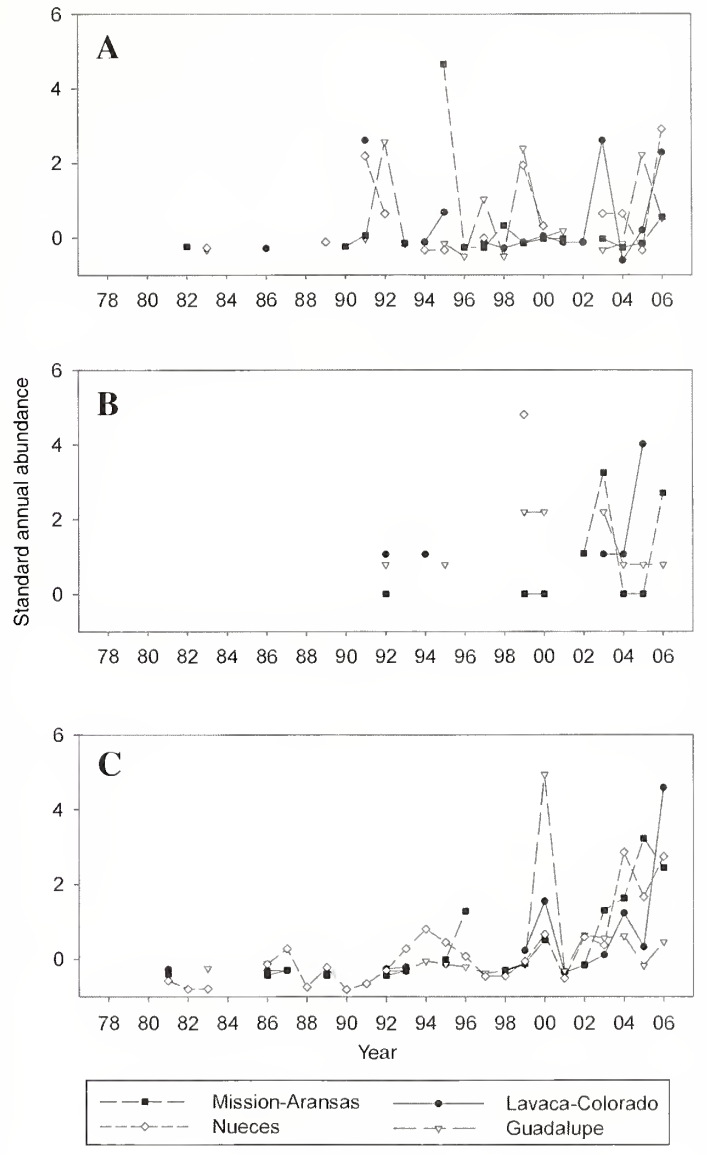

Figure 4

Time series of yearly catch rates for gray snapper (Lutjanus griseus) with (**A**) bag seines, (**B**) otter trawls, and (**C**) gill nets from four mid-coast Texas estuaries. To allow direct comparisons, each series has been standardized to a mean of zero and a unit variance of 1.

A link between large-scale climate drivers and biotic variability in the Gulf of Mexico has been attempted in only a few studies. Tolan (2006), however, did find a connection between short-phase NAO-AO forcing and Texas estuarine salinity patterns, and the greatest influence was found in three mid- and northern coast estuaries (Guadalupe, Lavaca-Colorado, and Sabine-Neches). An abrupt transition to positive phases of the NAO-AO index (wetter, warmer winters along the eastern U.S. coasts; Rajagopalan et al., 1998) occurred during the late 1970s, and the atmosphere generally remained in this positive mode through the 2005 winter season. During this 25 year interval, substantial negative phases of this pattern appeared only four times (1985, 1987, 1996, and 2001). The height of the current positive phase of the NAO-AO index (values from 1989 through 1995 represent some of the largest positive values ever recorded) temporally corresponds to the onset of the increase in gray snapper populations along the Texas coast. Zeeburg et al. (2008) identified a similar NAO-AO linked biological response in mid-1990s in the east central Atlantic Ocean off Africa. Their study showed that the response of Spanish sardine (*Sardinella aurita*) to changes in surface water temperatures (namely a surge in population numbers) began in 1995, around the same time that the temperature-mediated biological effects on gray snapper were seen in western Gulf of Mexico estuaries.

Recent increases in gray snapper appear to follow the "thermal opening of the estuary" theory that Hare

and Able (2007) presented for what the authors term as "outbursts" of Atlantic croaker (*Micropogonias undulatus*) populations along the east coast of the United States. Warmer winters result in higher juvenile survival, which allows for the formation of larger year classes. Sequential warm winters lead to sequentially large year classes that extend the duration of an outburst. In the Atlantic croaker example, the outburst allowed population ranges to expand north and, as a result, spawning extended farther north, supplying larvae to estuaries not normally inhabited. The outburst was continued as a result of additional juvenile habitat that was then available to the population. This appeared to be the case for gray snapper populations in the western Gulf of Mexico. A decade of nearly uninterrupted warm winters has allowed this species to flourish in estuaries where they were not historically encountered in great numbers. Following the winter temperature shift of 1993, the only precipitous dips in the exponential rise in gray snapper population numbers (declines seen in 1998 and 2002) followed years with sharply colder winters (1997 and 2001, see Fig. 3).

In the Hare and Able (2007) model, the role of larval supply was minimal, because the spatial expansion of the spawning range was a direct consequence of the outburst, not the cause. Temperature-related overwintering mortality of juvenile fish establishes year-class strength, and these strong year classes carry the population for 3–5 years. Based on established von Bertalanffy growth parameters (derived separately from Louisiana recreational harvest [Fischer et al., 2005] and eastern Florida commercial harvest [Burton, 2001]), the mean size of Texas gray snapper collected with gill nets represents 3–4 year-old fully mature fish. Fischer et al. (2005) found a multimodal distribution in gray snapper age structure from Louisiana and attributed the variation in year-class strength to intraspecific competition among juveniles for resources within the estuaries before recruiting to the offshore fisheries. The successive peaks in age-class abundance (strong year classes every 2–3 years) could also be attributed to juvenile overwintering mortality associated with thermal limits within the estuaries. Interestingly, year of birth distributions from Louisiana recreational catches from 1998 through 2002 (Fig. 5B in Fischer et al., 2005) showed that the largest percentage of gray snapper came from 1994, around the same time that the slope of seasonally detrended EOF mode 1 turned positive.

An alternative explanation for the exponential rise in the landings of gray snapper recorded from the northern Gulf may be attributed to a directed recreational fishing effort. To reverse the condition of overfishing of red snapper (*Lutjanus campechanus*), increasingly restrictive fish-size limits and bag limits were placed on the recreational fishing sector for red snapper in 1991. Anglers began to target the more nearshore populations of gray snappers once their bag limits of red snapper were reached. Peak landings of gray snapper in Louisiana generally coincided with the red snapper recreational season (April–October), and as a result, landings of gray snapper increased exponentially from 3.25 metric tons in 1983 to 175 metric tons in 2002 (Fischer et al., 2005). Even though the landing data for both Texas and Louisiana presented in Figure 5 were not adjusted for effort, it should be noted that both the fishery-independent and fishery-dependent indices of population abundance for each state both showed similar increases after the winter temperature shift of the mid-1990s. From 2000 to 2006, increasingly restrictive limits on red snapper have dramatically increased the fishing effort for gray snapper; yet the trends of the fishery-independent index (determined from TPWD gillnet effort over the period of record (1978–2007) has displayed similar temperature-related fluctuations as those displayed by the fishery-dependent indices.

Gray snapper are particularly susceptible to cold weather; their lower thermal limits range from 11° to 14°C (Starck and Schroeder, 1971). The effects of cold weather on marine organisms in Texas bays vary substantially, depending on how rapidly the temperature drops, on the severity and duration of the cold temperatures, on the physiographic characteristics of the affected area, and on

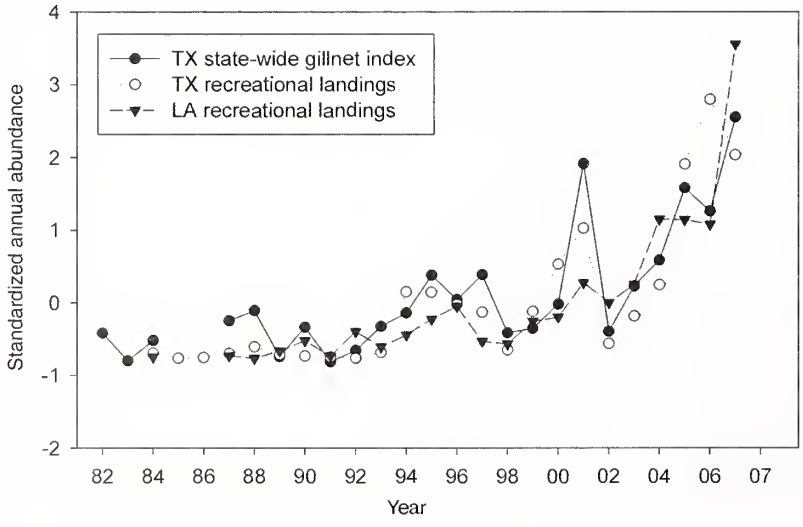

Figure 5

Time series of landing of adult gray snapper (Lutjanus griseus) from gill nets (Texas estuaries) and recreational landings (both Texas and Louisiana) from 1982 to 2006. To allow direct comparisons, each series has been standardized to a mean of zero and a unit variance of 1.

the life history, behavior, and population dynamics of the affected animals (McEachron et al., 1994). During our study period, three severe polar cold fronts caused coast-wide fish-kill events during December 1983, February 1989, and December 1989. In the absence of cold winters, this species has established semipermanent populations in nearly every estuary along the Texas coast, and these populations are likely to continue to flourish until the next polar front either diminishes these estuarine populations, or a series of successive cold winters creates a "thermal closure" of the nursery habitats (*sensu* Hare and Able, 2007). Gray snapper are far less abundant in the northernmost estuary (Sabine-Neches), presumably because the winter minimum temperatures regularly fall below 12°C. December 2004 was remarkable in that a strong cold front brought measurable snowfall to most of coastal south Texas for the first time in over 100 years and resulted in a localized cold kill of approximately 12,000 gray snapper on the gulf beach side of Boca Chica, near the lower end of the Laguna Madre estuary. Declines in gray snapper abundance after the snowfall event of 2004 can be seen in three of the four mid-coast estuaries shown in Figure 4C.

Although only a single species was examined in our study, there may well be many species along the Texas coast for which recruitment and population dynamics are linked to climatic forcing (e.g., sand drum, [*Umbrina coroides*]; common snook [*Centropomus undecimalis*]; tarpon [*Megalops atlanticus*], and African pompano [*Alectis ciliaris*], see Moore, 1975). In the past few years alone, both snook and tarpon have become exceedingly more common along the rock jetty passes at both Mansfield Pass (gulf connection at the far upper end of Lower Laguna Madre) and Aransas Pass (gulf pass connection for both the Nueces and Mission-Aransas estuaries). Connections between fish population dynamics and climate patterns need to be better quantified and incorporated into stock assessment models to ensure successful long-term management of fishery stocks.

Acknowledgments

We thank all the field staff and the technicians at the Coastal Fisheries Division of the Texas Parks and Wildlife Department for their diligent collection of the biotic and abiotic parameters used for this study. We especially thank J. W. Hurrell, Climate Analysis Section, National Center for Atmospheric Research, Boulder, Colorado, for providing the North Atlantic Oscillation–Arctic Oscillation index values used for this study. A. Nunez, Texas Parks and Wildlife Department, Coastal Fisheries Division, Corpus Christi, Texas, provided the December 2004 gray snapper fish-kill data. Although this project was never explicitly funded by research grants, the continued support of Sportfish Restoration Funds enabled the time necessary for data synthesis and interpretation.

Literature cited

Allman, J. A., and C. B. Grimes.
2002. Temporal and spatial dynamics of spawning, settlement, and growth of gray snapper (*Lutjanus griseus*) from the West Florida shelf as determined from otolith microstructures. Fish. Bull. 100:391–403.

Arcos, D. F., L. A. Cubillos, and S. P. Núñez.
2001. The jack mackerel fishery and El Niño 1997–98 effects off Chile. Prog. Oceanogr. 49:597–617.

Attrill, M. J., and M. Power.
2002. Climatic influences on a marine fish assemblage. Nature 417:275–278.

Burton, M. L.
2001. Age, growth, and mortality of gray snapper, *Lutjanus griseus*, from the east coast of Florida. Fish. Bull. 99:254–265.

Cronin, T. M., G. S. Dwyer, T. Kamiya, S. Schwede, and D. A. Willard.
2003. Medieval warm period, little ice age, and 20th century temperature variability from Chesapeake Bay. Global Planet. Change 36:17–29.

Delworth, T. L., and M. E. Mann.
2000. Observed and simulated multidecadal variability in the Northern Hemisphere. Clim. Dynam. 16:661–676.

Denit, K., and S. Sponaugle.
2004. Growth variation, settlement, and spawning of gray snapper across a latitudinal gradient. Trans. Am. Fish. Soc. 133:1339–1355.

Edwards, M., G. Beaugrand, P. C. Reid, A. A. Rowden, and M. B. Jones.
2002. Ocean climate anomalies and the ecology of the North Sea. Mar. Ecol. Prog. Ser. 239:1–10.

Enfield, D. B., A. M. Mestas-Nuñez, and P. J. Trimble.
2001. The Atlantic multidecadal oscillation and its relation to rainfall and river flows in the continental U.S. Geophys. Res. Lett. 28:2077–2080.

Fischer, A. J., M. S. Baker, Jr., C. A. Wilson, and D. L. Nieland.
2005. Age, growth, mortality, and radiometric age validation of gray snapper (*Lutjanus griseus*) from Louisiana. Fish. Bull. 103:307–319.

Gunter, G.
1941. Death of fishes due to cold on the Texas coast, January, 1940. Ecology 22:203–208.
1951. Destruction of fishes and other organisms on the south Texas Coast by the cold wave of January 28–February 3, 1951. Ecology 32:731–736.

Hare, J. A., and K. W. Able.
2007. Mechanistic links between climate and fisheries along the east coast of the United States: explaining population outbursts of Atlantic croaker (*Micropogonias undulatus*). Fish. Oceanogr. 16:31–45.

Hoerling, M. P., J. W Hurrell, T. Xu, G. T. Bates, and A. S. Phillips.
2004. Twentieth century North Atlantic climate change. Part II: Understanding the effect of Indian Ocean warming. Clim. Dynam. 23:391–405.

Holt, S. A., and G. J. Holt.
1983. Cold death of fishes at Port Aransas, Texas, January 1982. Southwest. Nat. 28:464–466.

Keiner, L. E., and X. Yan
1997. Empirical orthogonal function analysis of sea surface temperature patterns in Delaware Bay. IEEE Trans. Geosci. Rem. Sens. 35(5):1299–1306.

McEachron, L. W., G. C. Matlock, C. E. Bryan, P. Unger, T. J. Cody, and J. H. Martin.
1994. Winter mass mortality of animals in Texas bays. Northeast Gulf Sci. 13:121–138.

Moore, R. H.
1975. Occurrence of tropical marine fishes at Port Aransas, Texas 1967–1973, related to sea temperatures. Copeia 1975:170–172.
1976. Observations on fishes killed by cold at Port Aransas, Texas, 11–12 January 1973. Southwest. Nat. 20:461–466.

Nixon, S. G., B. A. Buckley, M. Lamont, and B. Rowell.
2004. A one hundred and seventeen year coastal water temperature record from Woods Hole, Massachusetts. Estuaries 27:397–404.

Okumura, Y., S. Xie, A. Numaguti, and Y. Tanimoto.
2001. Tropical Atlantic air-sea interaction and its influence on the NAO. Geophys. Res. Lett. 28:1507–1510.

Oviatt, C. A.
2004. The changing ecology of temperate coastal waters during a warming trend. Estuaries 27:895–904.

Parker, R. O., and R. L. Dixon.
1998. Changes in a North Carolina reef fish community after 15 years of intense fishing-global warming implications. Trans. Am. Fish. Soc. 127:908–920.

Perry, A. L., P. J. Low, J. R. Ellis, and J. D. Reynolds.
2005. Climate change and distribution shifts in marine fishes. Science 308:1912–1915.

Preston, B. J.
2004. Observed winter warming of the Chesapeake Bay Estuary (1949–2002): implications for ecosystem management. Environ. Manag. 34:125–139

Rajagopalan, R., Y. Kushnir, and Y. M. Tourre.
1998. Observed decadal midlatitude and tropical Atlantic climate variability. Geophys. Res. Lett. 25:3967–3970.

Randall, J. E.
1968. Caribbean reef fishes, 318 p. Tropical Fish Hobbyist Publications, Inc., Neptune City, NJ.

Rebstock, G. A.
2003. Long-term change and stability in the California Current System: lessons from CalCOFI and other long-term datasets. Deep-Sea Res. II 50:2583–2594.

Reid, P. C., M. Borges, and E. Svenden.
2001. A regime shift in the North Sea circa 1988 linked to changes in the North Sea horse mackerel fishery. Fish. Res. 50:163–171.

Roessig, J. M., C. M. Woodley, J. J. Cech, and L. J. Hansen.
2004. Effects of global climate change on marine and estuarine fishes and fisheries. Rev. Fish Biol. Fish. 14:251–275.

Rutherford, E. S., T. W. Schmidt, and J. T. Tilmant.
1989b. Early life history of spotted seatrout (*Cynoscion nebulosus*) and gray snapper (*Lutjanus griseus*) in Florida Bay, Everglades National Park. Bull. Mar. Sci. 44:139–154.

Rutherford, E. S., J. T. Tilmant, E. B. Thue, and T. W. Schmidt.
1989a. Fishery harvest and population dynamics of gray snapper, *Lutjanus griseus*, in Florida Bay and adjacent waters. Bull. Mar. Sci. 44:139–154.

Sirabella, P., A. Giuliani, A. Colosimo, and J. W. Dippner.
2001. Breaking down the climate effects of cod recruitment by principal component anaylsis and canonical correlations. Mar. Ecol. Prog. Ser. 216:213–222.

Smith, P. E., and H. G. Moser.
2003. Long-term trends and variability in the larvae of Pacific sardine and associated fish species of the California Current region. Deep Sea Res. II 50:2519–2536.

Snedecor, G. W., and W. G. Cochran.
1980. Statistical methods, 507 p. Iowa State Univ. Press, Ames, IA.

Starck, W. A., II, and R. E. Schroeder (eds.).
1971. Investigations on the gray snapper, *Lutjanus griseus*, 224 p. Univ. Miami Press, Coral Gables, FL.

Sullivan, M. C., R. K. Cowen, and B. P. Steves.
2005. Evidence for atmospheric-ocean forcing of yellowtail flounder (*Limanda ferruginea*) recruitment in the Middle Atlantic Bight. Fish. Oceanogr. 14:386–399.

Tolan, J. M.
2006. El Niño-Southern Oscillation impacts translated to the watershed scale: Estuarine salinity patterns along the Texas Gulf Coast, 1982 to 2004. Estuarine Coastal Shelf Sci. 72:247–260.

Woehrling, D., A. Lefebvre, G. Le Fevre-Lehoerff, and R. Delesmont.
2005. Seasonal and longer term trends in sea temperature along the French North Sea coast, 1975–2002. J. Mar. Biol. Assoc. U.K. 85:39–48.

Zeeburg, J., A. Corten, P. Tjoe-Awie, J. Coca, and B. Hamady.
2008. Climate modulates the effects of *Sardinella aurita* fisheries off Northwest Africa. Fish. Res. 89:65–75.

Dividing population genetic distance data with the software Partitioning Optimization with Restricted Growth Strings (PORGS): an application for Chinook salmon (*Oncorhynchus tshawytscha*), Vancouver Island, British Columbia

John R. Candy (contact author)[1]
R. Gregory Bonnell[2]
Terry D. Beacham[1]
Colin G. Wallace[1]
Ruth. E. Withler[1]

Email address for contact author: John.Candy@dfo-mpo.gc.ca

[1] Molecular Genetics Laboratory
Department of Fisheries and Oceans, Pacific Biological Station
3190 Hammond Bay Road
Nanaimo, British Columbia, Canada V9T 6N7

[2] Oceans and Habitat Enhancement Branch
Department of Fisheries and Oceans
4166 Departure Bay Road
Nanaimo, British Columbia, Canada V9T 4B7

Abstract—A new method of finding the optimal group membership and number of groupings to partition population genetic distance data is presented. The software program Partitioning Optimization with Restricted Growth Strings (PORGS), visits all possible set partitions and deems acceptable partitions to be those that reduce mean intracluster distance. The optimal number of groups is determined with the gap statistic which compares PORGS results with a reference distribution. The PORGS method was validated by a simulated data set with a known distribution. For efficiency, where values of n were larger, restricted growth strings (RGS) were used to bipartition populations during a nested search (bi-PORGS). Bi-PORGS was applied to a set of genetic data from 18 Chinook salmon (*Oncorhynchus tshawytscha*) populations from the west coast of Vancouver Island. The optimal grouping of these populations corresponded to four geographic locations: 1) Quatsino Sound, 2) Nootka Sound, 3) Clayoquot +Barkley sounds, and 4) southwest Vancouver Island. However, assignment of populations to groups did not strictly reflect the geographical divisions; fish of Barkley Sound origin that had strayed into the Gold River and close genetic similarity between transferred and donor populations meant groupings crossed geographic boundaries. Overall, stock structure determined by this partitioning method was similar to that determined by the unweighted pair-group method with arithmetic averages (UPGMA), an agglomerative clustering algorithm.

Manuscript submitted 26 March 2008.
Manuscript accepted 5 September 2008.
Fish. Bull. 107:45–56 (2009).

The views and opinions expressed or implied in this article are those of the author and do not necessarily reflect the position of the National Marine Fisheries Service, NOAA.

Genetic diversity in salmon species is thought to be maintained through high homing fidelity, which limits gene flow between spawning sites (Ricker, 1972; Quinn and Dittman, 1990). As a general rule, populations that are geographically close tend to be genetically similar, creating natural clusters of similar populations. Identification of genetically similar salmonid populations is important for fisheries management initiatives directed at conserving genetic diversity (Riddell, 1993; Waples et al., 2001). Consequently, managers are faced with the challenge of defining the number and size of these genetic groups. Furthermore, determining valid groupings of populations at a fine scale allows managers to make informed decisions regarding harvest levels and population-enhancement strategies. For British Columbia Chinook salmon (*Oncorhynchus tshawytscha*) populations, genetic markers have been used to determine genetic distance between populations and to provide considerable power for defining regional stock structure (Teel et al., 2000; Beacham et al., 2006a).

Clustering or grouping data are useful in many disciplines; as a result there is a wide assortment of methods available for representing data, measuring proximity between data elements, and grouping elements (e.g., Jain et al., 1999). For Pacific salmon, population-specific allelic frequencies are ascertained from spawning ground samples by using genetic markers at a number of loci. From these allelic frequencies, a metric of overall genetic difference between populations is used to estimate pairwise genetic distances. Three commonly used distance measures are Nei's distance, D_S (Nei, 1987), Nei's modified Cavalli-Sforza chord distance D_A (Cavalli-Sforza and Edwards, 1967; Nei et al., 1983), and Weir and Cockerham's (1984) estimator of F_{st}, the coancestory coefficient θ. Once a distance measure is selected, a proximity matrix is created which shows genetic distance between each pair of populations.

Clustering is often used to group populations, either by merging small clusters into larger ones (agglomerative) or by splitting larger clusters

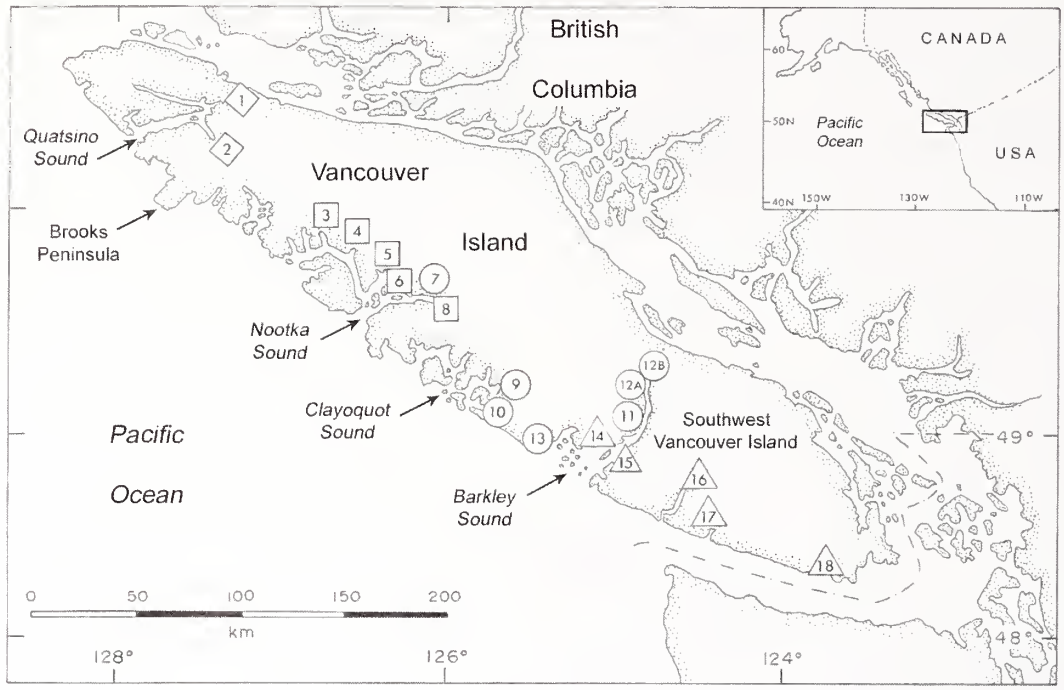

Figure 1

Location of the 18 sites on the west coast of Vancouver Island where Chinook salmon (*Oncorhynchus tshawytscha*) populations were sampled. Numbers correspond to stock codes in Table 1. The same population was sampled for Somas River (12A) and Robertson Hatchery (12B). Shapes around location numbers denote an genetic affiliation with one of the four regional groups: Quatsino Sound (diamonds), Nootka Sound (squares), Clayoquot+Barkley aounds (circles), and southwest Vancouver Island (triangles).

into smaller ones (divisive). A number of algorithms are available to decide which small clusters are merged or which larger clusters are split (e.g., Swofford et al., 1996; Jain et al., 1999). Groupings can be depicted as a branching tree or dendrogram where branch length is scaled to represent genetic distance. A drawback with the hierarchical approach is that the result is sensitive to initial groupings, which are not permitted to change once an assignment has been made. Furthermore, arbitrary tie-breaking actions, either in the original proximity data or during agglomeration, can cause instability in the tree structure (van der Kloot et al., 2005). Consensus from multiple tree constructions by bootstrapping across loci provides a measure of robustness of the apparent dominant tree structure (Felsenstein, 1985). A majority-rule consensus tree can provide a phylogeny with groups that occur in a majority of the bootstrap samples. However, the incorporation of variation from consensus trees appears to have limited quantitative application, and the optimum cluster number is not obvious.

This article provides a new method for partitioning genetic distance data by finding the optimal group membership and number of groupings. We validate the method using simulated data. To demonstrate the utility of this partition method, we applied it to genetic distance data calculated from samples taken from 18 Chinook salmon populations along the west coast of Vancouver Island, British Columbia (Fig. 1). The groupings determined by this method were evaluated with respect to known transfers of broodstock and histories of stock enhancement. Furthermore, results from both the simulated and Chinook salmon data sets were compared to results from a commonly used clustering method for genetic data.

Materials and methods

Pairwise cost function

A pairwise cost function used in the field of pattern recognition (Roth et al. 2003) minimizes the sum of mean intracluster distances. Minimized intracluster distance appears most desirable in grouping populations where two or more populations assigned to the same group contribute to total cost. Other clustering algorithms have been proposed which emphasize separation, combinations of compactness and separation, or conductivity measures (Buhmann, 2002).

Given row (i) and column (j) indices of an ($n \times n$) dissimilarity matrix D of populations with k groups, the pairwise cost function (CF) is

$$CF = \frac{1}{2}\sum_{v=1}^{k}\frac{\sum_{i=1}^{n}\sum_{j=1}^{n}M_{iv}M_{jv}D_{ij}}{\sum_{l=1}^{n}M_{lv}}. \quad (1)$$

For each population a binary assignment variable indicates group membership such that group membership (l) is assigned to each group (v) in an ($n \times k$) binary matrix (M), where

$$M \in \{0,1\}^{n\times k} : \sum_{v=1}^{k} M_{iv} = 1. \quad (2)$$

The optimal assignments of $\hat{M}$ are obtained through cost-function minimization ($\downarrow CF$) and visiting all combinations of group memberships. Unlike other cost functions (Hofmann and Buhmann, 1997), there is no penalty for increased numbers of partitions; thus adding more partitions will always reduce the cost where the output is nonconvex and $CF \rightarrow 0$ as $k \rightarrow n$. A nonpenalizing cost function was implemented so that the gap statistic (discussed later) could be used for determining the optimal number of groupings. Adding partitions creates more and smaller groups while lowering mean intracluster distance (the sum of all pairwise distances divided by the number of populations). Meanwhile, adding more groups increases the sum of the mean intracluster distances.

Implementation of the search algorithm

Testing all group memberships at different cluster sizes can generate large numbers of combinations. Structure detection through partitioning is considered a combinatorial optimization problem because visits to all combinations are computationally intensive. There is no guarantee of finding the optimal solution in a reasonable amount of time because the number of computations grows rapidly with increasing data (Puzicha et al., 1999). We describe two search methods that have been used for these data: simple random search and complete search.

Simple random search, a random set-partition assignment of the binary matrix, is an obvious way to visit combinations of group memberships, where i = 1 to n such that

$$M(i, rand_v) = 1. \quad (3)$$

Alternatively, all $n \times k$ combinations can be visited as a complete list of set partitions where, for example, three populations can be partitioned into the form

ABC AB|C AC|B A|BC A|B|C.

Set partitions are the union of nonempty disjoint subsets called blocks, where restricted growth strings (RGS) (strings of numbers used as a convenient way to represent partitions) were used to generate all blocks (Knuth, 2005). We called visits to all partitions while minimizing the cost function (Eq. 1), partitioning optimization using restricted growth strings (PORGS). The number of ways n populations can be partitioned into these nonempty sets is called the Bell number (Rota, 1964; Cameron, 1994). The total number of set partitions is the n^{th} Bell number, and the number of set partitions for each k is determined by the Stirling number of the second kind (Cameron, 1994).

Set partitions determined by RGS were used to configure the binary matrix to assign group membership. Although RGS can visit all possible partitions, they can also be used to generate partitions with "at most" r blocks (Knuth, 2005). This reduced search space allows bipartition (bi-PORGS) (r=2) such that an optimum split can be determined one partition at a time. Information from prior group membership is used to restrict future searches, where

$$M(i, v) = 1 \text{ for } i = 1 \text{ to } l, \text{ where } v = 1 \text{ or } 2. \quad (4)$$

A nested search occurs when all subgroups are sorted in descending order, and block combinations are selected when the cost function is minimized. Computational search time is reduced with the bi-PORGS method, thus allowing partitioning of larger sets of data.

The gap statistic

The objective of this analysis was to find an optimum number of groups, as well as the optimum partition solution, for k groups. Although there is no one criterion for deciding how many groups should be chosen to best represent the data, one guiding principle is that the appropriate number occurs when additional groups do not substantially change within-cluster dispersion. The gap statistic reveals within-cluster dispersion with that expected under an appropriate reference null distribution with methods of Tibshirani et al., (2001) such that

$$Gap_n(k) = \mathrm{E}^*_n\{\log(\downarrow CF)\} - \log(\downarrow CF), \quad (5)$$

where $\downarrow CF$ = the observed values from the minimized cost function for each k; and
$\mathrm{E}^*_n\{\log(\downarrow CF)\}$ = the log of the expected values from the reference distribution for each k.

The gap statistic is largest when the observed values fall the farthest below the reference curve. The estimate of the optimum number of groups will be the value where additional groups do not increase the gap statistic. The expected values for the reference distribution are generated by taking the mean PORGS values from bootstrapping the proximity matrix. Essentially, the mean values from the bootstrapped matrices remove the stock structure component from the reference data.

Simulated data

Simulated data were used to validate the PORGS method by comparing the known distribution of data points with

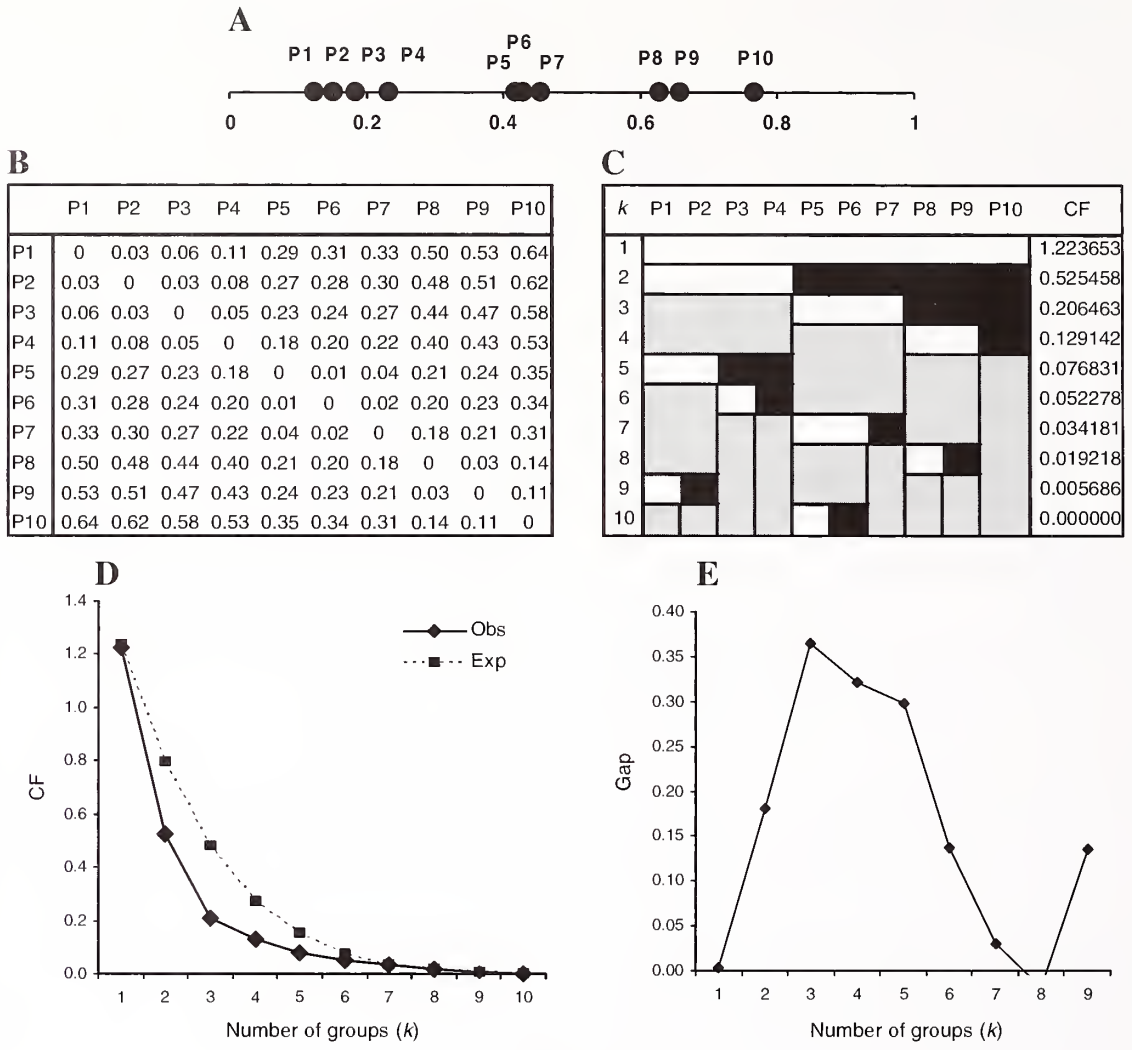

	P1	P2	P3	P4	P5	P6	P7	P8	P9	P10
P1	0	0.03	0.06	0.11	0.29	0.31	0.33	0.50	0.53	0.64
P2	0.03	0	0.03	0.08	0.27	0.28	0.30	0.48	0.51	0.62
P3	0.06	0.03	0	0.05	0.23	0.24	0.27	0.44	0.47	0.58
P4	0.11	0.08	0.05	0	0.18	0.20	0.22	0.40	0.43	0.53
P5	0.29	0.27	0.23	0.18	0	0.01	0.04	0.21	0.24	0.35
P6	0.31	0.28	0.24	0.20	0.01	0	0.02	0.20	0.23	0.34
P7	0.33	0.30	0.27	0.22	0.04	0.02	0	0.18	0.21	0.31
P8	0.50	0.48	0.44	0.40	0.21	0.20	0.18	0	0.03	0.14
P9	0.53	0.51	0.47	0.43	0.24	0.23	0.21	0.03	0	0.11
P10	0.64	0.62	0.58	0.53	0.35	0.34	0.31	0.14	0.11	0

k	CF
1	1.223653
2	0.525458
3	0.206463
4	0.129142
5	0.076831
6	0.052278
7	0.034181
8	0.019218
9	0.005686
10	0.000000

Figure 2

Partitions of simulated genetic distance data. (**A**) Populations P1–P10 are located randomly along a line from zero to one; (**B**) simulated proximity data were generated by using line distance between populations P1–P10; (**C**) results of the partitioning optimization using restricted growth strings (PORGS) analysis of simulated data, showing hierarchical group membership for k groupings and corresponding minimized cost function (CF) values; black, gray, and white represent status of the populations for a given cluster number. Black and white represent populations involved in partitions for a particular value of k, whereas gray populations were not involved; (**D**) expected CF values from the reference distribution and observed values plotted against number of groups k for the simulated data; and (**E**) the gap statistic plotted against number of groups, showing k=3 as the optimum number of groups with the simulated data for 10 populations.

optimal partitions and group membership obtained from the model.

To simulate genetic distance data, ten populations were assumed to be randomly located along a horizontal line, where i = 1 to 10 for a population $P(i)$ selected at random (Fig. 2A).

$$0<P(i)<1. \tag{6}$$

A proximity matrix of i rows and j columns of simulated data was constructed from the distances d between two populations (Fig. 2B) such that the values of each matrix element were

$$d(ij)=|P(i)-P(j)|. \tag{7}$$

Using the PORGS method, we partitioned the proximity matrix into optimal group membership for k = 1 to n groups by minimizing the cost function (Eq. 1; Fig. 2C). Ten bootstrapped variants of the proximity matrix were treated similarly, and the mean of the bootstrapped values provided a reference distribution to compare with

Table 1

Chinook salmon (*Oncorhynchus tshawytscha*) sampling data by region, stock code, population, years sampled, and annual and total sample size used in the bi-partitioning optimization using restricted growth strings (bi-PORGS) analysis. (H) indicates major hatchery facilities.

Region	Stock code	Population	Years sampled	Annual *n*	Total *n*
Quatsino Sound	1	Marble	1994, 1996, 1999, 2000	58, 98, 149 202	507
	2	Colonial	1999, 2004	40, 18	58
Nootka Sound	3	Zeballos	2002, 2004	4, 30	34
	4	Tahsis	1996, 1999, 2002, 2003	72, 87, 104 47	310
	5	Conuma (H)	1988, 1996, 1997, 1998	47, 214, 143 52	456
	6	Tlupana	2002, 2003	34, 32	66
	7	Gold	1983, 1985, 1986	9, 13, 71	93
	8	Burman	1976, 1985, 1986, 1989, 1990, 1991, 1992, 2000, 2002, 2003	8, 20, 2, 35 19, 56, 35 34, 51, 13	273
Clayoquot Sound	9	Tranquil	1996, 1999	209, 133	342
	10	Kennedy	1992, 2005	49, 190	239
Barkley Sound	11	Nahmint	1996, 2001, 2002, 2003, 2004	27, 56, 51 124, 135	346
	12A	Somas	1973	155	155
	12B	Robertson (H)	1996, 2003	155, 183	338
	13	Thornton	1992, 1999, 2000, 2001	37, 147, 150 184	518
	14	Toquart	1999, 2000	70, 17	87
	15	Sarita	1996, 1997, 2001	112, 157, 146	415
Southwest Vancouver Island	16	Nitinat (H)	1989, 1996, 2003	53, 153, 140	346
	17	San Juan	2001, 2002	80, 116	196
	18	Sooke	2004	58	58

the observed values of the original proximity matrix by using the gap statistic (Eq. 5; Fig. 2, D and E).

Genetic data for Chinook salmon from the west coast of Vancouver Island

Next we applied PORGS to genetic data derived from Chinook salmon populations. Tissue or scale samples were taken from Chinook salmon during times of broodstock collection and spawner enumeration along the west coast of Vancouver Island (Fig. 1). Genomic DNA was isolated from samples taken at 18 sites since the early 1970s (Table 1) and polymerase chain reaction analysis was conducted to amplify 12 microsatellite markers (*Ogo2, Ogo4, Oke4, Oki100, Ots100, Ots101, Ots104, Ots107, Ots2, Ots9, Omy325,* and *Ssa197*) by standard methods (Beacham et al., 2006a). All samples were combined over years except for one sample from the Robertson Creek Hatchery which was used to test the temporal stability of the microsatellites for population differentiation. Above the confluence with Sproat River, the Somas becomes Stamp River. Robertson Creek Hatchery lies on Stamp River downstream from Great Central Lake. The sample collected from Somas River in 1973 was considered to be the same stock as that represented by the sample from Robertson Creek Hatchery taken in 1996 and 2003. The Robertson Creek Hatchery stock was founded from Somas River fish collected from 1972 to 1976. and from additional broodstock collected from the river since then (Table 1, stock codes 12a and 12b).

For this analysis, we used Weir and Cockerham's (1984) co-ancestory coefficient θ, a widely used measure of genetic differentiation (Waples and Gaggiotti, 2006). A pairwise estimate of θ was calculated from data on multilocus genotypic distance between populations by using FSTAT software (Goudet, 1995).

History of Chinook salmon brookstock from the west coast of Vancouver Island

The west coast of Vancouver Island has three major hatcheries, Robertson Creek, Nitinat River, and Conuma River, which began enhancement of Chinook salmon in 1972, 1990, and 1979, respectively (Cross et al., 1991). Juveniles from these hatcheries have been transplanted into several river systems (Table 2). Robertson Creek Hatchery provided the founder stock for Thornton Creek Hatchery with transfers from brood years 1982–84. Since then, the hatchery-supported run has been perpetuated by returns to Thornton Creek. The Nitinat River Hatchery has transferred Nitinat River Chinook salmon to Toquart River (broods 1990–97 and 1999–2001) and

Table 2

History of transfers of Chinook salmon (*Oncorhynchus tshawytscha*) from the west coast of Vancouver Island, showing for each recipient population whether there was an indigenous stock, the enhancement status since transfers, the donor population, and the brood years transferred from donor to recipient sites.

Recipient population	Indigenous stock	Enhancement status	Donor population	Brood years transferred
Colonial	Yes	Not enhanced	Marble	1987–1989, 1991,1993,1998
Thornton	No	Enhanced: river returns only	Robertson	1982–1984
Toquart	Yes		Robertson	1989–1990
		Enhanced: river returns only	Nitinat	1990–1997, 1999–2001
Sooke	Yes	Enhanced: transfers plus river returns	Nitinat	1980–1984, 1987–1997, 1999–2006
Zeballos	Yes	Enhanced: river returns only	Conuma	1990–1998, 1999–2003

to Sooke River (brood years 1980–2006, except 1995, 1986, and 1998. Both Toquart River and Sooke River had existing Chinook salmon runs before hatchery releases, but populations were at a low abundance before transfers began. In addition, Marble River stock has been transferred to Colonial Creek, Goodspeed River (not sampled), and Coal Harbour, as well as various seapen release locations in Quatsino Sound. Other populations were either enhanced on-site or reared in a hatchery before being returned to the natal stream for release. For example, the Sarita River stock was reared in the Nitinat Hatchery, then returned to the Sarita River.

Comparison of PORGS method with standard genetic methods

To compare results obtained by the PORGS method with those from a standard hierarchical approach to clustering genetic data, the unweighted pair-group method using arithmetic averages (UPGMA) was applied to both the simulated and Chinook salmon data sets to generate a tree with PHYLIP software (Felsenstein, 1989). The UPGMA approach uses successive agglomeration with average-linking (Sneath and Sokal, 1973).

Results

When PORGS was applied to the simulated data, the first partition (k=2) occurred between P4 and P5 (Fig. 2C). The next partition occurred between P7 and P8; with k = 4, P10 was separated from the P7–P9 grouping. The last two populations to split were P5 and P6. The values of the optimized cost function decreases monotonically as the number of groups k increased (Fig. 2D). The expected data from the reference distribution (bootstrapped proximity matrix) also decreased monotonically (Fig. 2D); but followed a less concave curve than that for the observed data. The optimum k value occurred where the observed data fell the farthest below the expected curve, at k = 3 (Fig. 2E), which corresponded to the groupings P1–P4, P5–P7, and P8–P10 (Fig. 2C). According to the relative positions of these populations along the line in Figure 2A, the group memberships and optimum number of groups determined by PORGS appears reasonable. These data were re-analyzed by using the bi-PORGS method, which generated the same cluster groupings as PORGS.

These groupings are also consistent with the results depicted by an UPGMA tree (Fig. 3A). Figure 3A shows a vertical dashed line drawn to intersect branches that correspond to the three main clusters identified in the PORGS analysis. The UPGMA tree shows P10 with the longest branch length and P5–P6 with the shortest branch length, corresponding to both population location along the line (Fig. 2A) and the results from the application of the PORGS method (Fig. 2C).

The structure of the Chinook salmon data was evident when populations were sorted as an anti-Robinson matrix (Fig. 4; Robinson, 1951). In Figure 4 the smallest dissimilarity values appeared close to the main diagonal, resulting in a grouping of the most similar populations. Four main clusters were apparent, and the two Quatsino Sound populations, Marble River and Colonial Creek, were the most distinctive of all the populations (θ>0.04). Three other groups lay along the main diagonal, where θ<0.02, corresponding to northern (Nootka Sound), central (Clayoquot+Barkley sounds), and southwest Vancouver Island. The Toquart River and the Sarita River populations, although geographically part of Barkley Sound, clustered with southwest Vancouver Island populations. The Gold River population straddled the northern and central populations. The most genetically similar samples (θ=0.002) were those from Somas River in the early 1970s and those from the more recently sampled Robertson Creek hatchery.

Using the Chinook salmon data set, we were unable, in an initial attempt, to find an optimum solution from random set partitions. Although some partitions occurred only a few times, others were more common (Fig. 5). After 5.0×10^8 iterations, no cluster combinations were evaluated where block sizes were less than 2 or greater than 16. The expected number of occurrences for each k (Stirling number of the second kind)

indicated that considerably more iterations would be required to visit all set partitions.

Compared with random set partitions, PORGS reduces the number of cost function evaluations by eliminating redundant cluster combinations. However, if PORGS passes through all set partitions of the Chinook salmon data set, it would generate 5.8×10^{12} evaluations of the cost function (19th Bell number). Compared to the simulated data, where n=10, the Chinook salmon data set requires a much larger search (Fig. 5). Evidently, the number of combinations grows rapidly with an increasing number of populations, but not as fast as n factorial. (Knuth, 2005). An exhaustive search would still take a long time to execute, even with recent advances in computer processing speed. However, with bi-PORGS, the largest bipartition occurred for the first cluster with n=19 members, where 262,142 evaluations were generated.

During the bi-PORGS analysis for each value of k, the cost function minimizes the mean intracluster distance, then sums the means across all clusters. Because we were using the co-ancestory coefficient, θ, as a distance measure for the Chinook salmon data set, minimized cost function was referred to as the "mean sum theta" ($\Sigma\bar{\theta}$). For k=1 to 19, bi-PORGS values ($\downarrow CF$) represent optimal membership for each of these groups (Fig. 6A). The two most northerly Chinook salmon populations, Marble River and Colonial River (within the Quatsino Sound grouping), formed the first bipartition when ($\Sigma\bar{\theta}$=0.23). When k=4 ($\Sigma\bar{\theta}$=0.11) the remaining single cluster divided into 1) Nootka Sound, 2) Clayoquot+Barkley sounds, and 3) southwest Vancouver Island groups. Next, San Juan separated from the southwest Vancouver Island group,and the Quatsino group of Marble River and Colonial River split at k=6 ($\Sigma\bar{\theta}$=0.076). When eight groupings were optimized ($\Sigma\bar{\theta}$= 0.046) the Robertson-Creek–derived populations separated from Gold River and Nahmint River populations, as well as the Clayoquot Sound populations; and Sarita River populations split from the southwest Vancouver Island populations. The Burman River population split from the Nootka Sound populations at k=10 ($\Sigma\bar{\theta}$=0.029), and Clayoquot Sound populations (Tranquil River and Kennedy River) separated from the Barkley Sound populations (Gold River and Nahmint River). At k=12 ($\Sigma\bar{\theta}$=0.019) Thornton Creek split from Robertson Creek and Somas River, and the Gold and Nahmint Rivers split apart. At k=14 ($\Sigma\bar{\theta}$=0.011) Sooke River split from the Nitinat River and Toquart River populations, and Tranquil River and Kennedy River populations split. The last few remaining splits separated Tahsis River and Conuma River, Nitinat River and Toquart River, and finally Somas River and Robertson Creek populations (Fig. 6A).

As with the simulated data, the relationship between the number of groups and bi-PORGS evaluations decreases monotonically with increasing values of k (Fig. 6B); however, unlike the simulated situation, there appears to be more than one optimal point. The gap statistic indicates that the first optimum num-

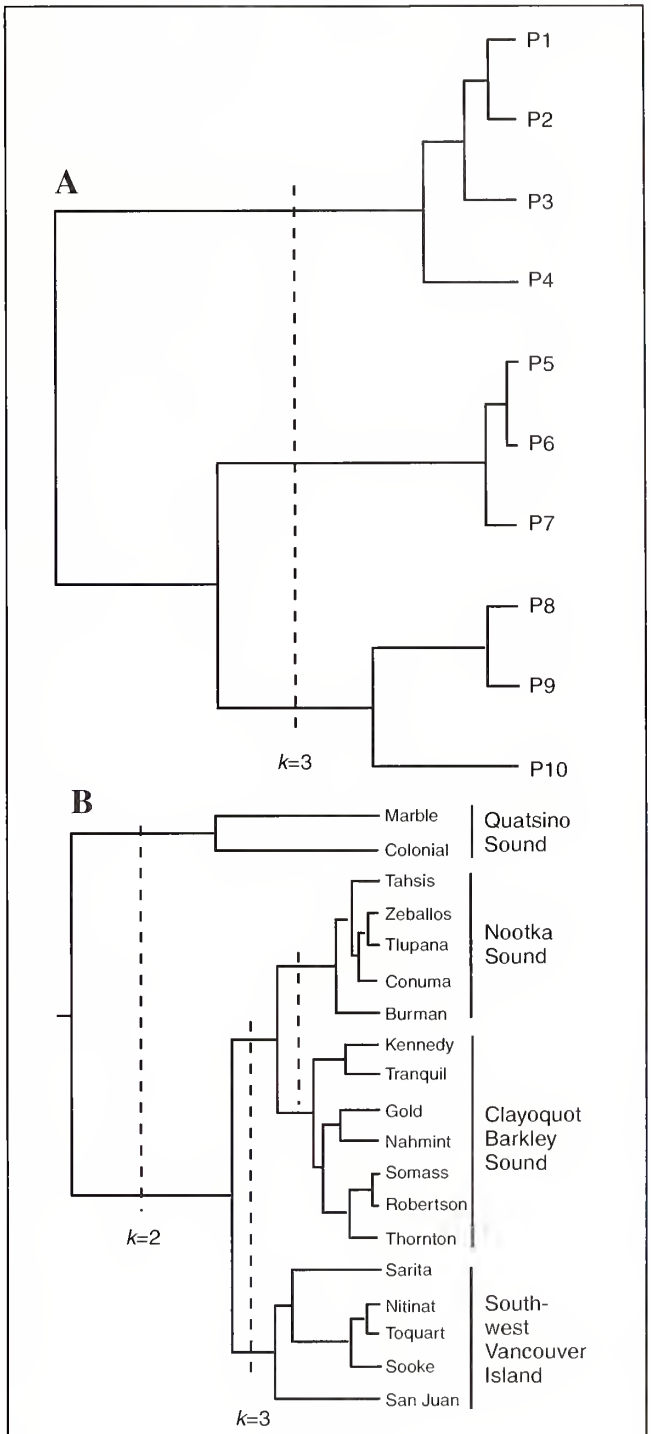

Figure 3

Dendrograms derived from (**A**) simulated genetic distance data clustered by the unweighted pair-group method using arithmetic averages (UPGMA) and from (**B**) genetic distance data for 18 populations of Chinook salmon (*Oncorhynchus tshawytscha*) from the west coast Vancouver Island clustered by using the co-ancestory coefficient θ. The dotted lines indicate corresponding groupings determined by bi-partitioning optimization using restrictive growth strings (bi-PORGS).

	Quatsino Snd		Nootka Sound					Clayoquot + Barkley sounds							Southwest Vancouver Island				
Population	Marble	Colonial	Zeballos	Tahsis	Conuma	Burman	Tlupana	Kennedy	Tranquil	<Gold>	Nahmint	Somas	Robertson	Thornton	San Juan	<Sarita>	<Toquart>	Nitinat	Sooke
Marble	0.000	0.040	0.050	0.053	0.059	0.061	0.058	0.051	0.048	0.040	0.036	0.037	0.043	0.052	0.054	0.063	0.069	0.072	0.076
Colonial	0.040	0.000	0.100	0.096	0.106	0.101	0.103	0.096	0.094	0.086	0.075	0.083	0.087	0.098	0.086	0.103	0.111	0.108	0.116
Zeballos	0.050	0.100	0.000	0.006	0.007	0.011	0.003	0.017	0.017	0.009	0.015	0.023	0.023	0.029	0.035	0.024	0.033	0.033	0.032
Tahsis	0.053	0.096	0.006	0.000	0.008	0.010	0.005	0.023	0.019	0.014	0.016	0.027	0.028	0.036	0.033	0.029	0.033	0.034	0.037
Conuma	0.059	0.106	0.007	0.008	0.000	0.013	0.003	0.027	0.024	0.018	0.025	0.034	0.035	0.043	0.046	0.034	0.042	0.041	0.044
Burman	0.061	0.101	0.011	0.010	0.013	0.000	0.008	0.022	0.021	0.014	0.019	0.031	0.031	0.040	0.042	0.029	0.038	0.038	0.043
Tlupana	0.058	0.103	0.003	0.005	0.003	0.008	0.000	0.027	0.025	0.017	0.023	0.032	0.035	0.042	0.044	0.035	0.042	0.043	0.043
Kennedy	0.051	0.096	0.017	0.023	0.027	0.022	0.027	0.000	0.009	0.014	0.015	0.018	0.017	0.021	0.031	0.027	0.037	0.037	0.042
Tranquil	0.048	0.094	0.017	0.019	0.024	0.021	0.025	0.009	0.000	0.014	0.015	0.015	0.014	0.021	0.030	0.021	0.034	0.035	0.044
Gold	0.040	0.086	0.009	0.014	0.018	0.014	0.017	0.014	0.014	0.000	0.010	0.009	0.011	0.019	0.033	0.027	0.035	0.036	0.034
Nahmint	0.036	0.075	0.015	0.016	0.025	0.019	0.023	0.015	0.015	0.010	0.000	0.013	0.013	0.019	0.027	0.024	0.030	0.033	0.037
Somas	0.037	0.083	0.023	0.027	0.034	0.031	0.032	0.018	0.015	0.009	0.013	0.000	0.002	0.008	0.030	0.032	0.044	0.046	0.046
Robertson	0.043	0.087	0.023	0.028	0.035	0.031	0.035	0.017	0.014	0.011	0.013	0.002	0.000	0.007	0.030	0.026	0.039	0.040	0.043
Thornton	0.052	0.098	0.029	0.036	0.043	0.040	0.042	0.021	0.021	0.019	0.019	0.008	0.007	0.000	0.036	0.030	0.043	0.046	0.053
San Juan	0.054	0.086	0.035	0.033	0.046	0.042	0.044	0.031	0.030	0.033	0.027	0.030	0.030	0.036	0.000	0.030	0.022	0.023	0.027
Sarita	0.063	0.103	0.024	0.029	0.034	0.029	0.035	0.027	0.021	0.027	0.024	0.032	0.026	0.030	0.030	0.000	0.018	0.016	0.029
Toquart	0.069	0.111	0.033	0.033	0.042	0.038	0.042	0.037	0.034	0.035	0.030	0.044	0.039	0.043	0.022	0.018	0.000	0.003	0.007
Nitinat	0.072	0.108	0.033	0.034	0.041	0.038	0.043	0.037	0.035	0.036	0.033	0.046	0.040	0.046	0.023	0.016	0.003	0.000	0.008
Sooke	0.076	0.116	0.032	0.037	0.044	0.043	0.043	0.042	0.044	0.034	0.037	0.046	0.043	0.053	0.027	0.029	0.007	0.008	0.000

Figure 4

Dissimilarity matrix of θ values for genetic distance data derived from Chinook salmon (*Oncorhynchus tshawytscha*) populations from the west coast of Vancouver Island. Values of θ where $\theta = 0$ are shown as white, $\theta < 0.02$ as light gray, $\theta < 0.04$ as dark gray, and $\theta \geq 0.04$ as black. Populations that show genetic affiliation but are outside the geographic region are denoted by < >.

ber of groups occurs at $k = 4$, corresponding to four geographic locations: Quatsino Sound, Nootka Sound, Clayoquot+Barkley sounds, and southwest Vancouver Island (Fig. 6C). At this point, additional groups do not cause the observed data to continue to drop substantially below the reference distribution. When k=9, a second peak in the optimum groupings occurred which corresponded to the partitioning of Barkley Sound and Clayoquot Sound populations, similar groupings were derived from the UPGMA tree; the vertical line in Figure 3B indicates the corresponding number of groups and group membership as determined by biPORGS. The four regional groups, Quatsino Sound, Nootka Sound, Clayoquot+Barkley sounds, and southwest Vancouver Island, each formed a cluster on the UPGMA tree; however, the optimum number of clusters is not obvious. The dendrogram appears to show greater genetic distance between the populations of Marble River and Colonial River than between populations of Nootka Sound and Clayoquot+Barkley sounds. Overall, the partition and agglomerative methods produced similar results.

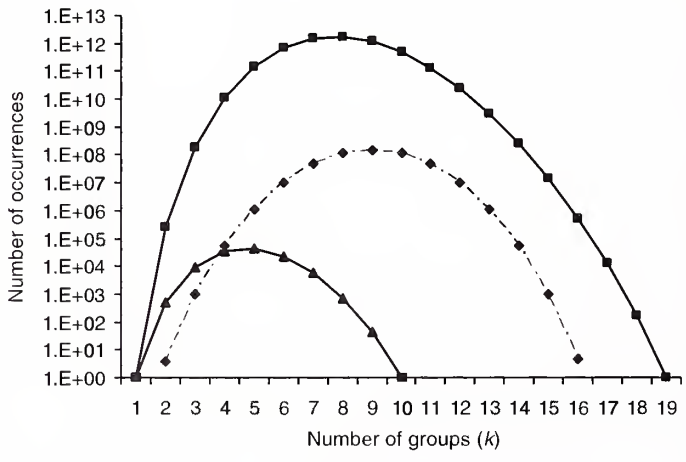

Figure 5

Number of occurrences by k groups for the simulated data set (—▲—) and for the Chinook salmon (*Oncorhynchus tshawytscha*) data set (n=19) with random search and 5.0×10^8 iterations (----◆----); and the total number of all set partition occurrences required for 19 populations (Stirling numbers of second kind (—■—).

Discussion

This article provides a new method for clustering genetic distance data by partitioning optimally with RGS, where acceptable partitions reduce intracluster distance. For this analysis, we used

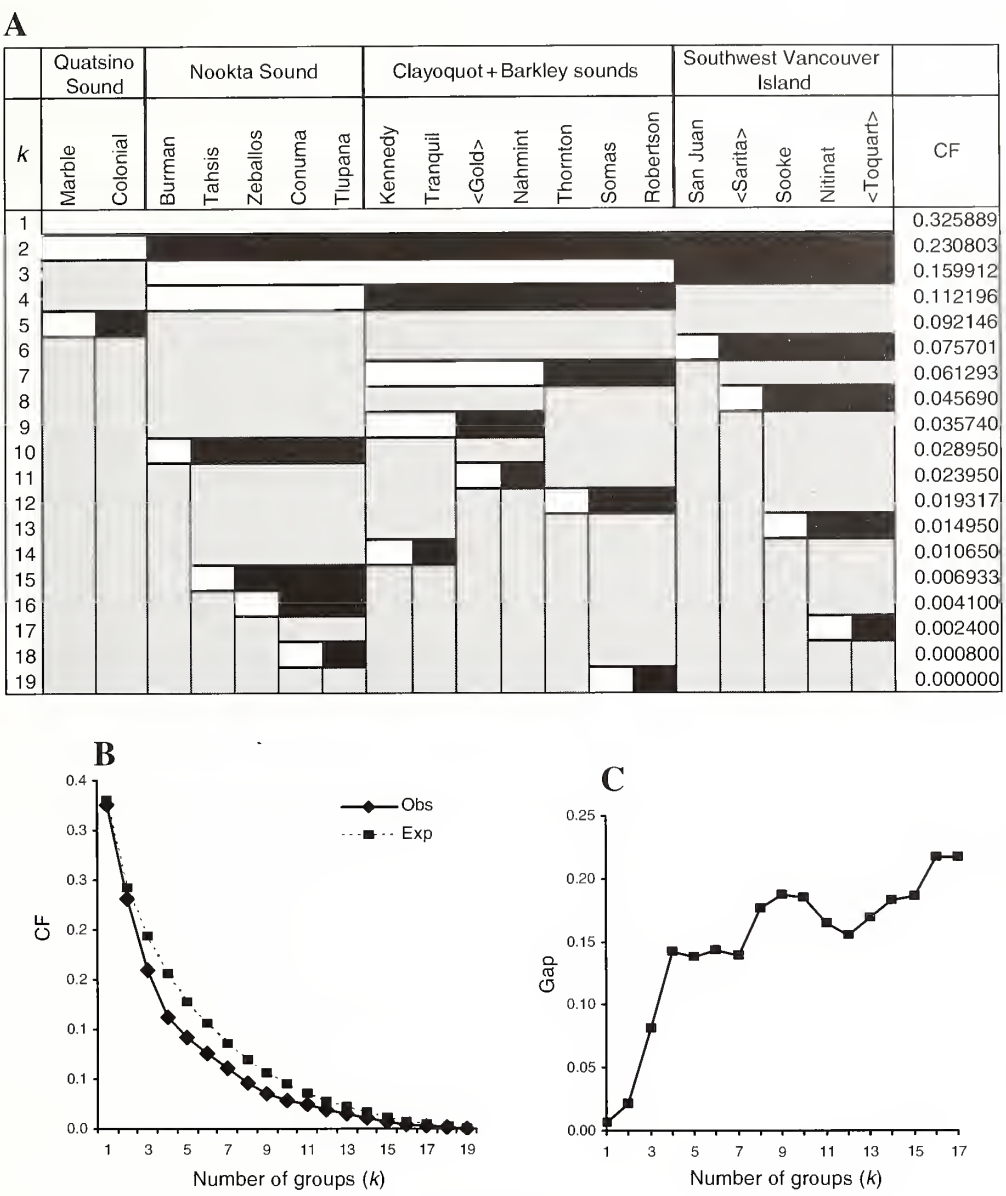

Figure 6

Clustering of genetic distance data for populations of Chinook salmon (*Oncorhynchus tshawytscha*) from the west coast of Vancouver Island. (**A**) Hierarchical group membership corresponding to minimized cost function (CF) by using bi-partitioning optimization using restrictive growth strings (bi-PORGS). Populations that show genetic affiliation but are outside the geographic region are denoted by < >. (**B**) Observed and expected values from the reference distribution plotted against k groups for the Chinook salmon data. (**C**) Gap statistic showing that the first optimum grouping occurs at k=4 and the second optimum grouping occurs at k=9. Black, gray, and white represent status of the populations for a given cluster number. Black and white represent populations involved in partitions for a particular value of k, whereas gray populations were not involved.

Weir and Cockerham's (1984) co-ancestory coefficient θ. A number of alternative distance measures could be tested with this method, but an examination of these measures is beyond the scope of this article. Also, determination and comparison of the optimal number of groupings directly from the multilocus genotypic data (e.g., Pritchard et al., 2000), instead of from the distance measures used here, would provide useful.

Unlike other clustering methods, PORGS does not have to embed distance data in vector space (i.e., mul-

tidimensional scaling); therefore, the underlying structure of the distance data remains intact, and resultant clusters can be compared between sets of populations. Successive increases in cluster numbers automatically lead to a hierarchical representation of the group structure. The gap statistic determines optimal number of groupings. In this example, $k=4$ was the first optimum number of groupings for Chinook salmon populations from the west coast of Vancouver Island. Except for populations impacted by straying fish and transferred fish, these groupings correspond to four geographic areas: Quatsino Sound, Nootka Sound, Clayoquot+Barkley sounds, and southwest Vancouver Island. Similar groupings were identified by agglomerative clustering seen in the UPGMA tree.

It was determined that random set partitions do not prevent visits to the same group memberships; therefore redundancy in cost function evaluations wastes processing time. Random search proves ineffective, except for very small n, because the prohibitively large number of iterations requires an unreasonable amount of time to find an optimal solution. However, an exhaustive search of the data space provided by a simple random search or a pass-through of all set partitions ensures that a globally optimized solution is found. By a globally optimal solution, we mean that no smaller cost function evaluations are possible for each k from a particular data set. Depending on available computational speed and the number of populations, PORGS can require an unreasonable amount of time. An alternative approach reduces the search by sequentially splitting into groups (bi-PORGS method) and evaluating subgrouping combinations to minimize the cost function. But like other hierarchical clustering methods, the nested search approach (bi-PORGS) means that prior cluster groups cannot be undone; therefore finding the optimal values may not always be possible. However, for the simulated data, PORGS and bi-PORGS methods produced the same results, indicating a globally optimal solution is possible with the nested search. The faster search method with bi-PORGS may forgo the guarantee of an optimal solution, but it can tackle larger problems, with the limitation being the number of populations in the first bipartition.

For large, coastwide data sets, a nested search requires bipartitioning a large number of populations simultaneously. Sparse data sets or optimization heuristics, such as thouse derived from deterministic annealing and mean field approximation, may be necessary when an exhaustive search is not possible (Puzicha et al., 1999). However, regional groupings could be recognized where each region could be run independently. This "divide and conquer" method requires that the subproblems be naturally disjoint, and that divisions be appropriate and of manageable size (Kirkpatrick et al., 1983). Ultimately, given the same set of genetic markers and distance measures, researchers will have a means of establishing groupings of varying size but representing similar levels of intracluster genetic variation.

Analysis of coded-wire tag data has indicated that straying Chinook salmon occur at a higher frequency between nearby spawning sites (e.g., Quinn, 1993; Candy and Beacham, 2000). Consequently, geographic distance between populations may be a good approximator of gene flow in salmon species; however, inferring barriers to migration on the basis of geographical or physical features alone can be misleading (Waples, 1991). The Gold River Chinook salmon population stands out by not conforming to the general rule of concordant genetic and geographic distance. According to geographic distance alone, Gold River Chinook salmon should be most genetically similar to Burman River Chinook salmon because less than 10 km separate the mouths of the two river systems. However, cluster analysis indicates that Gold River fish are most genetically similar to Barkley Sound fish, 125 km to the south (Fig. 1). Because the nearby Burman River population remains clustered with the Nootka Sound group, straying Barkley Sound fish must be extremely precise; apparently remaining in the Gold River only to spawn.

A number of factors could contribute to this restricted straying between Barkley Sound and the Gold River. Olfactory imprinting on waters near natal streams during out-migration is known to be important for successful homeward navigation (Harden Jones, 1968; Quinn, 1984). Consequently, the presence of pulp mills at the heads of both Muchalat (Gold River) and Alberni (Somas River) Inlets, and their effects on water chemistry, may increase straying between these two systems. Both systems lie at the head of long inlets, where the Gold and Somas Rivers have similar inlet and stream orientation. Also, both are lake-headed systems, possibly resulting in similarly modified river temperatures and flow regimes. Finally, approach to natal stream may be important for determining stray patterns. During the return migration to spawn, Barkley Sound, Chinook salmon heading south must first pass Nootka Sound, which provides an opportunity for these fish to eventually stray into the Gold River. The Gold River tissue samples collected in the early to mid-1980s, along with recent recoveries of thermally marked Robertson Hatchery fish in the Gold River, indicate that straying into the Gold River has likely occurred for quite a number of years.

Populations receiving transfers (Toquart, Thornton, and Sooke Rivers; Table 2) remain grouped to their respective donor stocks rather than to nearby populations, indicating that transfer history also plays an important role in establishing regional stock structure. The initial transfer of Robertson Creek fish to the Toquart River is not apparent from the bi-PORGS analysis, where Toquart River grouped with the second transfer source, Nitinat River. If native stocks existed in Toquart and Sooke Rivers before transfers into these systems, their continued existence there is not evident from the present study. However, populations with mixed ancestry may be better analyzed with individual-based clustering methods (Pritchard et al., 2000; Corander et al., 2003). The remaining two southwest Vancouver Island populations, where no transfers have occurred, remain quite distinctive.

Besides the history of transferred populations, other factors may determine genetic stock structure. Time of return to spawning grounds may provide a natural barrier to gene flow, preventing geographically superimposed populations from becoming genetically similar (Hendry and Day, 2005). Founder effects may play a role in shaping population structure, especially after recent colonization (Ramstad et al., 2004). Although multiyear sampling should address this problem, sampling error could be indistinguishable from allelic frequencies that are changed by some perturbing force. Indeed, small effective population size, where few related individuals are breeding, will hasten genetic drift (Waples, 1990). As a consequence of our inability to understand all mechanisms controlling gene flow, Waples (1991) warns against drawing inferences based on physical characteristics of the habitat without supporting biological information that links habitat differences to adaptations.

Little genetic variation with respect to population differentiation appears to have occurred in Robertson Creek over 23–30 years. Assuming that a majority of Robertson Creek fish return as four-year-olds (Healey, 1991), these years represent six to eight generations of Chinook salmon. The stability of microsatellite markers has been reported elsewhere for Atlantic salmon (*Salmo salar*) over a time frame of three to five generations (Tessier and Bernatchez, 1999). Furthermore, the genetic variation between populations with microsatellite markers was found to be 19 times greater than the interannual variation for sockeye salmon (*Oncorhynchus nerka;* Beacham et al., 2006b).

Microsatellites provide highly stable, reliable genetic markers for comparisons of genetic variation across the range of a species and are thus becoming an important tool for the management and conservation of genetic diversity of Pacific salmon species. Although genetic characters detected with these markers are neutral with respect to natural selection, it is likely that they are indicators of local adaptation in other encoding parts of the genome (Waples, 1991). Fine-scale grouping of genetically similar populations allows managers to make informed harvest and enhancement decisions. As was evident with Chinook salmon from the west coast of Vancouver Island, strictly geographically based assumptions regarding the level of genetic relatedness between populations can be incorrect.

Acknowledgements

The computer program PORGS, using the cost function (Roth et al., 2003) and RGS (Knuth, 2005; Algorithm 7.2.1.5H, modified for r blocks) is available from the contact author or for downloading from http://www.pac.dfo-mpo.gc.ca/sci/mgl/data_e.htm. We thank the staff at Robertson, Nitinat, and Conuma hatcheries, and R. Dunlop of the Nuu-chah-nulth Tribal Fisheries, for providing tissue samples for this analysis. We thank staff of the Molecular Genetics Laboratory (M. Wetklo, K. Jonsen, and J. Supernault) for laboratory work. We also thank the contributions of three anonymous reviewers who helped provide focus and clarity to the methods portion of this article.

Literature cited

Beacham, T. D., K. L. Jonsen, J. Supernault, M. Wetklo, L. Deng, and N. Varnavskaya.
2006a. Pacific Rim population structure of Chinook salmon as determined from microsatellite variation. Trans. Am. Fish. Soc. 135:1604–1621.

Beacham, T. D., B. McIntosh, C. MacConnachie, K. M. Miller, R. E. Withler, and N. Varnavskaya.
2006b. Pacific Rim population structure of sockeye salmon as determined from microsatellite analysis. Trans. Am. Fish. Soc. 135:174–187.

Buhmann, J. M.
2002. Data clustering and learning. *In* Handbook of brain theory and neural networks, 2nd ed. (M. A. Arbib, ed.), p. 308–312. MIT Press, Cambridge, MA.

Cameron, P. J.
1994. Combinatronics, Topics, Techniques, and Algorithms, 355 p. Cambridge Univ. Press, Cambridge, UK.

Candy, J. R., and T. D. Beacham.
2000. Patterns of homing and straying in southern British Columbia coded-wire tagged chinook salmon (*Oncorhynchus tshawytscha*) populations. Fish. Res. 4:41–56.

Cavalli-Sforza, L. L., and A. W. F. Edwards.
1967. Phylogenetic analysis: models and estimation procedures. Evolution 21:550–570.

Corander, J., P. Waldmann, and M. J. Sillanpää.
2003. Bayesian analysis of genetic differentiation between populations. Genetics 163:367–374.

Cross, C. L., L. Lapi, and E. A. Perry.
1991. Production of Chinook and Coho salmon from British Columbia hatcheries, 1971 through 1989. Can. Tech. Rep. Fish. Aquat. Sci. 1816, 48 p.

Felsenstein, J.
1985. Confidence limits on phylogenies: an approach using the bootstrap. Evol. 39:783–791.
1989. PHYLIP—Phylogeny inference package, vers. 3.2. Cladistics 5:164–166.

Goudet, J.
1995. FSTAT, a program to calculate F-statistics, vers, 1.2. J. Hered. 86:485–486.

Harden Jones, F. R.
1968. Fish migration, 134 p. St. Martin's Press, New York, NY.

Healey, M. C.
1991. Life history of Chinook salmon (*Oncorhynchus tshawytscha*). *In* Pacific salmon life history (C. Groot, and L. Margolis, eds.), p. 313–393. Univ. British Columbia Press, Vancouver, B.C.

Hendry, A. P., and T. Day.
2005. Population structure attributable to reproductive time: isolation by time and adaptation by time. Mol. Ecol. 14:901–916.

Hofmann, T., and J. M. Buhmann.
1997. Pairwise data clustering by deterministic annealing. IEEE Trans. Pattern Anal. Mach. Intel. 18:1–37.

Jain, A. K., M. N. Murty, and P. J. Flynn.
1999. Data clustering: a review. Assoc. Comput. Mach. Trans. Comput. Surv.31:265–322.
Kirkpatrick, S., C. D. Gelitt, and M. P. Vecchi.
1983. Optimization by simulated annealing. Science 220:671–680.
Knuth, D. E.
2005. The art of computer programming, vol. 4, fascicle 3, Generating all combinations and partitions, 150 p. Addison-Wesley, Reading, MA.
Nei, M.
1987. Molecular evolutionary genetics, 512 p. Columbia Univ. Press, New York, NY.
Nei, M., F. Tajima, and Y. Tateno.
1983. Accuracy of estimated phylogenetic trees from microsatellite DNA. Genetics 144:389–399.
Pritchard, J. K., M. Stephens, and P. Donnelly.
2000. Inference of population structure using multilocus genotype data. Genetics 155:945–959.
Puzicha, J., T. Hofmann, and J. Buhmann.
1999. A theory of proximity based clustering: structure detection by optimization. Pattern Recogn. 33:617–634.
Quinn, T. P.
1984. Homing and straying in Chinook salmon (*Oncorhynchus tshawytscha*) from the Cowlitz River hatchery, Washington. Can. J. Fish. Aquat. Sci. 41:1078–1082.
1993. A review of homing and straying of wild and hatchery-produced salmon. Fish. Res. 18:29–44.
Quinn, T. P., and A. H. Dittman.
1990. Pacific salmon migrations and homing: mechanisms and adaptive significance. Trends Ecol. Evol. 5:174–177.
Ramstad, K. M., C. A. Woody, G. K. Sage, and F. W. Allendorf.
2004. Founding events influence genetic population structure of sockeye salmon (*Oncorhynchus nerka*). Mol. Ecol. 13:277–290.
Ricker, W. E.
1972. Hereditary and environmental factors affecting certain salmonid populations. *In* The stock concept of Pacific salmon (R. C. Simon, and P. Larkin, eds.), p. 19–160. Univ. British Columbia Press, Vancouver, B.C.
Riddell, B. E.
1993. Spatial organization of Pacific salmon: what to conserve? *In* Genetic conservation of salmonid fishes (J. G. Cloud, and G. H. Thorgaard, eds.), p. 23–41. Plenum Press, New York, NY.
Robinson, W. S.
1951. A method for chronologically ordering archeological deposits. Am. Antiq. 16:293–301.
Rota, G. C.
1964. The number of partitions of a set. Am. Math. Mon. 71(5):498–504.
Roth, V., J. Laub, M. Kawanabe, and J. Buhmann.
2003. Optimal cluster preserving embedding of nonmetric proximity data. IEEE Trans. Pattern Anal. Mach. Intel. 5:1540–1550.
Sneath, P. H. A., and R. R. Sokal.
1973. Numerical taxonomy, 573 p. Freeman, San Francisco, CA.
Swofford, D. L., G. L. Olsen, P. J. Waddell, and D. M. Hillis.
1996. Phylogenetic inference. *In* Molecular systematics (D. M. Hillis and C. Mortiz, eds.), p. 407–514. Sinauer Assocs., Dunderland, MA.
Teel, D. J., G. B. Miller, G. A. Winans, and W. S. Grant.
2000. Genetic population structure and origin of life history types in Chinook salmon in British Columbia, Canada. Trans. Am. Fish. Soc. 129:194–209.
Tessier, N., and L. Bernatchez.
1999. Stability of population structure and genetic diversity across generations assessed by microsatellites among sympatric populations of landlocked Atlantic salmon (*Salmo salar* L.). Mol. Ecol. 8:169–179.
Tibshirani, R., G. Walther, and T. Hastie.
2001. Estimating the number of clusters in a data set via the Gap statistic. J. Royal Stat. Soc. 63(2):411–423.
van der Kloot, W. A., A. M. J. Spaans, and W. J. Heiser.
2005. Instability of hierarchical cluster analysis due to input order of the data: the Permcluster solution. Psychol. Methods 10:468–476.
Waples, R. S.
1990. Conservation genetics of Pacific salmon. II. Effective population size and the rate of loss of genetic variability. J. Hered. 81:256–276.
1991. Pacific salmon, *Onchorhynchus* spp., and the definition of "species" under the Endangered Species Act. Mar. Fish. Rev 53:11–22.
Waples, R. S., and O. Gaggiotti.
2006. What is a population? An empirical evaluation of some genetic methods for identifying the number of gene pools and their degree of connectivity. Mol. Ecol. 15:1419–1439.
Waples, R. S., R. G. Gustafson, L. A. Weitkamp, J. M. Myers, O. W. Johnson, P. J. Busby, J. J. Hard, G. J. Bryant, F. W. Waknitz, K. Nelly, D. Teel, W. S. Grant, G. A. Winans, S. Phelps, A. Marshall, and B. M. Baker.
2001. Characterizing diversity in salmon from the Pacific Northwest. J. Fish. Biol. 59:1–41.
Weir, B. S., and C. C. Cockerham.
1984. Estimating *F*-statistics from the analysis of population structure. Evolution 38:1358–1370.

The western blue groper (*Achoerodus gouldii*), a protogynous hermaphroditic labrid with exceptional longevity, late maturity, slow growth, and both late maturation and sex change

Peter G. Coulson
S. Alex Hesp
Norman G. Hall
Ian C. Potter (contact author)

Email address for contact author: I.Potter@murdoch.edu.au

Centre for Fish and Fisheries Research
School of Biological Sciences and Biotechnology
Murdoch University
South Street
Murdoch, Western Australia, 6150, Australia

Abstract—The western blue groper (*Achoerodus gouldii*) is shown to be a temperate protogynous hermaphrodite, which spawns between early winter and mid-spring. Because *A. gouldii* changes body color at about the time of sex change, its color can be used as a proxy for sex for estimating the size and age at sex change and for estimating growth when it is not possible to use gonads for determining the sex of this fish. The following characteristics make *A. gouldii* highly susceptible to overfishing: 1) exceptional longevity, with a maximum age (70 years) that is by far the greatest yet estimated for a labrid; 2) slow growth for the first 15 years and little subsequent growth by females; and 3) late maturation at a large total length (TL_{50}=653 mm) and old age (~17 years) and 4) late sex change at an even greater total length (TL_{50}=821 mm) and age (~35 years). The TL_{50} at maturity and particularly at sex change exceeded the minimum legal total length (500 mm) of *A. gouldii* and the lengths of many recreationally and commercially caught fish. Many of these characteristics are found in certain deep-water fishes that are likewise considered susceptible to overfishing. Indeed, although fishing effort for *A. gouldii* in Western Australia is not particularly high, per-recruit analyses indicate that this species is already close to or fully exploited.

Manuscript submitted 20 April 2008.
Manuscript accepted 9 September 2008.
Fish. Bull. 107:57–75 (2009).

The views and opinions expressed or implied in this article are those of the author and do not necessarily reflect the position of the National Marine Fisheries Service, NOAA.

Species of the family Labridae, which represents one of the largest and most speciose of all perciform families (comprising 82 genera and at least 600 species) are found in tropical and temperate coastal and continental shelf waters throughout the world (Westneat and Alfaro, 2005; Allen et al., 2006). On the basis of demographic analyses of large labrid species, Choat et al. (2006) concluded that they are characterised by relatively short life spans and indeterminate growth rates, namely, growth does not tend to an asymptote. However, a few species have substantial life spans; the oldest ages yet recorded for a labrid are 30–35 years (Gillanders, 1995a; Choat and Robertson, 2002; Choat et al., 2006).

Most of the biological studies on labrids have been undertaken on subtropical and tropical species (Denny and Schiel, 2002). These studies have shown that many members of this family are protogynous hermaphrodites, namely they change from female to male (e.g., Reinboth, 1970; Candi et al., 2004; McBride and Johnson, 2007). Sex change in these labrids is often accompanied by a change in body color and they are thus sexually dichromatic (Warner and Robertson, 1978; Shapiro, 1981; Gillanders, 1995a). Among labrids, a few species change from one sex to another and then back again, and thus undergo what is termed reversed sex change (Ohta et al., 2003; Kuwamura et al., 2007), and a number are gonochoristic, i.e., do not undergo sex change (Dipper and Pullin, 1979; Bentivegna and Benedetto, 1989; Sadovy de Mitcheson and Liu, 2008). However, a recent study of the green humphead parrotfish (*Bolbometopon muricatum*) has emphasised that a definitive conclusion as to whether certain species in this family are protogynous hermaphrodites or gonochorists can be difficult to ascertain, even when there is detailed information on such features as the size compositions of the two sexes and the histological characteristics of their gonads (Hamilton et al., 2008).

The western blue groper (*Achoerodus gouldii*) is found throughout southern Australia, southwards from the Houtman Abrolhos Islands at 28°30′S, 113°40′E on the west coast and eastwards along the south coast to Portland in Victoria at 38°21′S; 141°36′E (Hutchins and Swainston, 1986; Gommon et al., 1994) but is most abundant on the south coasts of Western Australia and South Australia. This species is reported to attain a maximum length of 175 cm (Gommon et al., 1994), which, among labrids, is apparently exceeded only by the humphead wrasse (*Cheilinus undulates*) (Sadovy et al., 2003). Although *A. gouldii* is the second most

commercially important species of scale fish on the south coast of Western Australia and is highly regarded by recreational anglers, detailed studies of its biology have been restricted to its foraging behavior, diet, and habitat, and how these change with body size (Shepherd, 2005; Shepherd and Brook, 2007). In contrast, several aspects of the biology of the congeneric eastern blue groper (*Achoerodus viridis*), which is distributed along the eastern and southeastern coasts of Australia and does not grow to as large a size as that of *A. gouldii* (Hutchins and Swainston, 1986), have been studied (e.g., Gillanders, 1995a, 1995b, 1997; Gillanders and Kingsford, 1998). The apparently detrimental effects of fishing on *A. viridis* led to this species being protected from both recreational and commercial fishing in 1969, although these restrictions were later eased to some extent in 1974 (Gillanders, 1999).

The present study demonstrates that *A. gouldii* is a protogynous hermaphrodite and provides data on the length and age compositions, growth, reproductive biology, recruitment variability, and stock status (mortality, and spawning potential ratio) of this species in southwestern Australian waters. The data were used to test the following hypotheses. 1) The far greater size of *A. gouldii* than the morphologically and ecologically similar congeneric eastern blue groper (*Achoerodus viridis*) is reflected in a greater maximum age and greater sizes and ages at which females become mature and later change sex. 2) It would then follow that *A. gouldii* has by the greatest longevity of any labrid species. Because protogynous labrids that exhibit sexual dichromatism tend to change color at about the same size and age as at which sex change occurs, the body colors of *A. gouldii* (typically green for females and blue for males) can be used as proxies for sex for determining the total length at which 50% of fish (TL_{50}) change color and the patterns of growth of females and males of this labrid. An ability to use color in this manner would be useful when, for example, fish cannot be dissected or the viscera have been removed. 3) Because environmental factors on the southwest coast of Australia, such as those brought about by marked variations in the strength of the Leeuwin Current (Pearce and Phillips, 1988), exhibit considerable interannual variations in winter, i.e., when *A. gouldii* spawns (see *Results* section), the recruitment success of this species on this coast differs among years. Lastly, inferences drawn from the biological data and stock assessment parameters are discussed for their applicability to management plans aimed at conserving the stocks of *A. gouldii*.

Materials and methods

Sampling regime and laboratory processing

Achoerodus gouldii was collected monthly or bimonthly between April 2004 and October 2007 from numerous sites in coastal waters between Albany (at 35°01′S, 117°58′E) and Esperance (at 33°45′S, 21°55′E) off the south coast of Western Australia. These fish were either caught by spear fishing in shallow (<20 m) inshore coastal waters or were obtained from commercial gill net fishing crews (mesh range=165–178 mm) operating in deeper (~20–100 m) offshore waters. A few *A. gouldii* (~3%) were also collected directly from commercial gillnet fishing vessels fishing in deeper, offshore waters at a latitude of ~32°S on the lower west coast of Australia. Although many of the individuals obtained from commercial gillnet fishing vessels were supplied as eviscerated and filleted frames, some were intact and therefore still contained their gonads.

Shallow, inshore water temperatures at Albany and Esperance, recorded by the Department of Fisheries, Western Australia, at intervals in the years 1994–2006, were pooled by month and used to calculate the average for each calendar month. Mean monthly offshore sea surface temperatures for Albany and Esperance in 2004–06 were derived by using a combination of data from National Oceanic and Atmospheric Administration (NOAA) advanced very high resolution radiometer (AVHRR) satellite imagery and from sea surface temperatures recorded by shipping and drifting buoys (Reynolds and Smith, 1994). The mean monthly water temperatures in inshore and offshore waters in the above two main sampling locations were plotted to elucidate the relationship between the initiation and duration of spawning and water temperature, which are typically related in teleosts (e.g., Lam, 1983).

The color (green or blue) and total length (TL, to the nearest 1 mm) of all *A. gouldii*, and the wet weight (W, to the nearest 0.1 g) of each of those individuals that had not been filleted, eviscerated, (or both), were recorded. The sex of each *A. gouldii* that had not been eviscerated and had a TL >~100 mm (the length above which the sex could be determined macroscopically) was also recorded. Because all of the large number of sexed fish <655 mm were females (see *Results*), the small number of fish <100 mm were recorded as this sex. Although the possibility cannot be excluded that some of the latter very small *A. gouldii* (<100 mm) may have been bisexual (i.e., possessed gonads containing both ovarian and testicular material), the fact that all individuals between the substantial length range of 100–655 mm were females means that this attribute would not have influenced the conclusions regarding whether this species is hermaphroditic and, if so, of which type (see *Discussion*). The gonads of each fish were removed and weighed to the nearest 0.01 g.

The relationship between TL and W was used to estimate the weights of *A. gouldii* collected from fish processors and recreational fishing crews and which had been filleted, eviscerated, or both, before they could be weighed. To facilitate comparisons between the lengths of *A. gouldii* and those of its congener *A. viridis*, the latter of which were recorded as standard lengths to the nearest 1 mm by Gillanders (1995a), standard lengths for 455 *A. viridis* were converted to total lengths by using the equation

$$TL = 1.19(SL) + 7.93,$$

where TL = total length;
SL = standard length; and

for which the value of the coefficient of determination was 0.99 ($P<0.001$).

Note that, because the tail of *A. gouldii* is not forked, the TL and fork lengths (FL) of this species are the same and thus the TL for this species can be compared directly with the fork lengths recorded for other labrid species (e.g., Choat et al., 2006).

Aging methods, length and age compositions, and growth patterns

Preliminary examination of the otoliths of a wide size range of *A. gouldii* before and after sectioning demonstrated that even the otoliths of small fish required sectioning to reveal all of their opaque zones. One sagittal otolith from each individual was embedded in clear epoxy resin and a section of ~0.3 mm thickness was cut transversely through the primordium with an Isomet Buehler low-speed diamond saw (Buehler Ltd., Lake Bluff, IL). The otolith sections were polished with wet and dry carborundum paper (grade 1200) and mounted on microscope slides with DePeX mounting adhesive (VWR International Ltd., Poole, England) and a cover slip. Electronic images of each section of otolith and of its peripheral region (at a higher magnification) were taken with transmitted light and an Olympus DP70 camera (Olympus Optical Co. Ltd., Tokyo, Japan) mounted on an Olympus BX51 compound microscope (Olympus Optical Co. Ltd., Tokyo, Japan). These images were used for counting opaque zones and measuring the distances required for marginal increment analysis, respectively. All images were examined by using Leica Image Manager 1000 (Leica Microsystems, Heerbrugg, Switzerland), which enabled the well-defined opaque zones (Fig. 1) to be marked and automatically counted and the distances required for marginal increment analysis to be measured precisely.

Validation that a single opaque zone is formed annually in the otoliths of *A. gouldii* was carried out by analyzing the trends exhibited throughout the year by the marginal increment on the otoliths, i.e., the distance between the outer edge of the single or outermost opaque zone and the otolith periphery. The marginal increment was expressed as the proportion of the distance between the primordium and the outer edge of the opaque zone, when one such zone was present, or as the proportion of the distance between the outer edges of the two outermost opaque zones when two or more such zones were present. All distances, which were recorded to the nearest 0.01 mm, were measured on the anterior surface of the otoliths and along the same axis as and perpendicular to the opaque zones.

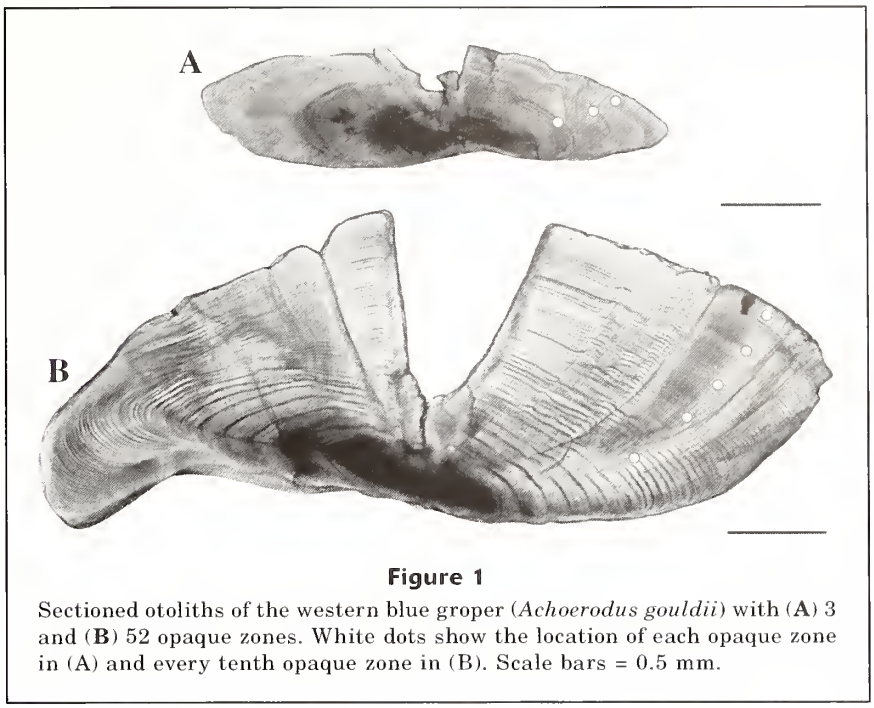

Figure 1

Sectioned otoliths of the western blue groper (*Achoerodus gouldii*) with (**A**) 3 and (**B**) 52 opaque zones. White dots show the location of each opaque zone in (A) and every tenth opaque zone in (B). Scale bars = 0.5 mm.

The opaque zones on the anterior surface in an image of each sectioned otolith were counted on three different occasions. The three counts were the same in 91.0% of otoliths with ≤20 opaque zones and 70.4% of those with >20 opaque zones. In the case of each otolith for which the three counts were not the same, if two of those counts were the same, these counts were the ones recorded for aging. The numbers of opaque zones in 150 otoliths from a wide size range of fish were counted by a second and experienced otolith reader (S. A. Hesp) and compared with those recorded by the senior author. The counts of 70 of the 100 otoliths with ≤20 opaque zones were the same and, where there were discrepancies, they differed by only 1 in 28 of the otoliths and 2 in the other two otoliths. For the 50 otoliths containing >20 opaque zones, the counts were the same or differed by 1 in 34 of those otoliths and differed by no more than 2 in a further seven otoliths. The maximum difference in the counts for otoliths with >20 opaque zones was 4. Following discussions between the two readers, it became apparent that the main reason for discrepancies in counts was due to the first reader, who through his extensive experience of examining the otoliths of *A. gouldii*, was able more consistently to detect the first zone. The level of agreement between the counts of the two readers was therefore high when his experience in detecting the first zone was taken into account.

Each fish was assigned an age based on its date of capture, the number of opaque zones in its otoliths, the time of year when newly formed opaque zones become

delineated from the otolith periphery, and on an appropriate birth date for *A. gouldii* (see *Results*). The von Bertalanffy growth equation, used for describing the growth of *A. gouldii*, **is**

$$L_t = L_\infty\left(1-\exp^{\left(-k(t-t_0)\right)}\right),$$

where L_t = the length (mm TL) at age t (years);
L_∞ = the mean asymptotic length (mm) predicted by the equation;
k = the growth coefficient (per year); and
t_0 = the hypothetical age (years) at which fish would have zero length.

Von Bertalanffy growth curves were fitted to the lengths at age of *A. gouldii* in the cases of 1) all fish irrespective of their sex; 2) females and males that had been sexed on the basis of an examination of their gonads; and 3) those fish that were a mixture of green and blue among the individuals used for constructing the growth curves for each sex in 2 (the above growth curves were fitted by using nonlinear regression in the Statistical Package for the Social Sciences, SPSS (vers. 11.0, SPSS Inc., Chicago, IL); and 4) von Bertalanffy growth curves for each sex were next fitted to the combination of the lengths at age of sexed and unsexed individuals, taking into account the probability that, from its total length and color, an unsexed fish would be a male or a female. For each unsexed fish, the expected length, $\hat{L}_j^s$, was first calculated as

$$\hat{L}_j^s = \begin{cases} L_\infty^f\left(1-\exp\left[-k^f\left(t_j-t_0^f\right)\right]\right) & \text{if } s=f \text{ or } t_j \le t_{\text{diverge}} \\ L_\infty^m\left(1-\exp\left[-k^m\left(t_j-t_0^m\right)\right]\right) & \text{if } s=m \text{ and } t_j > t_{\text{diverge}} \end{cases},$$

where s = sex ($s = f$ for a female and m for a male);
t_j = the age of fish j;
$t_{diverge}$ = the age at which it was assumed that female and male growth curves began to diverge;
L_∞^f and L_∞^m = the mean asymptotic lengths for females and males, respectively;
k^f and k^m = the growth coefficients for females and males, respectively; and
t_0^f and t_0^m = the hypothetical ages at which, assuming growth in accordance with the above von Bertalanffy growth equations, females and males, respectively, would have zero length.

Note that, if $L_{diverge}$ is the expected length of the females at age $t_{diverge}$, then

$$t_0^m = t_0^f - \left(1/k^f\right)\log_e\left[1-\left(L_{\text{diverge}}/L_\infty^f\right)\right] + \left(1/k^m\right)\log_e\left[1-\left(L_{\text{diverge}}/L_\infty^m\right)\right],$$

where $\log_e$ = the natural logarithm.

The observed lengths at age of fish were assumed to be normally distributed about the predicted lengths at age for each sex, and to have a common standard deviation.

The probability that fish j was of sex s was denoted by p_j^s, where $p_j^f = 1-p_j^m$ and where $p_j^m = 1$ if the fish possessed testes, $p_j^m = 0$ if the fish possessed ovaries and p_j^m = the value calculated with the logistic equation presented in the next section if the fish had been eviscerated and sex could not therefore be determined. The value of the normal probability density function, for fish j of sex s, ϕ_j^s, was calculated as

$$\phi_j^s = 1/\left(\sqrt{2\pi sd^2}\right)\exp\left[-\left(\left(L_j-\hat{L}_j^s\right)^2\right)/\left(2\,sd^2\right)\right],$$

where L_j = the observed length at age;
$\hat{L}_j^s$ = the predicted length at age;
sd = the standard deviation; and
π = the constant pi.

The log-likelihood, λ, determined as $\sum_j \log_e\left(\sum_s p_j^s \phi_j^s\right)$, was maximized by using Solver in Microsoft Excel to estimate the parameters L_∞^f, k^f, t_0^f, L_∞^m, k^m, $t_{diverge}$, and sd. Approximate 95% bootstrap confidence limits of the parameters were calculated as the 2.5 and 97.5 percentiles of the parameter estimates obtained by fitting the model to 1000 resampled data sets.

Reproductive biology

The gonadosomatic index (GSI) of each female with a length ≥ the TL_{50} at maturity (see *Results*) was calculated as

$$GSI = (W_1/W)\times 100,$$

where W_1 = wet gonad weight; and
W = wet body weight.

The criteria of Moore et al. (2007), adapted from Laevastu (1965), was used to allocate each gonad to one of the following maturity stages, I = virgin; II = immature or resting; III = developing; IV = maturing; V = prespawning; VI = spawning; VII = spent; and VIII = recovering or spent. Note that the TL_{50} at maturity was used as the cut off for determining the GSI of individuals because, outside the spawning period, it was not possible macroscopically to distinguish the gonads of virgins (stage I) from those of fish that had matured but were in a resting state (stage II).

Gonads from a large subsample of females and males in each month were placed in Bouin's fixative for 24 to 48 hr—the duration depending on the size of the gonad. They were then dehydrated in a series of increasing concentrations of ethanol and their mid-regions were embedded in paraffin wax and cut into 6-μm transverse sections, which were stained with Mallory's trichrome. The histological characteristics of the ovaries in that large subsample (see Coulson et al., 2005) were used to

validate the macroscopic staging. Note that comparisons of transverse sections through the anterior, middle, and posterior regions of the gonads of 10 *A. gouldii* over a wide size range demonstrated that the characteristics of those gonads remained similar throughout their length.

The length at which 50% of female *A. gouldii* attained maturity (TL_{50}) was determined by fitting a logistic curve to the probability that, during the spawning period, a female fish at a specific length would possess gonads at one of stages III to VIII. As such fish were potentially destined to become mature or had reached maturity during that period (see *Results*), they are, for convenience, referred to as mature in the present study. The logistic equation used for this analysis was

$$P = 1/\left\{1+\exp\left[-\log_e(19)(TL-TL_{50})/(TL_{95}-TL_{50})\right]\right\},$$

where P = proportion mature;
TL = total length in mm; and
TL_{50} and TL_{95} = the total lengths in mm at which 50% and 95% of fish were mature, respectively.

The logistic equation was fitted by using Markovian chain Monte Carlo simulation in WinBUGS (vers. 1.4.3, MRC Biostatistics Unit, Cambridge, U.K.) from 500,000 iterations, discarding the first 1000 iterations as the initial burn in set and using a thinning interval of 100 iterations. After assessment in WinBUGS that convergence was likely to have been achieved, the point estimates of the parameters of the logistic equation and their 95% confidence intervals, and of the probabilities of fish being mature at a range of specified lengths, were determined as the medians and the 2.5 and 97.5 percentiles of the estimates produced by WinBUGS.

Because the six fish with gonads containing both testicular and ovarian tissue all had lengths that lay within the range where the prevalence of females was decreasing and that of males was increasing, they were considered likely to be changing from female to male. Because the testicular tissue in those fish was more mature than the ovarian material, the data for these fish were combined with those for male *A. gouldii* for determining the length and age at which *A. gouldii* change sex. WinBUGS was then used as above to estimate the TL_{50} and TL_{95} for change in both sex and color, i.e., from green to blue (from female to male).

Logistic regression analysis was employed to relate the probability, p_j^m, that fish j was a male to its length L_j and color C_j (green=0, blue=1). p_j^m was determined as

$$\left[1+\exp\left(-\alpha-\beta_1 L_j-\beta_2 C_j\right)\right]^{-1},$$

where α, β_1, and β_2 are constants.

The probability that fish j possessed female gonads, p_j^f, was determined as $p_j^f = 1 - p_j^m$. The Akaike information criterion (AIC) (Burnham and Anderson, 2002) was used to determine which of the models, based solely on either length ($\beta_2=0$) or color ($\beta_1=0$), provided the better predictions. The AIC is determined by the following equation:

$$AIC = -2\lambda + 2K,$$

where λ = the log-likelihood; and
K = number of parameters.

The model with the lowest AIC value was selected as the better of the two models. The likelihood-ratio test (Cerrato, 1990) was then used to determine whether the model that contained both length and color significantly improved the prediction that a fish was a male.

Recruitment variability, mortality, and spawning potential ratio

The number of fish in each year class in each of three successive annual periods was determined. Because 1 August coincides with the birth date designated for *A. gouldii*, these estimates of numbers encompassed each of the three successive 12-month periods between 1 August and the following 31 July in the years 2004 to 2007.

Total mortality, Z, for *A. gouldii* was estimated from the age compositions of samples of fish collected during the above three successive 12-month periods (years) by using catch curve analysis and then relative abundance analysis (see below). We used data obtained from the commercial gillnet fisheries and assumed knife-edge recruitment into the fishery at 15 years, i.e., we restricted data to those for the descending limbs of the catch curves (Ricker, 1975).

Initially, an estimate of Z was calculated by using catch curve analysis, where recruitment was assumed to be constant. For a fish stock that experiences a constant level of Z from the age of full recruitment, $a = t_c$ years, the estimated proportion, $\hat{P}_{a,t}$, of fish at age a in year t is

$$\hat{P}_{a,t} = \left\{R_{t-a}\exp\left[-(a-t_c)Z\right]\right\} / \left\{\sum_{j=t_c}^{A} R_{t-j}\exp\left[-(j-t_c)Z\right]\right\},$$

where A = the maximum observed age;
j = an index of age, where $t_c \le j \le A$;
R_{t-a} = the number of fish of year class $t-a$ that recruited at age t_c years to the fully vulnerable portion of the fish stock in year $t\text{-}a+t_c$, and which, in year t, are of age a years; and
R_{t-j} = the number of fish of year class $t-j$ that recruited at age t_c years to the fully vulnerable portion of the fish stock in year $t\text{-}j+t_c$, and which, in year t, are of age j years.

It is assumed that the age composition of fish with ages $t_c \leq a \leq A$ observed in year t represents a random sample from a multinomial distribution and uniform selectivity from the age of full recruitment. Thus, by ignoring constants, the log-likelihood, λ, of the age compositions observed in the various years may be calculated as

$$\lambda = \sum_{t} \sum_{a=t_c}^{A} n_{a,t} \log\left[\hat{P}_{a,t}\right],$$

where $n_{a,t}$ = the observed number of fish of age a in year t.

An estimate of Z was obtained by maximizing the log-likelihood by using Solver in Excel (vers. 2003, Microsoft Corporation, Salem, MA).

Next, the constraint that recruitment is constant in the analysis just described was relaxed and an estimate of Z was determined with relative abundance analysis (Deriso et al., 1985). This latter analysis, which is an extension of catch curve analysis, involved initially setting the relative level of recruitment, R_y, for each year class, y, to 1. The relative levels of recruitment of the different year classes were then successively introduced as additional parameters to be estimated by the model, by using a stepwise forward selection algorithm (e.g., Sokal and Rohlf, 1995). The process was terminated when the introduction of R_y as a parameter to be estimated for any further year class failed to produce a statistically significant improvement in the fit of the model to the data, as determined with the likelihood-ratio test (Cerrato, 1990). At each stage, the relative levels of recruitment for year classes not included as parameters to be estimated in the model continued to be constrained to the average level, i.e., 1. The 95% confidence intervals for Z for *A. gouldii*, when either constant or variable recruitment was assumed, were obtained from the profile likelihood for Z (Hilborn and Mangel, 1997). All of the above calculations for Z were undertaken by maximizing the above log-likelihood with the Solver tool in Excel.

The point estimate and 95% confidence intervals for the natural mortality, M, of *A. gouldii* were determined by refitting, in SPSS, Hoenig's (1983) regression equation for fish to the values for mortalities and maximum ages for 82 unexploited or lightly exploited fish stocks (see Hall et al., 2004) and including the maximum recorded age for *A. gouldii*.

The approach of Hall et al. (2004) was used to determine the likelihood for M, calculated by using the likelihood for Z, as derived by using the relative abundance analysis and assuming variable recruitment. For this estimation it was assumed that, for each value of Z, there is a uniform probability that $M < Z$. The resulting likelihood for M was then combined with the estimate for M derived by refitting Hoenig's (1983) regression equation for fish.

A Monte Carlo resampling approach was used to derive estimates of F for the fully recruited age classes of each species. Estimates of Z (from the relative abundance analysis) and M (from the method of Hall et al., 2004) were randomly resampled, with replacement, from their respective probability distributions, and any pair of estimates for which the value for M was greater than Z was rejected. 10,000 sets of estimates of Z and M were produced, from which 10,000 estimates of F were determined with the equation $F = Z - M$. The point estimate of F and associated 95% confidence limits were taken as the median value and the 2.5 and 97.5 percentiles of these estimates.

The spawning stock biomass per age-0 recruit (SSB/R) of *A. gouldii* was calculated for each sex with the equation

$$SSB/R = \sum_{a=t_c}^{A} W_a P_{sex,a} P_{mat,a} \exp(-Za),$$

where Z = total mortality;
W_a = the weight of a fish at age a;
$P_{sex,a}$ = the proportions of each sex at age a; and
$P_{mat,a}$ = the proportions of mature females at each age a.

W_a was calculated by using the von Bertalanffy growth curves for each sex and the relationship between total body weight (g) and length (mm). For males, $P_{sex,a}$ was determined by using the growth curve and the logistic relationship describing the probability that a fish of a given length is a male, whereas, for females, $P_{sex,a}$ was calculated as 1 minus this probability. $P_{mat,a}$ was determined by using the logistic function describing the probability that a fish of a given length is mature, together with the lengths at age predicted by using the von Bertalanffy growth function. All males were assumed to be mature. Estimates of SSB/R were determined for each of the 10,000 values generated for F by the resampling procedure. The point estimates and associated 95% confidence limits for the current level of SSB/R were taken as the median and 2.5 and 97.5 percentiles of the resulting SSB/R values. The spawning potential ratio, SPR, was calculated as the ratio of SSB/R at a specified level of fishing mortality to that for an unfished population (Goodyear, 1993). For the per-recruit analysis we assumed that knife-edge recruitment to the fishery occurred at 15 years, total mortality for fully recruited fish was constant and the maximum age was 100 years.

Results

Aging methods, length and age compositions, and growth pattern

The mean monthly marginal increments on sectioned otoliths of *A. gouldii* with 2–10 zones remained relatively high (≥0.39) between July and October, before declining sequentially to 0.36 in November and to a minimum of 0.26 in January and February, and then

rising progressively in the ensuing months (Fig. 2). Although the numbers of otoliths with one opaque zone in each month were far less, their mean values could still be seen to follow a similar annual trend. Although the mean monthly marginal increments on otoliths with 11–20, 21–30, and >30 zones followed trends that were very similar to those described for otoliths with 2–10 zones, the minima of the last two groups were reached later. Consequently, as the number of zones in otoliths increases, the new opaque zone in otoliths becomes visually detectable later, i.e., in late summer to early autumn, rather than in late spring to mid-summer. The similar single decline and subsequent progressive rise in mean monthly marginal increments, irrespective of the number of opaque zones, demonstrate that a single opaque zone is formed annually in the otoliths of *A. gouldii*. The numbers of opaque zones in otoliths could therefore be used for aging this species.

From the trends exhibited by the mean monthly GSIs and prevalence in each month of females with stages V and VI ovaries, the approximate mid-point of the spawning period was estimated to be August, i.e., the end of the Austral winter. The small fish caught in November were ~40 mm in length, and those captured in February and March were ~60 and 90 mm, respectively. The otoliths of the latter (Feb. and Mar.) two collections of fish contained no opaque zones, which is consistent with these fish, on average, having been spawned in late winter and therefore not having had the opportunity to lay down the opaque zone that is deposited annually during that season in older fish. The first of these zones becomes delineated in the spring of the second year of life, i.e., when fish are ~140 mm in length and ~18 months old.

The individuals in samples of *A. gouldii* ranged in total length from 40 to 1162 mm and in age from a few months to 70 years (Fig. 3). The largest and oldest *A. gouldii*, from which the gonads had not been removed and could therefore be sexed, were 880 mm and 49 years, for females, and 1134 mm and 57 years, for males.

Although the 822 *A. gouldii* collected by spear fishing ranged from 40 to 1050 mm TL, the majority of those individuals measured between 100 and 600 mm, a range of TLs that corresponds to ages 1 to 11 years (Fig 4). The 1107 *A. gouldii* obtained from the commercial gillnet fishery ranged from 428 to 1162 mm (TL) and from 6 to 70 years, but most were between 500 and 800 mm (TL) and 10 and 34 years (Fig. 3).

A von Bertalanffy growth curve provided a good fit to the lengths at age of *A. gouldii* (r^2=0.84; Table 1, Fig. 4A). On the basis of the von Bertalanffy growth equation, *A. gouldii* attain lengths of 335, 509, 678, 741, 764, and 773 mm by ages 5, 10, 20, 30, 40, and 50 years, respectively. The marked similarity in the estimated lengths at 30, 40, and 50 years of age reflects the markedly asymptotic pattern of growth of *A. gouldii*, with relatively little overall growth occurring after 15 years with females and 30 years with males.

The von Bertalanffy growth curves fitted separately to the lengths at age of sexed fish demonstrated that, after the age at which some females had changed to males, the growth curve for males increasingly diverged upwards from that for females (Fig. 4B). Thus, for example, at 20, 35, and 50 years, the estimated lengths at age for males were 805, 923, and 965 mm, respectively; whereas those for females were 679, 737, and 746 mm, respectively. The above differences in growth

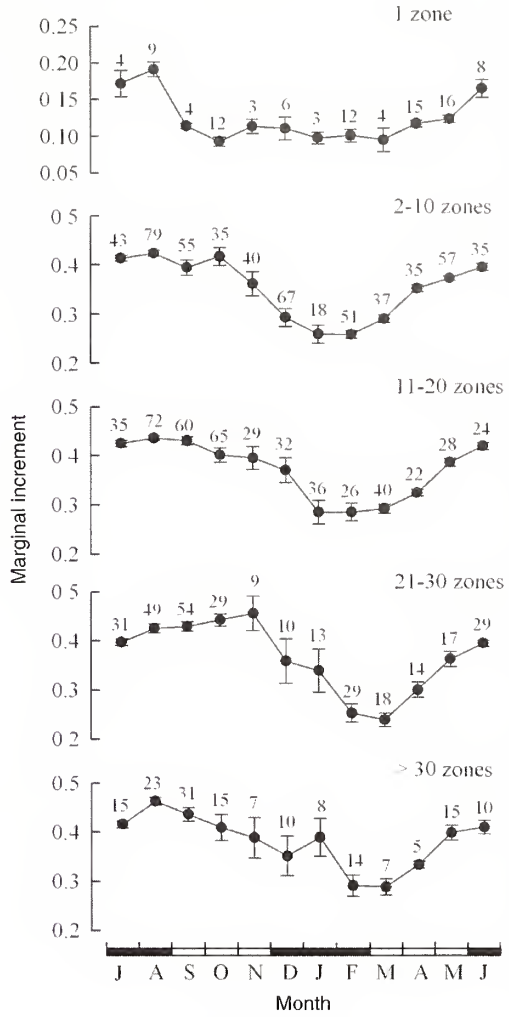

Figure 2

Mean monthly marginal increments ±1 standard error for sectioned sagittal otoliths of the western blue groper (*Achoerodus gouldii*) with different numbers of opaque zones. The marginal increment is expressed as a proportion of the distance between the primordium and the outer edge of the opaque zone, when one such zone was present, or as a proportion of the distance between the outer edges of the two outermost opaque zones when two or more such zones were present. Sample sizes are shown above each mean. Closed rectangles on the *x*-axis refer to winter and summer months and the open rectangles to spring and autumn months.

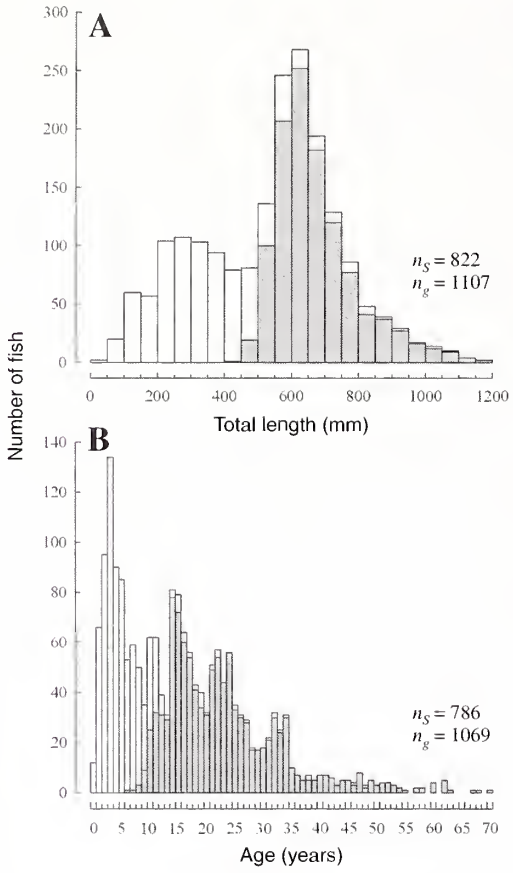

Figure 3

Length- and age-frequency distributions for the western blue groper (*Achoerodus gouldii*) caught by spear fishing (open histograms) and commercial gill netting (gray histograms). n_s and n_g, represent the number of fish caught by spear fishing and gill netting, respectively.

are reflected in a lower estimate for k for males (0.08/year) than for females (0.12/year), and in a reverse situation for L_∞, for which the respective values were 975 for males and 748 mm for females (Table 1).

When von Bertalanffy growth curves were fitted separately to the lengths at age of those individuals that were either green or blue, but that constituted the same subset of fish as those just used to describe the growth of males and females (Fig. 4B), the values for L_∞ and k for blue and for green fish were either identical or very similar to those for females and males, respectively (Fig. 4C; Table 1). Von Bertalanffy growth curves were next fitted to the lengths at age of fish, determined as females and males by using their gonadal characteristics (i.e., those used for Fig. 4B), and to the lengths at age of fish that could not be sexed by using gonads but could be assigned a sex on the basis of the combination of

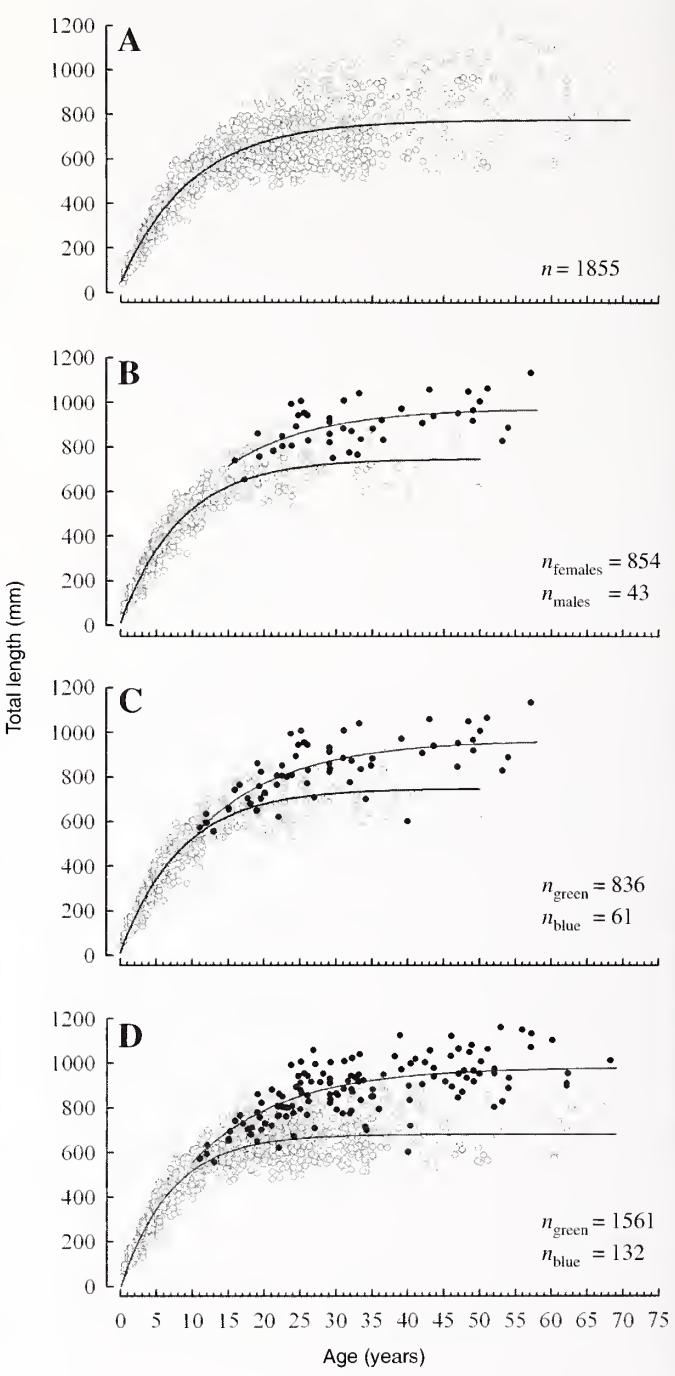

Figure 4

Von Bertalanffy growth curves fitted to the lengths at age of (**A**) all sexed and unsexed individuals, (**B**) females (open circles) and males (black circles) sexed on the basis of their gonadal characteristics, (**C**) the same individuals as in (B) but separated according to whether they were green (open circles) or blue (black circles), and (**D**) for females (open circles) and males (black circles), for which the sex of each individual had been designated by using either its gonadal characteristics or the probability of it being female or male on the basis of a combination of its body color and length. n = sample size.

Table 1

Estimates of the von Bertalanffy growth curve parameters L_∞, k, and t_0 (and their lower and upper 95% confidence limits [CLs]) for western blue groper (*Achoerodus gouldii*) caught off southwestern Australia (A) for all fish, (B) for females and males whose sex was determined from gonadal characteristics, (C) for the same fish as in B but according to whether they were green or blue, and (D) for fish whose sex was determined by using either gonad type or the likelihood of the fish being female or male on the basis of a combination of its length and color. L_∞ is the asymptotic length (mm), k is the growth coefficient (per year), t_0 is the hypothetical age (years) at which fish would have zero length, r^2 is the coefficient of determination, and n is the number of fish sampled.

Category			L_∞	k	t_0	r^2	n
A	All fish	Estimate	777	0.10	−0.65	0.84	1855
		Lower, upper CL	766, 789	0.09, 0.11	−0.90, −0.39		
B	Females	Estimate	748	0.12	−0.15	0.92	854
		Lower, upper CL	732, 764	0.11, 0.12	−0.30, 0.00		
	Males	Estimate	975	0.08	−0.91	0.35	43
		Lower, upper CL	879, 1072	−0.02, 0.19	−22.84, 21.03		
C	Green	Estimate	748	0.12	−0.17	0.92	836
		Lower, upper CL	731, 765	0.11, 0.12	−0.32, −0.02		
	Blue	Estimate	966	0.08	−0.10	0.53	61
		Lower, upper CL	867, 1055	0.03, 0.13	−8.38, 8.18		
D	Females	Estimate	682	0.14	0.06	0.93 for both sexes combined	1561
		Lower, upper CL	675, 692	0.14, 0.15	0.00, 0.10		
	Males	Estimate	982	0.08	−0.48		132
		Lower, upper CL	952,1013	0.07, 0.09	−1.09, −0.14		

its length and color (see *Results*). The resultant curves for the "females" and "males" fitted the length-at-age data very well (Fig. 4D), as is demonstrated by the high r^2 value of 0.93 for the model fitted to the data that produced the two separate curves (Table 1). Although the L_∞ estimated for the males shown in Fig. 4D was virtually identical to that derived for males in the subset of fish sexed on the basis of their gonadal characteristics in Fig. 4B, the L_∞ for females shown in Fig. 4D was less than that for females whose sex has been determined on the basis of their gonads, reflecting the presence of an increased number of older females and therefore an even greater tendency for the curve to reach an asymptote (Table 1).

The relationship between total length (TL) in mm and total weight (W) in g for *A. gouldii* is $\ln W = 3.041(\ln TL) - 11.017$ (r^2=0.997, P<0.001, n=756) and the relationship between standard length (SL) in mm and total length (TL) in mm is $TL = 1.201\ (SL) - 11.883$ (r^2=0.995, P<.001, n=101).

Reproductive biology

Temperatures in inshore and offshore waters at both Albany and Esperance underwent seasonal changes (Fig. 5, A and B). However, they were more pronounced, i.e., peaked earlier in mid-summer vs. early autumn, and reached their minima earlier, i.e., late-winter vs. mid spring, in inshore waters. Furthermore, the differences between water temperatures in inshore waters at the two locations in corresponding months were not as great as in offshore waters and, in some months, were greater at Esperance than at Albany. Although temperatures in deeper waters at Esperance on the south coast followed essentially the same seasonal trends as those at Albany, they were 1° to 1.5°C lower for each month.

The mean monthly GSIs for female *A. gouldii* ≥ the TL_{50} at maturity, i.e., 653 mm (see later), remained low, i.e., <0.50 between December and May and then rose sharply to a peak of 2.3 in July, before declining to ≤1.6 in August to October and 0.1 in November (Fig. 5C). The gonads of all females collected between November and May with lengths ≥ the TL_{50} at maturity possessed immature and resting ovaries (stage II). Female fish with ovaries at stages III and IV were caught in June and July and those with ovarian stages V and VI, between June and October (Fig. 5C). The above trends in the monthly female GSIs and the prevalence of females at different ovarian stages demonstrate that spawning occurs predominantly between June and October and that females with ovaries that develop beyond stage II will become mature during the spawning period.

The smallest mature female (i.e., with ovaries at one of stages III–VIII) caught during the spawning period measured 391 mm (Fig. 6A). The prevalence of mature females increased from 2% in the 350–399 mm length class to >40% in all length classes above 600 mm, and to 100% in fish >800 mm (Fig. 6A). The estimate for the TL_{50} for female *A. gouldii* at maturity (and its 95% confidence intervals) was 653 mm (623–693 mm).

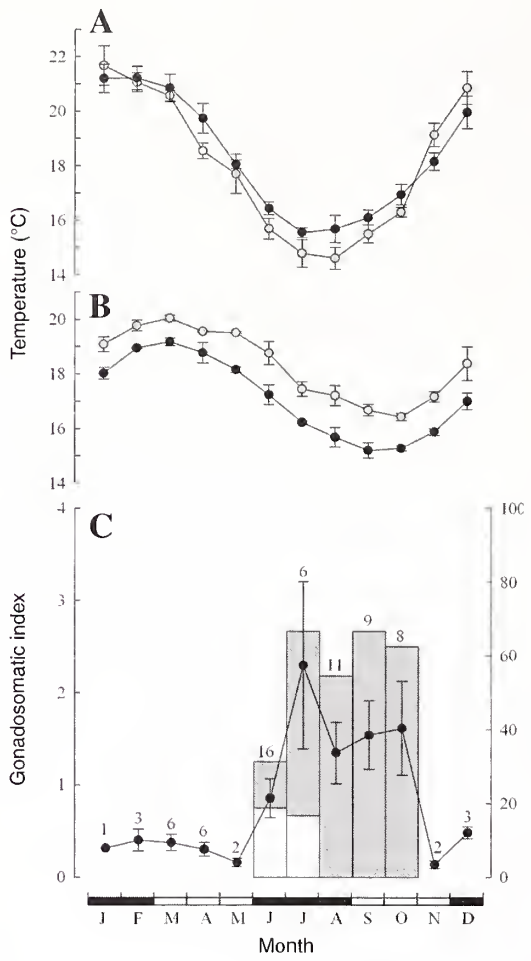

Figure 5

Mean monthly water temperatures ±1 standard error for (**A**) inshore and (**B**) offshore waters at Albany (gray circles) and Esperance (black circles) on the south coast of Western Australia and (**C**) mean monthly gonadosomatic indices ±1 SE for female western blue groper (*Achoerodus gouldii*) and mean monthly percent frequencies of occurrence of ovaries at stages III and IV (white) and V and VI (gray). Monthly sample sizes are shown on the figure. Closed rectangles on the *x*-axis refer to winter and summer months and the open rectangles to spring and autumn months.

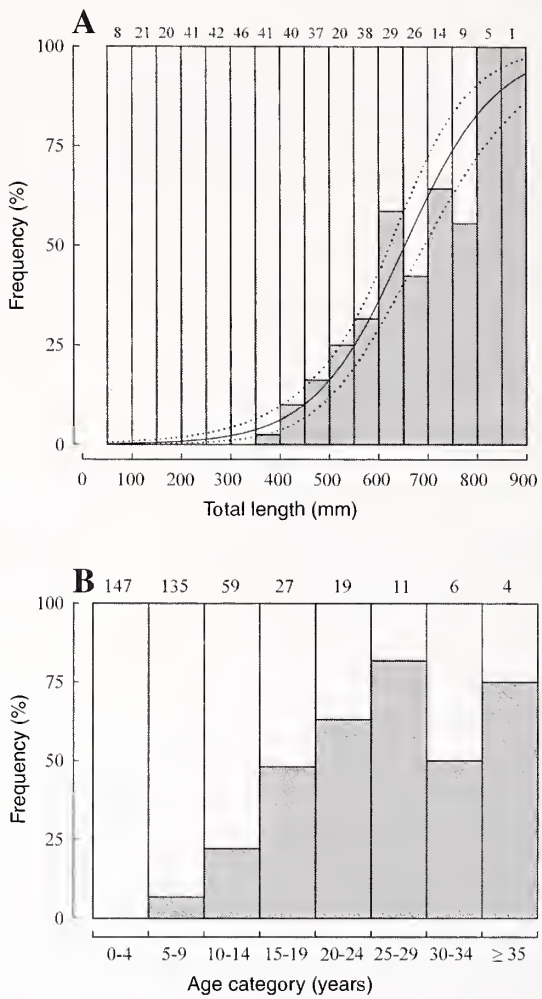

Figure 6

Percent frequency of occurrence of female western blue groper (*Achoerodus gouldii*) with mature gonads (gray histograms) in sequential (**A**) 50-mm length classes and (**B**) five-year age categories in samples obtained during the spawning period, i.e., from June to October. A logistic curve (solid line) and its 95% confidence limits (dotted lines) in (A) were derived from the probability that a fish at a given length is mature. Sample sizes are shown above the histograms for each 50-mm length class and each age category.

The youngest female that was mature during the spawning period was 5 years old. The prevalence of mature females in sequential five-year age categories increased from 7% in fish of 5–9 years to 63% in fish of 20–24 years (Fig. 6B). Although the prevalence of mature females caught during the spawning period reached 81% in fish of 25–29 years, it did not reach 100% in either the 30–34 age-class category or that comprising all older fish (Fig. 6B).

Among the 200 *A. gouldii* with lengths between 100 and 1041 mm and whose gonads were examined histologically, all 150 individuals <655 mm contained exclusively ovarian tissue (Fig. 7A) and were therefore females. All but six of the 50 individuals with lengths ≥655 mm contained exclusively either ovarian tissue (e.g., Fig. 7B) or testicular tissue (e.g., Fig. 7C). The gonadal tissue of those six exceptions—fish whose lengths ranged from 758 to 850 mm—comprised testicular

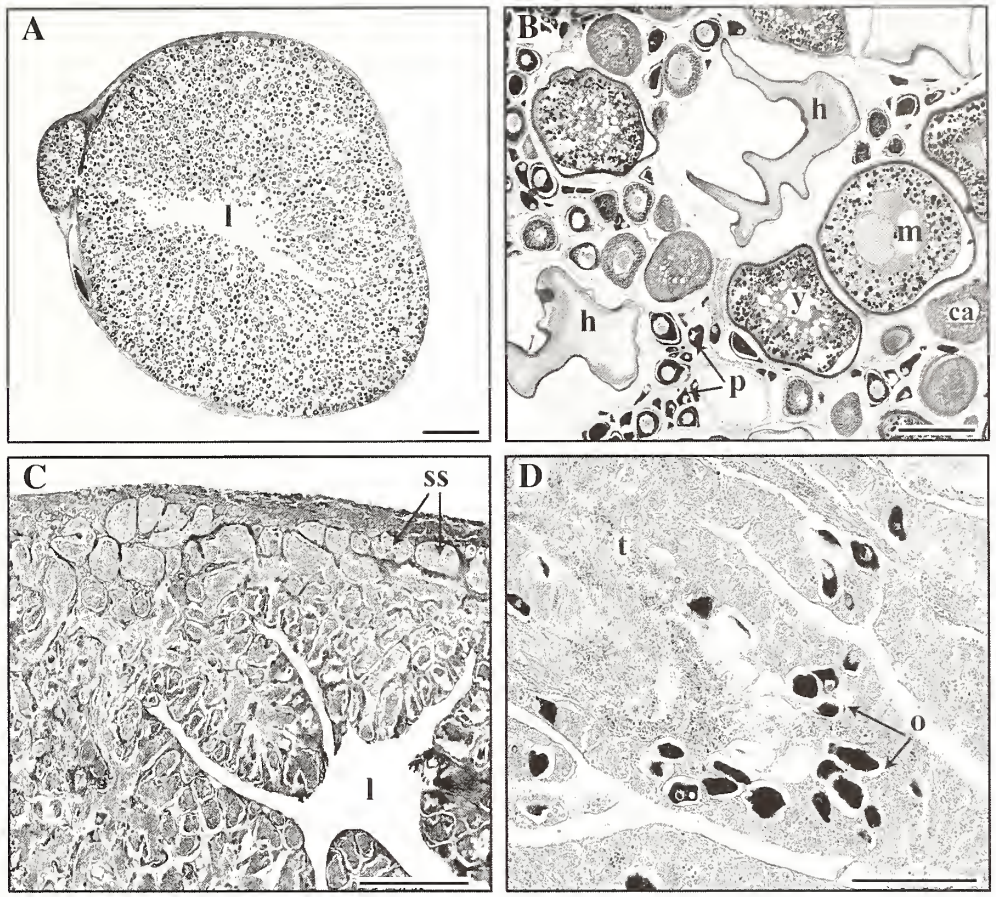

Figure 7

Histological sections of gonads of western blue groper (*Achoerodus gouldii*). (**A**) Ovary of immature female containing numerous previtellogenic oocytes and a prominent lumen (l); (**B**) ovary of mature female containing early previtellogenic oocytes (p), cortical alveolar oocytes (ca), yolk granule oocytes (y), migratory nucleolar oocytes (m), and hydrated oocytes (h); (**C**) mature testes with prominent lumen (l) and sperm sinuses (ss); and (**D**) gonad comprising mainly testicular tissue (t) and numerous previtellogenic oocytes (o). Scale bars = 1000 μm in (A) and 200 μm in (B–D).

tissue within which previtellogenic oocytes were scattered (Fig. 7D).

All immature ovaries, i.e., those containing only previtellogenic oocytes, possessed a prominent central lumen (Fig. 7A). This lumen was largely or fully occluded in mature and spawning ovaries (stages V and VI) (Fig. 7B). A conspicuous central lumen and peripherally located sperm sinuses (Fig. 7D) were present in all mature testes examined histologically.

On the basis of macroscopic examination of all gonads removed from fish and histological examination of a large subsample of those gonads, all *A. gouldii* <655 mm in length were females (Fig. 8A). The prevalence of male fish increased progressively from 3% in the 650–699 mm length class to 80% in the 850–899 mm length class, and to 100% among fish ≥900 mm (Fig. 8A). The TL_{50} at sex change was 821 mm (Table 2).

Among the 891 females, 866 (97%) were green and 39 of the 44 males (89%) were blue. All fish <550 mm were green (Fig. 8B). The prevalence of fish with blue coloration increased rapidly from 8% in the 550–599 mm length class to 86% in the 800–849 mm length class and reached 100% in all fish ≥900 mm (Fig. 8B). The confidence intervals for the TL_{50} of 779 mm at color change overlapped those for the TL_{50} of 821 mm at sex change (Table 2).

All fish <15 years old were females (Fig. 8A). The prevalence of males increased from 9% in fish of 15–19 years to 67% in those of 35–39 years and to 100% in those ≥50 years (Fig. 8A). The trend exhibited by the change from green to blue with increasing age broadly paralleled that for the change from female to male (Fig. 8, A and B). However, a few fish changed color at an even earlier age than the youngest age at which sex change was first found to occur.

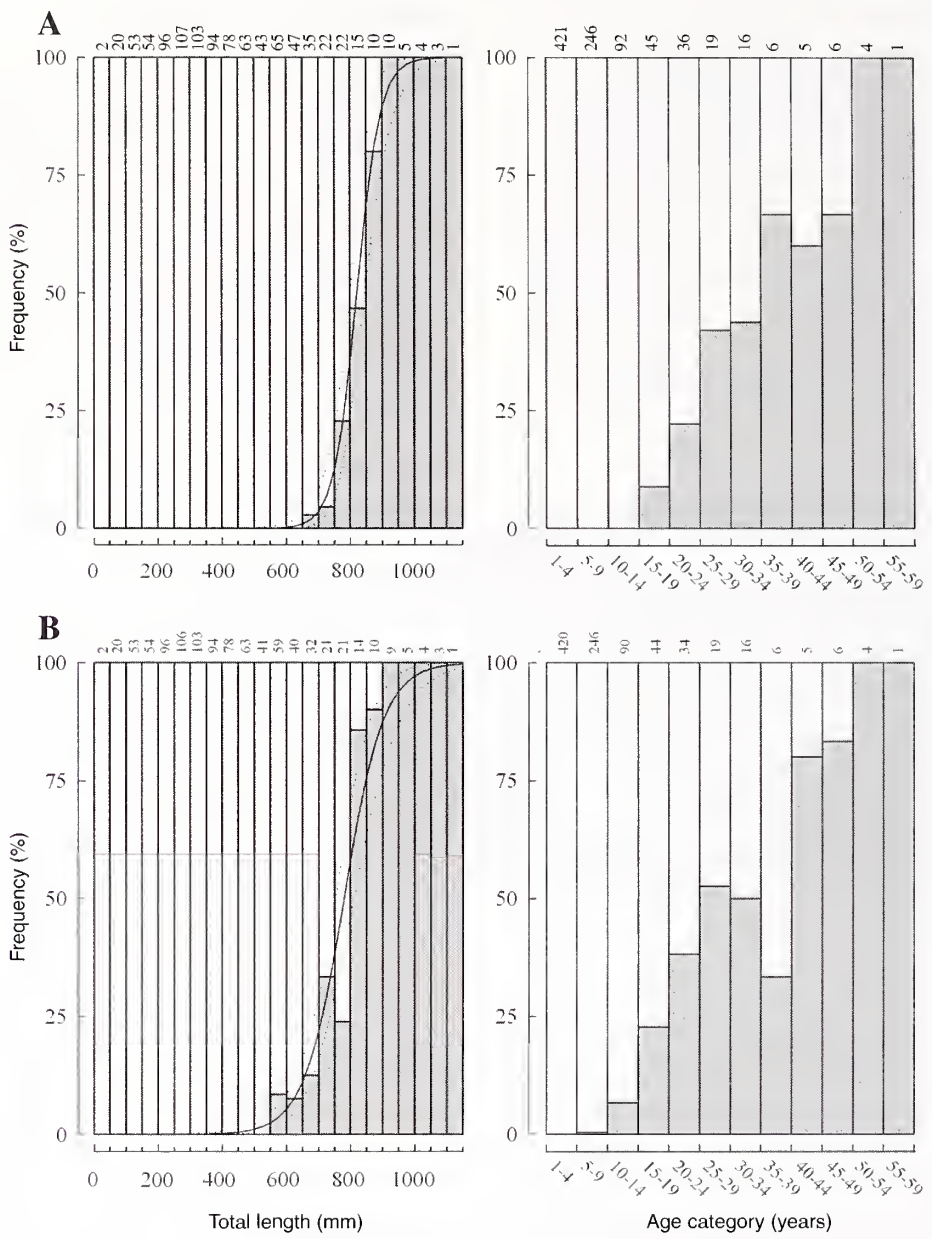

Figure 8

Percent frequencies of occurrence, in sequential 50-mm length classes and 5-year age categories, of the western blue groper (*Achoerodus gouldii*) with (**A**) testes, i.e., males (gray histograms), and (**B**) blue coloration (gray histograms). The logistic curves (solid line) and their 95% confidence limits (dotted lines) were derived from the probability that a fish at a given length is male in (A) and blue in (B). Sample sizes are shown above each histogram.

The values for the AIC showed that the dichotomous factor, color, is not as good a predictor as the continuous variable, length, that an individual is male (Table 3). However, the likelihood-ratio test demonstrated that the combination of color and length provided a significantly better fit than length alone (P=0.012).

Recruitment variability, mortality, and spawning potential ratio

From the data shown in Figure 3, it is assumed that *A. gouldii* becomes fully recruited to the commercial gillnet fishery by 15 years of age. Because a substantial

number of fish >35 years old were caught by this fishery and the distribution of the lengths of the males did not appear to be truncated, mesh selectivity did not apparently exert a major influence on the upper end of the length distribution.

Relative abundance analysis demonstrated that, in the three successive 12-month periods between August and July, 11 of the year classes between 1936 and 1992 differed significantly from the average level of recruitment. The strengths of the 1972, 1980, 1983, and 1990 year classes were 3.6, 2.6, 2.1, and 1.5 times greater, respectively, than the average level of recruitment (Fig. 9). Among the other year classes that differed significantly from the average level of annual recruitment, the 1981, 1958, 1971, and 1944 year classes were strong, whereas the 1991, 1992, and 1985 year classes were weak (Fig. 9).

The total mortality estimate, Z, of 0.086/year (0.08–0.092/year), derived from the catch curve analysis with the assumption of constant recruitment, was slightly less than the 0.093/year (0.08–0.092/year), derived for *Z* by using the relative abundance analysis and assuming variable recruitment. The estimate for *M*, derived by refitting Hoenig's (1983) equation for fish and inserting the maximum age for *A. gouldii*, was 0.072/year (0.022–0.180/year). The approach of Hall et al. (2004), which was used to refine the above estimate of *M*, yielded a lower value, i.e., 0.054/year (0.021–0.090/year). Fishing mortality, *F*, was estimated to be 0.039/year (0.003–0.073/year).

The spawning potential ratio at the current estimated level of *F*, on the basis of spawning stock biomass per recruit and calculated by using the von Bertalanffy growth curves for the females and males of *A. gouldii* shown in Figure 4D, was 0.88 (0.75–0.99) for females and 0.52 (0.27–0.96) for males (Fig. 10).

Table 2

Estimates of the total lengths (and their lower and upper 95% confidence limits [CLs], in mm) at which 50% (TL_{50}) and 95% (TL_{95}) of western blue groper (*Achoerodus gouldii*) change sex to male and the total lengths at which 50% and 95% of *A. gouldii* change from green (females) to blue (males) in southwestern Australia.

		TL_{50}	TL_{95}
Sex change	Estimate	821	930
	Lower CL	800	890
	Upper CL	845	1102
Color change	Estimate	779	961
	Lower CL	753	910
	Upper CL	809	1028

Table 3

Results of logistic regression analysis for determining whether color or total length (TL, in mm), or color and total length combined, were the best predictors of whether an individual of western blue groper (*Achoerodus gouldii*) was male. LL= log-likelihood; α, β_1, β_2 are constants; AIC = Akaike's information criterion.

Parameter	Color	TL	Color and TL
LL	−84.424	−48.644	−45.457
α	−4.631	−17.275	−15.505
β_1		0.021	0.018
β_2	4.979		1.477
AIC	172.847	101.289	96.913

Discussion

Demonstration of protogynous hermaphroditism

Our histological examination of the gonads of a large number of fish from throughout the year and covering a wide size range of *A. gouldii* fulfils one of the important requirements for demonstrating, with certainty, that a fish species is a functional hermaphrodite (Sadovy and Shapiro, 1987). Because all of the numerous *A. gouldii* captured with lengths of 100 to 655 mm were females and the prevalence of males subsequently rose with increasing body size to the extent where they constituted 100% of the larger fish, all males of *A. gouldii* are apparently derived from females. This conclusion is supported by the fact that all of the 164 individuals <15 years old, and whose gonads were examined histologically, were shown to be females. Moreover, the proportion of males subsequently increased progressively with age to the point where over 50% of individuals ≥35–39 years old were males. Because the length at which the prevalence of males reached 50% of fish (821 mm) was substantially greater than the TL_{50} at maturity (653 mm) for females and greater than that at which all female fish were apparently destined to become mature, a large number of male *A. gouldii* must have been derived from mature females. Thus, the characteristics of *A. gouldii* fulfil the criteria of Sadovy de Mitcheson and Liu (2008) for designating this species as a protogynous hermaphrodite. Although, on their own, these features do not provide concrete evidence that *A. gouldii* is monandric, i.e., all males are derived from mature females (Sadovy de Mitcheson and Liu, 2008), they do raise the strong possibility that this is the case for this labrid. As with other protogynous labrids (e.g., Reinboth, 1970; Sadovy and Shapiro, 1987), the presence of a central lumen in all mature testes of *A. gouldii* is considered to represent the retention of the ovarian lumen and to account for the peripheral location of the sperm ducts in those testes.

Aging methods, length and age compositions, and growth patterns

Although the von Bertalanffy growth curve provided a good fit to the lengths at age for all aged individuals

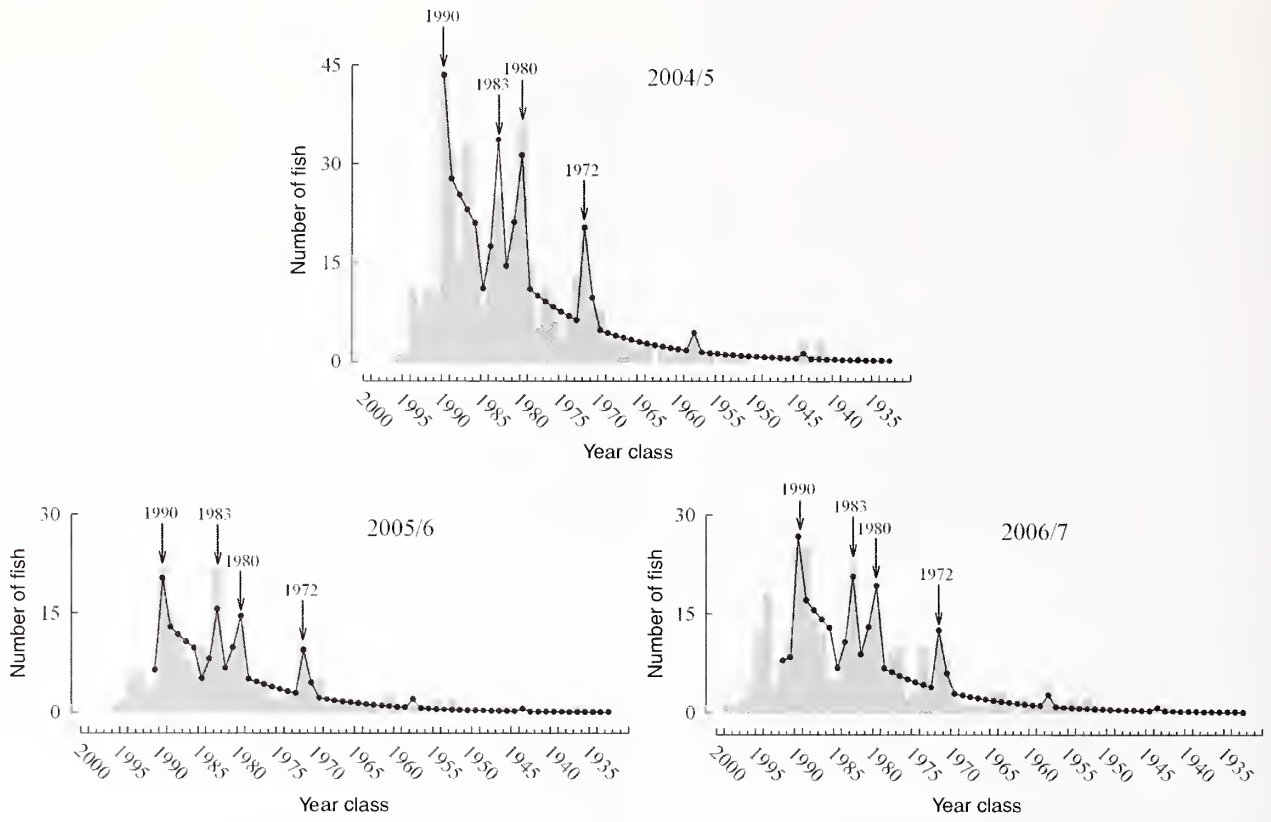

Figure 9

Observed numbers of individuals of each year class of western blue groper (*Achoerodus gouldii*) in commercial gillnet samples obtained from the south coast of Western Australia between August and July in 2004–5, 2005–6, and 2006–7 (histograms). Dotted lines represent the expected numbers of fish of each year class, as determined from a relative abundance analysis and were fitted to the observed frequency of abundance of fish in each year class in each of the three 12-month periods. Variable recruitment was assumed for creating the dotted lines; 1972, 1980, 1983, and 1990 (denoted with arrows) were years of particularly strong recruitment.

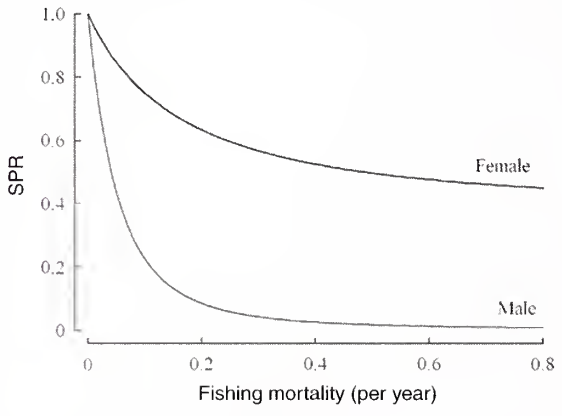

Figure 10

The effect of fishing mortality (F) on the spawning potential ratio (SPR) for females and males of the western blue groper (*Achoerodus gouldii*), calculated by using the age of 15 years (the age currently calculated to represent full recruitment into the commercial gillnet fishery).

of *A. gouldii*, irrespective of their sex, the variation in the lengths at age became very marked after ~25 years (Fig. 4A). This variation reflects a marked upward divergence in the growth of males from that of females among the larger and older fish (Fig. 4B). The fact that the von Bertalanffy growth parameters for green and blue fish were very similar to those derived for females and males, respectively, in data for the same subset of individuals, demonstrates that growth curves based on color provide a good proxy for those based on sex alone (Fig. 4, B and C).

A substantial number of the larger and older fish obtained during the study had been eviscerated before we collected them and therefore sex could not be determined and used to provide length-at-age data for constructing growth curves for the two sexes. Consequently, some caution must be exercised in drawing conclusions for the upper end of the growth curves constructed using fish of known sex, or for the same fish after separation by color. The AIC test used on the above subsample demonstrated that a combination of length and color provided a better indication of the sex

of a fish than either of those variables on their own. Although sex was determined for only a proportion of the large fish, the length and color of all fish were recorded. This enabled us to construct growth curves for females and males that incorporated the length at age for each individual of unknown sex, allowing for the probability that, from its length and color, it would be of a particular sex. Through increasing substantially the numbers of large fish from those whose sex was just determined from their gonads, the von Bertalanffy growth curves thereby derived for females and males are considered to provide better representations of the growth throughout life of the two sexes of *A. gouldii* than those derived solely from fish whose sex was unknown.

The greater length of males than females of *A. gouldii* at corresponding ages parallels the situation recorded for a number of other protogynous fishes, e.g., the cylindrical sandperch (*Parapercis cylindrica*), the heavybeaked parrotfish (*Chlorurus gibbus*), the greenfin parrotfish (*Chlorurus sordidus*), the swarthy parrotfish (*Scarus niger*), and the sixband parrotfish (*Scarus frenatus*) (Choat et al., 2006; Munday et al., 2004; Walker and McCormick, 2004), as well as its congener *Achoerodus viridis* (Gillanders, 1995a). Comparisons of the distributions of the lengths at age of the two sexes (Fig. 4B) strongly indicate that the fastest growing *A. gouldii* have the greatest tendency to change from female to male, a conclusion which parallels that drawn by Munday et al. (2004) for the labrid *S. frenatus*. However, some of the oldest fish were females (Fig. 4, B and D) and therefore some female *A. gouldii* were apparently not destined to become males, as is also the case with *Cheilinus undulatus* (Choat et al., 2006).

As hypothesized, the greater TL attained by *A. gouldii* (1162 mm) than by *A. viridis* (773 mm, after conversion from the SL given by Gillanders, 1995a), corresponded to a greater maximum age of 70 years for *A. gouldii* in comparison to 35 years for *A. viridis*. The maximum age of the large temperate *A. gouldii* is thus twice that estimated by Gillanders (1995a) for *A. viridis*, and by far the greatest yet recorded for any species of labrid, including the large tropical species *C. undulatus*, which attains a maximum age of 32 years (Choat and Bellwood, 1994; Choat et al., 2006). Although Hostetter and Munroe (1993) concluded that other large temperate labrids have long life spans, Choat et al. (2006) considered that the life spans of the large labrids that they used to make this generalization, typically <30 years of age, are relatively short. In the context of *A. gouldii*, the exceptional age attained by males was accompanied by a marked tendency for growth to an asymptote, which is not typically the case with the males of large tropical labrids (Choat et al., 2006).

Reproductive biology

The vast majority of the *A. gouldii* caught by spear fishing at numerous sites in nearshore waters were obtained from over the granite reefs that dominate the hard-structured substrate found in those waters along the south coast of Western Australia, and around the islands off the coast (Kendrick, 1999; Sanderson et al., 2000). Because the sizes of these fish, which were representative of the *A. gouldii* observed in those clear waters, were predominantly <600 mm and <12 years old, and therefore below the TL_{50} at maturity, the reef areas in nearshore waters constitute an important nursery habitat for juvenile *A. gouldii*. Large numbers of *A. gouldii* >500 mm, many of which were mature during the spawning season, were caught in deeper waters and this finding indicates that the individuals of this species move offshore as they increase in body size and become mature. This movement and the spawning of *A. gouldii* in offshore, deeper waters are consistent with the conclusions drawn by Shepherd and Brook (2007) for this species.

Our data indicate that, on the south coast of Western Australia, *A. gouldii* spawns in offshore waters between early winter and mid-spring, when water temperatures are declining to their minima (Fig. 5B); the preference for offshore waters and an early winter to mid-spring season for spawning parallels the situation with the congeneric *A. viridis* in eastern Australia (Gillanders, 1995a). Although there are no data on the larval phase of *A. gouldii*, Leis and Hay (2004) have shown that the larvae of *A. viridis* settle at 7–8 mm, metamorphose into juveniles by about 10 mm, and have hypothesized that the larvae of this species have some behavioral control over their movement from the shelf to their nearshore nursery habitats. Consequently, it is proposed that the spawning of *A. gouldii* in winter enables the larvae of this species to recruit into protected, nearshore coastal waters, at a time when the temperature and productivity in those waters have already started to increase (Fig. 5A) and winds are at their weakest and thus collectively provide an optimum environment for early juvenile growth.

The hypothesis that the greater length and age attained by *A. gouldii* than by *A. viridis* is accompanied by a greater length and age at maturity of females was confirmed by our results. With *A. gouldii*, the smallest mature female was 391 mm and the TL_{50} of females at maturity was as high as 653 mm. Furthermore, only one of the 164 females <5 years old was mature, and maturity was not attained by ~50% of females until they had reached 15–19 years in age. Although Gillanders (1995a) did not estimate the TL_{50} at maturity for female *A. viridis*, she recorded that females first matured at 200–220 mm SL (=246–270 mm TL) and that the majority had become mature by 240–280 mm SL (=294–341 mm TL). Gillanders (1995a) also found that, although a few female *A. viridis* became mature at the end of their second year of life, the majority matured between their third and fifth years of life. As with maturity, sex change occurred at a greater length and age in *A. gouldii* than in the smaller *A. viridis*. Thus, whereas sex change commenced in *A. gouldii* at ~650 mm and 15 years of age, and the TL_{50} at sex change was as high as 821 mm (TL), it began in *A. viridis* at lengths of ~600 mm (500 mm SL) and as early as 10 years of age (Gillanders 1995a).

Achoerdus gouldii undergoes the type of color change that is broadly associated with sex change in most protogynous labrids (e.g., Roede, 1972; Gillanders, 1995a; McBride and Johnson, 2007) and which, in *A. gouldii*, involves a shift from green to blue rather than from reddish brown to blue as in *A. viridis* (Gillanders, 1999). However, as with the latter congeneric species, some females (3%) were not of the initial color and some of the males (11%) did not have the terminal color. Furthermore, the continuous variable, length, was found to be a better predictor of sex than the dichotomous variable, color; however, a combination of both of these variables further improved one's ability to predict the sex of individuals of *A. gouldii*. The fitting of logistic curves to the length data for fish with testes and with blue coloration yielded TL_{50}s of 821 and 779 mm, respectively. Although these two TL_{50}s differed by 42 mm, their 95% confidence limits overlapped and therefore color can be used to derive an approximate value for the TL_{50} at sex change when it is not possible to record the sex of individuals because, for example, their viscera had been removed or fish were being viewed live during visual surveys. Our approaches to using color as a proxy for sex for estimating the TL_{50} at sex change and for enhancing the description of the growth of females and males are likely to be applicable to many of the numerous species that exhibit a similar form of sexual dichromatism.

Recruitment variability, mortality, and spawning potential ratio

The pattern of flow of the Leeuwin Current, the predominant current on the southwest coast of Australia in winter and therefore during the spawning period of *A. gouldii*, leads to the larvae of certain teleosts and the western rock lobster (*Panulirus cygnus*) being dispersed offshore (Pearce and Phillips, 1988; Gaughan, 2007). Thus, because *A. gouldii* is recruited into nearshore waters, it appears relevant that this species exhibited particularly strong recruitment in 1972, 1980, 1983, and 1990, when the Leeuwin Current was weak (Pearce and Phillips, 1988; Caputi et al., 1996), and very poor recruitment in 1991 and 1992 when the Leeuwin Current was especially strong.

Because the current level of fishing mortality for *A. gouldii* in southwestern Australian waters is estimated to be 74% of natural mortality, this species is apparently close to or at full exploitation in these waters (after applying a reference point $F_{lim} = {}^{2}/_{3}\,M$ based on Patterson [1992]). The conclusion that *A. gouldii* is close to or at full exploitation is consistent with the estimate for the spawning potential ratio (SPR) for the males of this protogynous hermaphroditic labrid. This value has therefore declined to 0.52 and, given the steepness of the curve relating SPR to fishing mortality, is rapidly approaching 0.30, which is often regarded as the level at which a stock is considered to be overfished (Goodyear, 1993; Mace and Sissenwine, 1993). Indeed, the lower 95% CL of 0.27 for the SPR lies below this reference point.

Implications for management

Most recreational line and spear fishing for *A. gouldii* on the south coast of Western Australia occurs in shallow and relatively accessible waters, where the individuals of this species are typically smaller than those in deeper waters and where most individuals are less than the TL_{50} of 653 mm at which females attain maturity. Furthermore, in deeper waters, 52% of the *A. gouldii* taken by the commercial fishery were less than the length at maturity and 88% were below the TL_{50} of 821 mm at which females change sex to males. Moreover, *A. gouldii* often suffers barotrauma when brought to the surface from particularly deep waters, as is the case with many other demersal species in Western Australia and elsewhere (e.g., St John and Syers, 2005; Parker et al., 2006), and with other labrids (e.g., Nardi et al., 2006). Thus, if the current minimum legal length of 500 mm is maintained, or slot (minimum and maximum length) limits are introduced, fishing crews should be encouraged to adopt fishing practices that minimize the loss of released fish. In this context, it would be of great value to undertake research into the effects of barotrauma on *A. gouldii* and the ways in which the loss of released fish may be minimized.

Although substantial fishing of protogynous species can lead to a marked decline in the relative abundance of their males (e.g., Coleman et al., 2000), the size at sex change of some protogynous species declines in response to the selective removal of large males by fishing (e.g., Platten et al., 2002; Hawkins and Roberts, 2003). Because it is not known whether the size at sex change of *A. gouldii* is labile, it would be prudent for managers to take the conservative view that this is not necessarily the case with this labrid.

Because fisheries for protogynous species, such as *A. gouldii,* have a greater effect on the spawning biomass of males than females, managers need to take into account the potential for fishing to lead to sperm limitation, reduced fertilization success, and social or behavioral changes, and to consider whether appropriate biological reference points need to be established to ensure that the sex and size structure of the fish stock is maintained (Alonzo and Mangel, 2004, 2005; Brookes et al., 2008). Because it would be useful for managers to have a rapid and inexpensive means for determining the sex of individuals of *A. gouldii*, our data are relevant in that they show that body color can be used as a broad surrogate for sex and it would enable rapid monitoring of the population to detect whether changes are occurring in the ratio of the biomasses of mature females and males and in the length at sex change, both of which could be used as the basis for an appropriate fishery control rule. In our estimates of the effect of increased fishing mortality on male spawning biomass per recruit, we did not assume that compensatory phenotypic or behavioral responses of the types explored by Alonzo and Mangel (2005) occurred in the pattern of sex change of *A. gouldii*. Consequently, our results provide a precaution-

ary evaluation of the implications of increased fishing mortality on the males.

Beamish et al. (2006) have recently drawn attention to the importance, when considering long-lived species, of understanding the effects of removing large numbers of the older age classes, which they referred to as longevity overfishing. In this context, managers need to recognize that our age-frequency distributions indicate that commercial gill netting captures the older age classes of *A. gouldii*. It is instructive to consider the potential for overfishing of the very long-lived (maximum age, 70 years) *A. gouldii* in the context of the response to heavy fishing by the smaller and earlier maturing but still quite large and relatively long-lived congener *A. viridis* (maximum age, 35 years). *Achoerodus viridis* suffered such heavy fishing mortality in eastern Australia that the waters of that region were closed to commercial and recreational fishing for that species and still remain closed to spear and commercial fishing (Gillanders, 1999).

When assessing which combination of typical fishery controls should be applied to *A. gouldii*, e.g., possession limits, controls on fishing gear or effort, minimum or maximum (fish) size limits (or both), and closed areas and seasons, consideration needs to be given to the effects of the various controls on both the commercial and recreational fishing sectors and the likely effectiveness of each control in helping to restore or maintain the reproductive potential of both the females and males of this species. In particular, managers should recognize that the inshore recreational fishery is a multispecies fishery, which, for *A. gouldii*, is a gauntlet fishery (i.e. a fishery largely restricted to catching fish of a limited period of their life cycle) that catches mainly smaller individuals. In contrast, the commercial fishery, which operates in deeper, offshore waters and targets elasmobranchs and a mix of other teleost species as well as *A. gouldii*, catches larger and older individuals of that species. Because the catches of the commercial fishery are buffered by the presence of a greater number of age classes than the recreational fishery, the commercial catches are less likely to experience the effects of recruitment variability. The use of a single control is therefore likely to have more effect on one fishing sector than the other. The strategies developed for managing *A. gouldii* in the future will need to balance the ways in which they affect the different fishing sectors. Furthermore, if fishing crews are to accept management controls, they will need to be informed of the implications of the particular biological characteristics of *A. gouldii* for the fishery and the effects of catches by different fishing sectors on the stocks of this species.

In summary, we have shown that the temperate *A. gouldii* is long lived (maximum age, 70 years), relatively slow growing and late maturing (~17 years)—characteristics that contrast with the those typically found in labrids, most of which are tropical. However, these characteristics are found with many large epinephelines (e.g., Morris et al., 2000) and numerous deep-water species (e.g., Koslow et al., 2000; Morato et al., 2006; Marriott et al., 2007), and they make these species particularly susceptible to overfishing. The variable recruitment of *A. gouldii* would also be likely to increase the susceptibility of this species to overfishing, as it does with other species (e.g., Koslow et al., 2000; Sadovy, 2001; Hawkins and Roberts, 2003). Furthermore, because *A. gouldii* does not typically change sex until a relatively old age (35–39 years), the abundance of the males of this protogynous hermaphrodite would be especially at risk of becoming depleted through fishing. The results of this study emphasize the need to acquire a thorough understanding of the life cycle characteristics of species that will almost inevitably become increasingly exploited in the future and, as Coleman et al. (2000) pointed out for reef fishes in North America, and not interpret a lack of such information as representing the absence of a potential problem.

Acknowledgments

Gratitude is expressed to S. Cossington and many colleagues at the Centre for Fish and Fisheries Research, Murdoch University, for help in the field and to recreational fisherman J. Stuart and commercial fishermen G. Campbell, J. Thornton, and C. Gulloti for their generous assistance with sampling. Many large fish were kindly provided by All Seas Fish Supply and Great Southern Seafoods. We thank K. Smith and J. Brown for providing water temperatures and F. Prokop, A. Pearce, and D. Gaughan for helpful comments. Special thanks are extended to G. Thompson for producing high quality histological slides of fish gonads and to B. Gillanders for kindly supplying length data for *Achoerodus viridis*. Financial support was provided by the Australian Fisheries and Research Development Corporation and Murdoch University. The project was carried out under animal ethics project number R1066/04.

Literature cited

Allen, G. R., N. J. Cross, C. J. Allen, M. Gomon, D. J. Bray, and D. F. Hoese.
2006. Labridae. *In* Zoological catalogue of Australia, vol. 35, part 2 (P. L. Beesley, and A. Wells, eds.), p. 1367. Australian Biological Resources Study and Commonwealth Scientific and Industrial Research Organisation Publishing, Victoria, Australia.

Alonzo, S. H., and M. Mangel.
2004. The effects of size-selective fisheries on the stock dynamics of and sperm limitation in sex-changing fish. Fish. Bull. 102:1–13.
2005. Sex-change rules, stock dynamics, and the performance of spawning-per-recruit measures in protogynous stocks. Fish. Bull. 103:229–245.

Beamish, R. J., G. A. McFarlane, and A. Benson.
2006. Longevity overfishing. Prog. Oceanogr. 68:289–302

Bentivegna, F., and F. Benedetto.
1989. Gonochorism and seasonal variations in the

gonads of the labrid *Symphodus* (*Crenilabrus*) *ocellatus* (Forsskål). J. Fish Biol. 34:343–348.

Brooks, E. N., K. W. Shertzer, T. Gedamke, and D. S. Vaughan.
2008. Stock-assessment of protogynous fish: evaluating measures of spawning biomass used to estimate biological reference points. Fish. Bull. 106:12–23.

Burnham, K. P., and D. R. Anderson.
2002. Model selection and multimodel inference: a practical information-theoretic approach, 2nd ed., 496 p. Springer-Verlag, New York, NY.

Candi, G., L. Castriota, F. Andaloro, M. G. Finoia, and G. Marino.
2004. Reproductive cycle and sex inversion in razor fish, a protogynous labrid in the southern Mediterranean Sea. J. Fish Biol. 64:1498–1513.

Caputi, N., W. J. Fletcher, A. Pearce, and C. F. Chubb.
1996. Effect of the Leeuwin Current on the recruitment of fish and invertebrates along the Western Australian coast. Mar. Freshw. Res. 47:147–155.

Cerrato, R. M.
1990. Interpretable statistical tests for growth comparisons using parameters in the von Bertalanffy equation. Can. J. Fish. Aquat. Sci. 47:1416–1426.

Choat, J. H., and D. R. Bellwood.
1994. Wrasses and parrotfishes. *In* Encyclopedia of fishes (J. R. Paxton, and W. N. Eschmeyer, eds.), p. 211–215. Univ. New South Wales Press, Sydney, Australia.

Choat, J. H., C. R. Davies, J. L. Ackerman, and B. D. Mapstone.
2006. Age structure and growth in a large teleost, *Cheilinus undulatus*, with a review of size distribution in labroid fishes. Mar. Ecol. Prog. Ser. 318:237–246.

Choat, J. H., and D. R. Robertson.
2002. Age-based studies on coral reef fishes. *In* Coral reef fishes: dynamics and diversity in a complex ecosystem (P. F. Sale, ed.), p. 57–80. Academic Press, New York, NY.

Coleman, F. C., C. C. Koenig, G. R. Huntsman, J. A. Musick, A. M. Ekland, J. C. McGovern, R. W. Chapman, G. R. Sedberry, and C. B. Grimes.
2000. Long-lived reef fishes: the grouper-snapper complex. Fisheries 25:14–21

Coulson, P. G., S. A. Hesp, I. C. Potter, and N. G. Hall.
2005. Comparisons between the biology of two co-occurring species of whiting (Sillaginidae) in a large marine embayment. Environ. Biol. Fish. 73:125–139.

Denny, C. M., and D. R. Schiel.
2002. Reproductive biology and population structure of the banded wrasse, *Notolabrus fucicola* (Labridae) around Kaikoura, New Zealand. N. Z. J. Mar. Freshw. Res. 36:555–563.

Deriso, R. B., T. J. Quinn II, and P. R. Neal.
1985. Catch-age analysis with auxiliary information. Can. J. Fish. Aquat. Sci. 42:815–824.

Dipper, F. A., and R. S. V. Pullin.
1979. Gonochorism and sex-inversion in British Labridae (Pisces). J. Zool. (Lond.) 187:97–112.

Gaughan, D. J.
2007. Potential mechanisms of influence of the Leeuwin Current eddy system on teleost recruitment to the western Australian continental shelf. Deep-Sea Res. II 54:1129–1140.

Gillanders, B. M.
1995a. Reproductive biology of the protogynous hermaphrodite *Achoerodus viridis* (Labridae) from south-eastern Australia. Mar. Freshw. Res. 46:999–1008.
1995b. Feeding ecology of the temperate marine fish *Achoerodus viridis* (Labridae): Size, seasonal and site-specific differences. Mar. Freshw. Res. 46:1009–1020.
1997. Comparison of growth rates between estuarine and coastal reef populations of *Achoerodus viridis* (Pisces, Labridae). Mar. Ecol. Prog. Ser. 146: 283–287.
1999. Blue groper. *In* Under southern seas (N. Andrew, ed.), p. 188–193. Univ. New South Wales Press, Sydney, Australia.

Gillanders, B. M., and M. J. Kingsford.
1998. Influence of habitat on abundance and size structure of a large temperate fish, *Achoerodus viridis* (Pisces, Labridae). Mar. Biol. 132:503–514.

Gommon, M. F., C. J. M. Glover, and R. H. Kuiter.
1994. The fishes of Australia's southern coast, 992 p. State Printer, Adelaide, Australia.

Goodyear, C. P.
1993. Spawning stock biomass per recruit in fisheries management. Foundation and current use. Can. Spec. Publ. Fish. Aquat. Sci. 120:67–81.

Hall, N. G., S. A. Hesp, and I. C. Potter.
2004. A Bayesian approach for overcoming inconsistencies in mortality estimates using, as an example, data for *Acanthopagrus latus*. Can. J. Fish. Aquat. Sci. 61:1202–1211.

Hamilton, R. J., S. Adams, and J. H. Choat.
2008. Sexual development and reproductive demography of the green humphead parrotfish (*Bolbometopon muricatum*) in the Solomon Islands. Coral Reefs 27:153–163.

Hawkins, J. P., and C. M. Roberts.
2003. Effects of fishing on sex-changing Caribbean parrotfishes. Biol. Conserv. 115:213–226.

Hilborn, R., and M. Mangel.
1997. The ecological detective: confronting models with data, 330 p. Princeton Univ. Press, Princeton, NJ.

Hoenig, J. M.
1983. Empirical use of longevity data to estimate mortality rates. Fish. Bull. 82:898–903.

Hostetter, E. B., and T. A. Munroe.
1993. Age, growth, and reproduction of tautog *Tautoga onitis* (Labridae: Perciformes) from coastal waters of Virginia. Fish. Bull. 91:45–64.

Hutchins, B., and R. Swainston.
1986. Sea fishes of southern Australia, 180 p. Swainston Publishing, New South Wales, Australia.

Kendrick, G.
1999. Western Australia. *In* Under southern seas (N. Andrew, ed.), p. 50–57. Univ. New South Wales Press, Sydney, Australia.

Koslow, J. A., G. W. Boehlert, J. D. M. Gordon, R. L. Haedrich, P. Lorance, and N. Parin.
2000. Continental slope and deep-sea fisheries: implications for a fragile ecosystem. ICES J. Mar. Sci. 57: 548–557.

Kuwamura,T., S. Suzuki, N. Tanaka, E. Ouchi, K. Karino, and Y. Nakahima.
2007. Sex change of primary males in a diandric labrid *Halichoeres trimaculatus*: coexistence of protandry and protogyny within a species. J. Fish Biol. 70: 1898–1906.

Laevastu, T.
1965. Manual of methods in fisheries biology, 51 p. FAO, Rome.

Lam, T.
1983. Environmental influences on gonadal activity in fish. *In* Fish physiology (W. S. Hoar, and D. J. Randall, eds), p. 65–116. Academic Press, London.
Leis, J. M., and A. C. Hay.
2004. Larval development of *Achoerodus viridis* (Pisces: Labridae), the Australian eastern blue groper. Ichthyol. Res. 51:46–51.
Mace, P. M., and M. P. Sissenwine.
1993. How much spawning per recruit is enough? *In* Risk evaluation and biological reference points for fisheries management (S. J. Smith, J. J. Hunt, and D. Rivard eds.). Can. Spec. Publ. Fish. Aquat. Sci. 120:101–118.
Marriott, R. J., B. D. Mapstone, and G. A. Begg.
2007. Age-specific demographic parameters, and their implications for management of the red bass, *Lutjanus bohar* (Forsskal 1775): A large, long-lived reef fish. Fish. Res. 83:204–215.
McBride, R. S., and M. R. Johnson.
2007. Sexual development and reproductive seasonality of hogfish (Labridae: *Lachnolaimus maximus*), an hermaphroditic reef fish. J. Fish Biol. 71:1270–1292.
Moore, S. E., S. A. Hesp, N. G. Hall, and I. C. Potter
2007. Age and size compositions, growth and reproductive biology of the breaksea cod *Epinephelides armatus*, a gonochoristic serranid. J. Fish Biol. 71:1407–1429.
Morato, T., R. Watson, T. J. Pitcher, and D. Pauly.
2006. Fishing down the deep. Fish Fish. 7:24–34.
Morris, A. V., C. M. Roberts, and J. P. Hawkins.
2000. The threatened status of groupers (Epinephelinae). Biodivers. Conserv. 9:919–942.
Munday, P. L., A. L. Hodges, J. H. Choat, and N. Gust
2004. Sex-specific growth effects in protogynous hermaphrodites. Can. J. Fish. Aquat. Sci. 61:323–327.
Nardi, K., S. J. Newman, M. J. Moran, and G. P. Jones.
2006. Vital demographic statistics and management of the baldchin groper (*Choerodon rubescens*) from the Houtman Abrolhos Islands. Mar. Freshw. Res. 57:485–496.
Ohta, K., J. K. Sundaray, T. Okida, M. Sakai, T. Kitano, A. Yamaguchi, T. Takeda, and M. Matsuyama.
2003. Bi-directional sex change and its steroidogenesis in the wrasse, *Pseudolabrus sieboldi*. Fish Physiol. Biochem. 28:173–174.
Parker, S. J., H. I. McElderry, P. S. Rankin, and R. W. Hannah.
2006. Buoyancy regulations and barotrauma in two species of nearshore rockfish. Trans. Am. Fish. Soc. 135:1213–1223.
Patterson, K.
1992. Fisheries for small pelagic species: an empirical approach to management targets. Rev. Fish Biol. Fish. 2:321–338.
Pearce, A. F., and B. F. Phillips.
1988. ENSO events, the Leeuwin Current, and larval recruitment of the western rock lobster. J. Cons. Int. Explor. Mer 45:13–21.
Platten, J. R., I. R. Tibbets, and M. J. Sheaves.
2002. The influence of increased line fishing on the sex ratio and age of sex reversal of the venus tuskfish. J. Fish Biol. 60:301–318.
Reinboth, R.
1970. Intersexuality in fishes. Mem. Soc. Endocrinol. 18:515–543.
Reynolds, R. W., and T. M. Smith.
1994. Improved global sea surface temperature analyses using optimal interpolation. J. Clim. 7:929–948.
Ricker, W. E.
1975. Computation and interpretation of biological statistics of fish populations. Bull. Fish. Res. Board Can. 191, 382 p.
Roede, M. J.
1972. Color as related to size, sex and behaviour in seven Caribbean labrid fish species (genera *Thalassoma*, *Halichoeres*, *Hemipteronotus*). Stud. Fauna Curaçao 138:1–264.
Sadovy, Y.
2001. The threat of fishing to highly fecund fish. J. Fish Biol. 59(suppl. A):90–108
Sadovy, Y. J., M. Kulbicki, P. Labrosse, Y. Letourneur, P. Lokani, and T. J. Donaldson.
2003. The humphead wrasse, *Cheilinus undulatus*: synopsis of a threatened and poorly known giant coral reef fish. Rev. Fish Biol. Fish. 13:327–364.
Sadovy, Y., and D. Y. Shapiro.
1987. Criteria for the diagnosis of hermaphroditism in fishes. Copeia 1987:136–156.
Sadovy de Mitcheson, Y., and M. Liu.
2008. Functional hermaphroditism in teleosts. Fish Fish. 9:1–43.
Sanderson, P. G., I. Eliot, B. Hegge, and S. Maxwell.
2000. Regional variation of coastal morphology in southwestern Australia: a synthesis. Geomorphology 34:73–88.
Shapiro, D. Y.
1981. Sequence of coloration changes during sex reversal in the tropical marine fish *Anthias squamipinnis* (Peters). Bull. Mar. Sci. 31:383–398.
Shepherd, S. A.
2005. Ontogenetic changes in diet, feeding behaviour and activity of the western blue groper, *Achoerodus gouldii*. *In* The marine flora and fauna of Esperance, Western Australia (F. E. Wells, D. I. Walker, and G. A. Kendrick, eds), p. 477–494. Western Australian Museum, Perth, Australia.
Shepherd, S. A., and J. B. Brook.
2007. Distribution and ontogenetic shifts in habitat and abundance of the temperate western blue groper, *Achoerodus gouldii* (Richardson). J. Fish Biol. 71:1457–1478.
Sokal, R .R., and F. J. Rohlf.
1995. Biometry: the principles and practice of statistics in biological research, 3rd ed., 887 p. W. H. Freeman, New York, NY.
St John, J., and C. J. Syers.
2005. Mortality of the demersal West Australian dhufish, *Glaucosoma hebraicum* (Richardson 1885) following catch and release: the influence of capture depth, venting and hook type. Fish. Res. 76:106–116.
Walker, S. P. W., and M. I. McCormick.
2004. Otolith-check formation and accelerated growth associated with sex change in an annual protogynous tropical fish. Mar. Ecol. Prog. Ser. 266:201–212.
Warner, R., and D. Robertson.
1978. Sexual patterns in the labroid fishes of the western Caribbean: 1. The wrasses (Labridae). Smithson. Contrib. Zool. 255:1–26.
Westneat, M. W., and M. E. Alfaro.
2005. Phylogenetic relationships and evolutionary history of the reef fish family Labridae. Mol. Phylogenet. Evol. 36:370–390.

Abstract—The diet and daily ration of the shortfin mako (*Isurus oxyrinchus*) in the northwest Atlantic were re-examined to determine whether fluctuations in prey abundance and availability are reflected in these two biological variables. During the summers of 2001 and 2002, stomach content data were collected from fishing tournaments along the northeast coast of the United States. These data were quantified by using four diet indices and were compared to index calculations from historical diet data collected from 1972 through 1983. Bluefish (*Pomatomus saltatrix*) were the predominant prey in the 1972–83 and 2001–02 diets, accounting for 92.6% of the current diet by weight and 86.9% of the historical diet by volume. From the 2001–02 diet data, daily ration was estimated and it indicated that shortfin makos must consume roughly 4.6% of their body weight per day to fulfill energetic demands. The daily energetic requirement was broken down by using a calculated energy content for the current diet of 4909 KJ/kg. Based on the proportional energy of bluefish in the diet by weight, an average shortfin mako consumes roughly 500 kg of bluefish per year off the northeast coast of the United States. The results are discussed in relation to the potential effect of intense shortfin mako predation on bluefish abundance in the region.

Recalculated diet and daily ration of the shortfin mako (*Isurus oxyrinchus*), with a focus on quantifying predation on bluefish (*Pomatomus saltatrix*) in the northwest Atlantic Ocean

Anthony D. Wood (contact author)[1]
Bradley M. Wetherbee[2]
Francis Juanes[3]
Nancy E. Kohler[4]
Cheryl Wilga[2]

Email address for contact author: awood@gso.uri.edu

[1] Graduate School of Oceanography
University of Rhode Island Bay Campus
215 South Ferry Rd.
Narragansett, Rhode Island. 02882
Present address: School for Marine Science and Technology (SMAST)
200 Mill Road, ATT 211,
Fairhaven, Massachusetts 02719

[2] University of Rhode Island
Biological Sciences
100 Flagg Rd.
Kingston, Rhode Island 02881

[3] Department of Natural Resources Conservation
160 Holdworth Way
University of Massachusetts
Amherst, Massachusetts 01003

[4] National Marine Fisheries Service, NOAA
Northeast Fisheries Science Center
Narragansett Laboratory
28 Tarzwell Drive
Narragansett, Rhode Island 02882

Manuscript submitted 11 July 2007.
Manuscript accepted 10 September 2008.
Fish. Bull. 107:76–88 (2009).

The views and opinions expressed or implied in this article are those of the author and do not necessarily reflect the position of the National Marine Fisheries Service, NOAA.

A top-down trophic system involves consumer control of the community structure and the population dynamics of an ecosystem. In many marine ecosystems many species of sharks are positioned at the top of the food chain, and through predation can potentially exert control upon their prey communities (van der Elst, 1979; Stevens et al., 2000; Heithaus and Dill, 2002). As management decisions become increasingly focused on the interactions between multiple species, it is important that the effects of predation be evaluated (Bax, 1998; Overholtz et al., 2000). One of the first steps in carrying out such an evaluation is through the examination of the food habits and daily rations of the top predators in a system (Wetherbee and Cortés, 2004). In the northwest Atlantic Ocean ecosystem the shortfin mako (*Isurus oxyrinchus*) is an abundant apex predator. We re-examine the diet and daily ration of shortfin makos in the northwest Atlantic and quantify an important predator-prey relationship that has existed for decades.

In the northwest Atlantic, the shortfin mako ranges from the Caribbean Sea and Gulf of Mexico, north to Nova Scotia, Canada, and the Grand Banks (Compagno, 2001). Starting in the early spring (mid to late May) shortfin makos appear in abundance off the northeast coast of the United States. The annual migration to this region from the south and from offshore locales coincides

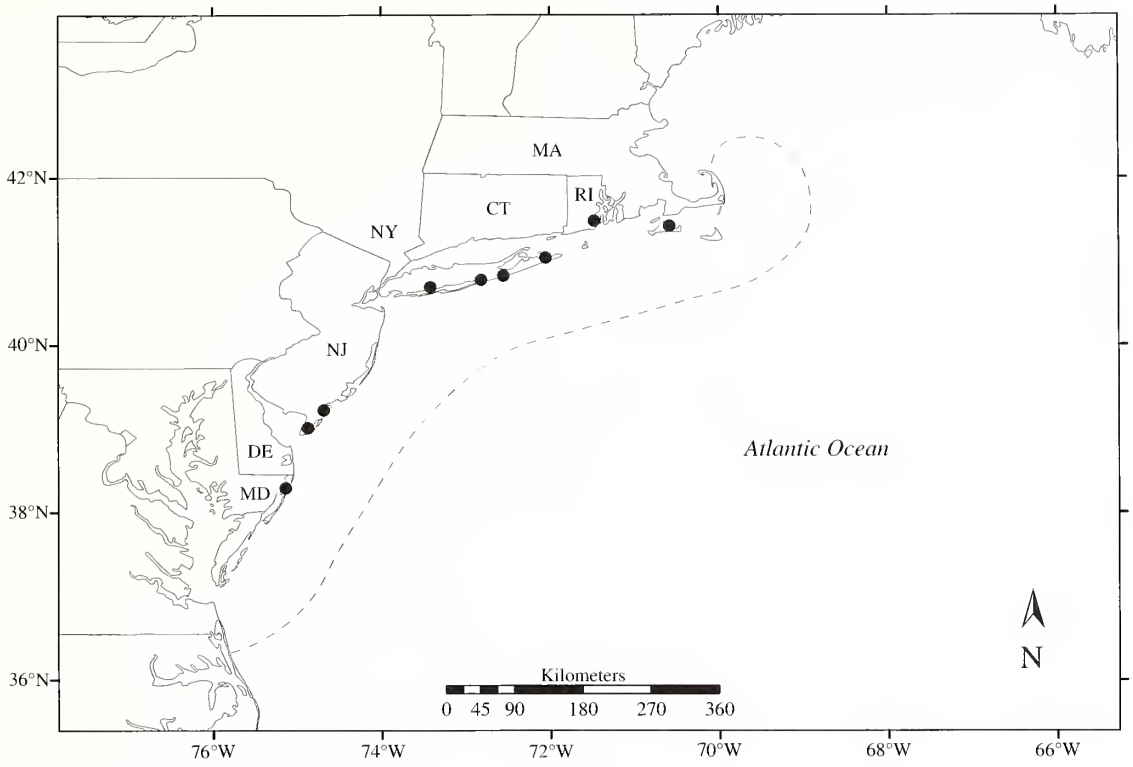

Figure 1

Map of the northeast coast of the United States showing the locations (●) of major shark fishing tournaments where shortfin mako (*Isurus oxyrinchus*) stomachs were collected from May through October of 2001 and 2002 to determine the diet of this species. An approximate boundary (- - -) indicates where fishing took place for these tournaments.

with the appearance of many teleost prey species. An early diet study from this region, during this seasonal residence, has indicated that teleosts make up 98% of the diet by volume, and that bluefish (*Pomatomus saltatrix*) account for 77.5% of prey by volume (Stillwell and Kohler, 1982). Bluefish are undoubtedly the most important prey species, but much has changed with the bluefish stocks since this initial examination of the shortfin mako diet. Throughout the 1980s and early 1990s the northwest Atlantic Ocean bluefish stock experienced a decline in both young-of-the-year abundance and spawning stock biomass (Shepherd and Packer, 2006). This decline was likely a result of many factors, including natural population fluctuation, environmental and physical stresses, fishing pressure (both commercial and recreational), and intense predation by shortfin makos and other bluefish predators.

To examine the current level of bluefish consumption by the shortfin mako, and to investigate whether predation on bluefish has changed over the past two decades, we 1) re-quantified the diet from stomach contents data collected from the late May through October of 2001 and 2002, and compared this current data with historical diet data (collected from 1972 to 1983); 2) back-calculated bluefish prey size to determine potential predator-size–prey-size relationships; 3) calculated daily ration from the 2001–02 data with a bioenergetics model and the method of Elliot and Persson (1978). We attempt to address from our results, focusing on bluefish as the most important prey, whether shifts in prey species abundance from historical levels are reflected in the shortfin mako diet. In addition, the potential regulatory effect of intense shortfin mako predation on bluefish in this region is investigated.

Materials and methods

Stomach collection

Stomach contents were examined from shortfin mako caught in shark fishing tournaments carried out from May to October of 2001 and 2002 along the northeast coast of the United States. (Fig. 1). For the purposes of comparison with historical inshore data, these samples were considered to have been caught <45 nmi from shore and at a water depth of <91 m. Historical data on shortfin mako diet were provided by the National Marine Fisheries Service (NMFS), Apex Predators Program, located at the Northeast Fisheries Science Center (NEFSC) Narragansett Laboratory, Narragansett, RI. These data were collected from late May through October from 1972 through 1983 by NMFS staff and charter boat fishing crews at many of the

Table 1

Digestive states (1–7) of prey items found in stomachs of shortfin makos (*Isurus oxyrinchus*) caught in fishing tournaments along the northeast coast of the United States, 2001–02, and the estimated digestion time (h) and the percentage of prey items found for each digestive state.

Scale number	Description of digestive state	Estimated digestion time (h)	Percentage of prey
1	Prey maintains original shape perfectly, skin also intact, pigmentation still bright.	0 to 2	2.4
2	Original shape almost completely retained, part or all of skin missing, pigmentation faded.	2 to 4	1.6
3	Flesh still recognizable on body, skeleton nearly complete.	4 to 7	15.7
4	Skeleton partially fragmented, flesh still attached to backbone.	7 to 10	27.6
5	Skeleton fragmented into many pieces, chunks of flesh remaining.	10 to 14	35.4
6	Prey reduced to mush consisting of flesh, skeletal fragments and scales, no recognizable body parts.	14 to 18	15.0
7	Opaque liquid only.	18 +	2.4

same shark fishing tournaments where the 2001–02 data were collected.

For the 2001–02 diet data, stomachs were extracted on location, bagged, placed on ice, and brought to the laboratory for examination within 48 to 72 hours of catch. In the laboratory, stomachs were carefully removed from surrounding organs and cut open for examination of the contents. Prey were identified to the lowest taxon possible, counted, sorted, and weighed individually (±0.01 g). When bluefish were found in stomachs, remaining bones were examined in more detail. In cases where one or more of five skull bones (maxilla, premaxilla, dentary, cleithrum, opercle) were found intact, and in good overall condition, these bones were collected for the purpose of back-calculating original bluefish size with a series of predictive equations (Wood, 2005). Unidentifiable prey items were designated as such and all prey items were given a value from 1 to 7 on a scale based on state of digestion (Table 1). This scale of digestion was used to eliminate suspicious prey items that could have been bait. All prey items were explored for clean (knife-edge) cuts, fish hook marks, and imbedded fish hooks, and any items identified as bait were removed from the samples. Typically, Atlantic mackerel (*Scomber scombrus*) pieces, butterfish (*Peprilus triacanthus*) pieces, and bluefish are used as bait by fishermen, and menhaden (*Brevoortia tyrannus*) oil and ground menhaden are used as chum.

Diet

The diet of the sharks sampled during the current study was quantified by three basic prey indices: percentage by number (%N), percentage by weight (%W), and percentage by occurrence (%O) (Hyslop, 1980); and a compound index of relative importance (IRI) was expressed as a percentage (%IRI) (Cortés, 1997).

Comparisons between the current and historical data were based on the index of number (%N), the index of weight (%W), and the index of occurrence (%O). For a direct quantitative comparison between the current and historical data, weight was used as a proxy for volume by assuming a constant prey density of 1.0 g = 1.0 mL. The %W index from the current data was compared to an index based on prey volume (%V) from the historical diet data.

Diet overlap between the current data and the historical data was examined with two measures of niche overlap, the percentage overlap measure and the simplified Morisita index (Krebs, 1999). A contingency table (both chi-square and G statistic) based on prey numbers was used to investigate whether significant differences existed between the current and historical diets in aggregate. For the contingency table analyses, prey items were grouped into seven categories (Pomatomidae, Clupeidae, Scombridae, other teleosts, unidentified teleosts, invertebrates, and mammals and elasmobranchs).

Cumulative prey curves were generated for the 2001–02 and historical diet data to determine whether the overall shortfin mako diet was adequately represented by the study samples. In addition, the rate of increase of the last 10 points in both curves was analyzed to determine whether an asymptote had been reached. A rate of increase of less than 5.0% was used as the cutoff (Baremore, 2007). A jackknife estimate of species richness was also calculated to estimate how many prey species were potentially missed by sampling. The cumulative prey curves and jackknife estimate were generated with PRIMER vers. 6.0 software (Clarke, 1993).

Predator-size–prey-size relationship

Measurements of bluefish bones collected from stomach contents were used to back-calculate sizes of prey

individuals with predictive equations (Wood, 2005). To explore predator-size–prey-size relationships a shortin mako size-bluefish size scatter plot was analyzed with least squares regression. Quantile regressions (5^{th} and 95^{th}) were used to determine changes in minimum and maximum prey size with increasing predator size. In addition, relative and cumulative frequency histograms were used to explore patterns in the size of prey consumed (Bethea et al., 2004).

Daily ration

Two methods were used to estimate daily ration of the shortfin mako: a bioenergetics approach and the use of the average weight of stomach contents (following Elliot and Persson, 1978). These approaches were both used so that a comparison between the resulting daily ration estimates could be made. In addition, both of these methods were previously used to calculate daily ration of shortfin makos (Stillwell and Kohler, 1982).

The bioenergetics approach used by Stillwell and Kohler (1982) did not include growth information and was based on the volume of oxygen consumption (VO_2) extrapolated from four species of squaloid sharks. More recently, VO_2 has been measured directly for the shortfin mako at various swimming speeds (U) (Graham et al., 1990). Stillwell and Kohler's (1982) estimate of VO_2 (284.2 mg/kg/h) was much lower than the values of VO_2 actually measured for the shortfin mako by Graham et al. (1990), who found an average VO_2 of 369 mg/kg/h for routine metabolism.

The bioenergetics model for this study followed a form commonly used for teleost fishes which has been successfully applied to blue sharks (*Prionace glauca*) (Schindler et al., 2002). To calculate daily consumption, the model incorporates growth rates, metabolism, and other energy parameters in an energy balance equation:

$$C = M + SDA + (F + Ur) + (G_t + Rp),$$

where
C = consumption rate;
M = metabolism;
SDA (specific dynamic action) = the amount of energy used for digestion;
F and Ur = energy lost to waste;
G_t = growth over time; and
Rp = the amount of energy allocated towards reproduction.

Metabolism (M) in the model was assumed to be active metabolism because shortfin makos are obligate ram ventilators (must continually swim in order to breathe). To generate a relationship between swimming speed (U) and mean VO_2, a least squares regression was fitted mean VO_2 data at a variety of swimming speeds taken from Graham et al. (1990)'s data. The resulting regression equation, along with observed rates of travel determined from satellite telemetry tracking of shortfin makos, was used to calculate active metabolism. An energy equivalence of 13.6 J/mg O_2 was used to convert the VO_2 consumed into energy (Schindler et al., 2002), and a Q_{10} value for the bonnethead shark (*Sphyrna tiburo*) of 2.3 (Carlson and Parsons, 1999) was used to adjust the final metabolic rate to 18.8°C (the preferred temperature of shortfin makos in the northwest Atlantic; Stillwell and Kohler, 1982).

Specific dynamic action (SDA) was set at a fraction of consumption rate (C) equal to $0.10C$ (Schindler et al., 2002), and the amount of energy lost to waste ($F + Ur$) was fixed at $0.27C$ (Stillwell and Kohler, 1982; Schindler et al., 2002). For growth, sex-specific growth rates (G_t) were taken from Natanson et al. (2006) who found that growth in length was best modeled by a three-parameter von Bertalanffy growth curve for males and a three-parameter Gompertz growth curve for females. Fork length (FL) was converted to weight with the relationship $WT = 5.2432 \times 10^{-6} FL^{3.1407}$, with weight in kg and FL in cm (Kohler et al., 1996). The energy density value used for the shortfin mako was 20.6 kJ/g dry weight, which was converted to wet weight energy by assuming a 73% water content for shortfin mako flesh (Steimle and Terranova, 1985). The resulting wet-weight energy assumed for all body sizes of the shortfin mako was 5562 kJ/kg which is very close to the average estimate calculated for all sharks of 5414 kJ/kg (Cortés and Gruber, 1990; Schindler et al., 2002).

Energy allocation to reproduction (Rp) was only calculated for females and was assumed insignificant in male sharks. Reproductive growth for mature females (>18 years; Natanson et al., 2006) was calculated by assuming the following reproductive characteristics: mean litter size = 11.1, mean size at birth = 74 cm total length (TL), 24-month gestation period, and 3-year reproductive cycle (Mollet et al., 2000). This reproductive information coupled with the energy density (5562 kJ/kg) for shortfin makos gave an estimated energy cost for reproductive growth.

The overall energy content of the shortfin mako diet was determined with species-specific energy values from Steimle and Terranova (1985). The resulting value was used to calculate daily ration based on the overall energy demand from the bioenergetics model. For comparison of daily ration estimates based on the bioenergetics model, the method of Elliot and Persson (1978) was applied to the stomach contents data collected in the present study. Previously, for the shortfin mako, time for 90% evacuation of a meal was estimated at 36 to 48 hours (Stillwell and Kohler, 1982). It is now known that the VO_2 of shortfin makos is in the same range as that of tunas (Graham et al., 1990; Korsmeyer et al., 1996), which is unsurprising given the similarities that exist between these pelagic predators (i.e., body form, prey, endothermic capability). Studies have revealed that evacuation time for larger species of tuna, such as yellowfin tuna (*Thunnus albacares*), can range from 6 to 20 hours for complete evacuation depending on the prey type (Olson and Boggs, 1986). Based on similarities with tunas, as well as on a markedly higher metabolic rate than that estimated in Stillwell and Kohler (1982),

a shorter evacuation rate of 18–20 hours (higher end of the tuna scale) was used as a more realistic estimate of gastric evacuation time. This range was used to generate values for evacuation rate (R) by assuming an exponential evacuation rate according to the equation: $S_t/S_0 = e^{-Rt}$ (Elliot and Persson, 1978), where S_t and S_0 are the final and initial amounts of the prey item, respectively, and S_t/S_0 is assumed to be 0.10 (or the time when 90% of the initial food has been evacuated from the stomach). With this estimate of gastric evacuation rate, daily ration was calculated with the equation: $\Sigma C(t) = 24\hat{S}R$, where $\hat{S}$ is the mean weight of the stomach contents data over a 24-hour period.

Results

Diet

The two years of seasonal sampling for the 2001–02 diet seemed to provide a very good sample, averaging 95 sharks per year. In total, 189 sharks (108 males and 81 females) were examined that ranged in size from 146 to 335 cm fork length (FL). The majority of sharks sampled (120) contained at least one prey item in their stomach. Overall, 63% of prey items collected from stomachs were at an advanced stage of digestion (levels 4 and 5) on the digestive state scale, and only 4.0% were designated as levels 1 and 2 (Table 1). Any fresh bait that shortfin makos would have encountered and eaten on the day of the tournament would have still been fresh in the stomachs at the time of dissection. The low prevalence of fresh prey items in the digestive scale ratings would indicate that bait was not an important factor in the analysis.

The historical diet data were collected over a much longer period (11 years) and averaged fewer sharks per year (27) than the 2001–02 data. Overall, 302 sharks ranging in size from 86 to 338.5 cm FL were sampled: 148 males, 54 females, and 100 unsexed sharks. A higher percentage of the historical shortfin makos (73.8%) contained at least one prey item in their stomachs. The size distributions of sharks sampled from the two data sets were similar except for the absence of sharks <140 cm in the 2001–02 data (because of restrictions on the size of sharks taken at tournaments implemented after the historical data were collected) (Fig. 2).

Bluefish dominated the current diet of shortfin makos, accounting for 71.2% of the prey by number, 92.6% by weight, 87.5% by occurrence, and 99.2% IRI (Table 2). Other observed prey items were Atlantic mackerel, two species of squid (*Loligo pealeii* and *Illex illecebrosus*), menhaden, and Atlantic herring (*Clupea harengus*). A graphical comparison of index calculations for the three subgroupings of sharks based on the 2001–02 data illustrated the similarity in diet among groups—a similarity primarily due to the predominance of bluefish in all diets (Fig. 3, A and B).

For the historical data, bluefish also dominated the diet, but to a lesser extent, accounting for 55.6% of the

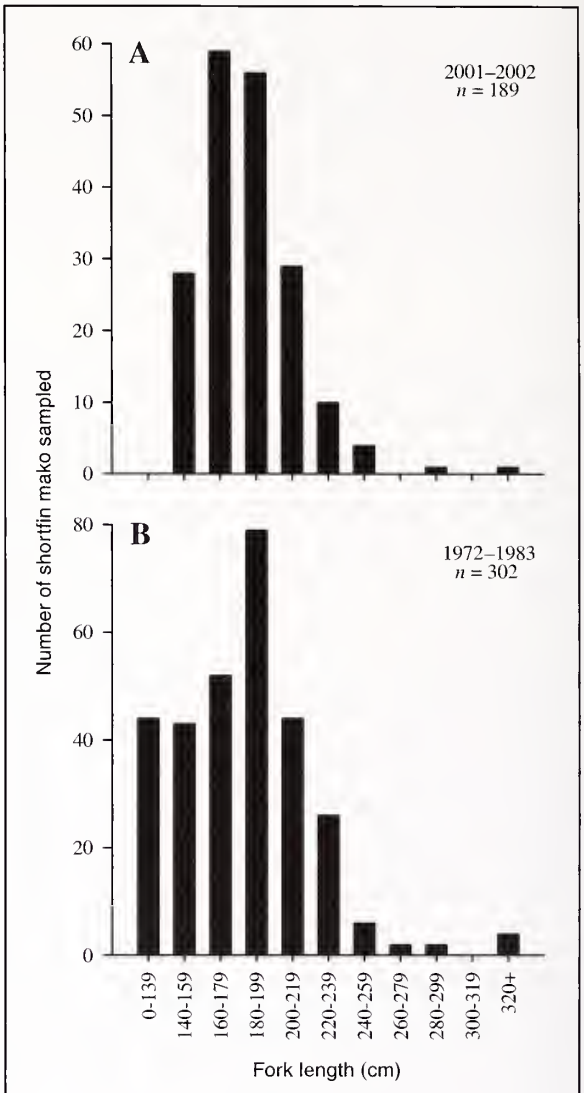

Figure 2

Length-frequency distributions for the shortfin mako (*Isurus oxyrinchus*) sampled in (**A**) the current study (2001–02), and (**B**) in the historical study (1972–83).

diet by number, 86.9% by volume, 78.5% by occurrence, and 97.2% IRI (Table 2). A variety of different prey items were found in the historical diet, mostly other teleosts. A comparison of prey families indicated that the current diet had prey from nine different families, plus prey from the group crustacea. In the historical diet 14 different fish families of prey were found, as well as crustaceans, mammals, and plants (Table 2). Some of the specific prey items present in the historical diet, but not found in the current diet, were saury (*Scomberesox saurus*), bullet mackerel (*Auxis rochei*), sand lance (*Ammodytes* sp.), and ocean pout (*Macrozoarces americanus*).

The 2001–02 diet data appeared to be a more accurate sample of the shortfin mako diet than the histori-

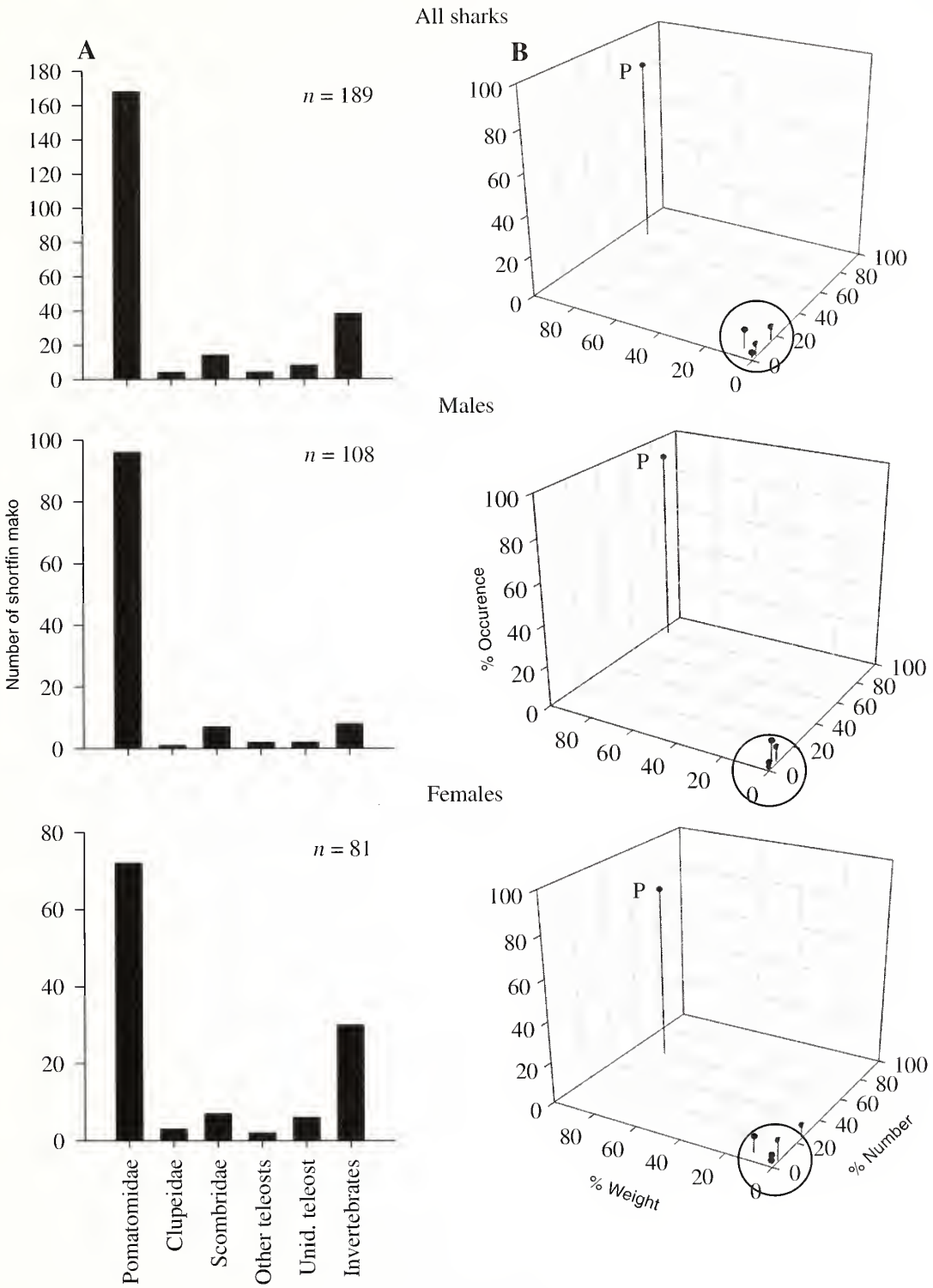

Figure 3

(**A**) Diet distribution by prey family for the three categories of shortfin mako (*Isurus oxyrinchus*)—all sharks, males, and females. Diet distribution was determined from the 2001–02 diet data. (**B**) Graphical representation of three diet index calculations for all sharks, for males, and for females. P = Pomatomidae, the predominant prey item, and the open circle surrounds a cluster of less important prey items: Clupeidae, Scombridae, other teleosts, unidentified teleosts, and invertebrates.

cal data. The rate of increase for the cumulative prey curve of the current diet was 3.0%, indicating that the diet was well sampled. Conversely, the cumulative prey curve for the historical diet showed a rate of increase of 6.24%, indicating more sampling may have captured the diet breadth better (Fig. 4). Jackknife estimates of species richness were 16 and 36 prey species for the 2001–02 and historical diet, respectively. The two measures of niche overlap used to compare the historical and 2001–02 diet data revealed slight

Table 2

Current and historical diet data for the shortfin mako (*Isurus oxyrinchus*) expressed as a percentage by number (%N), weight (%W), frequency of occurrence (%FO), volume (%V); and the index of relative importance expressed as a percentage (%IRI).

	Current diet				Historical diet			
Prey item	%N	%W	%FO	%IRI	%N	%V	%FO	%IRI
Crustaceans	10.60	0.03	0.83	0.07	0.96	0.15	1.79	0.02
Cephalapoda								
Ommastrephidae								
Illex illecebrosus	2.54	0.14	1.67	0.10	6.71	2.62	4.93	0.40
Loliginidae								
Loligo pealeii	2.96	0.42	4.17	0.14	0.72	0.28	1.35	0.01
Unidentifiable					7.19	2.81	7.18	0.34
Elasmobranchs								
Carcharhinidae								
Prionace glauca					0.24	0.19	0.45	0.00
Squalidae								
Squalus acanthias	0.42	0.02	0.83	0.00				
Teleosts								
Ammodytidae					1.44	0.02	0.45	0.01
Clupeidae					1.20	0.02	0.45	0.01
Brevoortia tyrannus	0.85	0.68	0.83	0.01	0.48	0.09	0.45	0.00
Clupea harengus	0.85	0.35	1.67	0.02				
Gadidae					0.24	0.24	0.45	0.00
Merluccius bilinearis					0.24	0.03	0.45	0.00
Malacanthidae								
Lopholatilus chamaeleonticeps	1.27	1.07	1.67	0.03				
Pomatomidae								
Pomatomus saltatrix	71.19	92.62	87.50	99.21	55.64	86.90	78.48	97.24
Scomberesocidae								
Scomberesox saurus					10.07	0.13	2.69	0.24
Scombridae					1.44	0.88	2.69	0.05
Auxis rochei					0.48	0.09	0.90	0.00
Euthynnus pelamis	0.85	0.81	1.67	0.02	0.24	0.39	0.45	0.00
Sarda Sarda					0.24	0.03	0.45	0.00
Scomber scombrus	3.80	0.93	6.67	0.22	2.39	0.68	4.04	0.11
Thunnus albacares	0.85	2.51	1.67	0.04	1.20	0.63	1.35	0.02
Serrandiae								
Centropristis striata	0.42	0.08	0.83	0.00				
Sparidae					0.24	0.06	0.45	0.00
Triglidae					0.24	0.05	0.45	0.00
Xiphidae								
Xiphias gladius					0.24	2.58	0.45	0.03
Zoercidae								
Macrozoarces americanus					0.24	0.06	0.45	0.00
Unidentifiable remains	3.39	0.34	5.83	0.15	7.19	0.94	8.52	0.60
Mammalia					0.48	0.14	0.90	0.01
Plant					0.24	0.00	0.45	0.00

differences in the diets and a percentage overlap equal to 70.3 and the simplified Morista's index equal to 0.937. The contingency table analysis indicated that the difference between the diets was significant according to a chi-square test and G-statistic ($P<0.001$). However, a subsequent contingency table analysis with the grouping "other teleosts" removed from both diets resulted in no significant difference.

Predator-size–prey-size relationship

An original fork length was back-calculated for 115 bluefish prey. The average bluefish prey length was 66.7 cm FL (minimum size=36.5 cm and maximum size=82.0 cm). Over 96% of the bluefish found in shortfin mako stomachs were greater than 50.0 cm FL. There was no significant relationship between the size of bluefish prey and predator size and none of the quantile regressions was significant. Investigation of prey size indicated that shortfin makos consume intermediate-size bluefish in relative to their own body size. Overall, 100% of bluefish consumed fell in the range of 0.2 to 0.5 prey-to-predator size ratio, and the majority (35%) were at a ratio of 0.35 (Fig. 5).

Daily ration

The linear relationship between mean VO_2 and swimming speed (U) was significant ($P<0.05$), and had a fairly good fit ($r^2=0.83$). The resulting regression equation was: $VO_2 = 506.42U + 201.39$. From a mean swimming speed of 0.5 body lengths per second (observed from pop-up satellite tag tracks) the active metabolic O_2 consumption rate for the bioenergetics model was calculated to be 454.4 mg/kg/h. Adjusting this value to reflect the average water temperature in which shortfin makos are found in the western North Atlantic ($Q_{10}=2.3$), we calculated an active metabolic O_2 consumption rate of 485.7 mg/kg/h. An oxycaloric conversion (13.6 J/mg O_2) of this metabolic demand resulted in an estimate of 6.61 kJ/kg/h of food energy for a shortfin mako to maintain active metabolism.

Total energy consumption increased with age until the onset of maturity for both sexes and slowly decreased (Fig. 6 shows energy consumption following the growth curves as they leveled off). After females reach the average age of maturity (18 years) the model calculated an average reproductive contribution of 86,299 KJ/yr.

The bioenergetic demands for the shortfin mako were higher than previously estimated, and higher than observed for any other species of shark. The average caloric value of the shortfin mako diet was calculated to be 4909 kJ/kg (Table 3). In order to satisfy the total energy demands from the bioenergetics model, shortfin makos must consume on average 4.48% of their body weight (BW) per day. Values of consumption by age ranged from 4.42–4.66 %BW/d for males and 4.42 to 4.56 %BW/d for females.

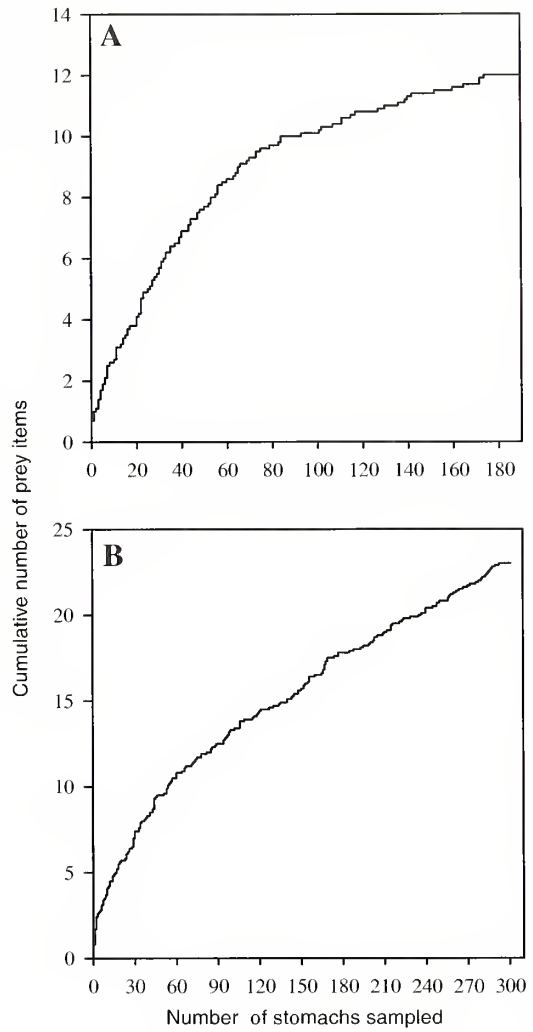

Figure 4

Cumulative prey curves calculated for prey items found in (**A**) the 2001–02 diet study, and (**B**) in the historical diet (1972–83) of shortfin makos (*Isurus oxyrinchus*) in the Northwest Atlantic Ocean.

The second method applied to estimate the daily ration of the shortfin mako yielded a result very similar to that from the bioenergetics model. We assumed all but 10% of a consumed food item was evacuated after a period of 18–20 hours, and a corresponding range of evacuation rates of 0.128 to 0.115/h were calculated. This range of evacuation rates, in conjunction with an observed average stomach contents weight of 1.02 kg, resulted in daily ration estimates of 2.82 to 3.13 kg per day. Daily ration was calculated to be 4.44 to 4.93 %BW/d for a 63.5-kg shortfin mako (the median weight of sharks from the 2001–02 study) according to this model (average of 4.68 %BW/d).

Based on the estimates of daily ration, and the high proportion of bluefish in the diet, a large amount of

Table 3

Percentage by weight and the energy content (kJ/kg) determined from the 2001–02 diet data for the shortfin mako (*Isurus oxyrinchus*) and broken down by species. All energy values were taken from Steimle and Terranova (1985).

Prey species	%W	kJ/kg	Diet contribution (kJ/kg)
Brevoortia tyrannus	0.68	7500	51.0
Centropristis striata[2]	0.08	4770	3.8
Clupea harengus	0.35	10,600	37.1
Crustaceans[1]	0.03	4450	1.3
Euthynnus pelamis[2]	0.81	6300	51.0
Illex illecebrosus	0.14	7100	9.9
Loligo pealei	0.42	5600	23.5
Lopholatilus chamaeleonticeps[2]	1.07	4770	51.0
Pomatomus saltatrix	92.62	4800	4445.8
Scomber scombrus	0.93	6000	55.8
Squalus acanthias	0.02	8600	1.7
Thunnus albacares[2]	2.51	6300	158.1
Unidentifiable pices[3]	0.34	5535	18.8
Total			4909.0

[1] Mean energy value for crustacea was used.
[2] Mean energy value for benthic and pelagic fish was used.
[3] Mean energy value for all fish was used.

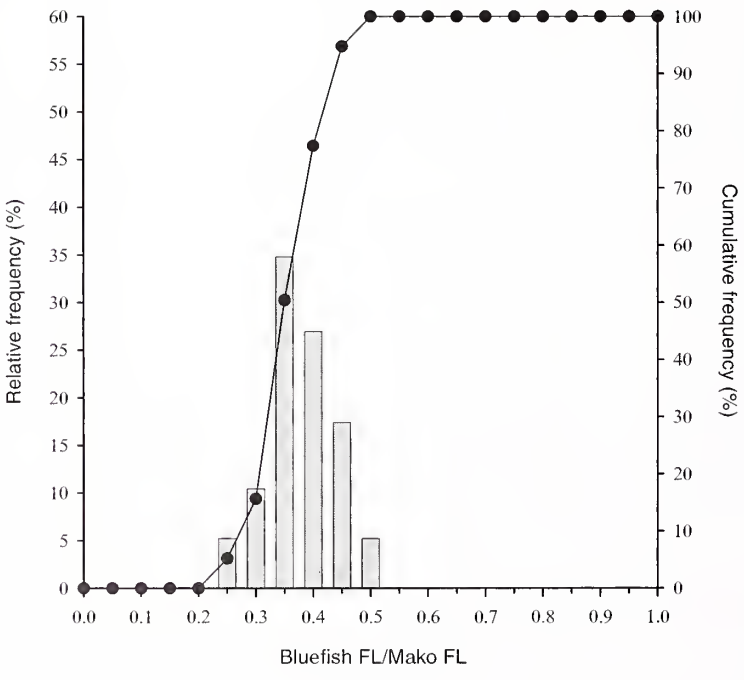

Figure 5

Relative frequency (bars) and cumulative frequency (line) plots showing the distribution of bluefish (*Pomatomus saltatrix*) size to shortfin mako (*Isurus oxyrinchus*) size ratios for the 2001–02 diet data.

bluefish could be consumed annually by shortfin makos in the northwest Atlantic Ocean. The average value for daily ration estimated by the two methods indicates that shortfin makos consume roughly 4.58% of their body weight per day. Considering the proportion by weight of bluefish in the diet (92.6%), an average shark (63.5 kg) could consume up to 1000 kg of bluefish per year (assuming a full year feeding cycle on bluefish).

Discussion

The level of top-down predation pressure that shortfin mako are able to exert on northwest Atlantic bluefish populations is still unclear. Quantifying this predator-prey relationship is difficult because it appears to only occur seasonally off the northeast coast of the United States. In offshore regions in the northwest Atlantic where bluefish are less abundant the shortfin mako diet is very different; the sharks focus mainly on squid species and other more prevalent teleosts (Stillwell and Kohler, 1982). It is not until these sharks migrate inshore that they shift

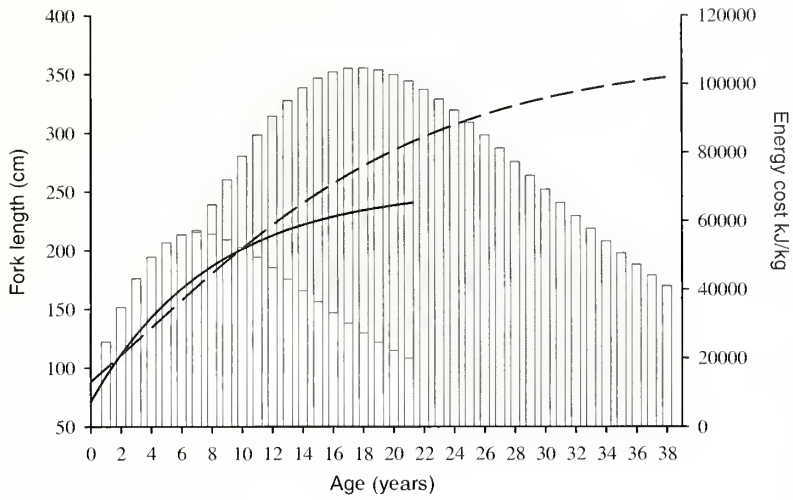

Figure 6

Growth curves for male (- - -) and female (----) shortfin mako (*Isurus oxyrinchus*), from growth equations in Natanson et al. (2006). The histogram represents energy costs (KJ/kg) for growth from age to age from the bioenergetics model derived from the 2001–02 diet data: The descending bars within the columns represents the cumulative frequency of these ratios.

their diet to focus on bluefish (MacNeill et al., 2005). In diet studies from the eastern Atlantic off of Portugal (Maia et al., 2006), and the Southwest Atlantic off Argentina (Vaske-Júnior and Rincón-Filho, 2003), bluefish were not found in the diet of shortfin makos, even though their distribution covers these regions and these sharks prey mainly on teleosts. The high concentration of bluefish in the northwest Atlantic Ocean, and the presence of large schools of bluefish that could be easily located by shortfin makos, is a likely reason for the predominance of bluefish in the diet.

There have been notable changes in the perceived abundance of bluefish in the northwest Atlantic Ocean since the historical diet data were collected. Nearing the end of the historical sampling period bluefish were very abundant with a total stock biomass of 104,000 metric tons (t) in 1982 (NEFSC[1]). At this time they were the most important prey species in the shortfin mako diet (86.9 %V). Since the early 1980s, fishing mortality of age-1 bluefish has increased fourfold, and recruitment for age-0 fish is thought to have declined from 75 million to 14 million (Shepherd and Packer, 2006). In addition, total stock biomass declined 72% (29,400 t) from 1982 to 1997 and was estimated to have increased since then to 40,000 t in 2004 (NEFSC[1]). This apparent decline in bluefish abundance from historical levels is not reflected in the current diet of the shortfin mako, and bluefish still represent a very high proportion of prey consumed.

The high numbers of bluefish in the 2001–02 diet indicate that even though abundance is lower than historical levels it is not limiting prey for shortfin mako. There appear to be suitable numbers of bluefish available for the shortfin mako population to prey almost solely on this species during their seasonal residence off the northeast coast of the United States. It is likely that shortfin mako abundance in this region has declined alongside bluefish since the historical diet data were collected. Therefore, although there may be a lower abundance of prey items to feed on, the predator abundance is lower as well. Unfortunately, the shortfin mako population in the northwest Atlantic Ocean has never been reliably quantified. The most recent stock assessment for large pelagic sharks was considered preliminary because of limitations on both the quality and quantity of the data, and came up short of providing reliable estimates. However, trends from catch-per-unit-of-effort indices derived from pelagic longline data for tuna and swordfish (*Xiphias gladius*) fisheries in the western North Atlantic have revealed a 43% decline in shortfin mako abundance since 1986 (Cortés et al., 2007). It is possible that any increased predation pressure on the depleted bluefish population is mitigated by a decreased abundance of shortfin makos from historical levels.

It appears that the importance of bluefish in the shortfin mako diet has not changed since the historical

[1] NEFSC (Northeast Fisheries Science Center). 2005. 41st Northeast Regional Stock Assessment Workshop (41st SAW). 41st SAW assessment report. Northeast Fish Science Center Reference Document 05-14, 237 p. Northeast Fisheries Science Center, National Marine Fisheries Service, Woods Hole Laboratory, 166 Water St., Woods Hole, MA 02543.

sampling; however, there has been an apparent decrease in species diversity in the diet. The cumulative prey curves indicate that the 2001–02 diet was well sampled, but more sampling was needed to better represent the historical diet. Additionally, the jackknife estimates of species richness indicate that 36 species would be represented in a fully sampled historical diet, and only 16 in the current diet. It is possible these results are an artifact of sampling. The total number of shortfin makos examined and the number of years over which the data were collected were both greater for the historical sampling, which likely affected prey diversity. On the other hand, some of the shift observed in the diet diversity over the past few decades could be due to temporal changes in the prey community structure of the northwest Atlantic Ocean. This ecosystem has experienced significant fluctuations in the relative abundance and biomass of many fish and invertebrate species (Overholtz et al., 2000). In addition, the community is now dominated by pelagic finfish such as Atlantic mackerel and Atlantic herring whose large concentrations draw a variety of piscivorous predators, such as bluefish (Overholtz et al., 2000). Large predatory schools of bluefish feeding on abundant pelagic finfish would themselves be easy prey for shortfin makos.

The schooling nature of bluefish is the likely explanation for their high concentration in the shortfin mako diet. Adult bluefish feed and also spawn in large schools as they migrate up the northeast coast of the United States in the spring and early summer (Juanes et al., 1996; Salerno et al., 2001). The focus of shortfin mako predation seems to be these adult bluefish. The length-frequency distribution of bluefish prey found in shortfin mako stomachs revealed that the majority (96%) of individuals fell in the 50- to 90-cm-FL size range. Bluefish at this size are around 2 years old and are likely mature individuals (Juanes et al., 1996; Salerno et al., 2001). The large feeding and spawning aggregations of these adult bluefish would be very easy to find and target for shortfin makos in the region. Intense predation on these large schools could potentially have a regulatory effect on bluefish abundance in the northwest Atlantic Ocean.

In order to quantify the level of shortfin mako predation on the bluefish population a reliable estimate of daily ration was needed. Recently available information on the metabolism, average swimming speed, and growth rate of the shortfin mako has allowed the development of a good bioenergetics model. The resulting estimates of daily ration are notably higher than those of many other elasmobranch species, which rarely exceed 3.0% BW/d (Wetherbee and Cortés, 2004). The highest published rate of consumption observed for an obligate ram ventilating shark was 3.54 %BW/d for juvenile scalloped hammerheads (*Sphyrna lewini*) (Bush and Holland, 2002). The most abundant pelagic shark in the North Atlantic, the blue shark, has a daily ration of approximately 1% BW/d, which is significantly less than that of the shortfin mako (Schindler et al., 2002). The high metabolic and high consumption rate of the shortfin mako can be attributed to its ability to thermoregulate. The endothermic capability of the shortfin mako increases its aerobic capacity, resulting in a higher metabolism and increased energy demand.

The estimates of daily ration from this study provide a means to quantify predation on bluefish on an individual predator basis. Because there is no estimate of the shortfin mako population size, a relevant exercise is to backcalculate the number of sharks it would take to match the fishing pressure. Bax (1998) determined that predation by fish can range from 2–35 times the loss to fisheries. However, we assumed that shortfin mako predation on bluefish was set equal to the amount of bluefish taken by fisheries in 2002. The total bluefish catch (commercial+recreational) in 2002 was 11,566 t (NEFSC[1]). Taking an average value of the daily ration estimates, it was determined that an average shortfin mako (63.5 kg) consumes up to 1000 kg of bluefish per year. For this estimate it is assumed that shortfin makos are feeding on bluefish all year long, which may not be the case. If shortfin makos spend around 6 months off the northeast coast of the United States.(May to October), that period results in around 180 days of intense predation on bluefish. During this feeding season an average shark would consume roughly 500 kg of bluefish. At this rate of consumption it would have taken only 23,132 sharks to equal the take of the fisheries in 2002. These are very simple calculations but they serve to illustrate that the level of predation by shortin mako on bluefish is likely much greater than the impact of the fisheries. If true, this would not be a unique case. Multiple studies have shown that predation mortality on a variety of important prey species exceeds fishing mortality, and in some cases even exceeds maximum sustainable yield of the prey population (Christensen, 1996; Bax, 1998; Overholtz et al., 2000).

The most important factor often attributed to the decline of bluefish stocks in the northwest Atlantic Ocean is fishing pressure (Shepherd and Packer, 2006), but it is evident that predation should not be disregarded. Bluefish mortality as a result of predation could exceed the loss to these fisheries, as has been shown in other predator-prey systems (Bax, 1998; Overholtz et al., 2000). It is becoming increasingly apparent that depressed fish stocks are very vulnerable to predation, but the mechanisms driving this vulnerability are still unclear. In recent studies there have been deeper probes into trophic interactions, such as efforts to quantify prey vulnerability to predation (Bundy and Fanning, 2005; Overholtz, 2006). The exact predator-prey dynamics that exist between shortfin makos and bluefish are still unclear; however, it is likely that predation has played a more important role in the decline of the northwest Atlantic Ocean bluefish population than previously thought.

Adding predation as a variable into the management of northwest Atlantic Ocean bluefish would increase the difficulty of an already complicated task. The highly

migratory nature of the bluefish, coupled with a variety of seasonal fisheries, creates a challenging situation for stock management. Bluefish in this region are currently managed as a single stock, and although the stock is still categorized as overfished, overfishing is not occurring (Shepherd and Packer, 2006). Decreases in fishing pressure have allowed biomass and abundance levels to slowly climb since 1997. However, heavily exploited fish populations tend to remain in a depressed state for a prolonged period following fishing reductions or moratoriums (Bakun and Curry, 1999; Hutchings, 2000; Bundy and Fanning, 2005). One theory offered for the lack of recovery in these populations is predation pressure (Bax, 1998; Bakun and Curry, 1999). In a depressed stock the spawning capability of the prey population is held in a depleted state by intense predation (Bakun and Curry, 1999). It is evident from this study that fisheries managers should consider predation as an important factor when managing the recovery of the bluefish population in the northwest Atlantic Ocean.

Acknowledgments

We thank the numerous fishermen and fishing tournament directors who allowed us behind the lines to collect samples. We also thank A. J. M. Wood, C. Butler, and M. Smith for their aid in the collection, transportation, and analysis of stomach contents. Funding for this study was provided by the Bluefish-Striped Bass Dynamics Research Program at Rutgers University in cooperation with the National Marine Fisheries Service (grant NA97FE0363), and the University of Rhode Island/National Oceanic and Atmospheric Administration/Cooperative Marine Education Research (grant NA03NMF4550395). Finally, we thank the many colleagues and anonymous reviewers whose suggestions helped to improve this manuscript.

Literature cited

Bakun, A., and P. Cury.
1999. The "school trap": a mechanism promoting large amplitude out-of-phase population oscillations of small pelagic fish species. Ecol. Letters 2:349–351.

Baremore, I. E.
2007. Feeding ecology of the Atlantic angel shark, *Squatina dumerili*, in the northern Gulf of Mexico. M.S. thesis, 79 p. Univ. Florida, Gainesville, FL.

Bax, N. J.
1998. The significance and prediction of predation in marine fisheries. ICES J. Mar. Sci. 55:997–1030.

Bethea, D. M., J. A. Buckel, and J. K. Carlson.
2004. Foraging ecology of the early life stages of four sympatric shark species. Mar. Ecol. Prog. Ser. 268:245–264.

Bundy, A., and L. P. Fanning.
2005. Can Atlantic cod (*Gadus morhua*) recover? Exploring trophic explanations for the non-recovery of the cod stock on the eastern Scotian Shelf, Canada. Can. J. Fish. Aquat. Sci. 62:1474–1489.

Bush, A., and K. Holland.
2002. Food limitation in a nursery area: estimates of daily ration in juvenile scalloped hammerheads, *Sphyrna lewini* (Griffen and Smith, 1834) in Kane'ohe Bay, Hawai'i. J. Exp. Mar. Biol. Ecol. 278:157–178.

Carlson, J. K., and G. R. Parsons.
1999. Seasonal differences in routine oxygen consumption rates of the bonnethead shark. J. Fish Biol. 55:876–879.

Christensen, V.
1996. Managing fisheries involving predator and prey species. Rev. Fish Biol. Fish. 6:417–442.

Clarke, K. R.
1993. Non-parametric multivariate analyses of changes in community structure. Aust. J. Ecol. 18:117–143.

Compagno, L. J. V.
2001. Sharks of the world: an annotated and illustrated catalogue of shark species known to date. FAO species catalogue for fishery purposes. No. 1, vol. 2. Bullhead, mackerel and carpet sharks (Heterdontiformes, Lamniformes, and Orectolobiformes), 269 p. FAO, Rome.

Cortés, E., C. A. Brown, and L. R. Beerkircher.
2007. Relative abundance of pelagic sharks in the western North Atlantic Ocean, including the Gulf of Mexico and Caribbean Sea. Gulf Caribb. Res. 19: 37–52.

Cortés, E.
1997. A critical review of methods of studying fish feeding based on analysis of stomach contents: applications to elasmobranch fishes. Can. J. Fish. Aquat. Sci. 54:726–738.

Cortés, E., and S. H. Gruber.
1990. Diet, feeding habits and estimates of daily ration of young lemon sharks, *Negaprion brevirostris* (Poey). Copeia 1990:204–218

Elliot, J. M., and L. Persson.
1978. The estimation of daily rates of food consumption for fish. J. Anim. Ecol. 47: 977–991.

Graham, J. B., H. Dewar, N. C. Lai, W. R. Lowell, and S. M. Arce.
1990. Aspects of shark swimming performance determined using a large water tunnel. J. Exp. Biol. 151: 175–192.

Heithaus, M. R., and L. M. Dill.
2002. Food availability and tiger shark predation risk influence bottlenose dolphin habitat use. Ecology 83:480–491.

Hutchings, J. A.
2000. Collapse and recovery of marine fishes. Nature 406:882–885.

Hyslop, E. J.
1980. Stomach contents analysis – a review of methods and their application. J. Fish Biol. 17:411–429.

Juanes, F., J. A. Hare, and A. G. Miskiewicz.
1996. Comparing early life history strategies of *Pomatomus saltatrix*: A global approach. Mar. Freshw. Res. 47:365–379.

Kohler, N. E., J. G. Casey, and P. A. Turner.
1996. Length-length and length-weight relationships for 13 shark species from the Western North Atlantic. NOAA Tech. Memo. NMFS-NE-110, 22 p.

Korsmeyer, K. E., H. Dewar, N. C. Lai, and J. B. Graham.
1996. Tuna aerobic swimming performance: Physiological and environmental limits based on oxygen supply and demand. Comp. Biochem. Physiol. 113:45–56.

Krebs, C. J.
1999. Ecological methodology, 2nd ed., 620 p. Addison

Wesley and Benjamin Cummins Publishing, New York, NY.

MacNeil, M. A., G. B. Skomal, and A. T. Fisk.
2005. Stable isotopes from multiple tissues reveal diet switching in sharks. Mar. Ecol. Prog. Ser. 302:99–206.

Maia, A., N. Queiroz, J. P. Correia, and H. Cabral.
2006. Food habits of the shortfin mako, *Isurus oxyrinchus*, off the southwest coast of Portugal. Environ. Biol. Fish. 77:157–167.

Mollet, H. F., G. Cliff, H. L. Pratt, and J. D. Stevens.
2000. Reproductive biology of the female shortfin mako, *Isurus oxyrinchus* Rafinesque, 1810, with comments on the embryonic development of lamnoids. Fish. Bull. 98:299–318.

Natanson, L. J., N. E. Kohler, D. Ardizzone, G. M. Cailliet, S. Wintner, and H. F. Mollet.
2006. Validated age and growth estimates for the shortfin mako, *Isurus oxyrinchus*, in the North Atlantic Ocean. Environ. Biol. Fish. 77:367–383.

Olson, R. J., and C. H. Boggs.
1986. Apex predation by yellowfin tuna (*Thunnus albacares*): independent estimates from gastric evacuation and stomach contents, bioenergetics, and cesium concentrations. Can. J. Fish. Aquat. Sci. 43:1760–1775.

Overholtz, W. J.
2006. Estimates of consumption of Atlantic herring (*Clupea harengus*) by bluefin tuna (*Thunnus thynnus*) during 1970–2002: an approach incorporating uncertainty. J. Northwest Atl. Fish. Sci. 36:55–63.

Overholtz, W. J., J. S. Link, and L. E. Suslowicz.
2000. Consumption of important pelagic fish and squid by predatory fish in the northeastern USA shelf ecosystem with some fishery comparisons. ICES J. Mar. Sci. 57:1147–1159.

Salerno, D. J., J. Burnett, and R. M Ibara.
2001. Age, growth, maturity, and spatial distribution of bluefish, *Pomatomus saltatrix*, off the northeast coast of the United States, 1985–96. J. Northwest Atl. Fish. Sci., 29:31–39.

Schindler, D. E., T. E. Essington, J. F. Kitchell, C. J. Boggs, and R. Hilborn.
2002. Sharks and tunas in the Central Pacific: fisheries impacts on predators with contrasting life histories. Ecol. Appl. 12:735–748.

Shepherd, G. R., and D. B. Packer.
2006. Essential fish habitat source document: Bluefish, *Pomatomus saltatrix*, life history and habitat characteristics, 2nd ed. NOAA Tech. Memo. NMFS-NE-144, 68 p.

Steimle, F. W., and R. J. Terranova.
1985. Energy equivalents of marine organisms from the continental shelf of the temperate northwest Atlantic. J. Northwest Atl. Fish. Sci. 6: 117–124.

Stevens, J. D., R. Bonfil, N. K. Dulvy, and P. A. Walker.
2000. The effects of fishing on sharks, rays, and chimaeras (chondrichthyans), and the implications for marine ecosystems. ICES J. Mar. Sci. 57:476–494.

Stillwell, C. E., and N. E. Kohler.
1982. Food, feeding habits, and estimates of daily ration of the shortfin mako (*Isurus oxyrinchus*) in the Northwest Atlantic. Can. J. Fish. Aquat. Sci. 39: 407–414.

van der Elst, R. P.
1979. A proliferation of small sharks in the shore-based Natal sport fishery. Environ. Biol. Fish. 4:349–362.

Vaske-Júnior, T., and G. Rincón-Filho.
2003. Stomach contents of blue sharks (*Prionace glauca*) and anequim (*Isurus oxyrinchus*) from oceanic waters of southern Brazil. Rev. Brasil. Biol. 58:445–452. [In Spanish].

Wetherbee, B. M., and E. Cortés.
2004. Food consumption and feeding habits. *In* Biology of Sharks and their Relatives: Food Consumption and Feeding Habits. (J. C. Carrier, J. A. Musick, and M. R. Heithaus, eds.), p. 223–244. CRC press, Boca Raton, FL.

Wood, A. D.
2005. Using bone measurements to estimate the original sizes of bluefish (*Pomatomus saltatrix*) from digested remains. Fish. Bull. 103:461–466.

A comparison between warm-water fish assemblages of Narragansett Bay and those of Long Island Sound waters

Abby Jane M. Wood (contact author)[1]
Jeremy S. Collie[2]
Jonathan A. Hare[3]

Email address for contact author: amclean@gso.uri.edu

[1] University of Rhode Island
Department of Fisheries, East Farm Campus
Kingstown Road
Kingston, Rhode Island 02881.

Present address: Rocky Hill School
530 Ives Road
East Greenwich, Rhode Island 02818.

[2] University of Rhode Island, Graduate School of Oceanography
South Ferry Road
Narragansett, Rhode Island 02882.

[3] National Marine Fisheries Service, NOAA
Northeast Fisheries Science Center
28 Tarzwell Drive
Narragansett, Rhode Island 02882.

Abstract—Fish species of warm-water origin appear in northeastern U.S. coastal waters in the late summer and remain until late fall when the temperate waters cool. The annual abundance and species composition of warm-water species is highly variable from year to year, and these variables may have effects on the trophic dynamics of this region. To understand this variability, records of warm-water fish occurrence were examined in two neighboring temperate areas, Narragansett Bay and Long Island Sound. The most abundant fish species were the same in both areas, and regional abundances peaked in both areas in the middle of September, four weeks after the maximum temperature in the middle of August. On average, abundance of warm-water species increased throughout the years sampled, although this increase can not be said to be exclusively related to temperature. Weekly mean temperatures between the two locations were highly correlated (r=0.99; P<0.001). The warm-water fish faunas were distinctly different in annual abundances in the two areas for each species by year (1987–2000), and these differences reflect the variability in the transport processes to temperate estuaries. The results reveal information on the abundance of warm-water fish in relation to trends toward warmer waters in these regions.

Manuscript submitted 27 January 2008.
Manuscript accepted 24 September 2008.
Fish. Bull. 107:89–100 (2009).

The views and opinions expressed or implied in this article are those of the author and do not necessarily reflect the position of the National Marine Fisheries Service, NOAA.

Temperate estuaries are subject to broad temperature variations related to seasonal warming and cooling. Resident fish species are able to survive these ranges in temperature, but these variations in temperature also create the conditions for seasonal habitat for boreal and subtropical fish species. These cold and warm-water species contribute significantly to the overall species diversity of temperate estuaries worldwide (Lenanton and Potter, 1987; Hutchins, 1991) and play a significant role in the trophic interactions in the ecosystem even though they are not present year round (Able and Fahay, 1998).

Temperature and faunal variations are well documented in temperate estuaries bordering the northeastern U.S. continental shelf ecosystem (Rountree and Able, 1992; Tremain and Adams, 1995), which extends from Cape Hatteras, North Carolina, to Nova Scotia, Canada (Fig. 1). Cape Hatteras is generally the northern barrier for warm-temperate fauna, but highly mobile species are able to move northward during warm seasons (Bigelow and Schroeder, 1953; Briggs, 1974). There are many estuaries stretching from Cape Hatteras to Nova Scotia, and estuarine fish assemblages have been well described in more southern estuaries, such as Chesapeake Bay (Murdy et al., 1997), Little Egg Inlet, New Jersey (Able and Fahay, 1998), and Sandy Hook, New Jersey (Grant, 1991). However, there is little information available regarding the abundance of warm-water fishes in estuaries farther north in the estuarine waters of Narragansett Bay (Narragansett Bay and several large salt ponds along the Atlantic coast of Rhode Island are hereafter referred to simply as Narragansett Bay) and Long Island Sound.

The goal of this study was to describe the warm-water fish fauna in the areas of the northeast U.S. continental shelf ecosystem represented by Narragansett Bay and Long Island Sound. We compiled a list of the warm-water fish species found in Narragansett Bay and Long Island Sound, calculated species richness, and compared species abundances between the two estuaries. Collected data were then used to address whether there had there been an increase in the occurrence of warm-water fishes

over time in response to warming of the coastal waters (Oviatt et al., 2002; Collie et al., 2008), and to determine whether similar oceanic processes are dominant in structuring the species composition in these two areas by examining the similarity in abundances of warm-water faunal assemblages.

Methods and materials

Data sources

Fish abundances were obtained from numerous long-term sampling programs in Narragansett Bay and Long Island Sound (Table 1). Concomitant environmental data were obtained when available, including surface temperature, bottom temperature, and salinity. Average water temperature (mean of surface and bottom temperature) was calculated for each week of the year.

Warm-water fishes (also called Carolinian, tropical, subtropical, transient, exotic species, in other literature) were identified by means of several regional ichthyofaunal guides (Smith, 1899; Bigelow and Schroeder, 1953). Important identifying characteristics included a significant portion of the life cycle, and usually the time and area of spawning (south of Cape Hatteras and only in late summer and fall months). It should be noted that northern puffer *(Sphoeroides maculatus)* were included because of the timing of their occurrence and their southerly distribution (Able and Fahay, 1998). In addition, the warm-water fishes that are caught in Narragansett Bay and Long Island Sound are generally found as juveniles.

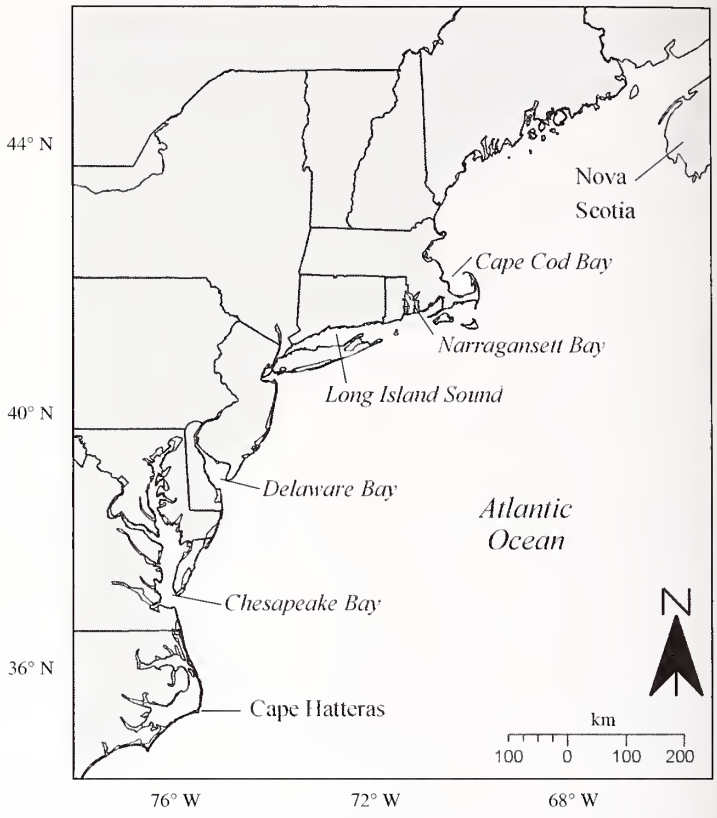

Figure 1

Map of Northwest Atlantic region between Cape Hatteras and Nova Scotia. Note the location of Narragansett Bay and Long Island Sound, which represent the sample sites for this study.

Data analysis

Timing, location, and frequency of sampling were different among the surveys considered here. Only the years in which sampling took place in all locations and during which consistent sampling methods were formed the data for the study. Sampling effort was not calculated for the different surveys but was consistent through each individual time series; therefore the accumulated data set represents internally consistent relative measures of the abundance of warm-water fishes. For area-specific analyses, data from 1987–2001 were included from surveys in Narragansett Bay, and data from 1984–2000 were included from surveys in Long Island Sound. For comparison between estuaries, only the data from overlapping years were used (1987–2000).

Describing and comparing warm-water fish fauna

Lists of warm-water species were generated for each area by using the sum of the species abundances during the different surveys. A rank correlation was calculated between total abundance of warm-water fish and year to evaluate whether species have increased in abundance through time. Correlations were then calculated between annual fish abundances in Narragansett Bay and Long Island Sound for all years, excluding 1994, during which extremely large catches of Atlantic moonfish (*Selene setapinnis*) were found in Narragansett Bay (59% of total Atlantic moonfish catch, 80% of 1994 catch, 29% of overall Narragansett Bay fish catch). Correlations were also calculated for the five most abundant individual species (representing 85% of the total catch): Atlantic moonfish, northern puffer, crevalle jack (*Caranx hippos*), planehead filefish (*Stephanolepis hispidus*), and bigeye (*Priacanthus arenatus*).

The observed species richness (S), or the number of different species present, was derived for both locations. Next, a jackknife estimation of species richness was conducted for both the Narragansett Bay and Long Island Sound data sets to estimate the number of species that were present but not sampled, following the method described by Krebs (1999). This estimation was made because, although the list of warm-water species was based on a large number of trawls and seine hauls, there are numerous species of warm-water fishes that have been observed by SCUBA divers and aquarists

Table 1

Description of data used from Narragansett Bay and Long Island Sound for this study, including the location of sampling site (RI=Rhode Island data from Narragansett Bay and the surrounding salt ponds, LIS=Long Island Sound), number of stations sampled, years when sampling occurred, sampling frequency, gear type used for sampling, and the source for the data.

Site	Number of stations sampled	Years	Sampling frequency	Gear type	Source
RI	2	1959 to present	Year round weekly	Trawl 10.4-m headrope 5.1 cm codend (*sic*) 30 min at 2 knots	University of Rhode Island Graduate School of Oceanography
	37	1987 to present	Year round monthly	Trawl 12.2-m headrope 0.95 cm codend (*sic*) 20 min at 2.5 knots	Rhode Island Department of Environmental Management
	5	1987 to present	April–November monthly	Seine 61-m net 6.4-mm mesh	
LIS	Random (about 80)	1984 to present	Fall	Trawl 9.1-m headrope 5.1 cm codend (*sic*) 30 min at 3.5 knots	Connecticut Department of Environmental Protection
	7	1984 to present	September	Seine 7.6-m net 6.4-mm mesh	
	6	1976 to present	Bi-weekly	Trawl 9.1 m headrope 6.4 mm codend liner (*sic*) 20 mins at 1.2–1.4 knots	Milford Laboratories
	5	1969 to present	May-November	Seine 9.14 m net 6.4-mm mesh	

that are not present in the databases represented in this study. In the jackknife estimation, the number of species present (S_i) was calculated with each of the years (i) removed in turn. The jackknife estimate was calculated by averaging together pseudovalues (Y_i), which represent the likely number of species for each year, by using the equation

$$Y_i = nS - (n-1)S_i,$$

where n = the number of years.

The jackknife mean and variance were calculated from the resulting pseudovalues (Y_i). The jackknife estimate was determined to obtain more likely values of species richness for each area. These estimates were compared between estuaries with a two-sample t-test (Johnson and Bhattacharyya, 2001) to determine if there was a significant difference in species richness. In addition, species accumulation curves were calculated for both populations and graphed together to assess whether the curves were similar for the two estuaries for the years 1987–2000.

A multidimensional scaling (MDS) analysis was conducted in the statistical analysis program PRIMER (PRIMER-E Ltd., Ivy Bridge, U.K.) to determine whether species composition of the annual abundances differed between Narragansett Bay and Long Island Sound. A Bray-Curtis measure of similarity was used for developing the similarity matrix (Krebs, 1999). Data were standardized, and a fourth root transformation was applied to the data to give less weight to abundant species. An MDS plot was computed for all of the years by species abundances in each location. A similarity percentage (SIMPER) analysis (in PRIMER) was then conducted to determine which of the species were driving the similarity and dissimilarity between the areas.

Timing of occurrence of warm-water fishes

Five aspects of the timing of the warm-water fauna were examined. First, the relationship between temperatures in the two estuaries was examined. Correlations were calculated between weekly mean temperatures in Narragansett Bay and Long Island Sound. Correlations were also calculated between the means of summer temperatures (June, July, and August combined) and semi-annual temperatures (May, June, July, August,

September, and October combined) because the warmest months are when these fishes are found.

Second, the relationship between the annual abundance of warm water fishes and water temperature was examined in both estuaries. Correlations were calculated between the mean annual, mean semi-annual, and mean summer temperatures and fish abundances by estuary.

Third, the weekly occurrence of the warm-water fishes was compared between estuaries. Catch abundances and means were derived for each week. Next, for each year, first appearance (at least 5% of the peak abundance), peak appearance, and last appearance were identified and a mean and standard deviation were calculated for each estuary. Correlations then were calculated for these measures of timing between estuaries. The weeks of first, peak, and last appearance were compared between estuaries by using a two-sample t-test and assuming equal variances (Johnson and Bhattacharyya, 2001).

Fourth, the weeks of first appearance, peak appearance, and last appearance were compared with estuarine temperatures. For each estuary, mean temperatures were derived at certain times of year. The weeks of first appearance were regressed upon temperatures for June 1 of each year, peak appearance weeks were regressed upon peak annual temperatures, and last appearance were regressed upon October 1 temperatures. June 1^{s}and October 1 were used because these are the dates between which the waters of Narragansett Bay and Long Island Sound are typically warm enough to sustain warm-water fishes.

Finally, the timing of northern puffer occurrence was examined in detail. This species was chosen for this analysis because of its abundance in both areas and because data were consistent enough to determine the peak week at which the species was captured. A correlation was calculated between weeks of peak appearance of the northern puffer in the two locations. In addition, correlations were calculated between the peak week of fish occurrence and temperature, as well as between the peak week of fish occurrence and the peak week for the 50% cumulative temperature for each year (calculated as the median temperature for the cumulative daily temperature degrees, termed "degree days").

Results

Comparison of warm-water fish fauna

The total number of warm-water fish sampled in Narragansett Bay (1987–2001) was 4683, and the total warm-water fish sampled in Long Island Sound (1984–2000) was 7075, for a total of 11,758 individuals. The most frequently occurring species was Atlantic moonfish (66.3%), followed by crevalle jack (9.6%), and northern puffer (8.1%) (Table 2).

The number of warm-water fishes has increased in more recent years of the survey. Most warm-water fish were caught in 1994, 2000, and 1998, whereas the fewest warm-water fish were caught in 1987, 1991, 1992, 1993, and 1995 (Fig. 2). A rank correlation between catch abundance and year indicated that the abundance of warm-water fish has increased (r=0.73; P=0.003).

The abundance of warm-water fish was correlated between Narragansett Bay and Long Island Sound. A correlation in abundance between areas that included data from all years was not significant (r=0.17, P=0.56), but when 1994 was excluded, a significant correlation was found (r=0.83, P=0.001). The annual abundances of the dominant species were also correlated between Narragansett Bay and Long Island Sound: Atlantic moonfish (omitting 1994) (r= 0.81, P=0.001), northern puffer (r=0.63, P=0.02), and planehead filefish (r=0.56, P=0.04). There was no significant correlation between the number of bigeye or crevalle jack caught in Narragansett Bay and Long Island Sound.

The observed species richness of warm-water fishes in Narragansett Bay and Long Island Sound were 26 and 28 species, and the resulting jackknife estimates of species richness were 33.9 and 39.2 species. Species richness did not differ significantly between estuaries (t=2.5, df=31, P>0.05). The species accumulation curves are similar in slope, although the curve for Long Island Sound is steeper and species

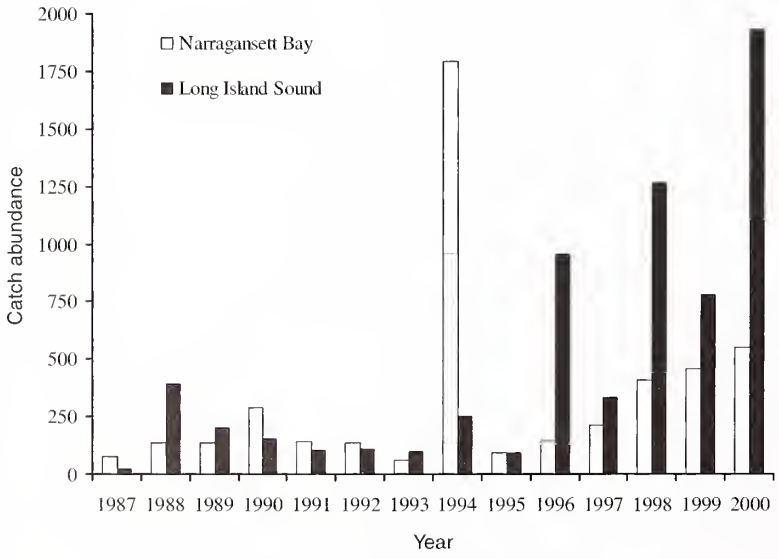

Figure 2

Sum of warm-water fish caught in trawl and seine surveys in Narragansett Bay and in Long Island Sound for the years 1987–2000.

Table 2

Warm-water fish species caught in regular monitoring surveys in Narragansett Bay and Long Island Sound waters (1987–2000). The number of each species caught in Narragansett Bay (NB) and Long Island Sound (LIS), total number caught, and percent of overall catch represented by each species are presented.

	Common name	Scientific name	Number caught in NB	Number caught in LIS	Total number caught	% of overall catch
1	Northern puffer	*Sphoeroides maculatus*	537	417	954	8.11
2	Crevalle jack	*Caranx hippos*	1059	64	1123	9.55
3	Atlantic moonfish	*Selene setapinnis*	2155	5639	7794	66.29
4	Planehead filefish	*Stephanolepis hispidus*	28	169	197	1.68
5	Bigeye	*Priacanthus arenatus*	71	55	126	1.07
6	Northern sennet	*Sphyraena borealis*	16	21	37	0.31
7	Flying gurnard	*Dactylopterus volitans*	9	38	47	0.40
8	Blue runner	*Caranx crysos*	109	2	111	0.94
9	Lookdown	*Selene vomer*	27	27	54	0.46
10	Bigeye scad	*Selar crumenophthalmus*	4	110	114	0.97
11	Bluespotted cornetfish	*Fistularia tabacaria*	15	92	107	0.91
12	Striped mullet	*Mugil cephalus*	8	133	141	1.20
13	Orange filefish	*Aluterus schoepfi*	2	30	32	0.27
14	Short bigeye	*Pristigenys alta*	2	21	23	0.20
15	Spot	*Leiostomus xanthurus*	29	0	29	0.25
16	Glasseye snapper	*Heteropriacanthus cruentatus*	2	19	21	0.18
17	Inshore lizardfish	*Synodus foetens*	0	19	19	0.16
18	White mullet	*Mugil curema*	0	112	112	0.95
19	Rough scad	*Trachurus lathami*	261	0	261	2.22
20	Gray triggerfish	*Balistes capriscus*	5	4	9	0.08
21	Sheepshead	*Archosargus probatocephalus*	332	0	332	2.82
22	Permit	*Trachinotus falcatus*	0	33	33	0.28
23	Red goatfish	*Mullus auratus*	0	17	17	0.14
24	Trunkfish spp.	*Lactophrys* spp.	0	12	12	0.10
25	Spotfin butterflyfish	*Chaetodon ocellatus*	0	8	8	0.07
26	Schoolmaster	*Lutjanus apodus*	0	7	7	0.06
27	Rough scad	*Trachurus lathami*	0	5	5	0.04
28	Sargassum fish	*Histrio histrio*	2	0	2	0.02
29	Spotted goatfish	*Pseudupeneus maculatus*	2	0	2	0.02
30	Cero	*Scomberomorus regalis*	2	0	2	0.02
31	Mahogany snapper	*Lutjanus mahogoni*	3	0	3	0.03
32	Atlantic needlefish	*Strongylura marina*	0	4	4	0.03
33	Pinfish	*Lagodon rhomboides*	0	4	4	0.03
34	Round scad	*Decapterus punctatus*	0	3	3	0.03
35	Mackerel scad	*Decapterus macarellus*	0	2	2	0.02
36	Filefish spp.		0	2	2	0.02
37	Striped burrfish	*Chilomycterus schoepfii*	0	2	2	0.02
38	French grunt	*Haemulon flavolineatum*	1	0	1	0.01
39	Guaguanche	*Sphyraena guachancho*	1	0	1	0.01
40	King mackerel	*Scomberomorus cavalla*	1	0	1	0.01
41	Snakefish	*Trachinocephalus myops*	0	1	1	0.01
42	Mullet spp.		0	1	1	0.01
43	Gag	*Mycteroperca microlepis*	0	1	1	0.01
44	Dwarf goatfish	*Upeneus parvus*	0	1	1	0.01

accumulate at a slightly faster rate than in Narragansett Bay (Fig. 3). The curve for Long Island Sound is slightly more asymptotic. Both curves for Narragansett Bay and Long Island Sound begin to plateau in 1994, which means it took seven years for the majority of the species to be sampled.

Multivariate species analyses indicated that the warm-water fish faunas were different between Narra-

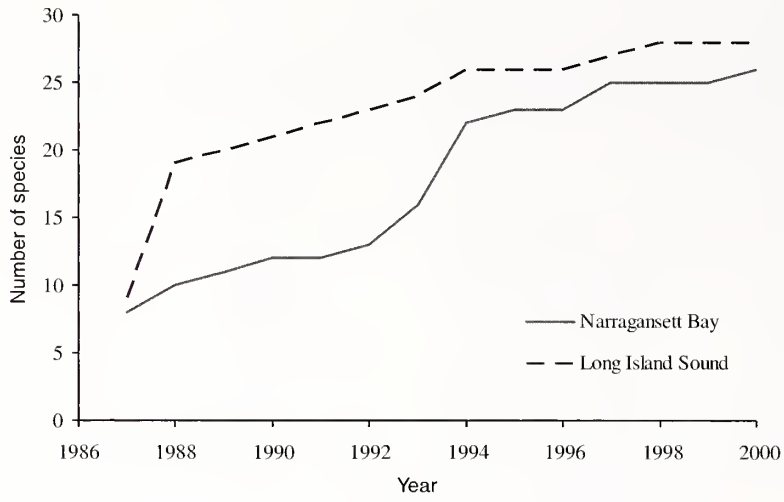

Figure 3

Species accumulation curves for Narragansett Bay and Long Island Sound warm-water fish species caught by trawl and seine surveys (1987–2000).

gansett Bay and Long Island Sound. Two groups were identified in the analysis, predominantly segregating on the basis of area (Fig. 4). Narragansett Bay data from 1993 was an outlier in the multivariate analysis (Fig. 4); the lowest abundance of warm-water fish in Narragansett Bay was present in this year.

The SIMPER analysis indicated that the species contributing most to the dissimilarity between Narragansett Bay and Long Island Sound were rough scad (*Trachurus lathami*), crevalle jack, blue runner (*Caranx chrysos*), flying gurnard (*Dactylopterus volitans*), bluespotted coronetfish (*Fistularia tabacaria*), and the orange filefish (*Aluterus schoepfi*). With the exception of crevalle jack, the species contributing to dissimilarity were found in moderate numbers and were present in greater abundance in one of the locations or during different years. The species that were most similar among locations were the most abundant, namely Atlantic moonfish, northern puffer, planehead filefish, and bigeye (Table 2).

Timing of occurrence of warm-water fishes

It was expected that because of the close spatial proximity of the sampling areas, that temperatures in Narragansett Bay and Long Island Sound would be similar. Temperatures were significantly correlated between the two estuaries. Of the several different correlations calculated, weekly mean temperatures in Narragansett Bay and Long Island Sound were significantly correlated (r=0.99; P<0.001), as were annual mean surface temperatures (r=0.83, P<0.001).

The relationship between annual fish catch and mean temperatures was equivocal. Annual abundance in Narragansett Bay was significantly correlated with mean summer temperatures and annual abundance on Long Island Sound was significantly correlated with semi-annual temperature (Table 3). However, annual abundance in Narragansett Bay was not correlated with semi-annual temperature and annual abundance in Long Island Sound was not correlated with summer temperature.

The general pattern of timing of fish occurrence was similar between estuaries. Fish were first caught in abundance (>5% of peak) in mid-July (week 30) in both Narragansett Bay and Long Island Sound at mean temperatures of 18°C in both areas (Fig. 5). Peak abundance occurred in mid-September in both estuaries. Last occurrence occurred in November in Narragansett Bay, and last occurrence, about 3 weeks later in Long Island Sound. Because of their nature, the species analyzed prefer warm conditions, and as expected, over 80% of the warm-water fishes were caught at temperatures between 17 and 21°C and the cumulative temperature reached 100% at 23°C (Fig. 6).

There were mixed results in the examination of the patterns of timing of fish appearance and disappearance. The time of first, peak, and last occurrence were not significantly different between Narragansett Bay and Long Island Sound (first: t=0.69, df=26; peak: t=1.3, df=26; last: t=2.8, df=26) (Fig. 7). However, there were no significant correlations between the interannual patterns in timing of first, peak, or last appearance among years in the two locations.

The peak week of occurrence of northern puffer was weakly correlated between the two areas during 1987–2000, but the annual means were very similar between estuaries, with a mean percent difference of only 0.32%. The final correlations of timing of occurrence were con-

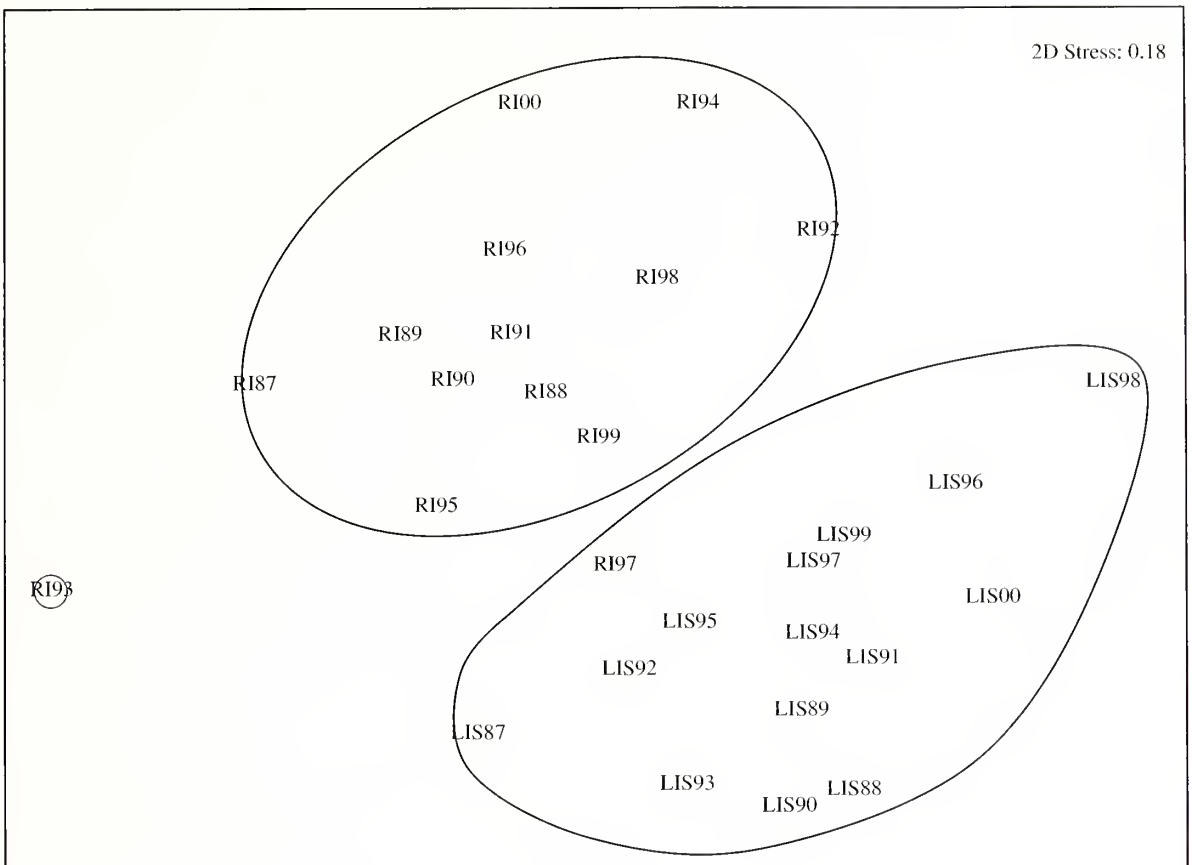

Figure 4

Multidimensional scaling plot of standardized, fourth-root transformed, fish abundance data by year (1987–2000) and location based on Bray-Curtis similarity. The two main groupings indicate that fish abundances in Narragansett Bay (RI) and Long Island Sound (LIS) were not similar to each other annually. The line contours describe 45% similarity from the clustering algorithm. Note that the year 1993 appears to be an outlier, lacking similarity to the Narragansett Bay or Long Island Sound populations. In addition, RI 97 seems equally similar to both the RI and the LIS groupings.

ducted for the weeks of peak fish occurrence and the temperature of that week, as well as the week of 50% minimum and maximum temperature as determined by cumulative degree days and both were significant (r=0.67; P=0.01 and r=0.67; P=0.01, respectively).

Discussion

Despite their brief seasonal appearance, warm-water fish species are an important part of the overall faunal assemblage in temperate estuaries worldwide. These summer visitors contribute significantly to the overall species diversity of temperate estuaries (Wallace et al., 1984; Francis et al., 1999), increasing both food sources and overall productivity (Chapin et al., 2000; Cardinale et al., 2002). The majority of the warm-water species found in this study have been recorded in the study areas only as juveniles; however, it is an open question whether this will always be the case. Many warm-water species are highly adaptable, and may eventually be able to over-winter in temperate estuaries, becoming part of the resident species assemblage. An influx of these new residents could affect the ecosystem structure and function in these estuaries.

The diversity and abundance of Narragansett Bay and Long Island Sound warm-water fish are increasing, apparently because of warming coastal waters. The species assemblages of both areas are similar. However, differences in both species presence and overall species abundance exist between the two data sets. For example, large schools of Atlantic moonfish were caught in a Narragansett Bay trawl survey in 1994, leading to a huge increase of overall catch abundance for that year. Schooling fishes, such as the Atlantic moonfish, caught during our study may influence the interpretation of the survey data. Another difference in species presence was indicated by the presence of a species in only one of the two areas surveyed uring the years of this study (1987–2000). Species such as the inshore lizard-

Table 3

Correlations (r) and probability values (P) between annual fish catch in Narragansett Bay and Long Island Sound and mean summer temperatures (June, July, August) and mean half-year temperatures (May, June, July, August, September, October) for each location (1987–2000). Catch columns are the total numbers of warm-water fishes caught in each location per year through both seining and trawl sampling.

	Narragansett Bay			Long Island Sound		
		Temperature °C			Temperature °C	
Year	Catch	Summer	Semi-annual	Catch	Summer	Semi-annual
1987	75	18.77	16.83	21	23.80	15.20
1988	138	19.16	16.59	392	20.57	17.80
1989	138	19.76	17.32	200	24.74	18.09
1990	289	19.25	17.34	150	21.33	17.50
1991	144	20.16	18.38	105	21.51	16.77
1992	137	18.69	16.98	109	22.87	15.74
1993	58	19.38	17.53	97	21.17	17.62
1994	1794	20.20	17.33	253	21.99	18.23
1995	91	20.09	19.16	94	20.37	14.82
1996	143	18.80	17.05	952	18.73	19.91
1997	213	18.51	16.75	335	17.94	19.51
1998	411	18.43	17.29	1267	22.93	19.83
1999	457	19.73	17.77	780	20.98	19.13
2000	550	18.99	16.83	1927	20.58	20.05
r		0.346	0.071		0.230	0.746
P		0.048	0.105		0.767	0.004

fish (*Synodus foetens*), spotfin butterflyfish (*Chaetodon ocellatus*), and striped burrfish (*Chilomycterus schoepfii*) were all recorded only in Long Island Sound during the years studied but are known to occur in Narragansett Bay as well. Spotfin butterflyfish have often been seen in Narragansett Bay (Meng and Powell, 1999), and catch records for inshore lizardfish were extremely high during the summer and fall of 2006. The data presented in this study may therefore represent only a snapshot of the areas that were sampled and may not completely represent the ecosystems being studied. Because of data limitations due to difficult sampling areas and a lack of frequency of sampling, it was important to look at overall estimates of species diversity, not just the actual numbers of species that were caught. The calculated species richness indicates that the number of warm-water species in the two locations is the same. Although the actual numbers of species found in each area are not equal (26 in Narragansett Bay vs. 28 in Long Island Sound), many additional species have been found by local aquarists and scuba divers in both areas that do not appear in the data sets. Examples of these include fishes seen mostly in rocky or vegetated habitats where sampling is difficult, such as foureye butterflyfish (*Chaetodon capistratus*) (Allen, 1985) and doctorfish (*Acanthurus chirurgus*) (Allen, 1985).

The annual abundance of warm-water species recorded in Narragansett Bay was similar to the abundances in Long Island Sound among the years used in this study (1987–2000). Annual abundance is correlated between locations for all warm-water fishes (omitting 1994 as an outlier), and for three of the five most abundant species. Despite these correlations, the multivariate analyses provided evidence of distinct species compositions in each location and indicated that the interannual variability in timing of occurrence is not correlated between areas. Based on the MDS analysis Atlantic moonfish, planehead filefish, and northern puffer contributed to the similarity in species composition and abundance between locations in the multivariate analyses. In contrast, the moderately and least abundant species, as well as the species that occurred in only one of the sampling areas, contributed to the differences in warm-water fishes present between locations. The recorded absence of species that were knowingly present in the estuaries, such as doctorfish and foureye butterflyfish, likely led to the resulting differences in the MDS plots between estuaries.

Based on the elusive nature of the juvenile warm-water fishes, the data set used for this study may have been compiled with insufficient sampling effort. For data sets with adequate effort, the species accumulation curves reach asymptotic levels quickly (Thompson et al., 2003). However, neither Narragansett Bay nor Long Island Sound data exhibited this pattern, which means that there were likely more species in the systems than there were samples to represent them. Species accumulation also occurs more quickly with increas-

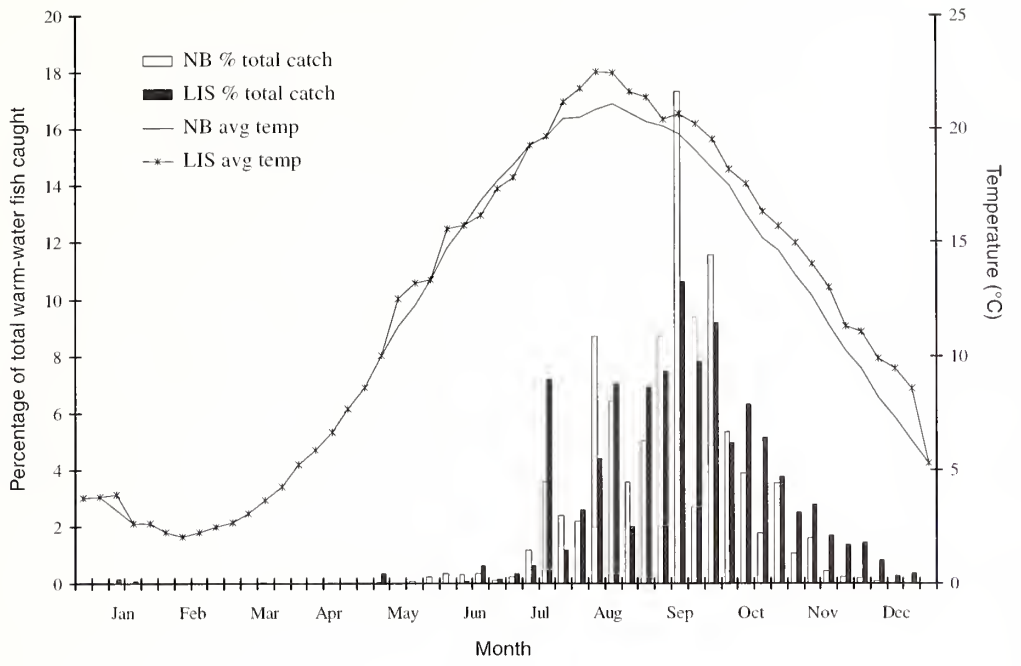

Figure 5

Weekly mean (surface and bottom) temperature data from Narragansett Bay, including all catch data from Narragansett Bay waters as well as from Rhode Island Salt Ponds, and Long Island Sound graphed with the percentage of total occurrences of warm-water fish caught in trawl and seine surveys in these two locations (1987–2000). The line graphs represent the mean annual temperatures, and the bar graphs represent the annual fish catch at each location.

ing sampling area and effort (Ugland et al., 2003). Because Long Island Sound is much larger than Narragansett Bay, there is a greater potential sampling area, which could explain the steeper increase and the more asymptotic nature of the species accumulation curve of the former area. The warm-water fish assemblages were largely similar between the two estuaries but there were spatially-specific variables that may have influenced the temporal occurrence of these species.

Timing of occurrence is an important factor in the structure of warm-water fish faunas; however, the processes that lead to the appearance of warm-water fishes in the early summer and to their disappearance in the fall are not completely understood. The mean weeks of first, last, and peak appearances are all very similar between Narragansett Bay and Long Island Sound and there is the same 4-week time lag between the week of peak temperatures (week 33) and the week of peak fish abundance (week 37)

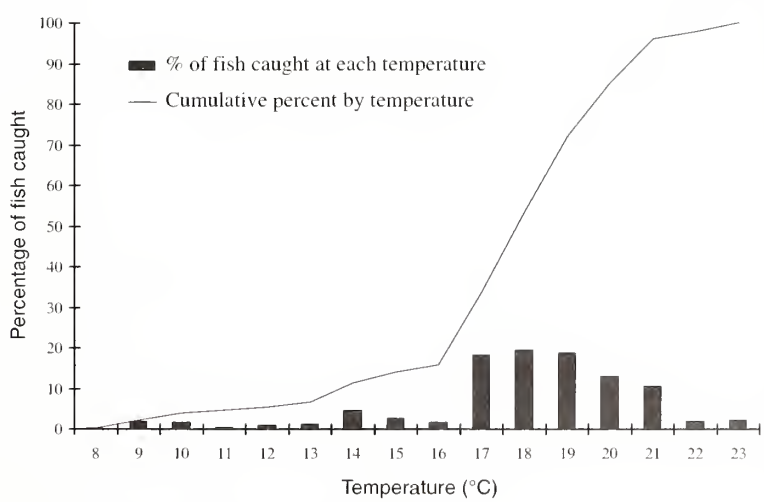

Figure 6

Percentage of warm-water fish sampled in Narragansett Bay and Long Island Sound (1987–2000) as a function of concomitant temperature data and the cumulative percentage of fish caught at each temperature. Bar graphs represent the percentage of total fish catch at each temperature, and the line represents the cumulative temperature percentage.

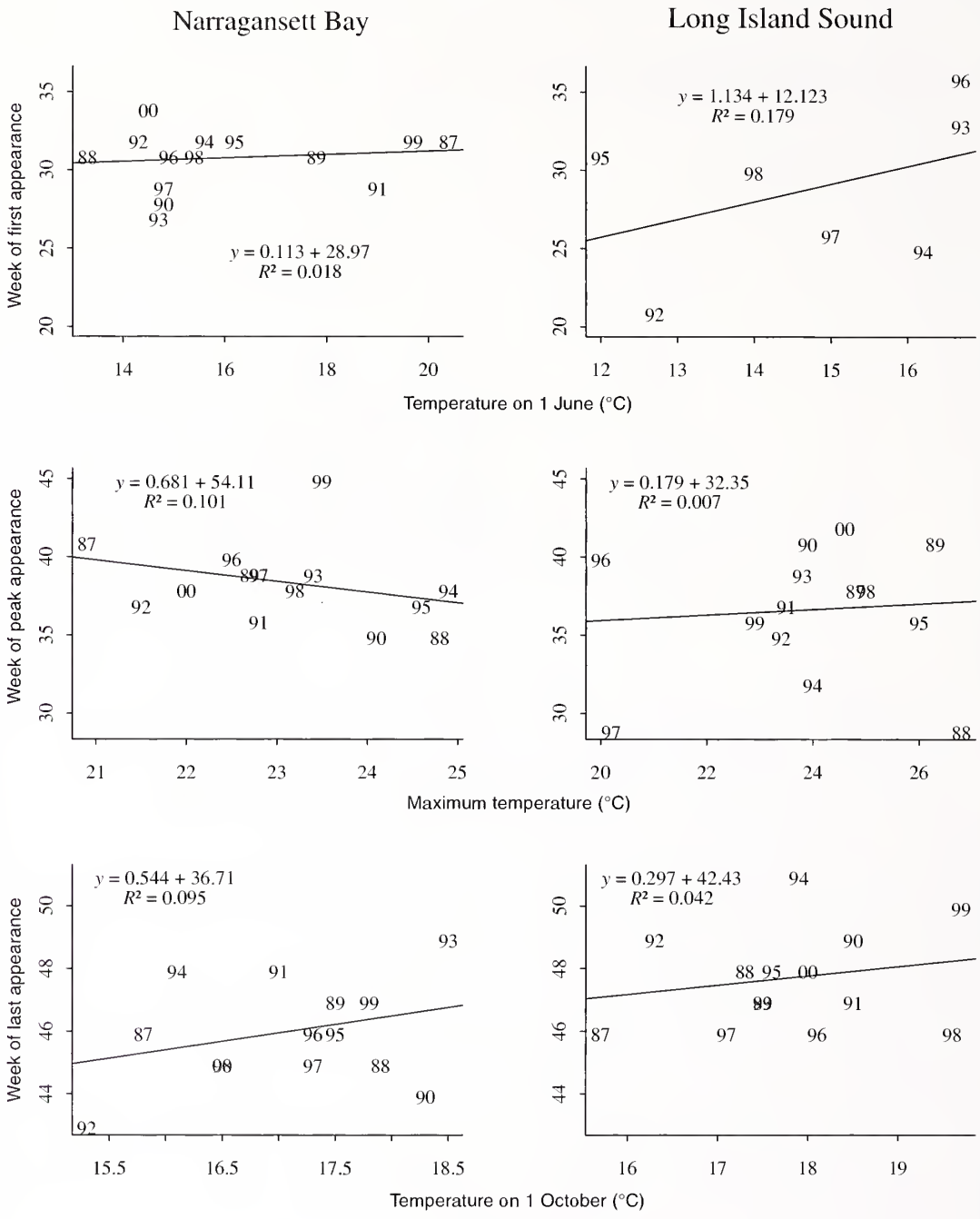

Figure 7

Correlations between temperatures and weeks of the year (1–52) of first (5% of peak), last, and peak appearance of warm-water fishes in both Narragansett Bay and Long Island Sound (1987–2000).

in both locations. In regard to their fall disappearance, warm-water fishes may experience different fates after seasonal periods in temperate estuaries. For some species, eastern Atlantic Ocean populations exist, raising the possibility that dispersal can range across the Atlantic Ocean (Markle et al., 1980), which is especially a possibility for species that are strong swimmers, such as the carangids (McBride and McKown, 2000). However, it is believed that most warm-water species do not successfully return to their place of origin, but die off as waters cool to temperatures below their physiological tolerances in the fall months. Moss (1973) conducted a series of experiments with planehead filefish and found that their lowest lethal temperature limit was 5.6°C,

which is slightly less than the suggested lowest lethal temperature of about 8°C for northern puffer (Hoff and Westman, 1966), 7.4° to 9°C for crevalle jack (Hoff, 1971), and 10°C for spotfin butterflyfish (McBride and Able, 1998). The rapidly decreasing temperatures in the fall cooling cycle determine the length of time the warm-water fish are able to survive in temperate waters before colder temperatures overtake them.

Trends in water temperature indicated that seasonal warming and cooling were the same between the two locations and that the warmer years were correlated with greater abundance of warm-water fishes. This has been observed in other estuarine waters as well, where major influxes of tropical and subtropical fish in New Zealand are linked to warm summers, although there have been several warm periods not accompanied by influxes (Francis et al., 1999). The incidence of warm-water fish is generally increasing with time, indicating that this pattern of increased warm-water fish abundance is likely to continue to rise as temperate coastal waters continually warm on a global scale. However, this increase in warm-water fish abundance may not be exclusively related to temperature. The majority of warm-water fishes are caught between 17° and 21°C, and very few fish are caught at temperatures greater than 21°C. It is possible that very few fish are caught at 21°C because temperatures are rarely recorded higher than 21°C in Narragansett Bay or Long Island Sound. In addition, not all warm years on record are accompanied by heightened warm-water fish catch, and this result highlights the possibility that nontemperature-related factors are contributing to the observed temporal trend. There are likely other processes that influence the abundance of these fishes, such as shifts in the transport mechanisms responsible for supplying warm-water fishes to more northern habitats.

It is hypothesized that the major mode of northward transport for warm-water fishes is the Gulf Stream Current. Because many warm-water fishes arrive as larvae or juveniles, larval transport mechanisms are important to their arrival to summer habitats (Flierl and Wroblewski, 1985; Hare et al., 2002). Western boundary currents such as the Gulf Stream and the Kuroshio Current, and their associated warm-core rings, meanders, and streamers provide physical mechanisms responsible for the pole-ward transport of many warm-water species (Craddock et al., 1992; Watanabe and Kawaguchi, 2003). The Gulf Stream and its associated currents consist of warmer Sargasso Sea water and introduce warm-water fish species into the continental shelf and slope waters near southern New England (Markle et al., 1980; Cowen et al., 1993). Hare et al. (2002) hypothesized four phases exist for northward larval transport and these are associated with warm-core rings. They hypothesized that larval fish were 1) entrained into the Gulf Stream, 2) transported to the northeastern shelf along the edge of the Gulf Stream, 3) carried in warm-core ring streamers from the Gulf Stream and across the Slope Sea (the region between the Gulf Stream and the shelf edge of Cape Hatteras), and 4) ejected from warm-core ring streamers at the shelf edge where larval fishes enter the shelf-slope frontal zone. This mode of transport is the most likely explanation for how warm-water fishes end up in Narragansett Bay and Long Island Sound, where they are observed in their early life stages.

The observations presented here have not been previously documented and provide valuable information regarding the community structure in these locations. Besides adding to our knowledge of the occurrence of warm-water fishes in northern estuaries, the changes in faunal assemblages noted in this study will become increasingly pertinent for future studies on climate change. If waters continue to warm on a global scale, it is thought that major western boundary current systems, such as that of the Gulf Stream Current, may weaken (Frank et al., 1990) and therefore would transport fewer juvenile warm-water fishes northward to temperate areas. It is also thought that the general fish assemblages of temperate estuaries may shift from more vertebrate species (fish) to more invertebrate species (crabs) with increasing water temperatures (Collie et al., 2008). These ideas are contradictory to the thought that warming temperate waters would support more warm-water fishes in temperate areas in the future. The information presented in this study may provide insight into future changes in species composition and abundance that may occur if warming trends continue in the coastal regions of the northwest Atlantic Ocean.

Acknowledgments

We are grateful to P. Howell (Connecticut Department of Environmental Protection), K. Gottschall (Connecticut Department of Environmental Protection), D. Danila (Dominion Resources Services), C. Powell (Rhode Island Department of Environmental Management), and T. Lynch (Rhode Island Department of Environmental Management) for extracting and sharing fish survey data for this study. The Graduate School of Oceanography Fish Trawl is funded by the University of Rhode Island. We greatly appreciate comments from A. D. Wood, C. Recksiek, and K. Castro on previous drafts of this paper, as well as earlier reviews by J. Manderson, D. Mountain, K. McKown, and two anonymous reviewers.

Literature cited

Able, K. W., and M. P. Fahay.
1998. The first year in the life of estuarine fishes in the Middle Atlantic Bight, 342 p. Rutgers Univ. Press, New Brunswick, NJ.

Allen, G. R.
1985. Butterfly and angelfishes of the world, vol. 2, 352 p. Aquarium Systems, Mentor, OH.

Bigelow, H. B., and W. C. Schroeder.
1953. Fishes of the Gulf of Maine. Fish. Bull., Fish. Wildl. Serv. 53: i–577.

Briggs, J. C.
1974. Marine zoogeography, 475 p. McGraw-Hill Book Co., New York, NY.

Cardinale, B. J., M. A. Palmer, and S. L. Collins.
2002. Species diversity increases ecosystem functioning through interspecific facilitation. Nature 415:426–429.

Chapin, F. S., III, E. S. Zavaleta, V. T. Eviners, R. L. Naylor, P. M. Vitousek, H. L., Reynolds, D. U. Hooper, S. Lavorel, O. E. Sala, S. E. Hobbie, M. C. Mack, and S. Diaz..
2000. Consequences of changing biodiversity. Nature 405:234–242.

Collie, J. S., A. D. Wood, and H. P. Jeffries.
2008. Long-term shifts in the species composition of a coastal fish community. Can. J. Fish. Aquat. Sci. 65:1352–1365.

Cowen, R. K, J. A. Hare, and M. P. Fahay.
1993. Beyond hydrography: Can physical processes explain larval fish assemblages within the Middle Atlantic Bight? Bull. Mar. Sci. 53(2):567–587.

Craddock, J. E., R. H. Backus, and M. A. Daher.
1992. Vertical distribution and species composition of midwater fishes in warm-core Gulf Stream meander/ring 82-H. Deep-Sea Res. 39(1):S203–S218.

Flierl, G. R., and J. Wroblewski.
1985. The possible influence of warm core Gulf Stream rings upon shelf water larval fish distribution. Fish. Bull. 83:313–330.

Francis, P. F., C. J. Worthington, P. Saul, and K. D. Clements.
1999. New and rare tropical and subtropical fishes from northern New Zealand. N. Z. J. Mar. Freshw. Res. 33:571–586.

Frank, K. T., R. I. Perry, and K. F. Drinkwater.
1990. Effects of climate change on fish. Trans. Am. Fish. Soc. 119:353–354.

Grant, D.
1991. Tropical waves. Underw. Nat. 20(2):26–27.

Hare, J. A, J. H. Churchill, R. K. Cowen, T. J. Berger, P. C. Cornillon, P. Dragos, S. M. Glenn, J. J. Govoni, and T. N. Lee.
2002. Routes and rates of larval fish transport from the southeast to the northeast United States continental shelf. Limnol. Oceanogr. 47(6):1774–1789.

Hoff, J. G.
1971. Mass mortality of the crevalle jack, *Caranx hippos* (Linneaus) on the Atlantic Coast of Massachusetts. Chesapeake Sci. 12:49.

Hoff, J. G., and J. R. Westman.
1966. Temperature tolerances of three species of marine fishes. J. Mar. Sci. 24(2):131–140.

Hutchins, J. B.
1991. Dispersal of tropical fishes to temperate seas in the Southern Hemisphere. J. R. Soc. West. Aust. 74:79–84.

Johnson, R. A., and G. K. Bhattacharyya.
2001. Statistics Principles and Methods, 4th ed., 723 p. John Wiley and Sons, Inc., New York, NY.

Krebs, C. J.
1999. Ecological Methodology, 2nd ed, 620 p. Harper and Row, Publishers, Inc., New York, NY.

Lenanton, R. C. J., and I. C. Potter.
1987. Contribution of estuaries to commercial fisheries in temperate Western Australia and the concept of estuarine dependence. Estuaries 10(1):28–35.

Markle, D. F., W. B. Scott, and A. C. Kohler.
1980. New and rare records of Canadian fishes and the influence of hydrography on resident and nonresident Scotian Shelf ichthyofauna. Can. J. Fish. Aquat. Sci. 37:49–65.

McBride, S. R., and K. W. Able.
1998. Ecology and fate of butterflyfishes, *Chaetodon* sp., in the temperate, Western North Atlantic. Bull. Mar. Sci. 63(2):401–416.

McBride, S. R., and K. A. McKown.
2000. Consequences of dispersal of subtropically spawned crevalle jacks, *Caranx hippos*, to temperature estuaries. Fish. Bull. 98:528–538.

Meng, L., and J. C. Powell.
1999. Linking juvenile fish and their habitats: an example from Narragansett Bay, Rhode Island. Estuaries 22(4):905–916.

Moss, S. A.
1973. The responses of planehead filefish, *Monacanthus hispidus*, to low temperature. Chesapeake Sci. 14(4):300–303.

Murdy, E. O., R. S. Birdsong, and J. A. Musick.
1997. Fishes of the Chesapeake Bay, 324 p. Smithsonian Institution Press, Washington DC.

Oviatt, C., A. Keller, and L. Reed.
2002. Annual primary production in Narragansett Bay with no Bay-wide winter-spring phytoplankton bloom. Estuarine Coastal Shelf Sci. 54(6):1013–1026.

Rountree, R. A., and K. W. Able.
1992. Fauna of polyhaline subtidal marsh creeks in southern New Jersey: composition, abundance, and biomass. Estuaries 15(2):171–185.

Smith, H. M.
1899. Fish fauna of the Woods Hole region. Science 10(259):878–881.

Thompson, G. G., P. C. Withers, E. R. Pianka, and S. A. Thompson.
2003. Assessing biodiversity with species accumulation curves; inventories of small reptiles by pit-trapping in Western Australia. Austral Ecol. 28:361–383.

Tremain, D. M., and D. H. Adams.
1995. Seasonal variations in species diversity, abundance, and composition of fish communities in the Northern Indian River Lagoon, Florida. Bull. Mar. Sci. 57(1):171–192.

Ugland, K. I, J. S. Gray, and K. E. Ellingsen.
2003. The species accumulation curve and estimation of species richness. J. Anim. Ecol. 72(5):888–897.

Wallace, J. H., H. M. Kok, L. E. Beckley, B. Bennett, and S. J. M. Blaber.
1984. South African estuaries and their importance to fishes. S. Afr. J. Sci. 80(5):203–207.

Watanabe, H., and K. Kawaguchi.
2003. Decadal change in abundance of surface migratory myctophid fishes in the Kuroshio region from 1957 to 1994. Fish. Oceanogr. 12(2):100–111.

Reconstruction of original body size and estimation of allometric relationships for the longfin inshore squid (*Loligo pealeii*) and northern shortfin squid (*Illex illecebrosus*)

Michelle D. Staudinger[1]

Francis Juanes[1]

Suzanne Carlson[2]

Email address for contact author: mstaudin@nre.umass.edu

[1] Department of Natural Resources Conservation
University of Massachusetts Amherst
Amherst, Massachusetts, 01003-9285

[2] School of Natural Science
Hampshire College
Amherst, Massachusetts, 01002

Quantification of predator-prey body size relationships is essential to understanding trophic dynamics in marine ecosystems. Prey lengths recovered from predator stomachs help determine the sizes of prey most influential in supporting predator growth and to ascertain size-specific effects of natural mortality on prey populations (Bax, 1998; Claessen et al., 2002). Estimating prey size from stomach content analyses is often hindered because of the degradation of tissue and bone by digestion. Furthermore, reconstruction of original prey size from digested remains requires species-specific reference materials and techniques. A number of diagnostic guides for freshwater (Hansel et al., 1988) and marine (Watt et al., 1997; Granadeiro and Silva, 2000) prey species exist; however they are limited to specific geographic regions (Smale et al., 1995; Gosztonyi et al., 2007). Predictive equations for reconstructing original prey size from diagnostic bones in marine fishes have been developed in several studies of piscivorous fishes of the Northwest Atlantic Ocean (Scharf et al., 1998; Wood, 2005). Conversely, morphometric relationships for cephalopods in this region are scarce despite their importance to a wide range of predators, such as finfish (Bowman et al., 2000; Staudinger, 2006), elasmobranchs (Kohler, 1987), and marine mammals (Gannon et al., 1997; Williams, 1999).

As with the bones and otoliths of prey fish, cephalopod beaks are often recovered from predator stomachs and may be used for identification of prey species and the reconstruction of original prey body size (Clarke, 1986). Many predators (e.g., marine mammals) cannot digest the chitinous beaks and thousands of beaks may accumulate in the stomachs until they are regurgitated (Clarke, 1980). Predictive equations for estimating body size in the two most common species of cephalopods in the Northwest Atlantic Ocean (Bowman et al., 2000) are either based on few observations (n=25) as seen in the longfin inshore squid (*Loligo pealeii*) (Gannon et al., 1997), or are nonexistent as is true for the northern shortfin squid (*Illex illecebrosus*).

Trophic niche breadth is the range of relative prey sizes consumed ontogenetically by a predator (Scharf et al., 2000). In previous diet studies, trophic niche breadth has been used to predict shifts in foraging modes and physical limitations on feeding patterns (Bethea et al., 2004; Beauchamp et al., 2007). Calculation of trophic niche breadth requires measurements of the total lengths of predators and prey. Depending on how a species is traditionally measured (e.g., fork length in fish, mantle length in squid) in population and other types of surveys, information on total length may not always be readily available. Therefore, knowledge of allometric relationships may be useful to accurately assess trophic interactions and predator-prey relationships. For the majority of cephalopod species, there are currently no predictive equations to estimate total length from mantle length and to account for variability in growth. To improve descriptions of the feeding habits of teuthophagous predators and to increase the number of evaluations of size-based predation on cephalopod prey we present 1) predictive equations for reconstructing original prey size and 2) allometric relationships of mantle length to total body length for the two most common species of cephalopods in the Northwest Atlantic Ocean, *L. pealeii* and *I. illecebrosus*.

Materials and methods

Loligo pealeii were collected by otter trawl from coastal waters off Massachusetts during the months of May through September of 2006 and 2007. *Illex illecebrosus* were collected from outer shelf waters from New Jersey to North Carolina during February 2007 on both the winter and spring bottom trawl surveys conducted by the National Marine Fisheries Service (Northeast Fisheries Science Center) (Azarovitz, 1981). All squid were preserved by freezing until they were processed in the laboratory. Specimens were thawed to room temperature and then measured for dorsal mantle length (DML), total length (TL), and maximum length (L_{Max}) to the nearest 1.0 millimeter. Dorsal mantle length was measured as the distance between the posterior

Manuscript submitted 2 June 2008.
Manuscript accepted 28 August 2008.
Fish. Bull. 107:101–105 (2009).

The views and opinions expressed or implied in this article are those of the author and do not necessarily reflect the position of the National Marine Fisheries Service, NOAA.

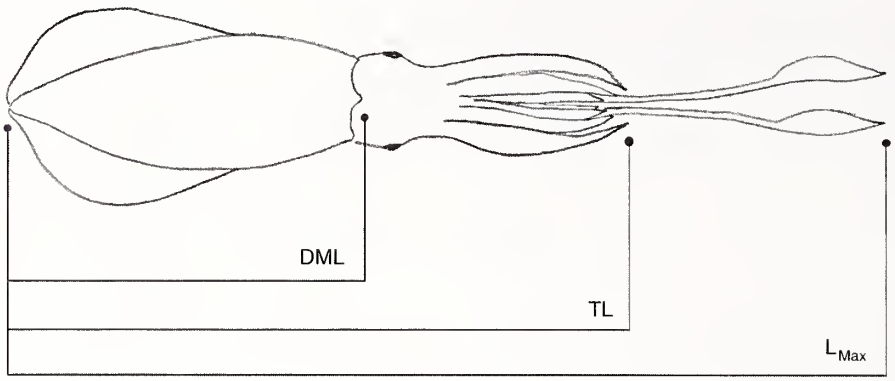

Figure 1

Morphological features used for measuring dorsal mantle length (DML), total length (TL), and maximum length (L_{Max}) of squid.

and anterior tips of the dorsal side of the mantle, total length was measured as the distance between the posterior tip of the mantle to the end of the longest arm, and maximum length was measured as the distance between the posterior tip of the mantle to the end of the longest tentacle (Fig. 1). Beaks were extracted from the buccal mass and the lower rostrum length (LRL) of the lower beak was measured to the nearest 0.01 millimeter. Lower beaks were held so that the rostrum tip was facing the observer and then turned to a left-facing orientation (Fig. 2); the lower beak was best viewed when held against a white background for contrast. The LRL of *L. pealeii* was measured by placing the tip of the moving arm of the calipers inside the jaw angle of the lower beak and extending it to the tip of the rostrum (Clarke, 1986) (Fig. 2A). The LRL of *I. illecebrosus* was measured from the tip of the rostrum to the jaw angle. In *I. illecebrosus* the shoulder forms a tooth which facilitates location of the jaw angle (Fig. 2B). Beaks from both species were measured either under a dissecting microscope or a magnifying glass.

Least squares regression analysis was used to estimate the relationship between mantle length and total length, mantle length and maximum length, and LRL and mantle length for both squid species. Using the PROC UNIVARIATE command in SAS, vers. 9.1 (SAS Institute Inc., Cary, NC), we found that all variables were in compliance with assumptions of normality and no outliers were detected. Linear models were used to develop predictive equations for all pairings of morphological structures. All statistical analyses were performed by using the PROC REG command in SAS.

Results

Total length (TL) and maximum length (L_{Max}) were strongly related to dorsal mantle length (DML) in both *L. pealeii* and *I. illecebrosus*. The r^2 values for all body size relationships ranged from 0.88 to 0.98 and were highly significant ($P<0.0001$) (Table 1). A total of 434 *L. pealeii* ranging in size from 1.9 to 28.0 cm (DML) and 158 *I. illecebrosus* ranging in size from 4.4 to 28.4 cm (DML) were measured to develop allometric relationships between DML, TL, and L_{Max}.

Equations for reconstructing original squid size (DML) from lower rostrum lengths (LRL) were highly significant ($P<0.0001$) in both *L. pealeii* and *I. illecebrosus* (Table 1). The model developed for *L. pealeii* improved the only known equation for this species by expanding the sample size from $n=25$ and the coefficient of determination (r^2) of 0.73 (Gannon et al., 1997) to $n=144$ and an r^2 of 0.83 (Table 1). Lower rostrum lengths (LRL) were measured from *L. pealeii* ranging from 2.6 to 24.7 cm (DML). The predictive model for estimating DML from LRL in *I. illecebrosus* was developed from 89 specimens ranging from 4.4 to 28.4 cm (DML). The relationship between LRL and DML in *I. illecebrosus* was stronger and less variable ($r^2=0.94$, coefficient of variation [CV]=8.15) in comparison to *L. pealeii* ($r^2=0.83$, CV=15.94). Measurement of the lower rostral length in *I. illecebrosus* is greatly facilitated by the presence of a tooth located in the angle point. This structure is absent in the lower beak of *L. pealeii*, and may make measuring beaks from this species more difficult and prone to error.

Discussion

The results of the present study are intended to assist and encourage quantitative assessments of cephalopod prey in the diets of a broad range of finfish, elasmobranch, marine mammal, and seabird predators. Although methods for identification and reconstruction of original body size from cephalopod beaks have

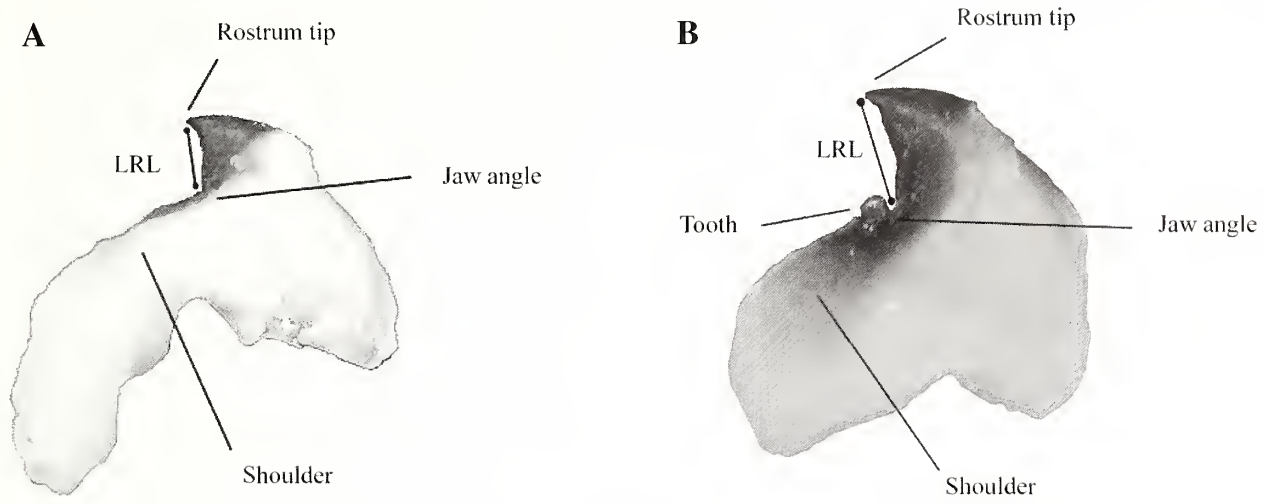

Figure 2

Orientation and key morphological structures of the lower beak of (**A**) the longfin inshore (*Loligo pealeii*) and (**B**) the northern shortfin (*Illex illecebrosus*) squids. Lower rostrum length (LRL) is measured from the tip of the rostrum to the jaw angle.

Table 1

Least squares regression equations for describing the relationship of total length (TL) to dorsal mantle length (DML) and maximum length (L_{Max}), and the relation of DML to the lower rostral length of the lower beak (LRL) in longfin inshore (*Loligo pealeii*) and northern shortfin (*Illex illecebrosus*) squids. All measurements are given in centimeters. n=sample size, r^2=coefficient of determination, F=the F-statistic, and P-value=significance of each model.

Species	Equation	n	r^2	F	P-value
Loligo pealeii	$TL = 1.29DML + 3.11$	434	0.97	14,818.7	<0.0001
	$L_{Max} = 1.52DML + 6.17$	434	0.88	3018.05	<0.0001
	$DML = 92.29LRL - 2.12$	144	0.83	639.2	<0.0001
Illex illecebrosus	$TL = 1.76DML - 1.43$	158	0.98	6624.16	<0.0001
	$L_{Max} = 2.05DML - 0.44$	158	0.97	4409.64	<0.0001
	$DML = 48.92LRL + 0.82$	89	0.94	1364.18	<0.0001

been available for several decades (Clarke, 1980, 1986), information on body-size relationships in the two most common species of squid found in the Northwest Atlantic Ocean has been lacking. Results presented here improved the fit of the only known model for reconstructing mantle length from the rostral length of the lower beak in *L. pealeii*. Clarke (1986) provided an equation for reconstructing body mass from the LRL in *I. illecebrosus*; however, to the best of our knowledge, an equation for reconstructing body length was not previously available for this species.

Mantle length is the universally measured characteristic to assess squid size in population and commercial surveys because it is easy to measure and exhibits less variation in comparison to other structures. We do not advocate changing the current method because, as shown here, morphological relationships for total length (TL) and maximum length (L_{Max}) can be reliably predicted from dorsal mantle length (DML). However, for the purposes of evaluating relative predator-prey body-size relationships, mantle length does not accurately represent total size. Squid swim with their arms extended in front of them or bent slightly downwards and rarely extend their two tentacles, which are longer than their eight arms, except during feeding and mating (Hanlon and Messenger, 1996). Therefore, when a predator attacks a squid it likely perceives the total body size of the squid as the sum of the arms and mantle, thus, making TL the appropriate measure for calculating relative body size. In response to predator

presence in laboratory conditions, squid have occasionally been observed swimming with their tentacles extended, perhaps to appear bigger and to deter attacks. Maximum length (L_{Max}) therefore could be used as an upper limit of predator-perceived squid size. Conversely, in studies where squid is considered the predator rather than the prey, maximum length may be useful to investigators interested in estimating the reach or striking distance of a squid.

All of the morphological relationships measured in this study were found to be highly accurate predictors of body size. The proposed models to back-calculate original size from the lower rostral length of squid beaks provide coefficients of determination similar to those found in previous studies where fish bones and eye lenses were used to calculate original prey size (Scharf et al., 1997, 1998; Wood, 2005). Although it appears that cephalopod beaks are less susceptible to digestion than fish bones, it is still possible that erosion may lead to some measurement bias (Tollit et al., 1997; Santos et al., 2001). The rostrum and shoulder are the sections of the beak formed earliest in development; they are most resistant to digestion and erosion and therefore ideal structures for reconstructing body lengths (Clarke, 1980). As is true with all allometric relationships, the techniques presented here are species specific and may not be reliable estimators of squid body size if applied to lengths beyond the ranges used to develop the predictive equations. Both longfin and shortfin squids attain body sizes larger than were included in the present study; however, our analyses include the most commonly observed lengths of squid found in predator diets and should be adequate for most diet studies. For example, <5% of longfin and shortfin squid prey sizes reported in Kohler (1987), Gannon et al., (1997), Williams (1999), Chase (2002), and Staudinger (2006) exceeded the largest mantle lengths measured here. It should also be noted that specimens collected for the present study were from a portion of the total distributional range of each species and were collected on a limited temporal scale (Macy and Brodziak, 2001; Hendrickson, 2004). If there is variation in squid allometry due to seasonal, interannual, and regional differences in population structure, our sampling regime may not have fully encapsulated these deviations.

Knowledge of size-selective feeding behaviors is fundamental to assessing trophic relationships and defining ecological niches (Bax, 1998). Some of the greatest consumers of cephalopods are large apex predators such as pelagic sharks, tunas, swordfish, and marine mammals; however, the majority of diet data collected on these and many other teuthophagous predators has been qualitative (Smale, 1996). Further, although it has been well established that marine predators are size-selective when feeding on piscine prey (Juanes and Conover, 1994, 1995; Juanes et al., 2001), evaluation of size-based predation on cephalopods has not been well explored. Perhaps the reason for this paucity of information, especially in the Northwest Atlantic Ocean, is the lack of available tools and techniques (Scharf et al., 1998). In previous studies where squid size has been taken into consideration, mantle length was used to calculate relative prey size and to evaluate trophic niche breadths (MacLeod et al., 2006; Ménard et al., 2006), or total length was estimated from anatomical drawings (Chancollon et al., 2006). These approaches are not recommended because they either considerably underestimate total squid size or fail to capture variation in size with growth, thereby introducing error into subsequent calculations.

To gain a complete understanding of the energetic demands of marine predators, it will be necessary for this key prey group to be accurately assessed. Discerning the squid sizes that are most important to supporting predator growth will improve evaluations of age- and size-based consumption rates of squid predators, natural mortality rates of squid populations, competition among species, and resource sharing between the commercial fishing industry and marine predators.

Acknowledgments

Funding for this study was provided by the Woods Hole Oceanographic Institute Sea Grant and the University of Massachusetts School of Marine Sciences. We thank the scientists at the National Marine Fisheries Service (Northeast Fisheries Science Center) and the staff of the Marine Resources Center (Marine Biological Laboratory), in Woods Hole Massachusetts for their help collecting squid specimens. Special thanks to N. Jacobson and C. McGarigal for helping to measure squid, and M. Clarke for providing expertise and advise during the analysis of cephalopod beak structures.

Literature cited

Azarovitz, T. R.
1981. A brief historical review of the Woods Hole Laboratory trawl study time series. *In* Bottom Trawl Surveys (W. G. Doubleday, and D. Rivard, eds.). Can. Spec. Publ. Fish. Aquat. Sci. 58:62–67.

Bax, N. J.
1998. The significance and prediction of predation in marine fisheries. ICES J. Mar. Sci. 55:997–1030.

Bethea, D. M., J. A. Buckel, and J. K. Carlson.
2004. Foraging ecology of the early life stages of four sympatric shark species. Mar. Ecol. Prog. Ser. 268:245–264.

Beauchamp, D. A., D. Wahl, and B. M. Johnson.
2007. Predator-prey interactions. *In* Analysis and Interpretation of Inland Fisheries Data (C. S. Guy, and M. L. Brown, eds.), p 765–842. Am. Fish. Soc., Bethesda, MD.

Bowman, R. E., C. E. Stillwell, W. L. Michaels, and M. D. Grosslein.
2000. Food of Northwest Atlantic fishes and two common species of squid. NOAA Tech. Memo. NMFS-NE-155, 137 p.

Chancollon, O., C. Pusineri, and V. Ridoux.
2006. Food and feeding ecology of Northeast Atlantic

swordfish (*Xiphias gladius*) off the Bay of Biscay. ICES J. Mar. Sci. 63(6):1075–1085.

Chase, B.
2002. Differences in diet of Atlantic bluefin tuna (*Thunnus thynnus*) at five seasonal feeding grounds on the New England continental shelf. Fish. Bull. 100:168–180.

Claessen, D., C. Van Oss, A. M. De Ross, and L. Persson.
2002. The impact of size-dependent predation on population dynamics and individual life history. Ecology 83(6):1660–1675.

Clarke, M. R.
1980. Cephalopoda in the diet of sperm whales of the Southern hemisphere and their bearing on sperm whale biology. Discovery Rep. 37, 324 p.
1986. A handbook for the identification of cephalopod beaks, 273 p. Clarendon Press, Oxford, UK.

Gannon, D. P., A. J. Read, J. E. Craddock, and J. G. Mead.
1997. Stomach contents of long-finned pilot whales (*Globicephala melas*) stranded on the US mid-Atlantic coast. Mar. Mamm. Sci. 13(3):405–418.

Gosztonyi, A. E., L. Kuba, and L. E. Mansur.
2007. Estimation of body size using morphometric relationships of head bones, pectoral fin bones and bony precaudal distance in *Raneya brasiliensis* (Kaup, 1856) (Pisces, Ophidifformes, Ophidiidae) in Patagonian waters. Rev. Biol. Mar. Oceanogr. 42(1):1–5.

Granadeiro, J. P., and M. A. Silva.
2000. The use of otoliths and vertebrae in the identification and size-estimation of fish in predator-prey studies. Cybium 24(4):383–393.

Hanlon, R.T., and J. B. Messenger.
1996. Cephalopod behaviour, 232 p. Cambridge Univ. Press, Cambridge.

Hansel, H. C., S. D. Duke, P. T. Lofy, and G. A. Gray.
1988. Use of diagnostic bones to identify and estimate original lengths of ingested prey fishes. Trans. Am. Fish. Soc. 117:55–62.

Hendrickson, L. C.
2004. Population biology of northern shortfin squid (*Illex illecebrosus*) in the Northwest Atlantic Ocean and initial documentation of a spawning area. ICES J. Mar. Sci. 61:252–266.

Juanes, F., and D. O. Conover.
1994. Rapid growth, high feeding rates, and early piscivory in young-of-the-year bluefish (*Pomatomus saltatrix*). Can. J. Fish. Aquat. Sci. 51(8):1752–1761.
1995. Size-structured piscivory: Advection and the linkage between predator and prey recruitment in young-of-the-year bluefish. Mar. Ecol. Prog. Ser. 128:287–304.

Juanes, F., J. A. Buckel, and F. S. Scharf.
2001. Predatory behaviour and selectivity of a primary piscivore: Comparison of fish and non-fish prey. Mar. Ecol. Prog. Ser. 217:157–165.

Kohler, N. E.
1987. Aspects of the feeding ecology of the blue shark, *Prionace glauca* in the western North Atlantic. Ph.D. diss., 163 p. Univ. Rhode Island, Kingston, RI.

MacLeod, C. D., M. B. Santos, A. Lopez, and G. J. Pierce.
2006. Relative prey size consumption in toothed whales: Implications for prey selection and level of specialization. Mar. Ecol. Prog. Ser. 326:295–307.

Macy, W. K., and J. K. T. Brodziak.
2001. Seasonal maturity and size at age of *Loligo pealeii* in waters of southern New England. ICES J. Mar. Sci. 58:852–864.

Ménard, F., C. Labrune, Y. J. Shin, A. S. Asine, and F. X. Bard.
2006. Opportunistic predation in tuna: A size-based approach. Mar. Ecol. Prog. Ser. 323: 223–231.

Santos, M. B., M. R. Clarke, and G. J. Pierce.
2001. Assessing the importance of cephalopods in the diets of marine mammals and other top predators: Problems and solutions. Fish. Res. 52:121–139.

Scharf, F. S., J. A. Buckel, F. Juanes, and D. O. Conover.
1997. Estimating piscine prey size from partial remains: Testing for shifts in foraging mode by juvenile bluefish. Environ. Biol. Fishes 49(3):377–388.

Scharf, F. S., R. M. Yetter, A. P. Summers, and F. Juanes.
1998. Enhancing diet analyses of piscivorous fishes in the northwest Atlantic through identification and reconstruction of original prey sizes from ingested remains. Fish. Bull. 96:575–588.

Scharf, F. S., F. Juanes, and R. A. Rountree.
2000. Predator size-prey size relationships of marine fish predators: Interspecific variation and effects of ontogeny and body size on trophic-niche breadth. Mar. Ecol. Prog. Ser. 208: 229–248.

Smale, M. J.
1996. Cephalopods as prey. IV: Fishes. *In* The role of cephalopods in the world's oceans (M. R. Clarke, ed.), p. 1067–1081. Philos. Trans. R. Soc. Lond. B. 351.

Smale, M. J., G. Watson, and T. Hecht.
1995. Otolith atlas of southern African marine fishes. Ichthyol. Monogr. J. L. B. Smith Inst. Ichthyol., 253 p. + 149 plates.

Staudinger, M. D.
2006. Seasonal and size-based predation on two species of squid by four fish predators on the northwest Atlantic continental shelf. Fish. Bull. 104:605–615.

Tollit, D. J., M. J. Steward, P. M. Thompson, G. J. Pierce, M. B. Santos, and S. Hughes.
1997. Species and size differences in the digestion of otoliths and beaks: Implications for estimates of pinniped diet composition. Can. J. Fish. Aquat. Sci. 54(1):105–119.

Watt, J., G. J. Pierce, and P. R. Boyle.
1997. A guide to the identification of North Sea fish using premaxillae and vertebrae. Co-operative Research Report No. 220, 231 p. Int. Council Explor. Sea. Copenhagen, Denmark.

Williams, A. S.
1999. Prey selection by harbor seals in relation to fish taken by the Gulf of Maine sink gillnet fishery. M.S. thesis, 62 p. Univ. of Maine, Orono, ME.

Wood, A. D.
2005. Using bone measurements to estimate the original sizes of bluefish (*Pomatomus saltatrix*) from digested remains. Fish. Bull. 103:461–466.

Fishery Bulletin

Guidelines for authors

Content of manuscripts

Contributions published in *Fishery Bulletin* describe original research in marine fishery science, fishery engineering and economics, as well as the areas of marine environmental and ecological sciences (including modeling). Preference will be given to manuscripts that examine processes and underlying patterns. Descriptive reports, surveys, and observational papers may occasionally be published but should appeal to an audience outside the locale in which the study was conducted. Although all contributions are subject to peer review, responsibility for the contents of papers rests upon the authors and not on the editor or publisher. *Submission of an article implies that the article is original and is not being considered for publication elsewhere.* **Articles** may range from relatively short contributions (10–15 typed, double-spaced pages, tables and figures not included) to extensive contributions (20–30 typed pages). **Notes** are reports of 5 to 10 pages without an abstract and describe methods or results not supported by a large body of data. Manuscripts must be written in English; authors whose native language is not English are strongly advised to have their manuscripts checked by English-speaking colleagues before submission.

Manuscript Preparation

Title page should include authors' full names and mailing addresses and the senior author's telephone, fax number, and e-mail address, and a list of key words to describe the contents of the manuscript. **Abstract** should be limited to 200 words (one-half typed page), state the main scope of the research, and emphasize the author's conclusions and relevant findings. Do not review the methods of the study or list the contents of the paper. Because abstracts are circulated by abstracting agencies, it is important that they represent the research clearly and concisely. **Text** must be typed in 12 point Times New Roman font throughout. A brief introduction should convey the broad significance of the paper; the remainder of the paper should be divided into the following sections: **Materials and methods, Results, Discussion** (or **Conclusions**), and **Acknowledgments**. Headings within each section must be short, reflect a logical sequence, and follow the rules of multiple subdivision (i.e., there can be no subdivision without at least two items). The entire text should be intelligible to interdisciplinary readers; therefore, all acronyms, abbreviations, and technical terms should be written out in full the first time they are mentioned. Include FAO common names for species in the list of keywords and in the introduction. Regional common names may be used throughout the rest of the text if they are different from FAO common names which can be found at http://www.fishbase.org/search.html. Follow the U.S. Government Printing Office Style Manual (1984 ed.) and the CBE Style Manual (6th ed.) for editorial style; for fish nomenclature follow the most current issue of the American Fisheries Society's Common and Scientific Names of Fishes from the United States and Canada. Dates should be written as follows: 11 November 2000. Measurements should be expressed in metric units, e.g., 58 metric tons (t); if other units of measurement are used, please make this fact explicit to the reader. Write out the numbers zero through nine unless they form part of measurement units (e.g., nine fish but 9 mm). Refrain from using the shorthand slash (/), an ambiguous symbol, in the general text

Literature cited comprises published works and those accepted for publication in peer-reviewed literature (in press). Follow the name and year system for citation format in the "Literature cited" section (that is say, citations should be listed alphabetically by the authors' last names, and then by year if there is more than one citation with the same authorship). If there is a sequence of citations in the text, list chronologically: (Smith, 1932; Green, 1947; Smith and Jones, 1985). Abbreviations of serials should conform to abbreviations given in the Serial Sources for the BIOSIS Previews Database. Authors are responsible for the accuracy and completeness of all citations. Literature citation format: Author (last name, followed by first-name initials). Year. Title of report or manuscript. Abbreviated title of the series to which it belongs. Always include number of pages. Cite all software and special equipment or chemical solutions used in the study, not in a footnote but within parentheses in the text (e.g., SAS, vers. 6.03, SAS Inst., Inc., Cary, NC).

Tables and figures—general format

- Zeros should precede all decimal points for values less than one.
- Sample size, n, should be italicized.
- Capitalize the first letter of the first word in all labels within figures.
- Do not use overly large font sizes in maps and for units of measurements along axes in figures.
- Do not use bold fonts or bold lines in figures.
- Do not place outline rules around graphs.
- Do not use horizontal lines through graphs to indicate measurement units.
- Use a comma in numbers of five digits or more (e.g. 13,000 but 3000).
- Maps require a North arrow and degrees latitude-longitude (e.g., 170°E).

Tables are often overused in scientific papers; it is seldom necessary or even desirable to present all the data associated with a study. Tables should not be excessive in size and must be cited in numerical order in the text. Headings should be short but ample enough to allow the table to be intelligible on its own. All unusual symbols must be explained in the table legend. Other incidental comments may be footnoted with italic numeral footnote markers. Use asterisks to indicate probability in statistical data. Do not type table legends on a separate page; place them above the table data. *Do not submit tables in photo mode.*

Figures include line illustrations, photographs (or slides), and computer-generated graphs and must be cited in numerical order in the text. Graphics should aid in the comprehension of the text, but they should be limited to presenting patterns rather than raw data. Figures should not exceed one figure for every four pages of text. Figures must be labeled with author's name and number of the figure. Avoid placing labels vertically (except of y axis). Figure legends should explain all symbols and abbreviations and should be double-spaced on a separate page at the end of the manuscript. Please note that we do not print graphs in color.

Failure to follow these guidelines and failure to correspond with editors in a timely manner will delay publication of a manuscript.

Copyright law does not apply to *Fishery Bulletin*, which falls within the public domain. However, if an author reproduces any part of an article from *Fishery Bulletin* in his or her work, reference to source is considered correct form (e.g., Source: Fish. Bull 97:105).

Submission

The Scientific Editorial Office encourages authors to submit their manuscripts as a *single* PDF (preferred) or Word (zipped) document by e-mail to Fishery.Bulletin@noaa.gov. Please use the subject heading, "Fishery Bulletin manuscript submission". *Do not* send encrypted files. For further details on electronic submission, please contact the Scientific Editorial Office directly (see address below). Or you may send your manuscript on a compact disc in one of the above formats along with four printed copies (one original plus three copies [stapled]) to the Scientific Editor, at the address shown below.

Richard D. Brodeur, Ph.D.
Scientific Editor, *Fishery Bulletin*
Northwest Fisheries Science Center
2030 S. Marine Science Dr.
Newport, Oregon 97365-5296

Once the manuscript has been accepted for publication, you will be asked to submit a final electronic copy of your manuscript. When requested, the text and tables should be submitted in Word or Word Rich Text Format. Figures should be sent as PDF files, Windows metafiles, tiff files, or EPS files. Send a copy of figures in the original software if conversion to any of these formats yields a degraded version.

Questions? If you have questions regarding these guidelines, please contact the Managing Editor, Sharyn Matriotti, at

Sharyn.Matriotti@noaa.gov

Questions regarding manuscripts under review should be addressed to Richard Brodeur, Scientific Editor, at Rick.Brodeur@noaa.gov

Fishery Bulletin

Subscription form

Superintendent of Documents **Publications** Order Form

*5178

☐ YES, please send me the following publications:

____ Subscriptions to Fishery Bulletin
for $36.00 per year ($50.40 foreign)

The total cost of my order is $ _____ . Prices include regular domestic postage and handling and are subject to change.

_____
(Company or Personal Name) (Please type or print)

_____
(Additional address/attention line)

_____
(Street address)

_____
(City, State, ZIP Code)

_____
(Daytime phone including area code)

_____
(Purchase Order No.)

Charge your order. IT'S EASY!

Please Choose Method of Payment:

☐ Check Payable to the Superintendent of Documents
☐ GPO Deposit Account ☐☐☐☐☐☐☐–☐
☐ VISA or MasterCard Account
☐☐☐☐☐☐☐☐☐☐☐☐☐☐☐☐
☐☐☐☐ (Credit card expiration date)

To fax your orders (202) 512-2250

_____
(Authorizing Signature)

Mail To: Superintendent of Documents
P.O. Box 371954, Pittsburgh, PA 15250-7954

Thank you for your order!

Also available online at http://bookstore.gpo.gov/collections/fishery-bulletin

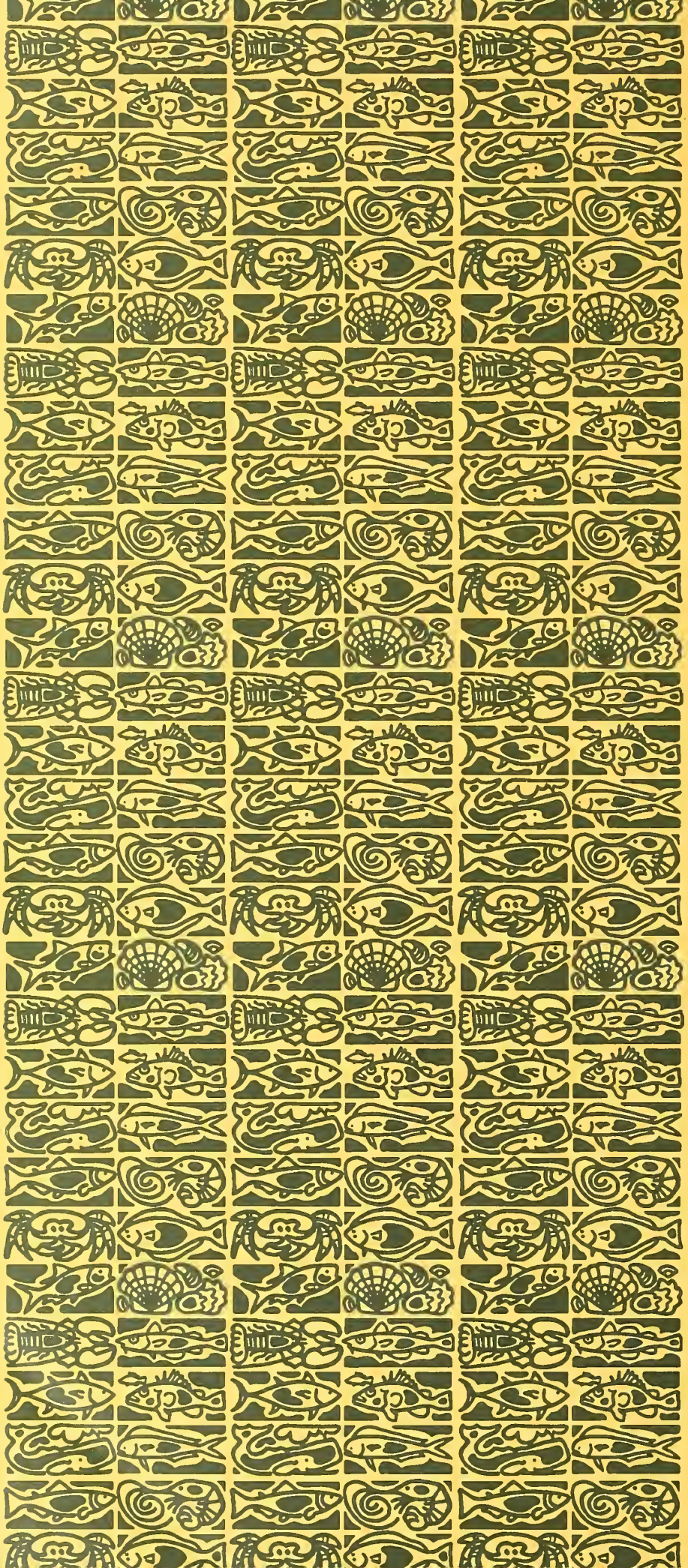

SMITHSONIAN INSTITUTION LIBRARIES
3 9088 01479 6742